Anatomy of Mesenchyme and the Pharyngeal Arches

2

Michael H. Carstens

Introduction

Our previous discussion centered on the anatomic components of the neuromeric system and the identification of their derivatives. The emphasis was on mesenchyme (neural crest and mesoderm) because so many structures (bone, muscles, fascia, and dura) arise from it. We examined how the mesenchyme of any particular structure could be traced back ("assigned") to one or more neuromeric zones in the developing embryo. Excess, deficiency, or outright absence of a developmental field can be attributed to pathologic processes occurring at a neuromeric level very early in development. Craniofacial developmental fields function much like Lego® pieces built one upon another in a tightly regulated sequence. When a field "goes wrong," neighboring fields cannot form correctly. The result is a facial cleft.

We shall now focus on the actual process by which such clefts occur. Our discussion has two parts, static and dynamic. We begin with a detailed analysis of individual fields, where they come from, in what order they form, and what anatomic consequences are seen in the event of field failure. Contributions of various types of mesenchyme will be discussed. We shall then describe the physical manner by which fields are assembled over time. As we shall see, the clinical observations made by Paul Tessier regarding patterns of craniofacial cleft formation (derived on a strictly empiric basis) match closely patterns of neural crest migration [1–3].

Three Caveats

1. *This subject is dense and difficult…but don't be daunted*! Take time to study the definitions section at beginning of the previous chapter and the illustrations section at the back of this chapter. This will give you a visual orientation to the terminology and concepts we are about to discuss. The legends make each illustration self-explanatory. Because one must reference these figures time and again, I have elected to keep them in one section, in a fixed intellectual order that is not in sync in the manuscript. Figure numbers in the text will therefore be out of order. Visualizing gastrulation is key to understand how the neuromeric plan is initiated and carried out. Start with Figs. 2.1, 2.2, 2.3, 2.4, 2.5, 2.6, 2.7, and 2.8
   (a) Figures 1.17–1.19 demonstrates the transformation of a single layer epiblast made of totipotent cells to a bilaminar embryo (stage 4). Note how the hypoblast (primitive endoderm) is derived for the "drop-out" of epiblast cells.
   (b) Figure 2.1 starts with the bilaminar embryo (stage 5). Here you will see the fate map of the epiblast as it gets organized with a primitive streak, but prior to the ingression of mesodermal cells that produces a trilaminar embryo.
   (c) Figure 2.2 is a traditional view of gastrulation (stage 6–7). It is static and therefore deceptive because the

M. H. Carstens (✉)
Wake Forest Institute of Regenerative Medicine, Wake Forest University, Winston-Salem, NC, USA
e-mail: mcarsten@wakehealth.edu

M. H. Carstens (ed.), *The Embryologic Basis of Craniofacial Structure*, https://doi.org/10.1007/978-3-031-15636-6_2

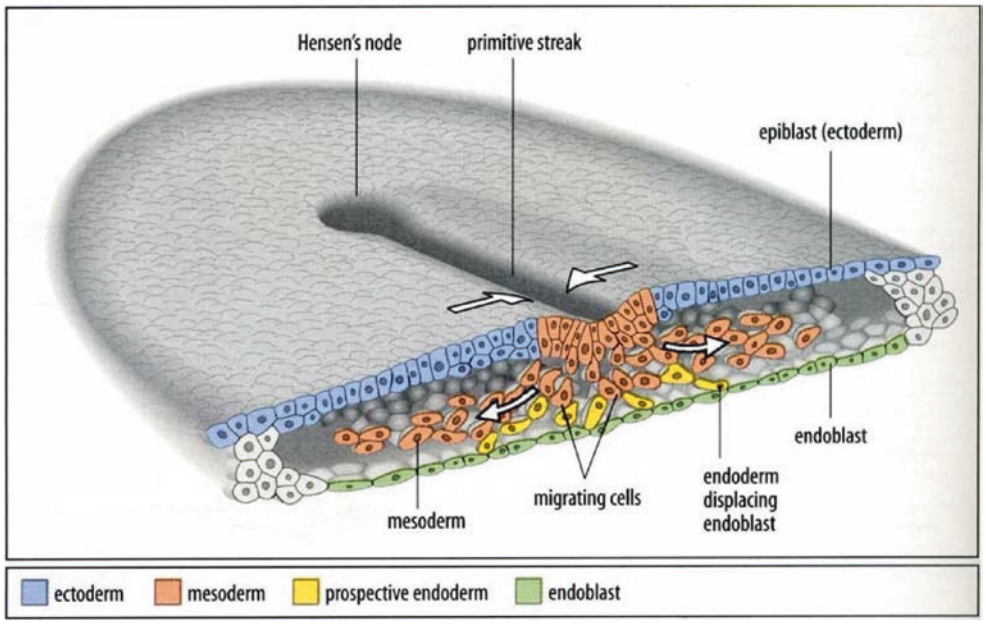

Fig. 2.1 Gastrulation: ingression of mesoderm. This figure shows the classic model of gastrulation. We will expand on this in Figs. 2.2 and 2.3. Note that at each neuromeric level the first wave of cells, future endoderm (yellow) displaces the primitive endoderm (endoblast) outside the boundaries of the embryo proper. The second wave of cells, the future mesoderm (red) moves into the potential space between the epiblast (blue) and the endoderm (yellow). Cells migrating anteriorly through Hensen's node become prechordal plate and anterior-most notochord. Populations just behind them become notochord and somites. Intermediate level of the streak makes intermediate mesoderm (GU system) and lateral plate mesoderm. The most posterior cells of the streak produce the extraembryonic mesoderm. The entire streak ratchets backwards producing these distinct cell populations at every neuromeric level. (Reprinted from Gilbert SF, Barresi M. Developmental Biology, 11th ed. Sinaurer: Sunderland, MA, 2016. Reproduced with permission of the Licensor through PLSclear)

three-dimensional sorting out of germ layers does not happen simultaneously at all levels of the embryo. It is a process that sweeps backward, being directed by the cranio-caudal maturation of neuromeres, each with its unique homeotic signature.

(d) Figure 2.3 goes into greater depth by demonstrating the regional origins of mesoderm and its migrations from initial to mid-streak (stage 6) to definitive streak (7) to neurulation (stage 8). You will see how, with time, lateral plate mesoderm surrounds paraxial mesoderm and is itself surrounded by extraembryonic mesoderm. Physical continuity between LPM and EEM means that blood vessels formed in both of these layers are in continuity, creating the eventual connection between intraembryonic LPM vessels and the placental blood supply.

2. *Consider this a conversation, not a lecture*. Our purpose is to explore an entirely new framework for understanding head and neck anatomy. Get curious! Works by Carlson, O'Rahilly, Gilbert, Liem, Kjaer will greatly enhance your understanding of development [4–8].
3. *This work is interpretive, but testable*…concepts from diverse specialties are woven together to paint a coherent picture of how development might work. The model is my own best guess as to how this system works. You are encouraged to take it further.

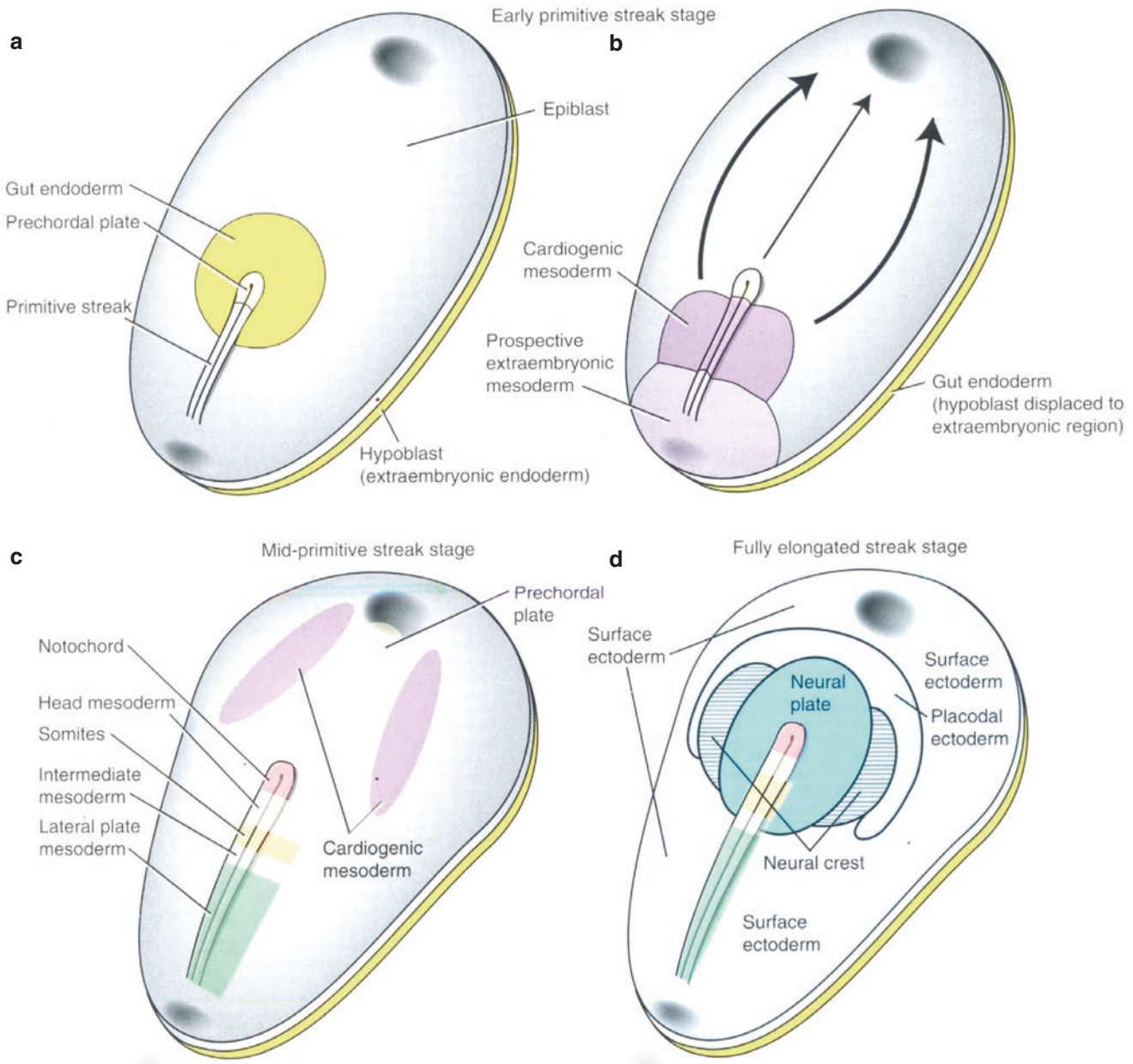

Fig. 2.2 Gastrulation: reorganization of the bilaminar disc. Source: Fate maps of the epiblast (chick + mouse data) showing the regions of epiblast that undergo ingression through and primitive striate and subsequent differentiation. To form the principle components of the trilaminar disc. (**a**) Initial primitive streak stage: Blastoderm consists of upper epiblast(yellow) and a lower hypoblast, (the future extraembryonic endoderm). Note that this layer contains within it the cells that will eventually become mematopoeietic stem cells and somatic stem cells. The prochordal plate is surrounded by prospective true gut endoderm. Oval zones indicated the future buccopharyngeal and cloacal membranes. Even at this stage, the entire epiblast has a primitive set of coordinates. (**b**) Early primitive streak stage: Cardiogenic mesoderm and extra-embryonic mesoderm. Curved arrows indicate the forward flow of cardiogenic mesoderm. Straight arrow shows the forward progression of the prechordal plate. Note that at this stage definitive gut endoderm has displaced the hypoblast to the peripheraly where it becomes the extraembryonic endoderm. (**c**) Mid-primitive streak stage: Demonstrates locations of prospective mesoderm within the epiblast and around the primitive streak. This includes the prospective notochord, head mesoderm (somitomeres) PAM somites, intermediate mesoderm, and lateral plate mesoderm. Note that at this stage the prechordal plate and cardiogenic mesoderm have entered the primitive streak and are now relocated deep to the epiblast. (**d**) Late primitive streak stage shows neural plate, definitive ectoderm, neural crest cells, and placodal ectoderm more peripherally. Cells in the cranial half of the disc have now ingressed. The stage is set for gastrulation. (Reprinted from Schoenwolf GD, Beyl SB, Brauer PB, Phillipa-West PH (eds). Larsen's Human Embryology, 5th ed. Philadelphia, PA: Churchill Livingstone; 2014. With permission from Elsevier)

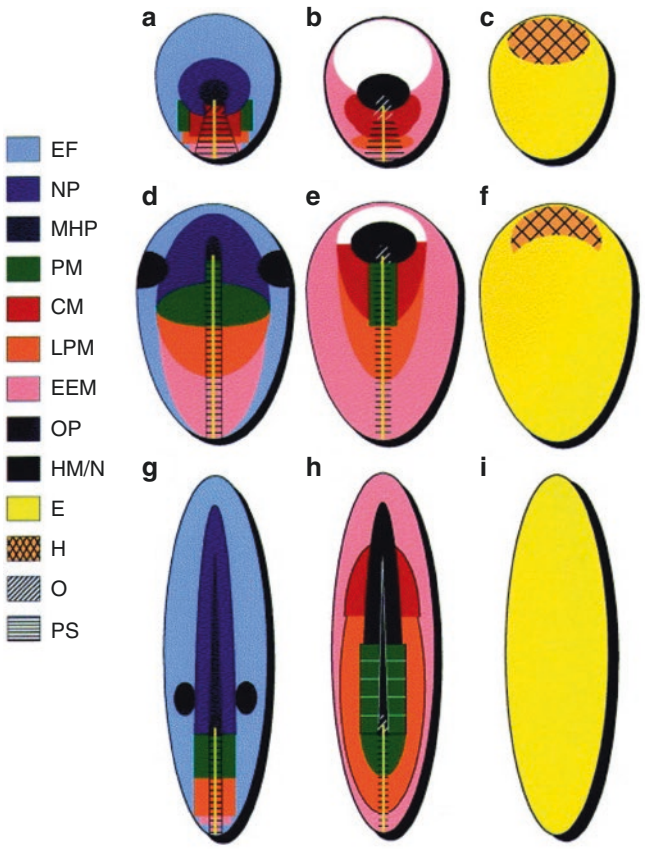

Fig. 2.3 Detail of gastrulation. Prospective fate maps of the avian blastoderm at three stages: (**1**) Stage 6: initial-to-mid-streak; (**2**) stage 7: definitive primitive-streak, and (**3**) stage 8: mid-neurula. The epiblast is shown in (**a**), (**d**), and (**g**), the ingressed mesoblast in (**b**), (**e**), and (**h**), and the ingressed endoderm/hypoblast in (**c**), (**f**), and (**i**). At all three ranges of stages, the epiblast contains a peripheral epidermal ectoderm (EE) and a central prospective neural plate (NP), subdivided into prospective median hinge point (MHP or floor plate), neuroepithelial cells and lateral neuroepithelial cells (that is, L neuroepithelial cells and DLHP neuroepithelial cells). The neural plate lies in close proximity to the Organizer (O) at all stages, with the latter located at the rostral end of the primitive streak (PS). At the later two ranges of stages, cells of the prospective otic placodes (OP) are intermixed on each side near the rostrocaudal level of the Organizer with cells of the prospective epidermal ectoderm and neural plate. In more caudal levels of the blastoderm, the central epiblast and primitive streak contain prospective mesodermal cells. At initial-to-mid-streak stages (**a**–**c**), prospective mesoderm is ingressing through the primitive streak in the following rostrocaudal sequence: (1) prospective head mesoderm (HM or prechordal plate; not shown in epiblast); (2) prospective cardiac mesoderm (CM); (3) prospective lateral plate mesoderm (LPM); and (4) prospective extraembryonic mesoderm (EEM); prospective paraxial mesoderm (PM) occupies the epiblast lateral to the primitive streak. At definitive primitive-streak stages (**d**–**f**), prospective mesoderm is ingressing through the primitive streak in the following rostrocaudal sequence: (1) prospective head mesoderm (not shown in epiblast); (2) prospective rostral heart mesoderm (that is, conotruncus; not shown in epiblast); (3) prospective paraxial mesoderm; (4) prospective lateral plate mesoderm; and (5) prospective extraembryonic mesoderm. At mid-neurula stages (**g**–**i**), prospective mesoderm is ingressing through the primitive streak in the following rostrocaudal sequence: (1) prospective notochord (N); (2) prospective paraxial mesoderm; (3) prospective lateral plate mesoderm; and (4) prospective extraembryonic mesoderm. Endoderm (E) is ingressing through the primitive streak at all ranges of stages shown, displacing the hypoblast (H) rostrally to an extraembryonic location. (Reprinted from Schoenwolf G, Smith JL. Neurulation: coming to closure. Trends Neurosci 1997; 20(11): 510–517. With permission from Elsevier)

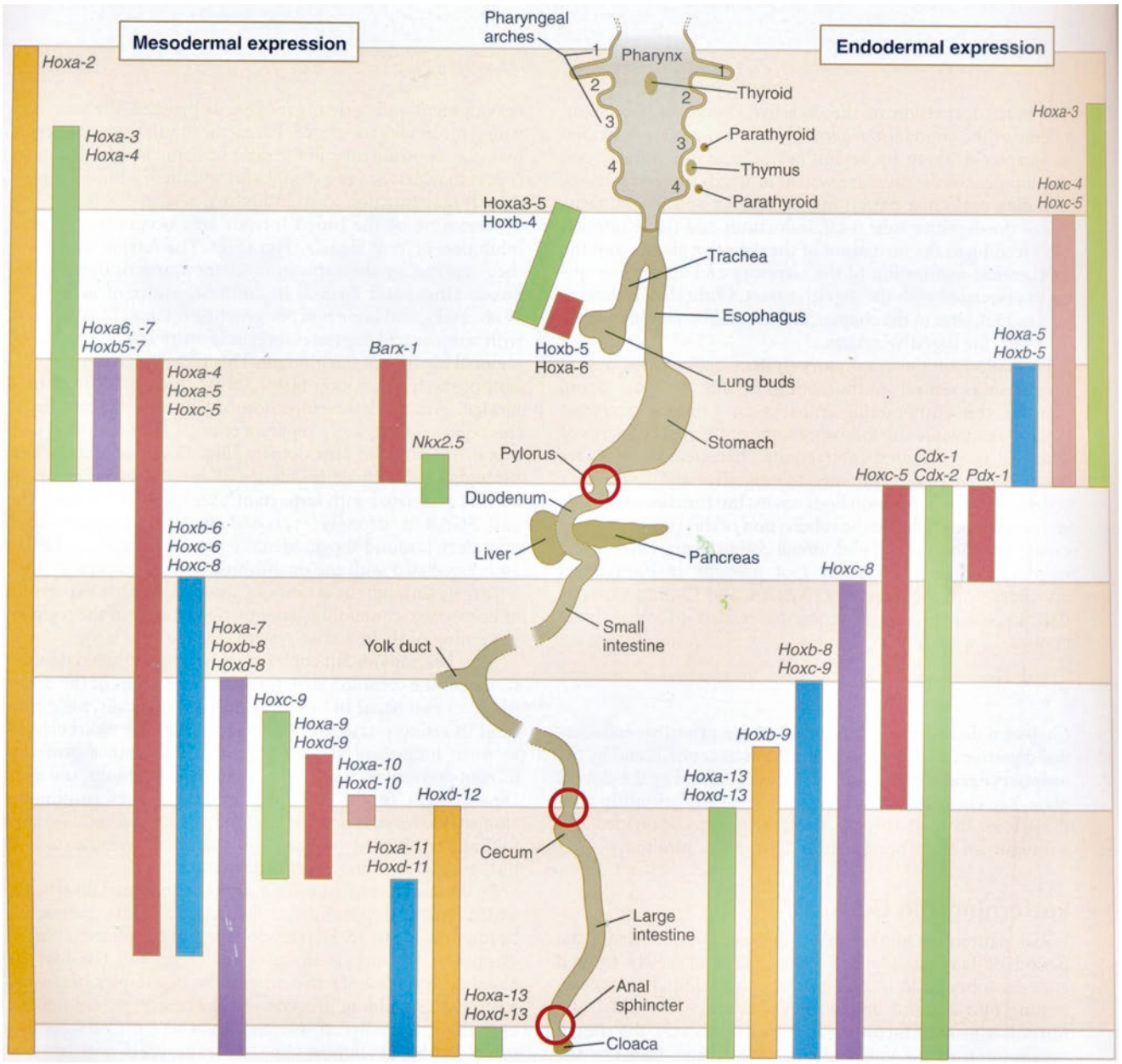

Fig. 2.4 Hox gene expression along the digestive tract. Expression patterns along the mesoderm (left) and the endoderm (right) differ. This shows how, at gastrulation, homeotic coding is imprinted, first, into the endoderm (right), and secondarily into the lateral plate mesoderm (left). For this reason, expression patterns for the same region differ between mucosa and its mesenchymal surround. (Reprinted from Carlson BM. Human Embryology and Developmental Biology, 6th edition. St. Louis, MO: Elsevier; 2019. With permission from Elsevier)

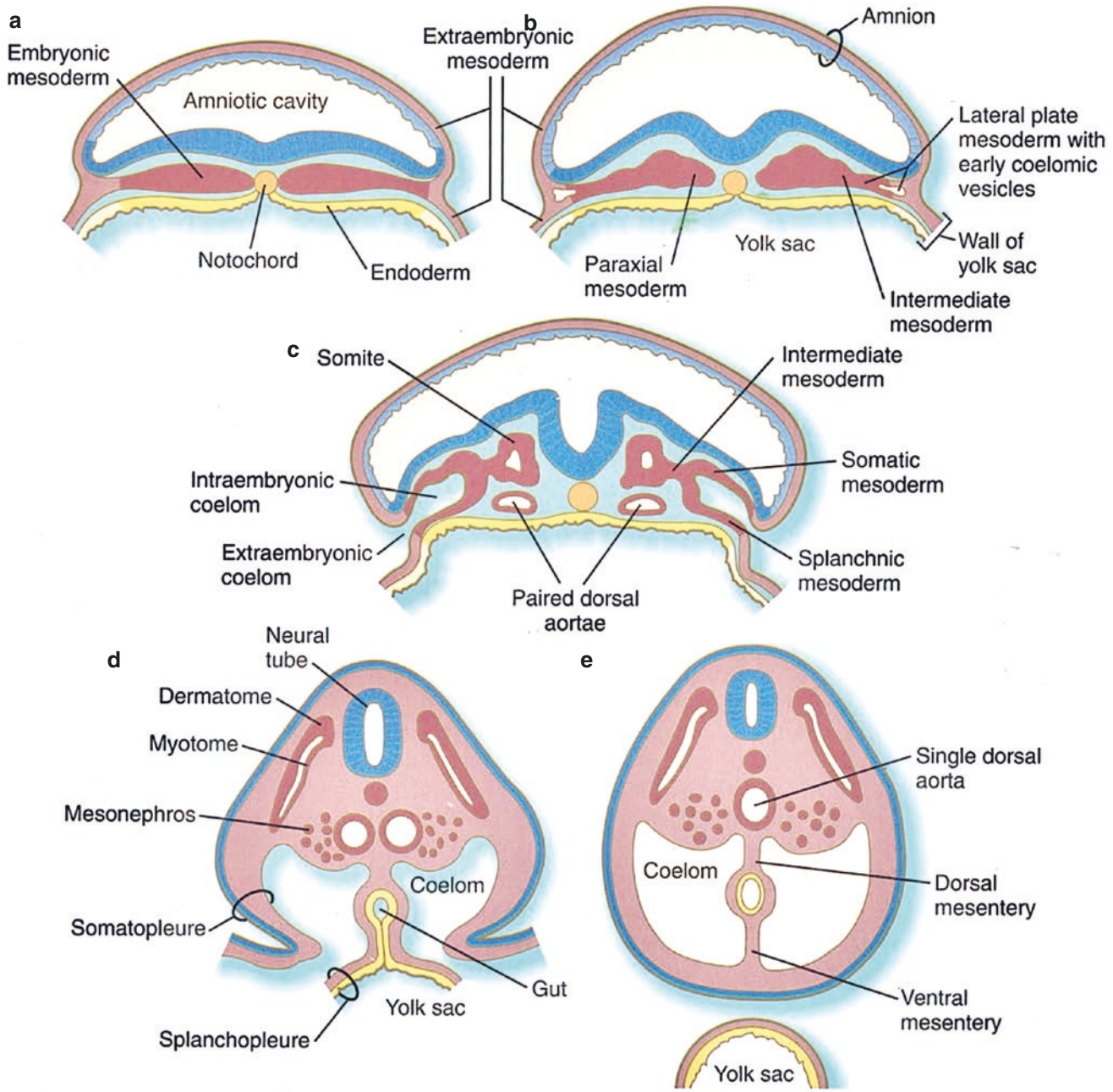

Fig. 2.5 Mesoderm development, both extra and intraembryonic, in staged cross sections. Note: (1) Vesicle formation causing splitting of the lateral plate. (2) Paired dorsal aortae are seen caudal to the heart. In the head, aortic arches ascending through the pharyngeal arches connect to the dorsal aortae (these latter will fuse). (3) Somatic mesoderm **LPMs** makes up body wall, the limb bones, and "programs" the muscles of the extremities. (4) Visceral mesoderm **LPMv** remains closely applied to the endoderm, forming the muscle layers surrounding the gut. (Reprinted from Carlson BM. Human Embryology and Developmental Biology, 6th edition. St. Louis, MO: Elsevier; 2019. With permission from Elsevier)

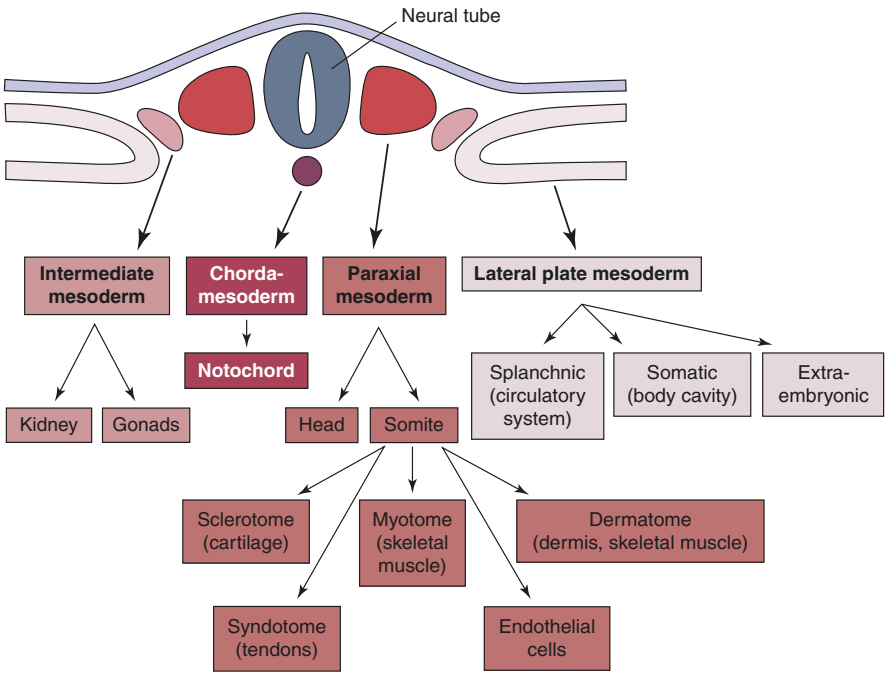

Fig. 2.6 Developmental fate of mesoderm. Blood vessels form in each of the mesodermal compartments. Ectoderm and endoderm are incapable of forming blood vessels. Note that lateral plate is programmed by skin or mucosa. LPM muscles include possibly sternocleidomastoid and trapezius. Also important are diaphragm and lining tissues of body cavities (serosal membranes). Cutaneous contributions are the dermis of the trunk and extremities, and adipose tissue. LPM vascular components populate the fat with stem cells. Thus, stem cells could potentially have neuromeric identities early in their development which separate them into distinct populations. (Reprinted from Gilbert SF, Barresi M. Developmental Biology, 11th ed. Sinaurer: Sunderland, MA, 2016. Reproduced with permission of the Licensor through PLSclear)

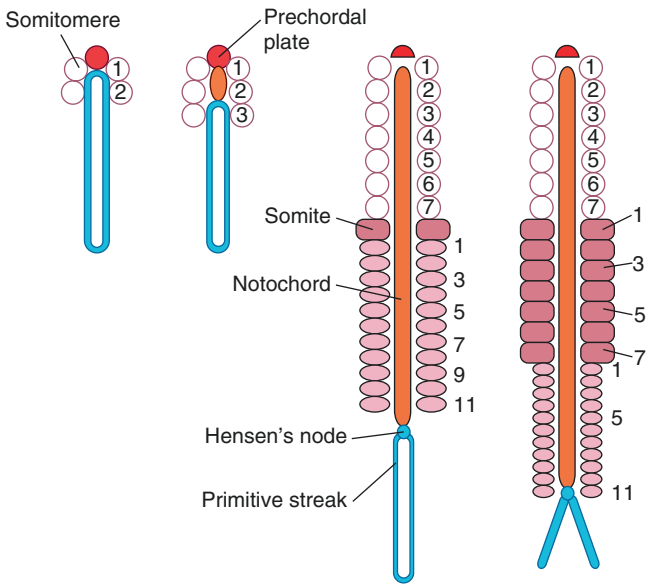

Fig. 2.7 Relationship between somitomeres and somites. Mesoderm segments at four somitomeres per day. Cranial somitomeres (open circles) take shape along Hensen's node until seven pairs appear. All somitomeres caudal to Sm7 have a different fate (ovals): they become transformed into somites (rectangles). At formation of the 19th somitomere, Sm8 becomes the 1st somite (S1). Through the duration of the process, the equilibrium between somitogenesis anteriorly and somitomeres synthesis posteriorly keeps the number of caudal somitomeres at 11. (Reprinted from Carlson BM. Human Embryology and Developmental Biology, 6th edition. St. Louis, MO: Elsevier; 2019. With permission from Elsevier)

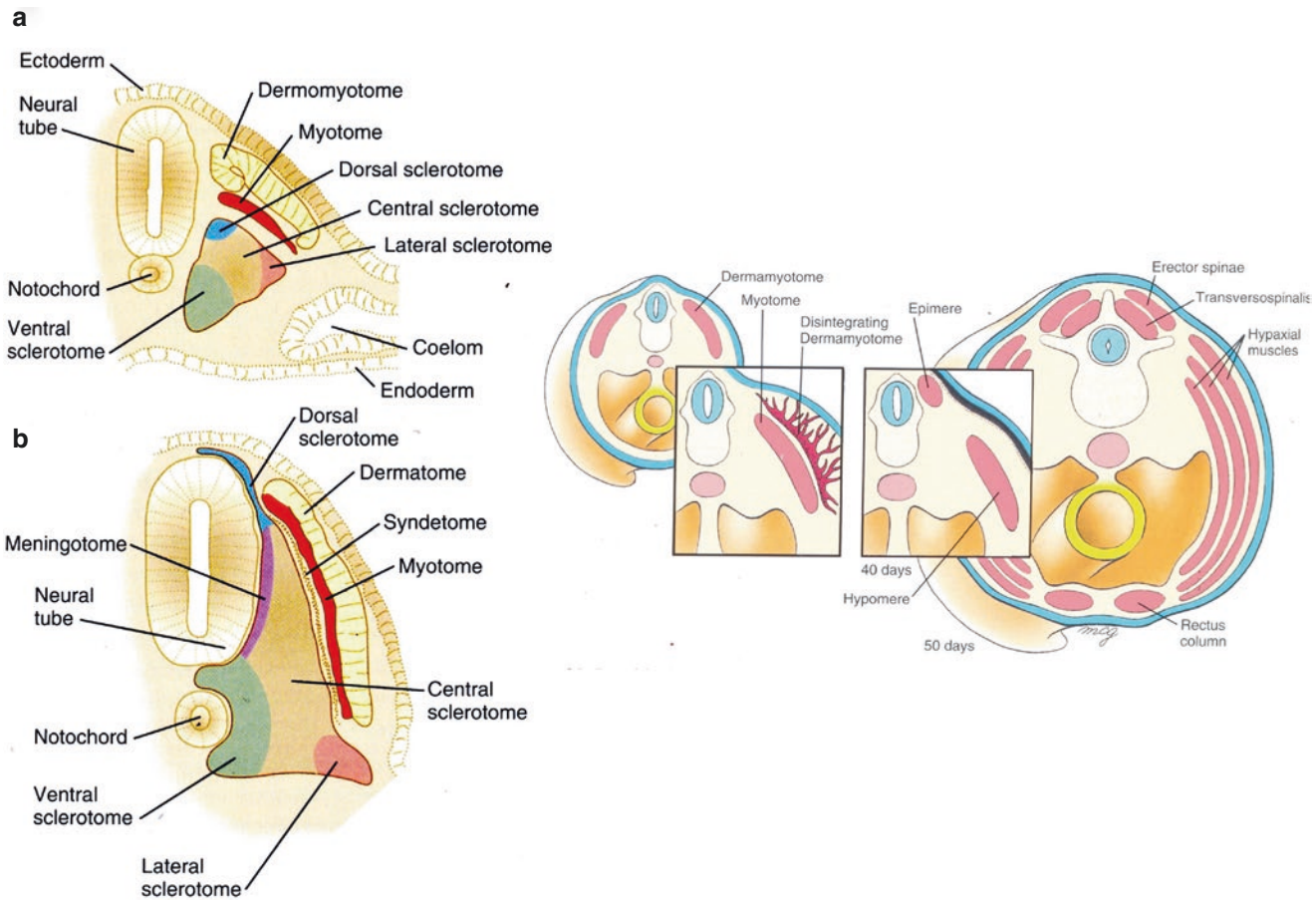

Fig. 2.8 Organization of somites: epaxial vs. hypaxial muscles. Organization of somites at early (**a**) and late (**b**) stages. Fate of the dermomyotome and myotome (cervical neuromere c2 and below). The dermamyotome produced subjacent myotome and dermis. Percursors of dermis (possibly pre-pericytes) migrate up to the surface of their corresponding neuromere. There they interact with lateral plate mesoderm to form the definitive substrate of the future dermis. Meanwhile, the myotome slits into a dorsal epimere and a ventral hypomere. The epimere forms the deep muscles of the back. The hypomere in the thorax forms three layers of the chest wall. In the abdomen, a fourth division ventral segment splits off to form the rectus. This multilevel muscle arises from a vertical fusion from neuromeric levels t12 to 15. (Left: Reprinted from Carlson BM. Human Embryology and Developmental Biology, 6th edition. St. Louis, MO: Elsevier; 2019. With permission from Elsevier. Right: Reprinted from Schoenwolf GC, Beyl SB, Brauer PR, Francis-West PH. Larsen's Human Embryology, 5th ed. Philadelphia, PA: Churchill-Livingstone; 2014. With permission from Elsevier)

Anatomy of Craniofacial Mesoderm

Craniofacial clefts result from hypoplasia or absence of recognizable anatomic structures, such as bone, cartilage, muscle, or dermis. These all originate from mesenchyme; this is to be distinguished from epithelium. Let's get these definitions straight. Epithelial cells are *polar*. One surface faces an external, extracellular environment (such gut lumen or air), while the other surface is joined with a supporting cellular network. Epithelial cells are *interconnected* with tight junctions, gap junctions, and the like. They display *internal polarity*. Organelles such as mitochondria are localized to certain regions within each cell. Mesenchymal cells are *nonpolar*; they do not have "sides." Mesenchymal cells are *not attached* to each other; they can migrate within an extracellular environment. Mesenchymal cells are *internally homogeneous*; organelles are not concentrated in specific zones within the cell.

Mesenchyme of the head and neck come from two main sources: paraxial mesoderm and neural crest. Neural crest mesenchyme will be discussed in a later section of this paper. Paraxial mesoderm results from the physical act of gastrulation, the creation of a trilaminar embryo. During stages 5–6, the embryo is converted from a single layer of cells into a bilaminar structure consisting of two epithelial layers, a dorsal *epiblast* and a ventral *hypoblast* (also known as the *primitive endoderm*). The hypoblast floats on top of the yolk sac. During stage 6, a midline *primitive streak* forms in the epiblast and appears first at its caudal end, the *connecting stalk*; it extends forward about 2/3 of the distance of the epiblast. The primitive streak provides a means by which cells living near its border lose their epithelial characteristics and

become individual mesenchymal cells capable of independent migration. The process of gastrulation takes place at stage 7 when these cells pass into the primitive streak. At any given neuromeric level, they form specific new structures *depending upon the timing of their passage into the primitive streak and their anterior-posterior position along the neuraxis* (Figs. 2.1, 2.2, and 2.3).

The first cells to ingress cluster beneath the midline to form the *notochord*; these multiply rapidly in a lateral direction. This causes the hypoblast cells to be pushed out laterally [4]. Eventually, the new layer completely covers the undersurface of the epiblast and lines the yolk sac. It is now called the *definitive endoderm*. Endoderm does not demonstrate overt signs of segmentation. Nevertheless, it is organized into developmental zones, *endomeres*, in perfect register with the neuromeres of the neural plate. Like the notochord, each endomere bears a unique pattern of homeobox gene expression. The gut is organized into homeotic zones [9] (Fig. 2.4).

The next population of epiblast cells to enter the primitive streak now migrates between the epiblast above and the endoderm below to form the mesoderm. They contain a high concentration of glycosoaminoglycans that absorb water, thereby pushing the epiblast and hypoblast apart. Mesoderm fills in this potential space. It consists of three zones. As demonstrated by work of Tam et al., the identities of these zones are determined by timing of epibast cell ingression and this in turn has everything to do with the spatial positioning of these cells prior to ingression [9–14] (Figs. 2.5 and 2.6).

The first zone is produced by the migration of cells closest to the primitive streak. These cells aggregate close to the midline to form the *paraxial mesoderm* (PAM). Genes elaborated in the midline notochord and in the midline neural plate induce the paraxial mesoderm (PAM) in two zones. Anterior to Hensen's node at r0 is *prechordal plate mesoderm*. This specialized mesoderm will play a role in the development of the midbrain and forebrain and of their accompanying vascular supply [15]. Posterior to Hensen's node, PAM rounds up into discrete structures on either side of the notochord called *somitomeres*, as first described by Jacobson [16, 17]. As gastrulation proceeds in an orderly cranio-to-caudal sequence, somitomeres make their appearance at regular time intervals. The first seven somitomeres are incompletely segmented. The PAM cells are oriented around a central cavity, the *somitocoele*. When 11 somitomeres are produced (stage 10), the end of the CNS (i.e., r11) is reached. The function of PAM is the production of the axial skeleton (including the cranial base) and striated muscles. This process begins with the transformation of the eighth somitomere into the first somite and continues throughout the axis of the embryo [18–20].

The second zone is produced by mesodermal cells originating from more peripheral regions of the epiblast. This intermediate mesoderm forms a thin cord of *intermediate mesoderm* (IM) running the length of the embryo. IM gives rise to the genitourinary system [21].

The third zone is called *lateral plate mesoderm* (LPM). Gene products in the lateral aspect of the epiblast will induce the LPM to form a dorsal, *somatic* layer (LPMs) and a ventral, *visceral* layer (LPMv). It makes sense that the LPMs is in register with its overlying ectomere and the LPMv is in register with the underlying endomere (Fig. 2.10). LPMs synthesizes the appendicular skeleton, dermis of the trunk, dura of the spinal cord, and the non-craniofacial fasciae. LPMv produces the cardiovascular system, smooth muscle, and the viscera (internal organs). Note that LPM is unsplit until it reaches level c1. Lateral plate mesoderm is intensively angiogenic. In the head, more than 90% of LPM cells are angioblasts and they invade medially into the pharyngeal arches and the body of the embryo to produce (with assistance from neural crest cells) the craniofacial vascular system [21].

Paraxial Mesoderm: Somitomeres and Somites

The CNS is flanked by a continuous column of PAM. *Head mesoderm* is incompletely segmented up to somitomere 8 and segmented after that. It provides the endothelial components of all blood vessels of the CNS and pharyngeal arches. The first seven somitomeres form the cranial base of the middle cranial fossa. The posterior aspect of the vertebrate braincase is produced, not from somitomeres, but from their conversion products, the *occipital somites*. Fusion of their sclerotomes produces the cranial base: the basioccipital, exoccipital, and supraoccipital bones. Finally, PAM in its somitomeric form produces the myoblasts of all craniofacial striated muscles, save those of the tongue. The myotomes of occipital somites 1–4 are responsible for, going forward, the tongue (pre-hyoid hypobranchial group), and going backward, the sternocleidomastoid and trapezius. Muscles connecting the pharyngeal arches (post-hyoid hypobranchial group) arise from cervical somites 1–4 (Figs. 2.7 and 2.8) (Table 2.1).

The number of occipital somites varies with the organism. Avian embryos possess five, while mammalian embryos possess four (abbreviated O1–O4). Let us first examine the avian model. At the appearance of the 19th somitomere, an anatomic transformation of the 8th somitomere takes place. The caudal end of Sm7 becomes completely separate from that of the eighth somitomere. The cranial end of Sm7 remains incompletely separated from Sm6. One might ask: *is this an anatomic basis for the para segmentation pattern seen in all subsequent somite derivatives*?

In birds, somitomere 7 also develops a sclerotome and a myotome, but *no dermatome*. It becomes the first occipital somite. Production of the 13th somitomere coincides with

Table 2.1 Somitomeres and their derivatives

Somitomere	Motor nerve	Neuromere	Derivative muscles
Sm1	III	m1	Inferior rectus, medial rectus
Sm2	III	m2	Superior rectus, inferior oblique
Sm3	IV	r0	Superior oblique
Sm4	V3	r3	Mastication, quadratus pyramidalis?
Sm5	VI, VII	r4	Lateral rectus, facial?
Sm6	VI, VII	r5	Lateral rectus, mastication, facial
Sm7	IX/X	r6–r7	Palate, pharynx
Sm8//S1	X, XI, XII	r8	Pharynx, larynx//tongue, SCM-trapezius
Sm9//S2	X, XI, XII	r9	Pharynx, larynx//tongue, SCM-trapezius
Sm10//S3	X, XI, XII	r10	Tongue, SCM-trapezius
Sm11//S4	X, XI, XII	r11	Tongue, SCM-trapezius

Sm somitomere, *S* somite
Somitomeres 1–7 constitute the head mesoderm
All somitomeres from and after Sm8 undergo transformation to somites

the transformation of the eighth somitomere into the first occipital somite. This is the first completely epithelialized somite; both its cranial and caudal borders are distinct. Elegant studies by Huang have mapped the avian mastoid process, sternocleidomastoid, and trapezius muscles to the level of the seventh somitomere/first occipital somite. The spatial pattern in which the five avian sclerotomes amalgamate to produce the skull base is well demonstrated as well [22, 23].

In mammals, the pattern is slightly different. The eighth somitomere is transformed into the first occipital somite. This structure is completely epithelialized. All remaining somite formation proceeds in exactly the same manner to produce the vertebral column and peripheral mesodermal structures, all of which are unified in a segmental fashion by the peripheral nervous system. Despite these differences, the topology used by mammalian sclerotomes to produce the cranial base can be considered to follow an analogous pattern. O'Rahilly and Mueller document the contributions of each occipital somite in human material [24].

The notochord and neural tube serve as an axis dividing the embryo into dorsal and ventral sectors. All structures relating to the notochord and nervous system are considered *epaxial*; these are innervated by dorsal motor and sensory nerves. All other structures of the embryo are considered *hypaxial*; these are innervated by ventral motor and sensory nerves. Craniofacial PAM thus has two primary fates.

- Epaxial PAM remains in situ next to the CNS where it forms the endothelial skeleton of blood vessels surrounding the primitive brain (primitive head plexus and hindbrain channels) and later those arising within the brain itself (but always external to the pia mater). Because the eye is considered part of the brain, the extraocular muscles can be considered epaxial as well.
- Hypaxial PAM provides protection for the brain: it forms part of the *chondral neurocranium*. This refers to bone structures of the skull base posterior to the pituitary (but not posterior fossa) and the petro-mastoid complex. PAM from the fourth somitomere also contributes to the parietal bone. Craniofacial blood vessels such as the dorsal aortae and aortic arches and all remaining muscles are considered hypaxial.

Three Types of Cranium

The craniofacial skeleton consists of three parts. These will be discussed in depth in a subsequent chapter. The oldest, *chondrocranium*, has been mentioned. In evolution, with the advent of gills, *splanchnocranium* arises as the mechanism to support feeding and respiration. The derivation of its mesenchyme is exclusively from neural crest (Fig. 2.19). Careful mapping of derivatives in the chick embryo by Noden demonstrates great homology with mammals [25–28]. This is true across the phylogenetic spectrum (Fig. 2.9).

Note that in the phylogeny (biologic history) of the skull, neural crest cells are almost as primitive as mesoderm. Their forebears appear in the protochordate sea squirts. So, in the production of chordates, with the invention of gills the splanchonocranium and chondrocranium appear simultaneously. In evolution, the transition between chondrichthyans (fishes with an exclusively cartilaginous skeleton, such as sharks) and osteichthyans (bony fishes) demonstrates with the invention of a new covering layer appearing over the skull, the *dermatocranium*. These membranous bones are almost always neural crest with some exceptions, the parietal bone in humans being one of them (Figs. 2.10, 2.11, and 2.12).

Second Iteration of Cranial Mesoderm: The Pharyngeal Arches

The pharyngeal arches of mammals are five in number, the fifth one being vestigial. fifth arch 5 does even not merit its own artery. Pharyngeal arches are sectors of embryo epithelium which, like balloons, are "inflated" with neural crest and project downward from the neuraxis. Each arch is in reg-

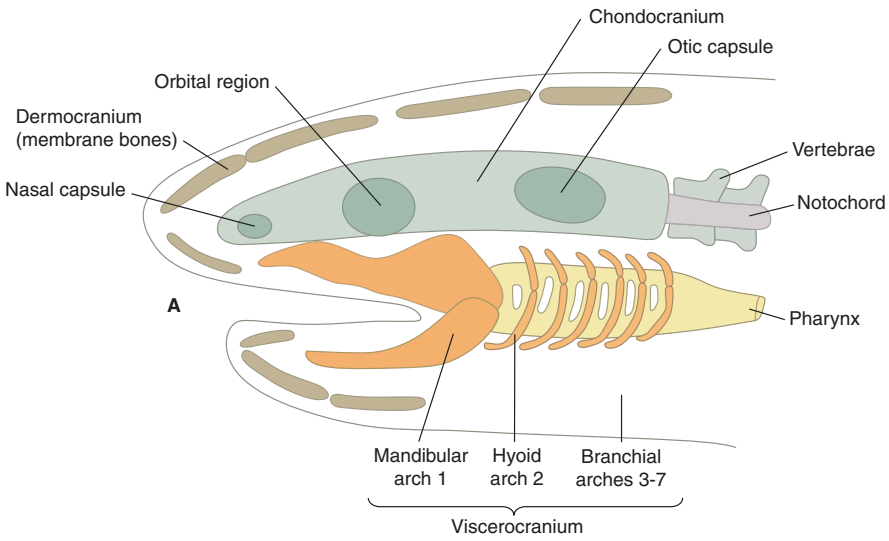

Fig. 2.9 Organization of major component of vertebrate skull. Primitive aquatic vertebrate showing chondrocranium (green), viscerocranium (orange), and dermatocranium (brown). (Reprinted from Carlson BM. Human Embryology and Developmental Biology, 6th edition. St. Louis, MO: Elsevier; 2019. With permission from Elsevier)

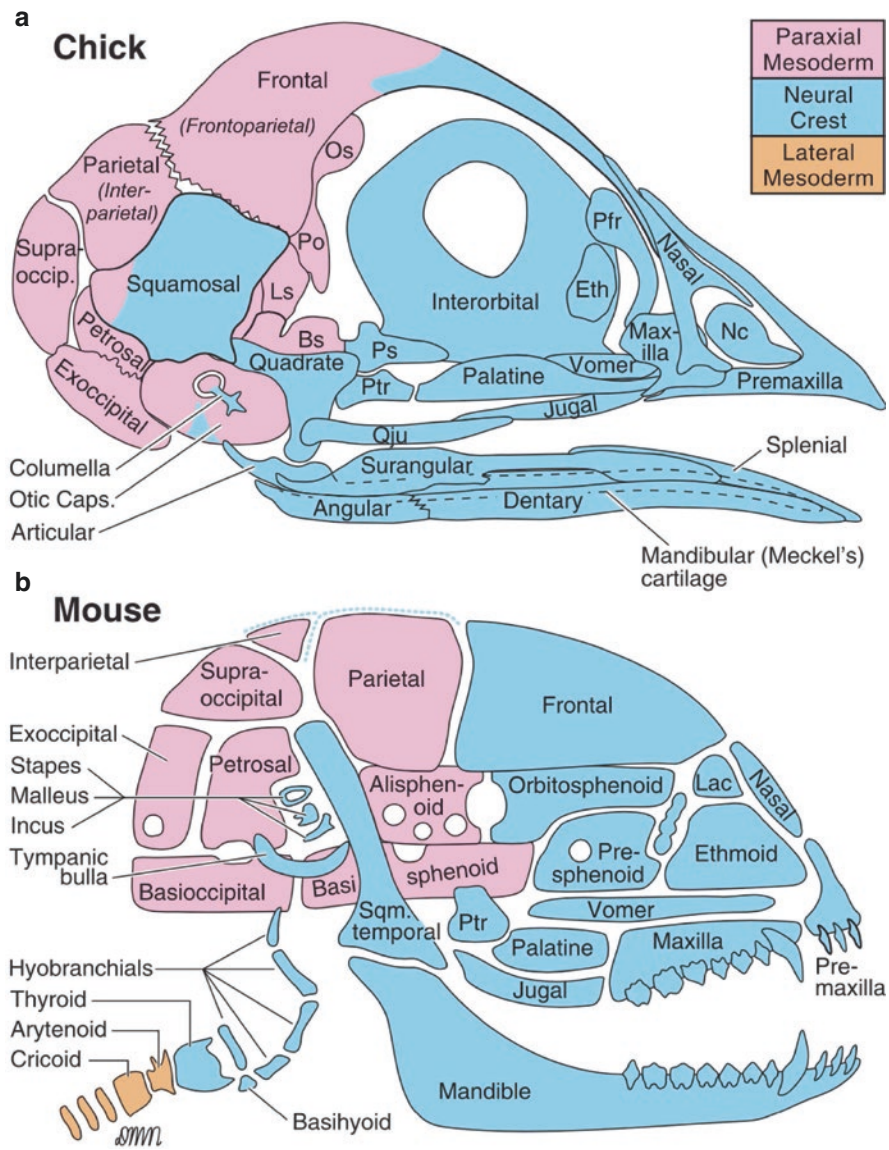

Fig. 2.10 Embryonic skull—avian versus mammal. In mammals, all cartilages anterior to pituitary fossa are neural crest. Schematic (**a**) chick and (**b**) mouse skulls showing the contributions of neural crest, paraxial and lateral mesoderms to the cranial skeleton. The avian map is based on transplantation and retroviral lineage tracings in the chick embryo; hyobranchial structures, all of which are derived from neural crest cells, are not shown. The mouse map is based largely on the location of neural crest cells, as identified by expression of *LacZ* driven by a *Wnt1* promoter in *cre-lox* transgenic embryos [28]. Origins of mouse laryngeal cartilages are by extrapolation from avian data, with the caveat that birds do not have a thyroid cartilage. Blue dots indicate the locations of crest cells present at sites of calvarial sutures. Abbreviations (Figs. 2.5, 2.9 and 2.11): *Ang* angular, *Art* articular, *Bs* basisphenoid, *Den* dentary, *Eth* ethmoid, *Lac* lacrimal, *Ls* laterosphenoid*, *Mc* mandibular cartilage, *Nc* nasal capsule, *Os* orbitosphenoid*, *Pal* palatine, *Pfr* prefrontal, *Po* postorbital, *Ps* presphenoid, *Ptr* pterygoid, *Qd* quadrate, *Qju* quadratojugal, *San* surangular, *Sqm* squamosal, *regions of the pleurosphenoid. (Reprinted from Noden DM, Trainor P. Relations and interactions between cranial mesoderm and neural crest populations. J Anat 2005 207: 575–601. With permission from John Wiley & Sons)

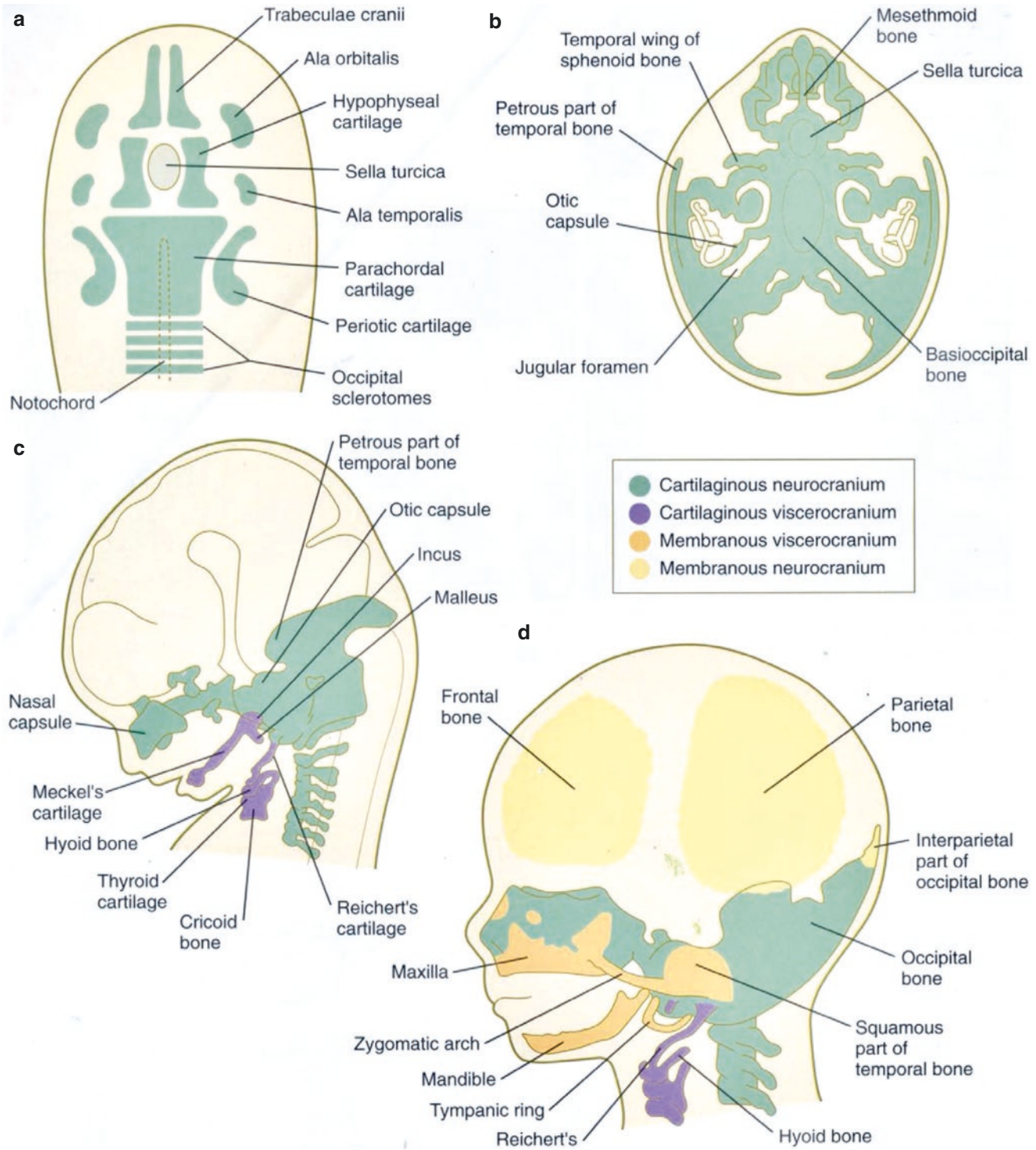

Fig. 2.11 Modern model of the cranium classified by developmental pattern. Note that neural crest can form intermediate cartilages that develop into membranous bone *or* go on to form chondral bone. PAM is exclusively chondral with the exception of scapula where some PAM portions develop in membrane. (Reprinted from Carlson BM. Human Embryology and Developmental Biology, 6th edition. St. Louis, MO: Elsevier; 2019. With permission from Elsevier)

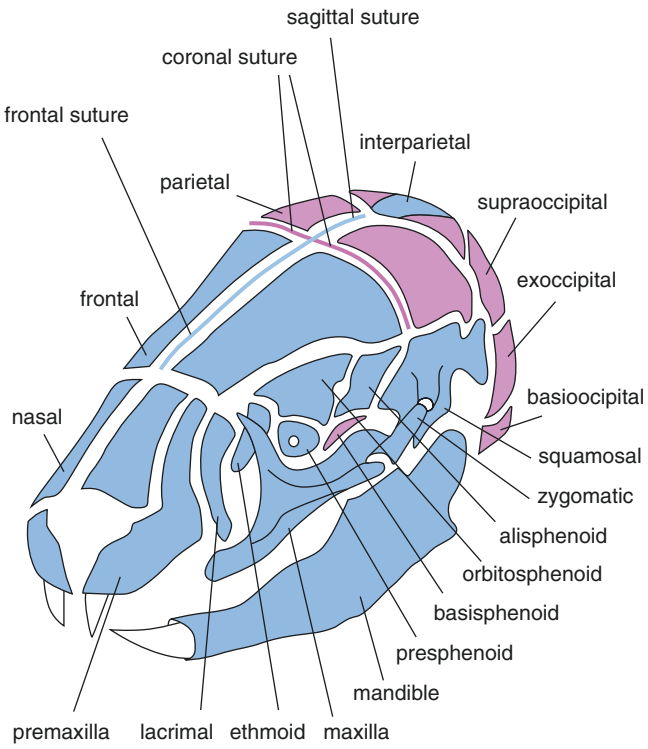

Fig. 2.12 Bones of the skull. Note interparietal has multiple origins—it originally consisted of four distinct bone fields. (Reprinted from Mishima Y, Taylor NS. Neural crest signaling pathways critical to cranial bone development and pathology. *Exp Cell Res* 2014; 325(2):138–147. With permission from Elsevier)

ister with two rhombomeres from which it obtains its neural crest mesenchyme: first arch = r1–r2, second arch = r4–r5, third arch = r6–r7, fourth arch = r8–r9, and fifth arch = r10–r11. Note that the most anterior two rhombomeres, r0 and r1, are not involved in pharyngeal arch formation. Recent evidence supports the existence of a theoretical *premandibular arch* [29, 30]. This structure is better understood as midbrain neural crest (m1–m2, r0–r1) which migrates forward to surround the eye and cover to the anterior forebrain. It is responsible for synthesis of the anterior cranial base (i.e., presphenoid, sphenoid complex, the ethmoid complex, frontal bone, and the superomedial orbit), part of the orbit, and the frontonasal mesenchyme of the upper face and forehead. The importance of the frontonaso-orbital mesenchyme will be stressed time and again in this text.

Head has no bone or cartilage representation in the pharyngeal arches. Its contribution in the arches is very limited: striated muscles. Derivatives of each arch come from spatially distinct sectors of PAM which we have designated as somitomeres. Immediately upon gastrulation, head mesoderm is divided by the otic placode into two distinct zones. *Preotic* PAM refers to the first seven semi-segmented somitomeres. *Postotic* PAM (starting with somitomere 8) is organized into somites, one for each neuromere. These are distinguished by the expression patterns of genes unique to each sector of the arch [31–34].

Somitomeric PAM is assigned to the pharyngeal arches in a pattern that is distinct from that of neural crest. Each arch is in genetic register with two rhombomeres. Neural crest cells from each rhomberomere are distributed to distinct sectors of their "target" arch. For example, r2 forms the cranial half of the first arch (maxillary-zygomatic-palatine complex), while the caudal half of first arch derived from r3 produces mandible and squamous temporal bone. The remainder of the arches are organized along the same principle (Fig. 2.13).

The clinical model of *macrostomia* suggests that an embryologic "fault line" exists along the axis of the first and secondary pharyngeal arches. Embryonic folding turns these arches 90° into contact with the ventral surface of the prosencephalon. The future mesenchyme of the maxilla (r2 neural crest) is now dorsal to that of the mandible (r3 neural crest). We note that second arch fuses into first arch almost as soon as it develops. The lateral facial cleft (#7) running from the oral commissure toward the ear reproduces this genetic boundary zone [22] with r2/r4 being cranial to the cleft and r3/r5 being caudal to it [35]. We shall see (vide infra) that these boundaries follow a common system of Distal-less (Dlx) genes for each arch [36, 37] (Fig. 2.14).

In contrast, the assignment of somitomeric muscle precursors to the arches is *not* symmetric, but *is* related to the location of their motor neurons within the hindbrain. The eye receives Sm1–Sm3 and Sm5 because their motor nerves belong to the *medial motor column* reserved for non-pharyngeal arch muscles. Muscles innervated from the *lateral motor column* are distributed as follows. first arch (Sm4), second arch Sm6, third arch (Sm7), fourth arch (Sm8 and Sm9), and fifth arch (Sm9/10?).

Somitomeres are transient structures. Their derivatives go elsewhere, either directly or becoming somites. In this model, PAM behaves quite differently depending on whether its destination is epaxial or hypaxial. Some epaxial PAM does not transition through an intermediate structure. It retains a physical relationship to the CNS, surrounds the neural tube, and supplies blood vessels. Although vascular PAM is not overtly segmented, the arterial supply it eventually produces is neuromerically organized to serve each developmental unit of the brain and spinal cord (see Chap. 6). Another destiny of PAM is to supply the pharyngeal arches with muscles. The organization of this mesoderm also follows neuromeric principles since each arch is in register with two rhombomeres.

Muscle groups appear to be divided along somitomeric lines. In birds, both Sm5 and Sm6 contain distinct muscles for lateral rectus having motor nuclei in r4 and r5. Upper and lower facial muscles may be supplied by rhombomeres r4 and r5, respectively. Superior constrictor arises from Sm7.

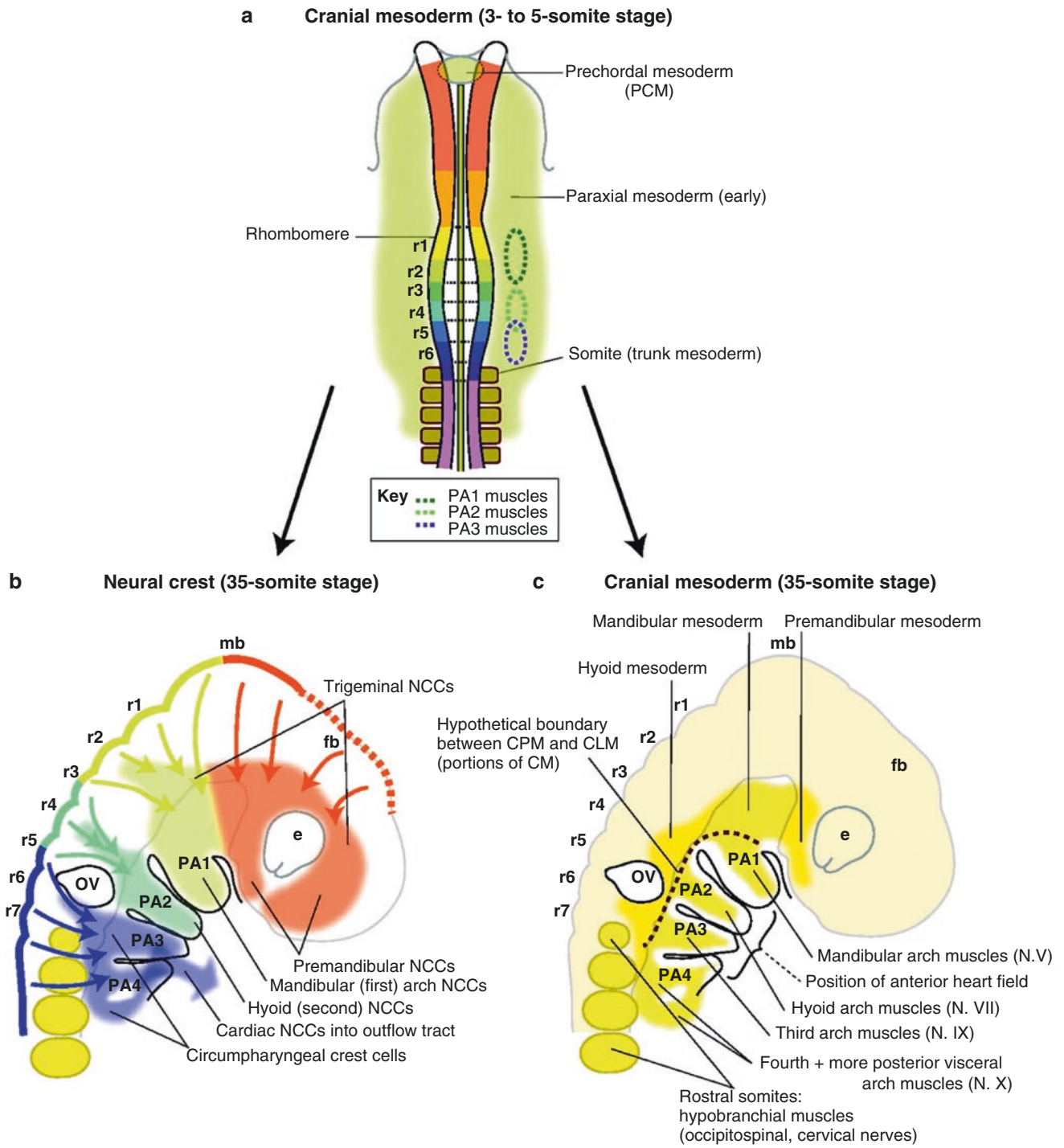

Fig. 2.13 Migration of PAM and neural crest to pharyngeal arches. Note: avian model includes somitomere 7 as the first somite. In mammals this transition occurs at somitomere 8. (Reprinted from Ramkumar Sambasivan, Shigeru Kuratani, Shahragim Tajbakhsh. An eye on the head: the development and evolution of craniofacial muscles. Development 2011;138: 2401–2415. With permission from The Company of Biologists)

The space above it and the skull base, the *sinus of Morgagni*, transmit ascending palatine artery from second arch facial and palatine branch of third arch ascending pharyngeal, thus demarcating a boundary between second and third arch. The cranial base just above it is probably Sm5–Sm6 in register with second arch, while the superior constrictor per se represents myoblasts in register with third arch (Fig. 2.15).

Fig. 2.14 Macrostomia. (Reprinted with permission from Gurgel do Amaral Teles G, Maarques Perfeito D. Surgical correction of unilateral and bilateral macrostoma: case report and review of the literature. *Revista Brasileira de Cirurgia Plástica* 2016; 31(2):273–277)

The third destiny of PAM is to occupy an intermediate state as a somites. Epaxial somite derivatives provide skeletal cover and muscles for the spinal cord. These structures are segmented along rigidly neuromeric lines. Hypaxial somite sclerotomes demonstrate *parasegmentation*. This is most easily recognizable in vertebral column. Each vertebral body is formed from the sclerotome of two adjacent somites. This pattern, in which the cranial half of somite *n* combines with the caudal half of the somite above it, *n* − *1*, is known as *parasegmentation*. For example, the third thoracic vertebra forms from the cranial half of somite T3 and the caudal half of somite T2. This segmentation pattern changes in the skull base. Occipital somites 1–3 are fused and incorporate the rostral half of S4 [38–40].

The occipitocervical junction (OCJ) is a critical evolutionary zone. Fishes have but three occipital somites and no joint between the head and body. Parasegmentation in fishes begins between the third occipital somite and the first cervical somite, i.e., level S3–S4. Tetrapods add an additional somite to the posterior fossa and attach it to three cervical somites. Parasegmentation is pushed backward to the S4–S5 level. In so doing, this tetrapod innovation produces a neck and OCJ zone. The atlas is formed from cervical somites 1

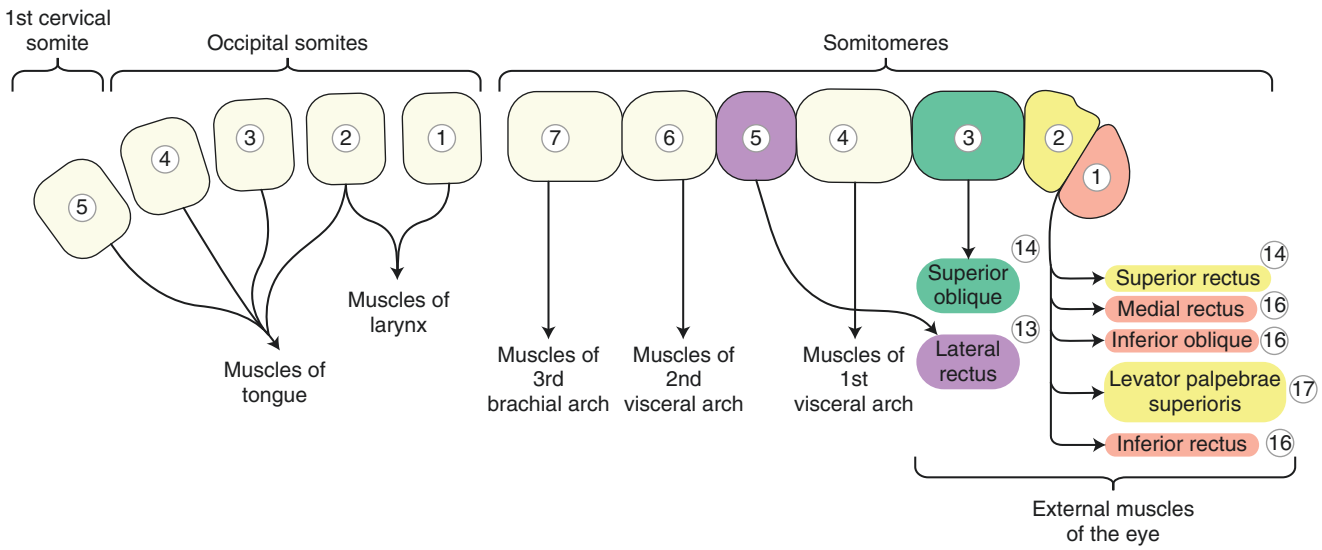

Fig. 2.15 LR/Sm5[13], SO/Sm3[14], SR/Sm2[14], MR/Sm1[16], MR/Sm1[16], IO/Sm1[16], IR/Sm1[16], LPS derived from SR/Sm2[17] First three somitomeres spatially positioned anterior to the notochord and are referred to as *prechordal mesoderm.* Somitomeres 4–5 are positioned at the tip of the notochord. Thus, all are in position to access the globe. Avian model (depicted) has five occipital somites. In mammalian model, with four occipital somites, tongue muscles arise from S1 to S4

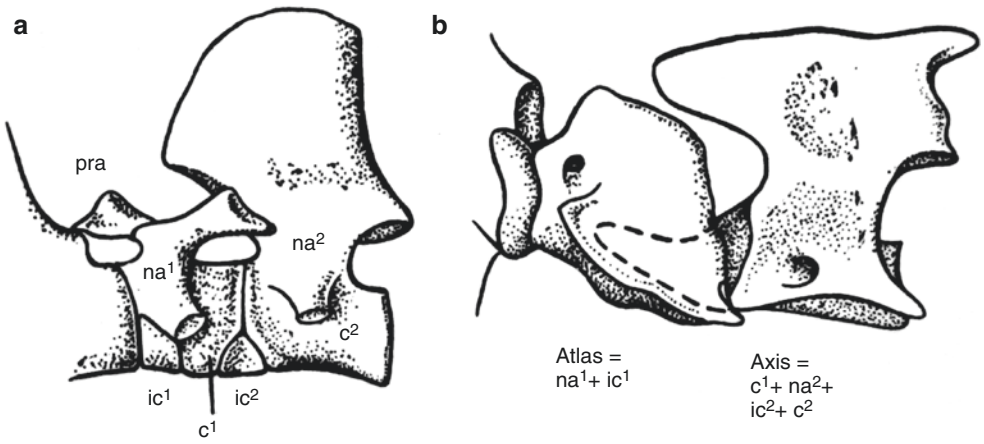

Fig. 2.16 Proatlas (pra) is seen in a primitive reptile (**a**) versus mammal (**b**). Absorption is marked by appearance in mammals of two occipital condyles on the skull base. (Reprinted from Romer AS. Vertebrate Paleontology, 3rd ed. University of Chicago Press; 1956. With permission from University of Chicago Press)

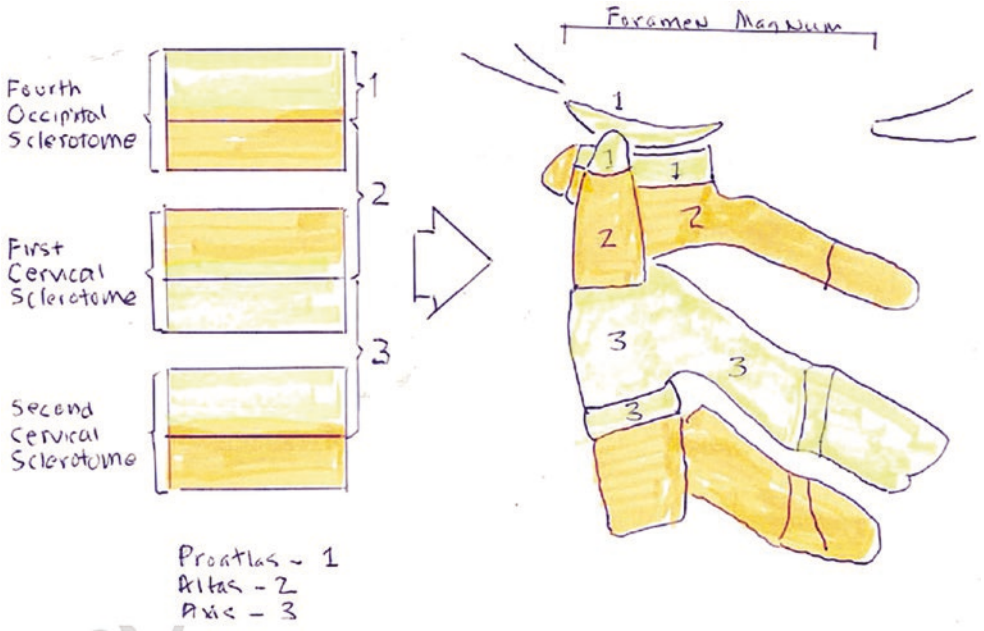

Fig. 2.17 Formation of proatlas. (Courtesy of Michael Carstens, MD)

and 2. The ancient *proatlas* (now incorporated into the foramen magnum) is formed from occipital somite 4 and cervical somite 1 [41] (Figs. 2.16, 2.17, and 2.18).

The sutures of the skull represent distinct segmental field boundaries. Those bones (arising from rhombomeric levels 1–7) do not manifest parasegmentation. The mammalian parietal bone is produced by epaxial PAM from somitomeres 4 and r3–r4 neural crest, while the temporal bone is synthesized from r5 to r6 neural crest and somitomeres 6 and 7. In mammals, PAM from somitomeres 5–7 forms petromastoid. Segmentation from occipital somites 1–4 has been mapped out into a series of concentric rings. The basioccipital, exoccipital, and supraoccipital bones each receive contributions from all four occipital somites. These bones are *composite fields*. Remaining bones of the membranous neurocranium are exclusively neural crest.

Let us digress, for the sake of completeness to the behavior of PAM assigned to the neck, trunk, and extremities. We have seen that, in somites, the lateral dermatome and myotome form the skin and muscles of the body wall and extremities. Because trunk musculature develops in a very straightforward segmental manner, the ventral (hypaxial) motor and sensory nerves that supply it are arranged in a logical, linear, spatial pattern. Muscles such as the external oblique arise from multiple myotomes. Their motor nerves receive contributions from several neuromeres. Sensory nerves, such as the iliohypogastric, reflect multiple dermatomes.

Muscles assigned to the extremities have a different neuroanatomy. They arise from a unique portion of the somitic myotome and undergo complex migratory patterns to seek out their levels of insertion. For this reason, the ventral motor and sensory nerves supplying the limbs are organized into complex "switchyards" called *plexuses*. The topologic arrangement of the roots, trunks, divisions, cords, and branches of each plexus is a *faithful replica of the migratory patterns of the target muscles.*

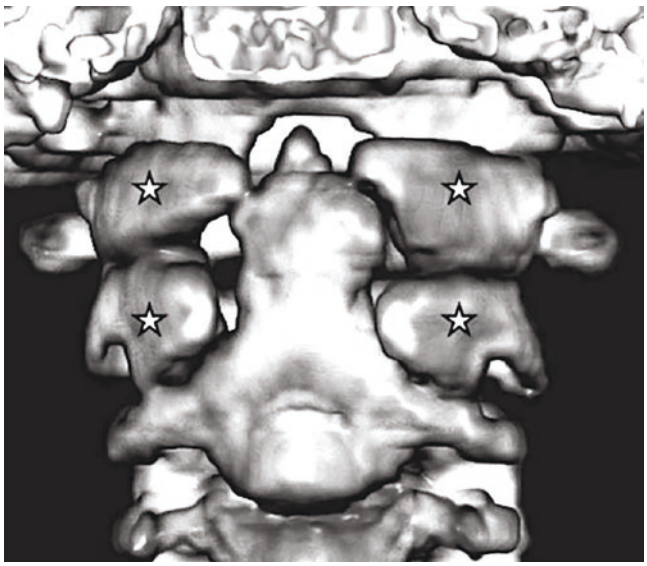

Fig. 2.18 Clinical case of proatlas in 8-year-old boy, anterior view showing the two lateral masses (upper two asterisks) and the dens. Note upper 1/3 of dens belongs to proatlas, lower 2/3 belongs to atlas and axis (although it appears to arise from the axis alone). (Reprinted from Spittank H, Goehmann U, Hage H, Sacher R. Presistent proatlas with persistent segmentation of the craniovertebral junction—the Tsuang-Goehmann malformation. *J Radiology Case Reports* 2016; 10(10):15–23. https://www.radiologycases.com/index.php/radiologycases/article/view/2890. With permission from Journal of Radiology Case Reports)

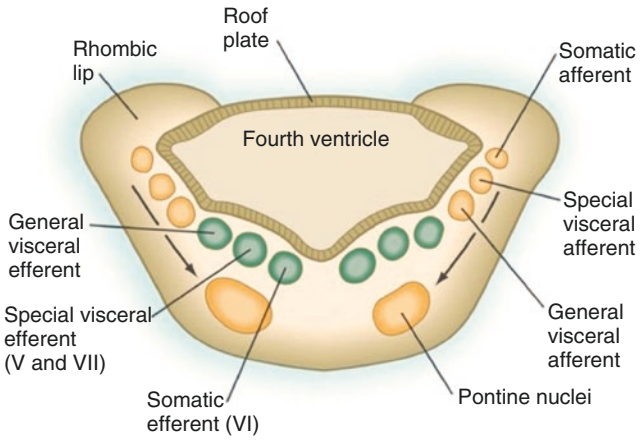

Fig. 2.19 Functional organization of cranial nerves. Medial and lateral motor column. In the brainstem, parasympathetic column, *special visceral efferent*, is interposed between them. (Reprinted from Carlson BM. Human Embryology and Developmental Biology, 6th edition. St. Louis, MO: Elsevier; 2019. With permission from Elsevier)

The muscles of the neck are a mixture of these two models. Its epaxial muscles are strictly neuromeric. The hypaxial muscles, both the vertebral muscles and the strap muscles, derived from the ancient *coracomandibularis* muscle, are supplied by the cervical plexus. We shall deal with the cervical plexus in a later chapter.

Let us refocus on paraxial mesoderm, its organization, and its relationship to the pharyngeal arches. As previously stated, shortly after gastrulation PAM originating from rhombomeres r0–r7, the so-called *head mesoderm*, has three distinct types of derivatives: (1) the *material prima* of cerebral blood vessels, (2) cartilages of the cranial base posterior to the hypophysis, and (3) craniofacial striated muscles.

- With the process of neurulation, as the neural plate rolls up upon itself to form the neural tube, it drags some PAM upward with it. This mesoderm covers the CNS in its entirety, like the paint over a newly constructed house. It provides the angioblasts which will form the *primitive head plexus* which nourished the embryonic brain between stages 6 and 8 until such time as the internal carotid and longitudinal neural arteries develop at stage 9. It explains the presence of the pial plexus. This model of PAM continues to provide all the way down the spinal cord.
- The second product of somitomeric PAM is the *materia prima* of parachordal cartilages and the otic capsule. This mesoderm remains sessile and is located beneath the CNS. Cranial base bones anterior to the hypophysis are neural crest.
- Striated muscles are the third product of head mesoderm. These been mapped to seven individual structures within the head mesoderm, somitomeres, which also appear beginning at stage 7 and are produced at the rate of approximately 4 per day. Recall that by day 25 with the appearance of the 19th somitomere, the process of somitogenesis begins at Sm8 when it is transformed into the first occipital somite. The ultimate destiny of myoblasts within a particular somitomere is determined by the neuromeric level from which the PAM originated and the motor nerve associated with that level. Thus, muscles innervated by the *medial motor column* III, IV, and VI are destined for the eye regardless of the spatial position of the somitomere. All remaining somitomeric muscles are innervated by the *lateral motor column* and supply the pharyngeal arches. It should be noted that craniofacial muscles and their motor nerves migrate into position well after the initial formation of the pharyngeal arches themselves (Fig. 2.19).

Let's look a little more closely into the biologic rationale for the timing of this arch/somite sequence. Once again, we must return to gastrulation. Cells exiting the primitive streak at any given neuromeric level do so in a rigid spatiotemporal sequence [42]. This is seen clearly in the distribution of the various muscle blastema within the pharyngeal arches. We can think of an arch as a "pocket" into which mesodermal cells migrate. The earliest cells to enter travel most distally: *they fall to the bottom of the pocket*. They are vascularized first. Subsequent migrations occupy progressively more

superficial levels of the pocket. When each pocket is full of cells, a finite amount of time has elapsed and a new pocket begins to form at the next most caudal neuromere.

Maturation and migration of cells also follow a timing sequence. The most distal cells of the pocket are the "oldest;" these are more likely to undergo population expansion than more recently arrived cells. If the distal zone of each arch is vascularized first, this transformation will precede that of the proximal population. Thus, *muscle development in the pharyngeal arches follows the spatial-temporal order of blood supply: caudal-to-cranial, deep-to-superficial, and lateral-to-medial*.

In development, the "decision" as to what zone of mesoderm is fated to become lateral plate and what zone will be transformed into paraxial mesoderm is a chemical one determined by gene products expressed in the overlying ectoderm and neural tube. One could think of these chemical signals as radio waves emitted from broadcasting towers located at specific anatomic zones of the embryo. Signals from the ectoderm induce LPMs, from the endoderm LPMv, and signals from the notochord and neural tube induce PAM. Each chemical signal diffuses outward, its concentration decreasing at greater distances from its source. Mesodermal cells closer to the neuraxis will "listen" more attentively to the stronger signals from the midline than to those from the periphery. They will organize first as somitomeres and then, from Sm8 onward, as somites.

In similar fashion, we can consider each somitomere and somite to be made up of distinctive zones, each one reflecting the presence of specific combinations of gene products unique to that zone. This "genetic map" specifies all future structures (dermis, muscle, cartilage, or bone) that will develop from that somitomere. This process is not spatially obvious in somitomeres. They appear as simple balls of cells around a central cavity. The advent of somitogenesis begins at Sm8 (which we all learned in medical school): sclerotome, myotome, and dermatome. But *the final determination of muscle "identity" is determined by signals received once the myoblasts have arrived at their final destination*, be it the eye, the arches, the pharynx, or the tongue.

Genetic zones exist with each pharyngeal arch using a common "street map" of HOX and DLX genes to establish spatial zones of epithelium. These interact with the incoming neural crest cells to create patterns that determine future structures. For example, on either side of the longitudinal axis of the first arch, the same genes are expressed that will determine tooth-bearing fields. Thus, from distal to proximal, maxillary fields of Mx1 (incisors/canines), Mx2 (premolars), and Mx3 (molars) are set directly opposite Mn1, Mn2, and Mn3. Sensory nerves and arteries will be assigned to each of these fields. This provides a *genetic basis for occlusion*. We shall see later that this order determines the eruption of teeth in a very logical sequence (Figs. 2.20, 2.21, 2.22, and 2.23).

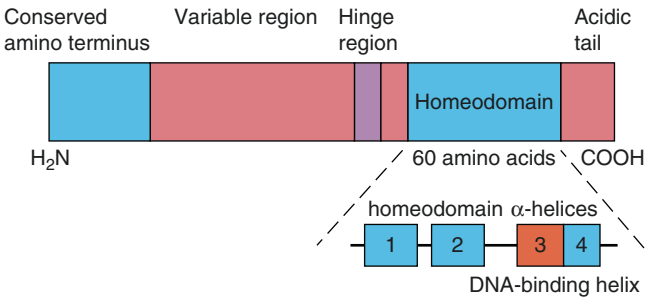

Fig. 2.20 Structure of a homeodomain protein. This highly conserved region contains 60 amino acids that form a DNA-binding helix-loop—helix structure. These are encoded by a180 nucleotide region called a homeobox. Humans contain 39+ *HOX* genes found in four clusters of four different chromosomes. Neuromeres rostral to r3 are encoded by non-Hox homeotic genes. (Reprinted from Carlson BM. Human Embryology and Developmental Biology, 6th edition. St. Louis, MO: Elsevier; 2019. With permission from Elsevier)

In this regard, we should note that *the presence of one blastema determines the physical location of a subsequent blastema*. One muscle cannot displace its predecessor. This is well demonstrated by the four extrinsic muscles of the tongue. These muscles arise from occipital somites 1–4 and their motor has four distinct nuclei from r8 to r11. It is reasonable to assume the muscles arise in cranio-caudal order. Thus, styloglossus migrates from S1, assumes a proximal insertion from stylomandibular ligaments, and a distal insertion into the mucosa along the lateral aspect of the tongue. Chondroglossus, hyoglossus, and genioglossue migrate from S2, S3, and S4, respectively, and insert in progressively more medial positions, with genioglossus occupying the midline (Fig. 2.24).

We conclude this important section by stating that all cells of a particular pharyngeal arch share a common *Hox* gene code with their corresponding neuromeric zone in the central nervous system. However, the development specifics of individual structures are based on a very simple system of cellular age and distance from important sources of gene products produced in surrounding structures.

This system is readily seen in the relative amounts of neural crest material "assigned" to form pharyngeal arches versus occipital somites. As one proceeds caudally, the *relative size* of each pharyngeal arch becomes smaller and smaller compared to its corresponding somite. There is also a change in the type of product produced by the pharyngeal arch mesenchyme. Beginning with the fourth pharyngeal arch, neural crest mesenchyme ceases to be transformed into bone. Instead, it forms cartilage.

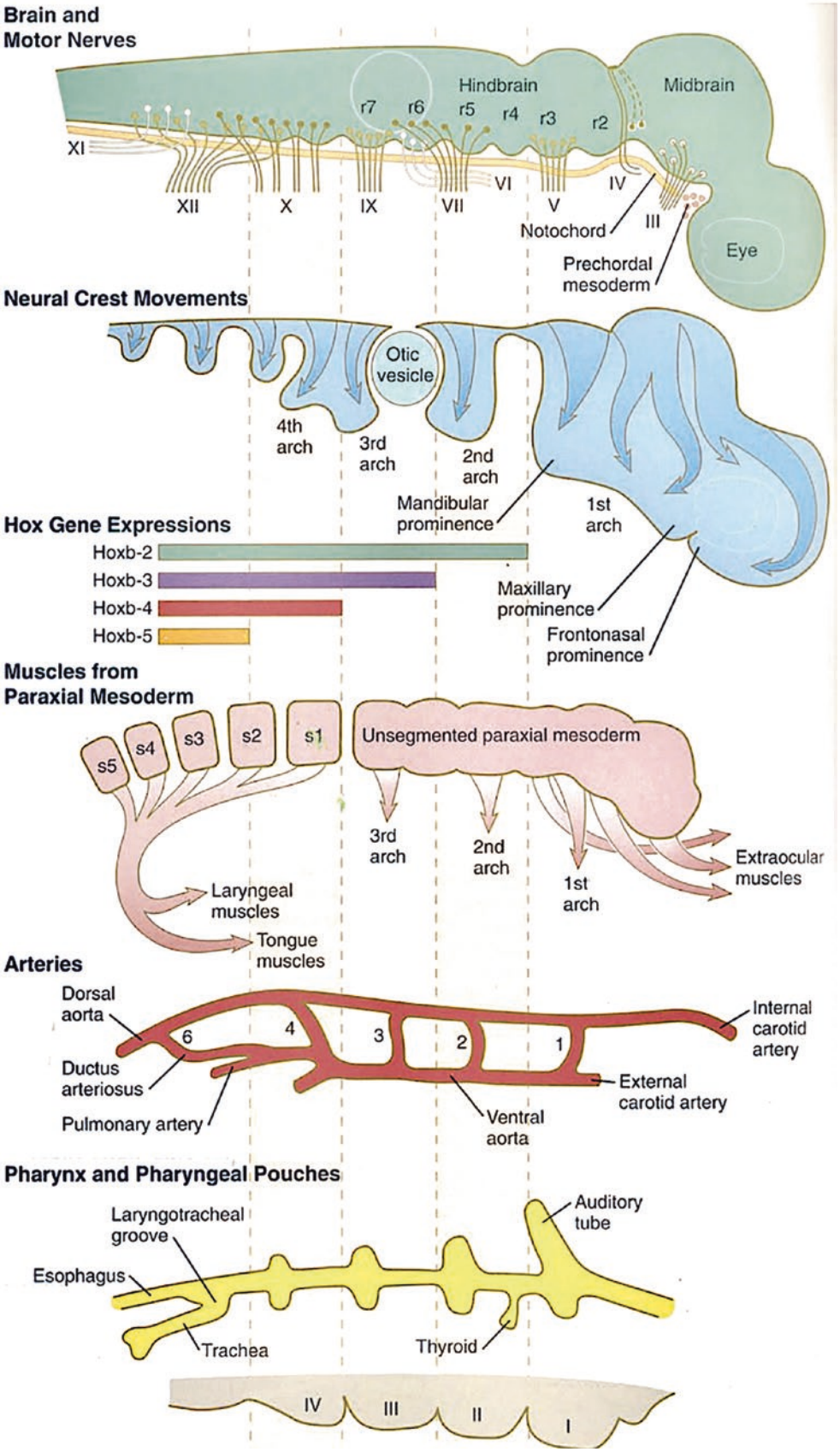

Fig. 2.21 Lateral view of organization of head and pharynx of a 30 day old human embryo with individual tissue components in register. The identity of germ layer derivatives with respect to the neuromeric level or origin is maintained throughout ontogeny. Unsegmented head mesoderm divided into seven somitomeres (not depicted here). Homeotic genes of Hox series encode from r3 caudal, while neuromeres from r2 rostral are encoded by non-hox homeotic genes. Patterns of gene expression in relation to neuroanatomic landmarks in early mammalian embryo. Bars define craniocaudal limits of expression for gene products. Cranial sensory nerves derived from neural crest and placodal precursor are laid out in proper register. *CRABP* cytoplasmic retinoic acid-binding protein, *RAR* retinoic acid receptor. **Grand generalization** (1) All pharyngeal arches are in register with pairs of rhombomeres. (2) Motor control and general sensory perception for pharyngeal arch structures are in strict neuromeric register with the brainstem via the lateral motor column and the lateral sensory column. Neurons dedicated to a specific arch may arrive at their destination either directly or indirectly, using a different nerve to gain access. (3) ***Pharyngeal arch structures should be classified, not by the individual nerves that supply them, but by the neuromeres which supply the neurons in the first place.*** (Reprinted from Carlson BM. Human Embryology and Developmental Biology, 6th edition. St. Louis, MO: Elsevier; 2019. With permission from Elsevier)

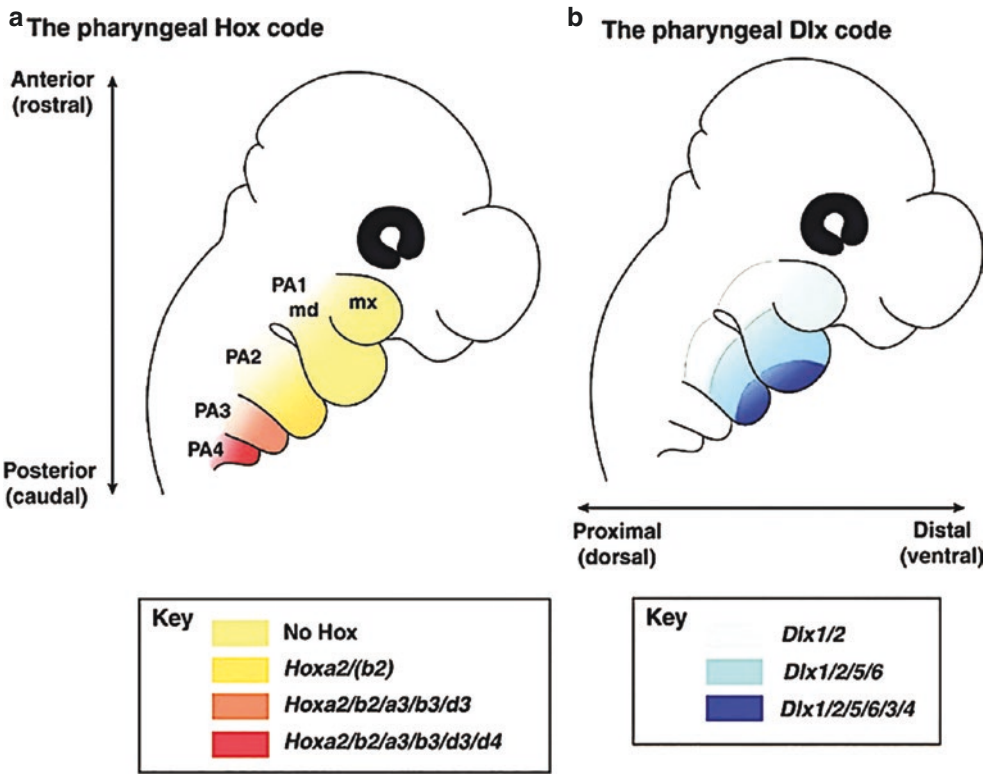

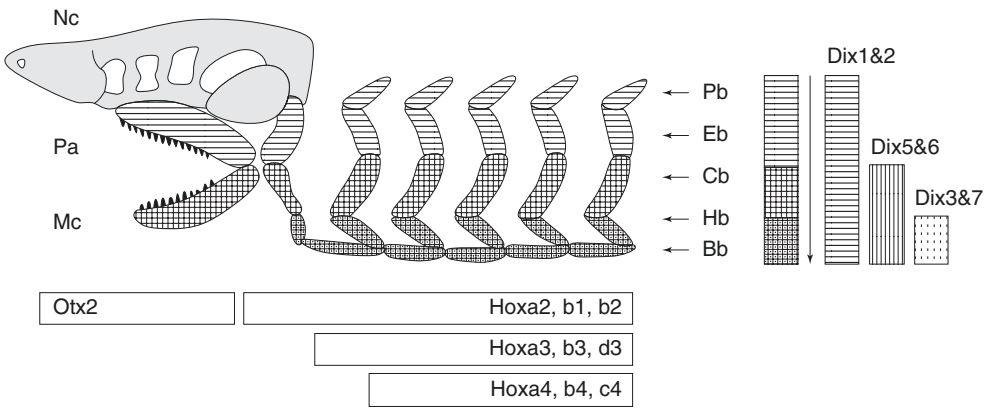

Fig. 2.22 (**a**) Hox vs. (**b**) Dlx system. Universal system of Dlx genes defines anterior-posterior zones of pharyngeal arches. (Reprinted from Minoux M, Rijli FM. Molecular mechanisms of cranial neural crest cell migration and patterning in craniofacial development. Development 2010; 137: 2605–2621. With permission from The Company of Biologists)

Fig. 2.23 Dlx system Note the neural crest cartilage components of the branchial arches. In humans, these are recapitulated in the formation of bone of second, third, and fourth arches. *PB* prebranchial, *EB* epibranchial, *CB* ceratobranchial, *HB* hypobranchial, *Bb* basibranchial, *NC* nasal cartilage, *Pa* palatoquadrate cartilage, *Mc* Meckel's cartilage. Note that the homeotic coding of first pharyngeal is based, not on Hox genes, but on Otx genes. (Reprinted from Olsson L, Ericsson R, Cerny R. Vertebrate head development: Segmentation, novelties, and Homology. Theory in Biosciences. 2005 124(2): 143–163. With permission from Springer Nature)

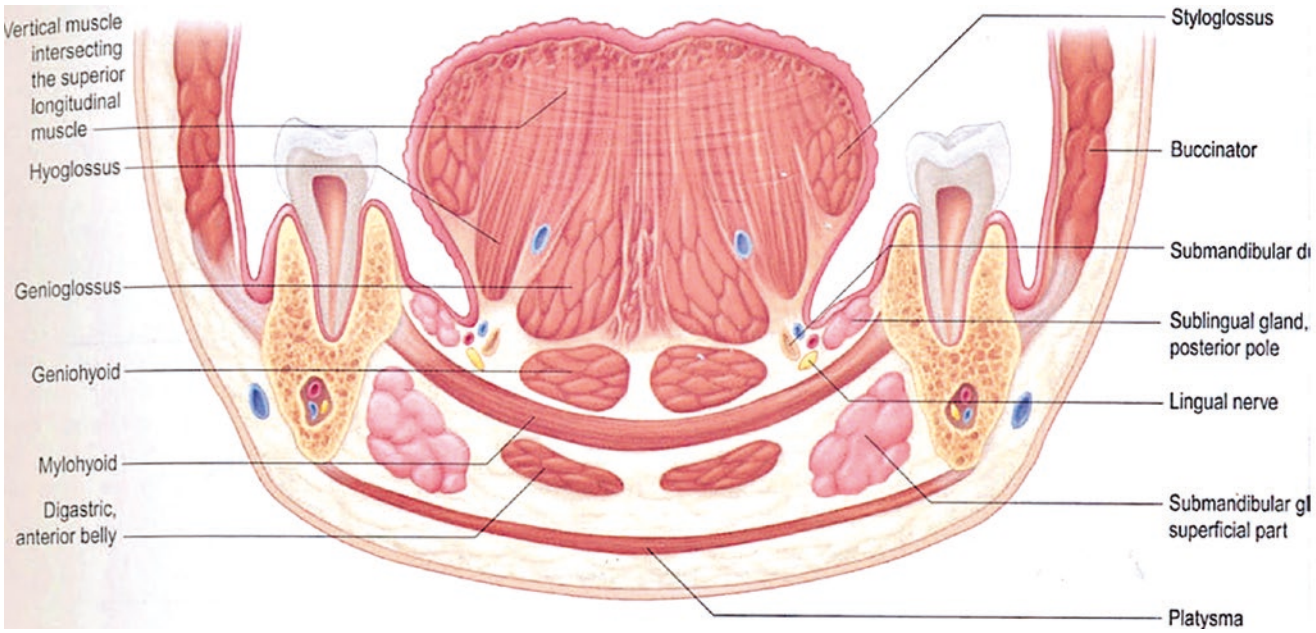

Fig. 2.24 Stacking of the muscles of the tongue. Lateral to medial: styloglossus (S1), hyoglossus (S2), chondroglossus (S3), genioglossus (S4), thus matching the four motor roots of hypoglossal nerve. (Reprinted from Standring S (ed). Gray's Anatomy: The Anatomic Basis of Clinical Medicine, 40th ed. London, UK: Churchill Livingstone; 2008. With permission from Elsevier)

Table 2.2 Derivatives of pharyngeal arches

Pharyngeal arch	Rhombomere/ nerve	Derivatives
First (mandibular)	r2–r3/V2, V3	Maxilla complex, mandible
First (mandibular)	r2–r3/V3	Non-jaws, mastication
Second (hyoid)	r4–r5/VII	Mastication, animation
Third (glossopharyngeal)	r6–r7/IX, X	Sup constrictor, palate
Fourth (pharyngolaryngeal)	r8–r9/X	Middle constrictor, larynx
Fifth (internal laryngeal):	r10–r11/X	Inferior constrictor

Blood supply: (1) external carotid, (2) stapedial

Fate of Pharyngeal Arch PAM (Table 2.2)

The Mammalian System of Pharyngeal Arches

The pharyngeal arches, numbering five in mammals, appear during embryogenesis between stages 10 and 15 and represent a transient stage in the development of the head and neck. Each arch consists of a mesenchymal core of hindbrain neural crest from paired rhombomeres, surrounded by a discrete epithelium. The arches are situated between the body wall above and the aortic outflow tract that was tucked at stage 9 to lie immediately ventral to the future pharynx. Running the core of each arch is an aortic arch artery spanning from the aortic outflow tract ventral to the future pharynx and the dorsal aorta running along the axis of the embryo. The arteries are constructed from angioblasts that invade from lateral plate mesoderm, from which develops a tube of endothelial cells that subsequently recruit surrounding neural crest to form pericytes that ensheath the vessel.

We have previously pointed out the fallacy of the sixth pharyngeal arch. Its components are in register with r10–r11. Aortic arch 6 is unlike its predecessors. It forms as two distinct plexuses, one from the dorsal aorta and the other from the outflow tract. The ventral plexuses extend into the future pulmonary anlagen. On the left side only, a transient connection exists between outflow tract and dorsal aorta; this forms ductus arteriosus. The components of these vascular struc-

tures are in register with r10 and r11, but there are no epithelial structures or neural crest populations associated with these vessels.

Fifth arch does indeed exist but is vestigial. Because fifth aortic arch either disintegrates or fails to form, it is dependent for its survival upon the blood supply to fourth arch, superior thyroid artery. fifth arch neural crest from r10 to r11 is a putative source for cricoid cartilage and the inferior fibers of inferior constrictor (cricothyodeus).

The rhombomeres that are the source of neural crest are even-odd pairs with the even-numbered rhombomere being cranial. Within the arch, neural crest is organized into topographic sectors by a system of *distal-less* (*Dlx*) genes. In knock-out experiments conducted on the first arch, genetic expression in the distal zone affects the mandible, while those causing disturbances in the proximal zone affect the maxilla. Myoblasts for each arch arise from a discrete somitomere, immediately invade the mesenchyme, and are distributed to Dlx-determined compartments as well [36, 43].

Evolutionary Considerations

The evolutionary design of pharyngeal arches follows the neuroanatomic organization of the basal gnathostome. Early agnathic fishes had, in general, 8 branchial arches, all of which were respiratory. However, in some primitive armored fishes (placoderms), up to 15 branchial arches have been identified. This is an intriguing detail. If we assume two neuromeres per arch, this means that in mammals, the primitive genetic marker for arch production could extend back to somite 24, i.e., the t12–11 junction between thorax and abdomen. A 9-arch system in humans would extend up to and including neuromere c8. More modern jawless craniates are represented today by hagfishes and the slightly more advanced lampey eel, *Petromyzon marinus*. They have a total of seven arches which, in humans, would encompass neuromeric levels r2–c4. As we shall see, descent of the thymus along pretracheal fascia can lead to ectopic locations as far distal as the pericardium (level c4).

The earliest chondricthyan (represented today by sharks) modified the seven-arch system, converting the first two branchial arches into jaws and hyoid structures capable of providing support. This brings the total number of respiratory branchial units to 5. An external carotid artery developed to supply the lower jaw. *The conversion of neural crest from gill structures to jaws was accompanied by the invention of the stapedial system.* Osteicthyces (bony fishes) lost the seventh arch, so assume a 2 + 4 system. Tetrapods further modified this to 2 + 3 configuration (two arches for the jaws and additional visceral arches) (Fig. 2.25).

Examination of the original gnathostome model is very instructive. Arches 1 and 2 have been modified to form jaws and arch 3–7 are respiratory The primitive gill arch (branch)

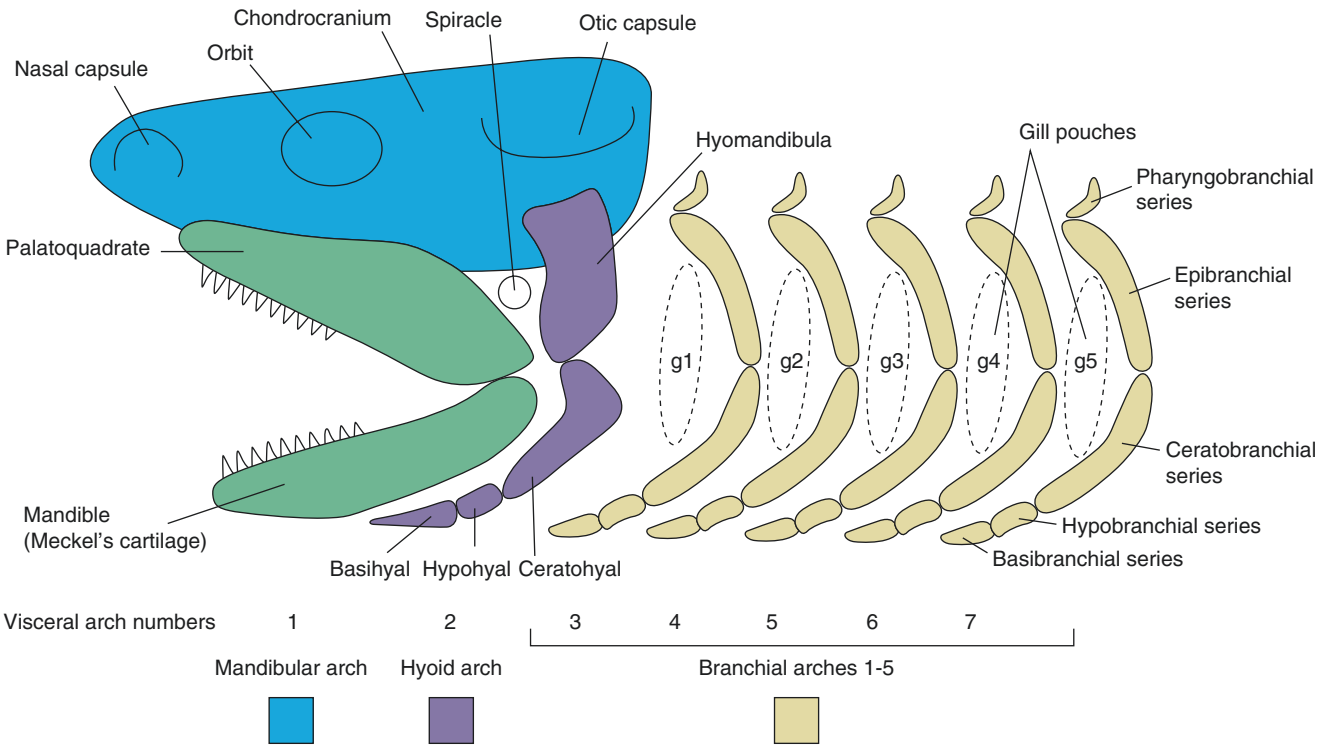

Fig. 2.25 Head segmentation. Jawless fishes: 7 respiratory arches (in primitive forms, up to 15). Cartilagenous fishes: 2 + 5 respiratory arches. Bony fishes: 2 + 4 respiratory arches. Tetrapods: 2 + 3 pharyngeal arches. (Courtesy of William E. Bemis)

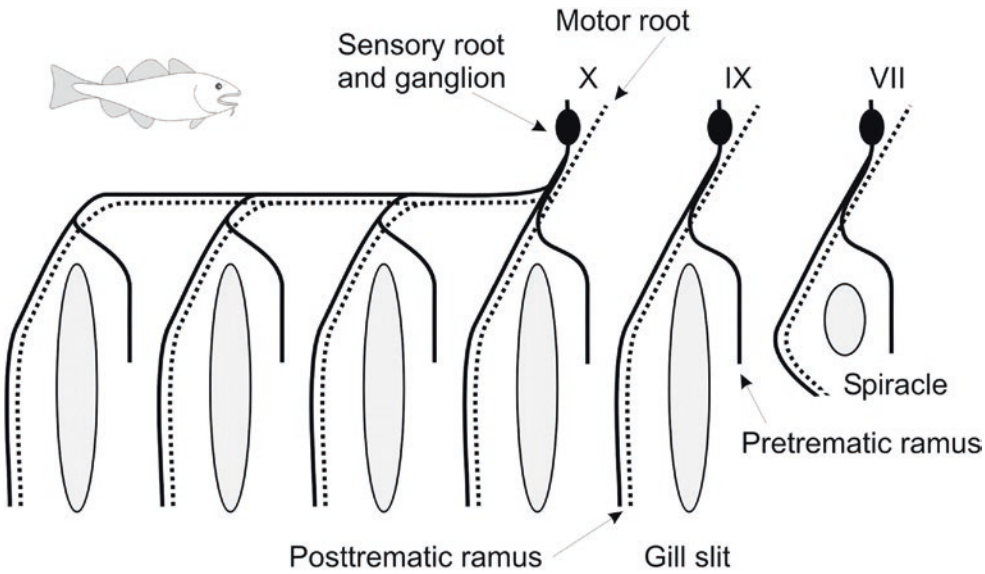

Fig. 2.26 Innervation of branchial arches. Sensory nerves are both pretrematic and posttrematic. Motor nerve is posttrematic and accompanies the aortic arch artery in the posteromedial quadrant. (Reprinted from Evans DH, Piermarini PM, Choe KP. The Multifunctional Fish Gill: Dominant Site of Gas Exchange, Osmoregulation, Acid-Base Regulation, and Excretion of Nitrogenous Waste. Physiol Rev. 2005;85(1):97–177. With permission from The American Physiological Society)

consists of anterior and posterior walls surrounding a gill slit. Each branch is supplied by a mixed motor and sensory nerve that emanates from a ganglion. *The dorsal part of the ganglion is placodal and the ventral part is placodal*. This neuroanatomy exists to this day. As the nerve approaches the gill slit, it branches into three functional parts: (1) a deeply placed *sensory nerve to the pharynx*, (2) a *pretrematic sensory nerve*, and (3) a *postrematic sensory-motor nerve*. The main cranial nerve for each banchiomere is located in the caudal zone of the arch [44, 45].

Reconfiguration of branchial arch structures is seen in the asymmetry of the pharyngeal arch. The gill slit is gone, but is replaced by the pharyngeal pouch. Cross-section of the branchiomere shows four quadrants. The endodermal side has branchiomeric muscle anterior and the skeletal rod posterior. The ectodermal side has the cranial nerve anterior and the aortic arch artery posterior (Figs. 2.26 and 2.27).

In the mammalian example, spatial asymmetry is reflected in the timing with which various anatomic structures make their appearance. This depends upon how quickly they are vascularized. Hypothetically, the aortic arch artery develops from below upwards. Tissues that are distal and caudal are more efficiently supplied. The mandible (r3) forms before the maxilla (r2). Malleus (r3) appears before incus (r2).

Let's take a closer look at the two ear bones. The malleus is a homolog of the *articular*—a dermal bone (neural crest) that ensheaths the proximal end of *Meckel's cartilage* (mandible). Thus, the malleus is an r3 derivative. In fishes, the primitive *palatoquadrate cartilage* of the upper jaw is the analog of Meckel's cartilage because the maxilla will be constructed around it. It has three components seen in the acanthodian skull. Of all jawed fishes (gnathostomes), the acanthodians have the earliest fossil record. The anterior palatoquadrate is known as the *autopalatine cartilage*. This provides the basis for the maxilla and palate. Immediately behind is the *metapterygoid (epipterygoid) cartilage*, the future template for the alisphenoid bone. Most posterior is the *quadrate cartilage*. This is the origin of the incus. Not surprisingly, it is anchored to the *prootic* temporal bone. Hence, the incus (an r2 derivative) lies internal to the malleus (an r3 derivative). Malleus forms before incus (Fig. 2.28).

The same pattern obtains to derivatives of the second and third arches. Facial muscles develop in an absolutely stereotypical manner: from ventral to dorsal, deep to superficial, and lateral to medial [46]. It is logical to "assign" the muscles of the upper division of the facial nerve in r4 and those of lower division to the nucleus of VII in r5. The source for the upper half and lesser cornu of the hyoid and the styloid process should be r5 neural crest. The hyoid appears well before the styloid, but the latter is attached to the temporal bone. Future work with labelling should tease out these spatiotemporal relationships.

Do somitomeres produce any derivatives prior to being transformed into somites? As previously stated, Sm1–Sm11 are closely applied to the cranial base. They interact with lateral plate angioblasts to produce the *primitive vascular tubes* that will later become the internal carotid and vertebrobasilar arteries. In particular, Sm8–Sm11 produce the caudal longitudinal neural arteries that extend downward from cranial nerve 6 to the foramen magnum. The muscles of the larynx have been traced to somitomeres 8–9. They are not classified as somatic structures. Once Sm8–Sm11 become somites, they make use of somite subdivisions (dermatome, myotome, and sclerotome) to make *non*-pharyngeal arch structures, such as tongue muscles, sternocleidomastoid, and trapezius.

In sum, prior to their conversion into somites 1–4, somitomeres 8–11 produce perineural vasculature and myoblasts

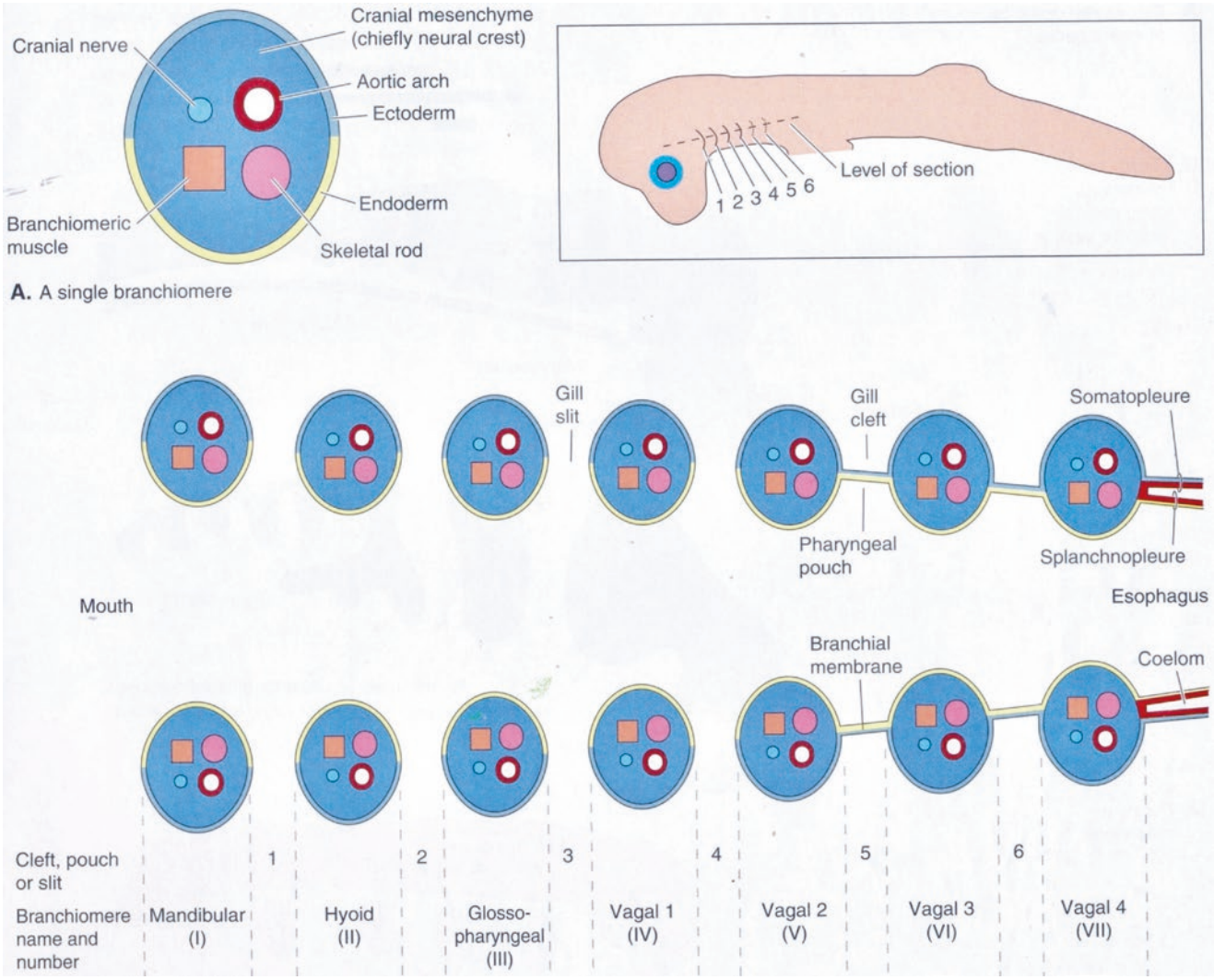

Fig. 2.27 Petromyzon seven-arch system showing the asymmetric position of the artery. Vascularization sequence of the pharyngeal arches likely determines the developmental maturation sequence of arch muscles. (Courtesy of William E. Bemis)

dedicated to pharyngeal arches 4–5. Once out of the head region, paraxial mesoderm in its somitomeric state from Sm12 caudally could potentially provide immediate vascular coverage for the future spinal cord. All further derivatives, including dura, will develop from specific regions of the somite.

Do somitomere and somites have any effect upon neural crest migration routes into the arches? The answer is no; however, there are selective routes by which migration takes place. *Although neural crest cells are produced at each neuromeric level, they appear to migrate out from only even-numbered rhombomeres*. Thus, all neural crest migration into PA1 proceeds via r2, migration into PA2 proceeds via r4, and migration into PA3 proceeds via r6. The pattern is disrupted for the fourth arch as it receives neural crest directly from r8 to r9 (Fig. 2.29).

Some investigators postulate that something "goes wrong" with neural crest cells at odd neuromeric levels. But this flies in the face of evidence regarding programming of neural crest that is neuromere-specific. For example, neural crest cells with the *hox* gene "tattoo" of r3 are never found in the maxillary part of first arch. If one transplants r3 neural crest cells into the proximal portion of PA1, two mandibles are produced. So the selective pathways are "permissive" routes by which neural crest from odd-numbered rhombomeres is forced to migrate with its even-number predecessor.

At this juncture, we have a clear picture of how a pharyngeal arch is constructed. Furthermore, we can "assign" individual bones and muscles to neural crest and PAM from specific neuromeric levels. Kjaer and her coinvestigators painstakingly catalogued the order of appearance of craniofacial bones. When one applied neuromeric mapping to these

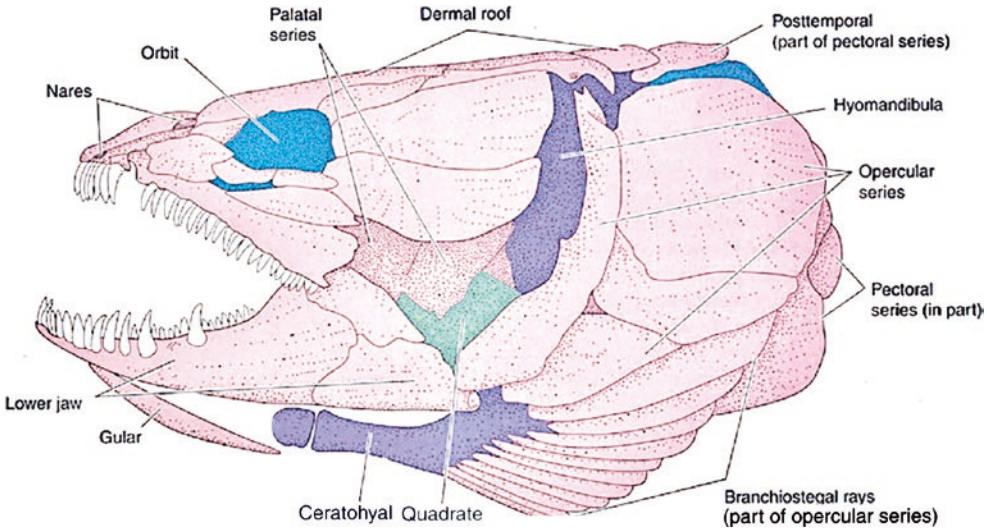

Fig. 2.28 *Amia* skull: palatal series. Anterior part of palatoquadrate ensheaths the maxilla followed by entopterygoid, ectoptyerygoid, metapterygoid, then quadrate. (Courtesy of William E. Bemis)

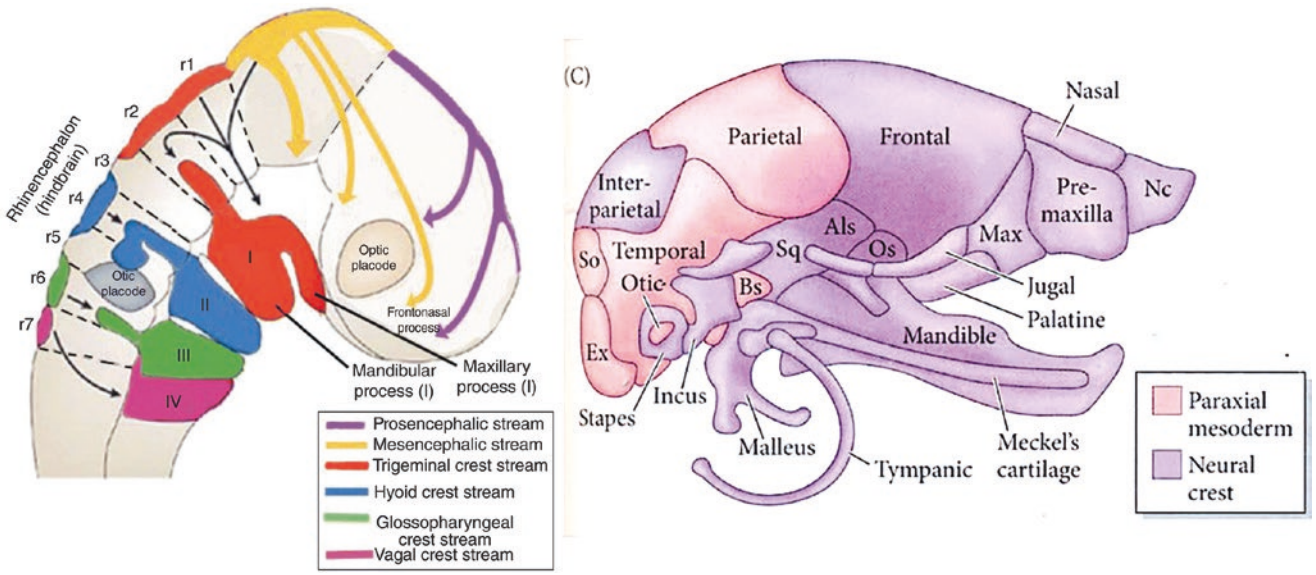

Fig. 2.29 Cranial neural crest migration routes and derivatives. Note that neural crest from r0 to r1 and m1 to m2 acts in concert to populate the frontnasal and periorbital zones. Note that PNC creates the frontonasal skin cover. Neural crest bone map shows interparietal as an "island" between paraxial mesoderm bones. (Left: Reprinted from Carlson BM. Human Embryology and Developmental Biology, 6th edition. St. Louis, MO: Elsevier; 2019. With permission from Elsevier. Right: Reprinted from Gilbert SF, Barresi M. Developmental Biology, 11th ed. Sinaurer: Sunderland, MA, 2016. Reproduced with permission of the Licensor through PLSclear)

structures, the initial results often appear contradictory and confusing. If the maxilla comes from level r2 and the mandible from r3, why should mandibular structures appear first? Why should dental development follow a mesial-to-distal plan? What sense can be made of these patterns?

Vascularization of the Pharyngeal Arches: Nutritional Basis of Derivatives

Lateral plate mesoderm is the primary source for angioblasts in the developing embryo, constituting more than 90% of the LPM cell population. They are highly invasive and populate the surrounding tissues with angioblasts in all directions as soon as gastrulation occurs at stage 7. As the LPM spreads out, its anterior-most population occupies a position forward from the future brain, anterior to prechordal plate mesoderm and to the buccopharyngeal membrane. This zone is known as the primitive heart field. At the same time, LPM angioblasts invade paraxial mesoderm to create the major intraembryonic vessels such as dorsal aortae, the head plexus, and primitive hindbrain channels. At stage 9, head folding at the mesencephalic flexures forces the heart field and its accompanying LPM angioblasts into a position just ventral to the developing pharyngeal arches. This puts LPM angioblasts associated with the aortic outflow tract in direct opposition to

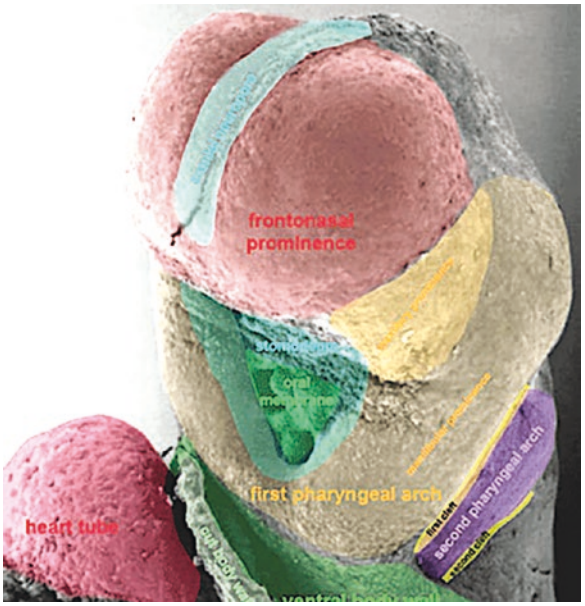

Fig. 2.30 Stage 11–12 Closure of rostral neuropores. First and second pharyngeal arches fully developed with third arch in formation. Note buccopharyngeal membrane (green). Oral ectoderm (blue-green) leading back to BPM is r2–r3 with no expression of second arch ectoderm (purple) in the oral cavity. On the surface, first arch ectoderm will cover over the second arch back to the exernal auditory meatus. (Courtesy of Prof. Kathleen K. Sulik, University of North Carolina)

those found in the vicinity of the dorsal aortae. From these two opposing sources, blood vessels bud outward, migrating toward each other through the intervening neural crest mesenchyme of the pharyngeal arches. The result of this process is the production of a succession of aortic arch arteries beginning with at stage 10 with AA2 (Figs. 2.30 and 2.31).

Successive sprouting of aortic arches from the heart occurs in a strict spatiotemporal sequence [47–51]. Recall that at stage 8, just prior to embryonic folding, the primitive heart is located in front of the forebrain in the anterior most aspect of the embryonic disc. The proximal atrial ends of the primitive heart are connected to the vitelline, umbilical, and cardinal veins, while the distal outflow tract is connected to the dorsal aortae. Pharyngeal arch formation begins at stage 9, with the folding of heart from the anterior aspect of the embryonic disc in front of the forebrain to a new position beneath the future mouth and pharynx. When this takes place, the heart dorsal aortae are dragged downward and backward, creating, passively, paired first aortic arch arteries. During stages 10–12, the ventricular outflow tracts give off an additional aortic arch artery, each one supplying a pharyngeal arch. The fifth aortic arch involutes leaving PA5 dependent upon AA4 for survival. The sixth aortic arches dedicated to the pulmonary circulation appear at stage 14

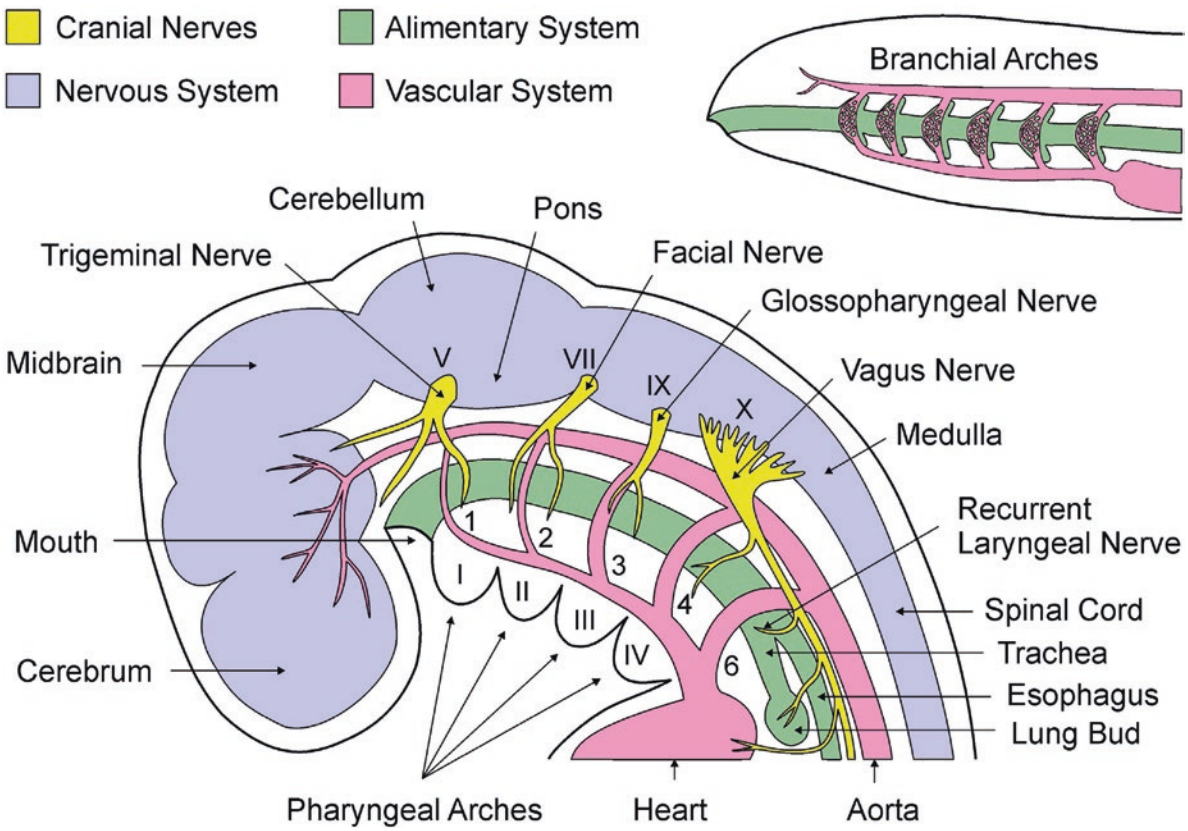

Fig. 2.31 Pharyngeal arches in tetrapods versus fishes. AAs are transient—they unite the ventral aortic outflow tract with dorsal aortae and then undergo extensive remodeling. AA5 involutes—its target, PA5 is supplied by AA4. AA6 assigned to pulmonary circulation There is ***no*** *sixth pharyngeal arch* in tetrapods. (Reprinted from Carlson BM. Human Embryology and Developmental Biology, 6th edition. St. Louis, MO: Elsevier; 2019. With permission from Elsevier)

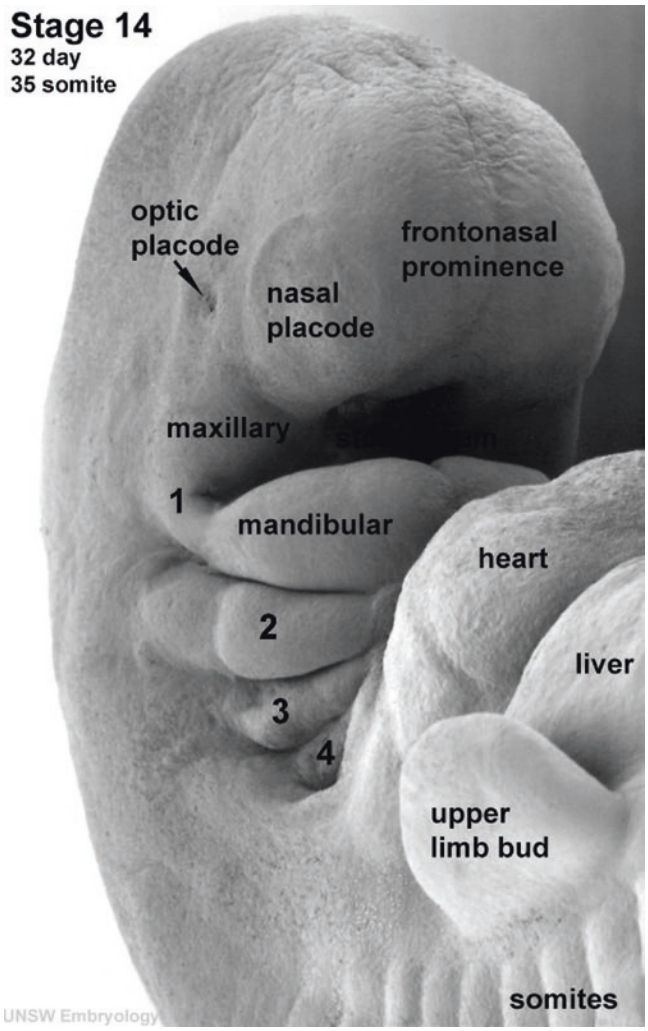

Fig. 2.32 Pharyngeal arches, stage 14: Arch synthesis (stages 9–14) now complete. Arches not melded together; rearrangement begins at stage 15. First cervical somite (S5) barely visible (next to UNSW Embryology). Occipital somites fused and not seen. (Courtesy of Prof. Kathleen K. Sulik, University of North Carolina)

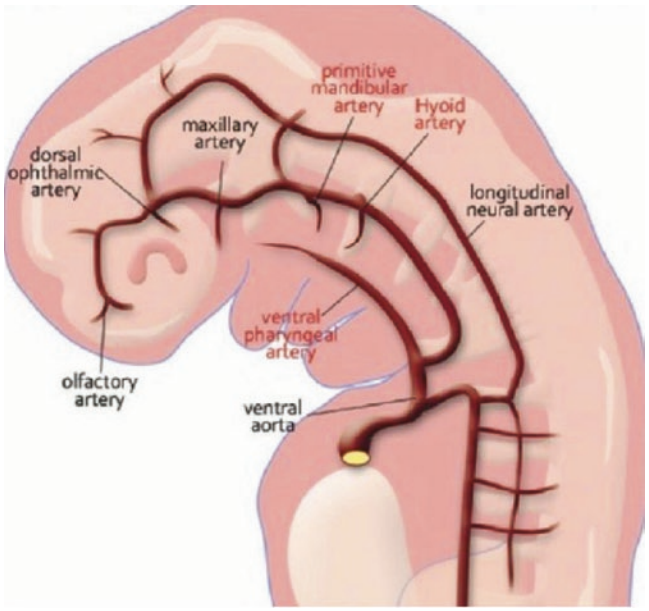

Fig. 2.33 Schematic drawing of embryonic vascular system at stages 14–15 immediately prior to initiation of the stapedial system. Third and fourth arches are present, primitive internal carotid supplies optic vesicle first, via the primitive maxillary and now, at stage 14, by primitive dorsal ophthalmic. (This causes PrMax to be re-directed to the hypophysis.) At stage 12, Internal carotid has joined the longitudinal neural arteries hindbrain channels at the midbrain-hindbrain junction. Segmental arteries such as trigeminal become unnecessary and involute. Obliteration of AA1 and AA2 leaves behind dorsal remnants, mandibular and hyoid arteries, respectively. The first three arches are supplied by ventral pharyngeal artery which originates from the base of the truncus arteriosus in the segment common to both AA3 and AA4. It will morph to external carotid in the next stage. At stage 15–16, hyoid artery gives off the stem of stapedial, sending it upward into tympanic cavity. (Reprinted from Tanoue S, Kayoso H, Mori H. Maxillary Artery: Functional and Imaging Anatomy for Safe and Effective Transcatheter Treatment. Radiographics 2013; 33(7) 209–229. With permission from the Radiological Society of North America)

and the pharyngeal arch period of embryonic development comes to an end by stage 15 (Figs. 2.31 and 2.32).

During the aortic arch period, each successive stage leads to a reconfiguration of the system. In the process of melding first arch and second arch together, their respective aortic arch arteries disintegrate, with blood supply being reestablished from extracranial stapedial and the external carotid system. Paired AA3s create the extracranial segment of internal carotid. The AA4s give rise to the right subclavian artery, but only the left side persists as a segment of aortic arch from which left subclavian arises.

In this process, three remnant arteries deserve mention. Cranial to AA1, the primitive internal carotid gives off the misnamed *primitive maxillary artery*. This vessel constitutes the initial supply for the developing eye, but with the advent of the definitive ophthalmic artery primitive maxillary is subsequently reconfigured as the *inferior hypophyseal artery*. When AA1 breaks down, it leaves behind a *primitive mandibular artery* dangling from the dorsal aortae. This vessel involutes. The breakdown of AA2 also gives a dorsal remnant, one that will have an important future. *Hyoid artery* gives off the all-important *stapedial* system which will supply the dura, orbit, and jaws (Fig. 2.33).

The exact anatomic manner in which the outflow tract from the heart supplies the pharyngeal arches is remarkably simple and elegant. Diagrams in books based on the gill arches of fishes are quite misleading. A typical illustration depicts a core artery running up the center of each gill arch in ventral-dorsal fashion to anastomose with the dorsal aorta. How might this happen? One never sees a central vascular core running through the axis of a muscle. Instead, arteries and motor nerves travel in the interstices between muscles, i.e. they follow fascial planes. Each muscle unit is penetrated from without by a nerve. *The arterial supply is derived by induction from the nerve via VEGF* [52]. The arterial supply of the arch arises when neural crest Schwann cells cause the surrounding mesoderm to create a vascular conduit.

In the head and neck, all muscles are surrounded by fascia, derived exclusively from neural crest cells. As neural crest cells spread over each pharyngeal arch, they penetrate the PAM via natural cleavage planes separating genetically myoblast populations. Spatial relationships among the fascial planes reflect the order of development of the muscles. Furthermore, the relative positions of motor neurons in the neural plate (and neural tube) faithfully replicate the spatial location of their muscle "targets". Muscles close to the vertebral axis such as the paraspinous group are classified as *epaxial*. Their motor neurons lie close to the midline in the *medial lamina of the medial motor column* (MMCm). Muscle groups hypaxial to the midline but not assigned to the extremities have neurons in the *lateral lamina of the medial motor column* (MMCl). Muscle groups of the extremities have motor neurons still more laterally located in the neural plate. These form the lateral motor column. Ventral muscles of the limbs are supplied by neurons from the LMCm. Dorsal muscles of the limbs are supplied by neurons from the LMCl. All motor nerves to striated muscles use Schwann cells for axonal insulation. These Schwann cells are of neural crest derivation. *Because neural crest defines the fascial planes between muscles, it is logical that all neurovascular structures make use of these planes in order to access their target muscles*.

The spatiotemporal order of appearance of muscles within the pharyngeal arches has a great deal to do with blood supply. The overall pattern is ventral to dorsal, caudal to cranial, and medial to lateral (in that relative order). Muscle development requires metabolic activity; this in turn requires blood supply. Thus, ***the order in which muscles develop within a pharyngeal arch reflects the pattern of the arterial development to that arch***.

Hypothetical Model of Vascular Development

The heart and outflow tract are rapidly embraced by pharyngeal arches filled with neural crest. From stages 10–14, stems appear simultaneously from both the outflow tract and the dorsal aorta. These follow the core of the pharyngeal arches and unite to create pharyngeal arch arteries. Muscles within the arches are vascularized in a fixed order, depending on their location. This pattern, in turn, determines the temporal and spatial order in which they appear.

Important deductions about the neuromeric basis of the intracranial arterial system can be made from a careful analysis of dural innervation. The meninges consist of *leptomeninx*, the pia mater and arachnoid, and *pachymeninx*, the dura. The leptomeninges are exclusive neural crest structure created by the immediate migration of local neural crest. They are admixed with PAM with forms of the blood vessels found between pia and arachnoid. Pachymeninx covers only the prosencephalon and cerebellum. Intracranial dura is a neural crest tissue. Below the tentorium cerebelli, the midbrain and hindbrain are covered only by pia and arachnoid. The innervation of the entire prosencephalic dura comes from V1 to V3 with small contributions from VII and IX (via X) to the basisphenoid/basioccipital. The periosteum covering the bones of the middle cranial fossa arises from PAM, but shares a common innervation because second and third arches sensation is routed exclusively to the trigeminal nucleus (Fig. 2.34).

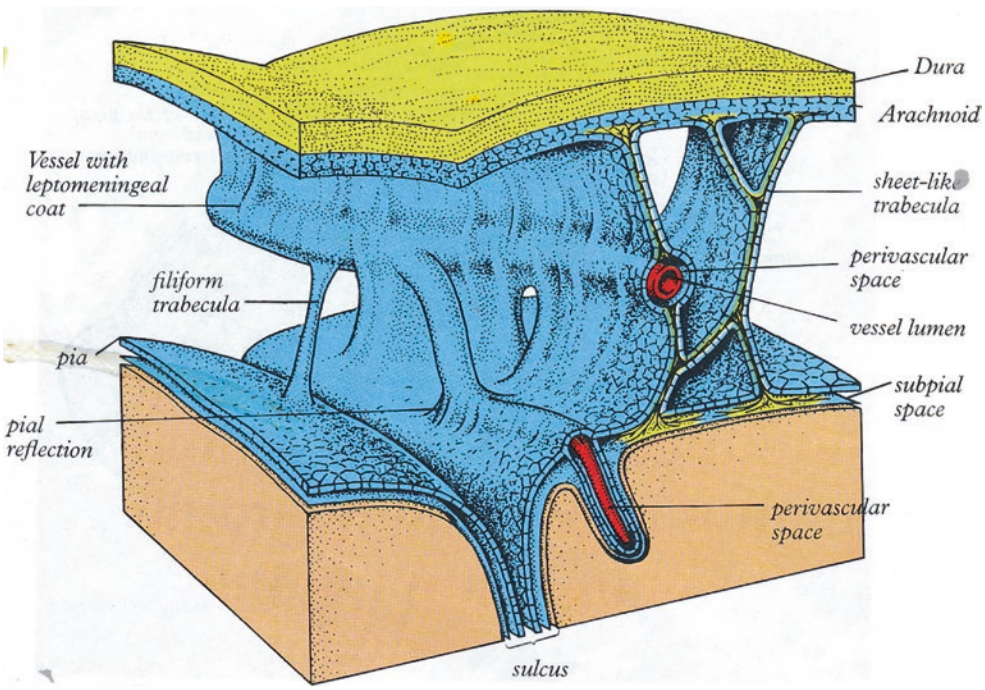

Fig. 2.34 Meninges. First wave of local neural crest is admixed mesoderm containing angioblasts to form leptomeninx (pia and archanoid). Second wave of neural crest from hindbrain forms the pachymeninx (dura). (Reprinted from Williams PL (ed). Gray's Anatomy, 38th ed. Philadelphia, PA: Churchill Livingstone; 1997. With permission from Elsevier)

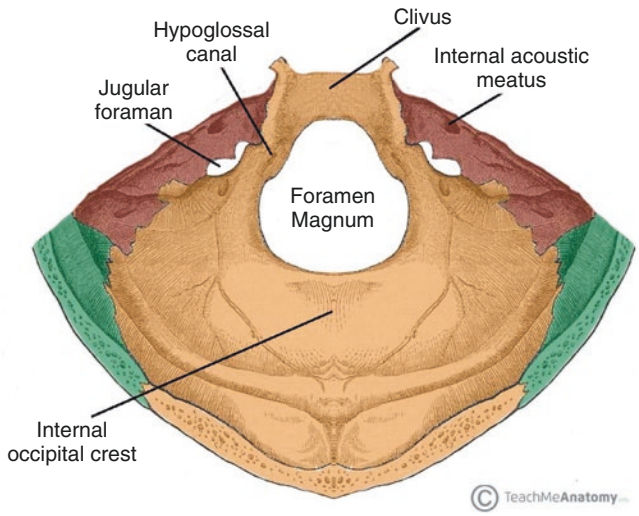

Fig. 2.35 Blood supply of posterior fossa dura: occipital (representing second arch), ascending pharyngeal (representing third arch). Innervation of posterior fossa dura: IX, X via jugular foramen, foramen magnum supplied by branches of C1, C2. (Reprinted from TeachMeAnatomy, courtesy of Dr. Oliver Jones)

As far as the occipital lobes are concerned, they retain V3 innervation. Recall that the cerebral hemispheres arose as balloons from their initial location anterior to pituitary fossa. The parietal and occipital lobes extend backwards to enclose the diencephalon. As such, their dura remains r3 neural crest and is innervated by V3. Periosteal lining (endosteum) of the middle cranial fossa is associated with the neuromeres associated with its bone components, but the innervation remains the same.

Posterior cranial fossa is different. Here, sensory branches of glossopharyngeal and vagal enter the cranium via jugular foramen and are directed anterior to the foramen magnum. The periosteum of this zone refers to IX and X as well as to V3. Thus, the symptom nausea and vomiting are seen with increased intracranial pressure. Posterior to foramen magnum, the periosteum covering the cranial base is mesoderm. Although these bones arise from the occipital somites, their periosteum arises from mesoderm originating from second and third cervical somites that enter the posterior cranial fossa via foraen magnum. For this reason, it is innervated by C2–C3. This explains the stiff neck seen in basilar meningitis. The innervation to the remainder of the calvarium mimics that of the overlying scalp. The dura of the spinal cord from foramen magnum caudal is PAM and is innervated by a strictly neuromeric manner (Fig. 2.35).

Fate of Non-pharyngeal Arch PAM

Not all paraxial mesoderm participates in the formation of pharyngeal arches (strictly hypaxial structures). Somitomeres 1–3 are exclusively dedicated to the extraocular muscles. Sm5 produces lateral rectus and possibly contributes to the petrous temporal complex. Let's look at specific components of the skull formed from paraxial mesoderm [27, 53]. The parietal bone is synthesized from r2 to r3 neural crest and from Sm4 paraxial mesoderm. The squamous temporal bone is formed from r3 neural crest and r4 PAM. Sm6 forms the petrous temporal bone and Sm7 the mastoid temporal bone. The temporal complex likely receives neural crest from r4 to r6. Sm8–Sm11 are subsequently converted into occipital somites with sclerotomes. In the vertebral column proper, the sclerotomes of each somite combine to form vertebral bodies. Signals involved in the induction of the medial somite arise from the notochord and neural tube. Hence, it is not surprising that the vertebral bodies encase these structures. Remnants of the notochord persist as the *nucleus pulposus*.

This situation exists in the cranial base as well. Sm 11 and Sm12 combine to form the proatlas (the first true cervical vertebra, bringing the total to 8). In mammals, a vestigial proatlas (the original first cervical bone) persists as three structures: the rostral tip of the dens, the dento-occipital ligament, and the condyles of the exoccipital bone. The course of the rostral notochord is as follows. Via the dens and the dentooccipital ligament, it gains access to the basioccipital bone (BO). BO is formed as the fusion of sclerotomes from occipital somites 1–4. The notochord then passes through the core of basioccipital bone up to the basisphenoid bone (BS). BS is produced from the PAM of Sm4. The notochord terminates at the junction of the PAM basisphenoid and neural crest presphenoid. Thus, the notochord occupies the center of PAM-derived basicranium, running from r11 forward to r1.

Blood Supply to the Face: An Overview

Summary of Circulations as Determined by Neural Crest

As previously discussed, the rostral rhombencephalon consists of six neuromeres: r2–r7. The first two pharyngeal arches unite as a single functional unit. For evolutionary reasons, both arches produce derivatives very different from their original design. The reassignment of selected first arch derivatives to jaws and dura was so radical that it required an entirely separate system of perfusion. Specifically, *all bone structures of the first arch relating to the jaws and the bones that connect them with the skull are supplied by the extracranial stapedial system*. By this we refer to V2 and V3 neuroangiosomes that depart from the axis of the external carotid maxillary artery. *All non-jaw structures of the first arch (muscles of mastication and their fasciae), glands, and subcutaneous tissue are supplied by the ligual, facial, and*

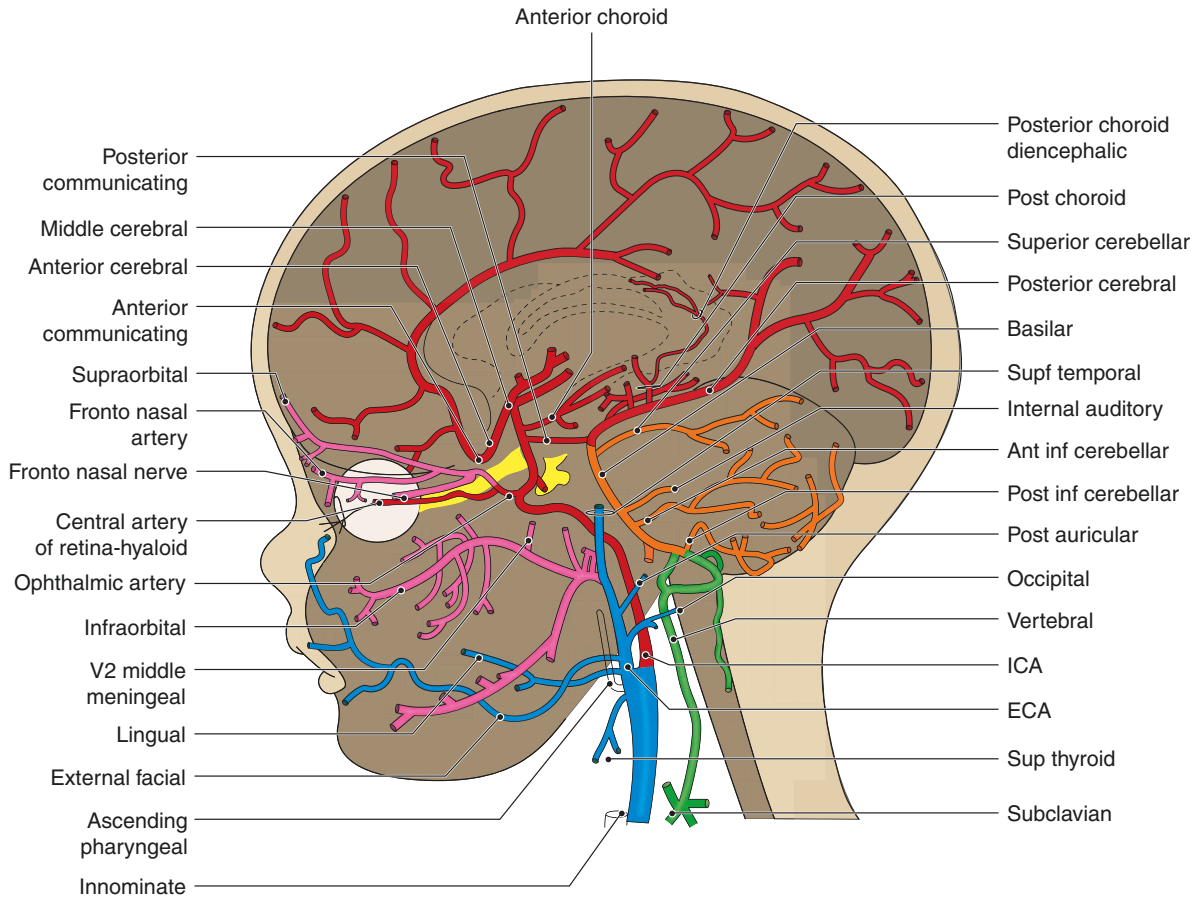

Fig. 2.36 Fetal state. **Stapedial system** (not previously depicted) originates at stage 17 and produces (1) **meningeal aa**, (anast with **external carotid**), (2) **StV1 extraocular ophthalmic aa** (anast with **primitive ophthalmic**), and (3) **StV2 and StV3 sphenopalatine aa** (anast with **external carotid**). (Courtesy of Michael Carstens, MD)

superficial temporal branches of external carotid artery. All remaining arches are supplied by arteries of the external carotid system (Figs. 2.36, 2.37, 2.38, and 2.39).

In evolution, the earliest jawless fishes had eight (or more) gill, or branchial, arches, and a simple circulatory system consisting of parallel ventral and dorsal aortae. Oxygen poor blood pumped by the heart through the ventral aortae passed through gills and the oxygenated blood circulated through the body via the dorsal aortae. This system can still be seen in the agnathic lamprey and hagfish.

In Sum

Frontonasal derivatives containing forebrain neural crest and midbrain neural crest

- Stapedial neuroangiosomes supplied by StV1

Pharyngeal arch derivatives containing hindbrain neural crest

- Stapedial neuroangiosomes supplied by StV2 and StV3
- External carotid neuroangiosomes

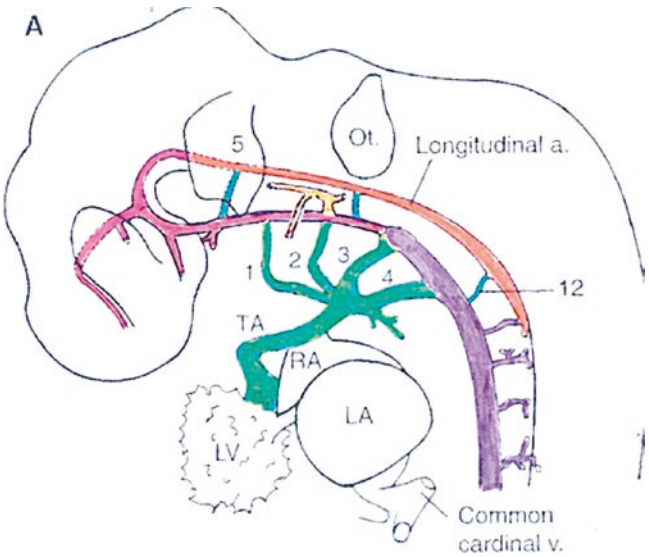

Fig. 2.37 Vascular stages 13–14. **Primitive ICA** to forebrain and midbrain, **Longitudinal neural** (future **basilar**) to hindbrain, connecting **presegmentals** (trigeminal, hyoid, otic, hypoglossa), **aortic arches** (future **external carotid**), **dorsal aorta** giving off **dorsal intersegmentals** (these will later unite longitudinally as the **vertebral artery**). (Courtesy of Michael Carstens, MD)

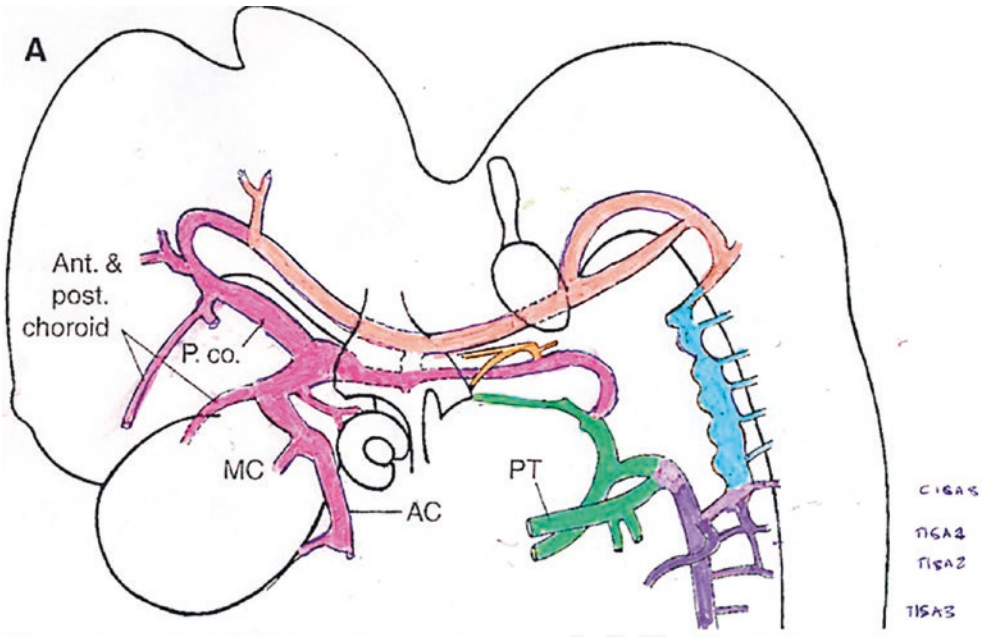

Fig. 2.38 Vascular stage 17. Ventral pharyngeal artery converting to external carotid. Extracranial division of stapedial (yellow) arrives at V3, meets with ventral pharyngeal artery, and forms distal external carotid to the first arch. (Courtesy of Michael Carstens, MD)

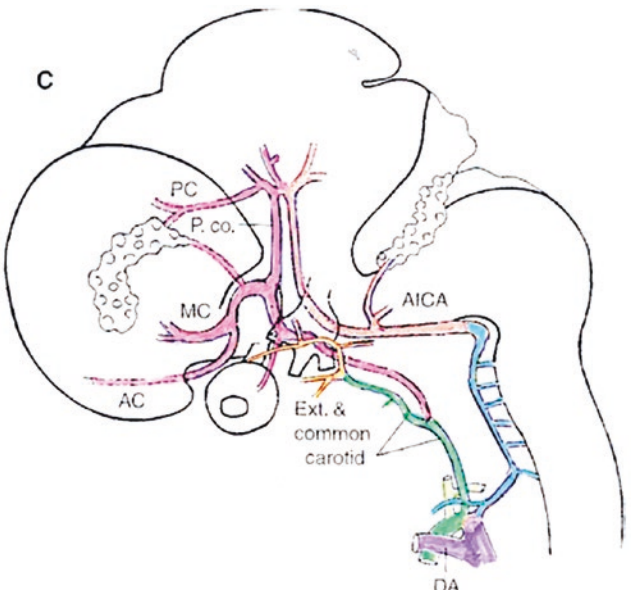

Fig. 2.39 Vascular stage 21. Stapedial connections now complete. Superior division has reached the orbit and united with ophthalmic. (Courtesy of Michael Carstens, MD)

Aortic Arch Precursors

The jawed fishes (gnathostomes) reassigned neural crest from their anterior gill arches to make jaw structures. This change took place in two steps (1) Early cartilagenous fishes (chondrichthyans) such as sharks lose the first branchial arch, the tissues being reassigned from respiration to the creation of jaws. A vascular innovation is required to support tissues reassigned from gill structures to jaws. The upper jaw, eye, and face are supplied by a *stapedial artery* originating from the dorsal aorta at its junction with the second branchial arch. The lower jaw is supplied by an *external carotid* originating from the ventral part of the first collector loop, located junction between second and third arches. Thus, sharks have five gills. (2) Bony fishes (osteoichthyces) reassign *both* first *and* second branchial arches as a composite unit. The hyoid arch is converted into a bony suspension for the jaws. They have four gills. In these species, external carotid now extends to the tissues covering upper jaw as well.

The relationship between the stapedial and external carotid circulations has passed through several iterations during evolution which we shall discuss in a subsequent chapter dealing with vascular embryology. We can summarize the circulations as follows (Fig. 2.40).

Amalgamation of the first and second pharyngeal arches with transformation into jaws requires the dissolution of the original aortic arch arteries AA1 and AA2 in stage 12. In stage 13, assembly of the stapedial and external carotid systems is underway. AA2 leaves behind a dorsal stem, the *hyoid artery* dangling from the dorsal aorta. AA3 and AA4 dissociate. AA3 forms the common carotids and connects an intermediate ventral pharyngeal artery which subsequently morphs into external carotid. The hyoid gives off stapedial, as the first branch of the extracranial internal carotid. Stapedial enters the tympanic cavity and divides, giving off an intracranial *superior division* and an extracranial *inferior division* which exits via the pterotympanic fissure.

Extracranial stapedial follows chorda tympani to the root of V3, at which point it joins with the maxillary branch of external carotid to form the *maxillomandibular artery*. MMA is a hybrid that contains stapedial vessels designated for the

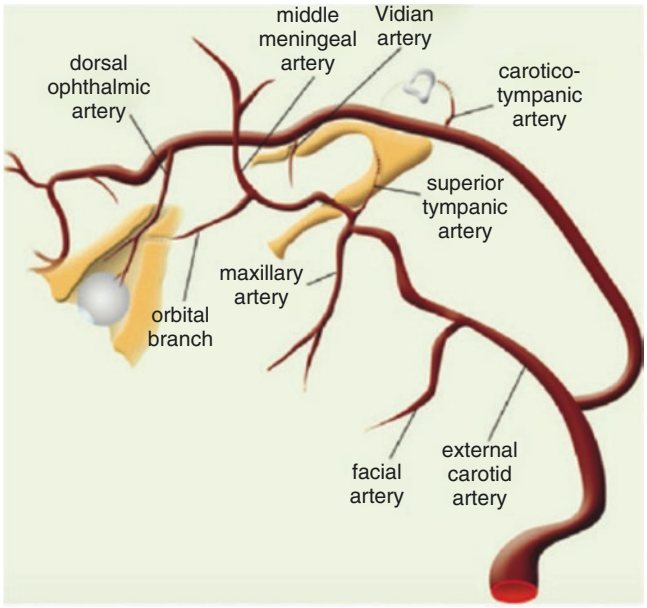

Fig. 2.40 Stapedial contributions to ophthalmic and maxillomandibular systems—embryonic stapedial system has been replaced. **Stapedial stem** originated from the hyoid artery, the remnant of which is *carotico-tympanic artery.* It proceeded through stapes and divided. The **inferior maxillomandibular division** followed CN VII chorda tympani nerve to exit the skull and access the external carotid system at the root of V3 in the infratemporal fossa. The adult remnant of this is *superio tympanic artery.* The **superior supraorbital division** (disintegrated) followed CN VII superior petrosalnerve and then trigeminal ganglion V1 and V2 to supply dura branches and the orbital branch. Secondary connection between the two systems was provided by V3-induced middle meningeal which accessed the intracranial division, completing the middle meningeal system. Orbital branch was accessed by ophthalmic making the original connection with middle meningeal optional—thus the meningo-orbital branch of MMA is usually not present in the adult. This topic is discussed in depth in Chaps. 6 and 7. (Reprinted from Tanoue S, Kayoso H, Mori H. Maxillary Artery: Functional and Imaging Anatomy for Safe and Effective Transcatheter Treatment. Radiographics 2013; 33(7):209–229. With permission from the Radiological Society of North America)

jaws and supporting bone fields and external carotid vessels assigned to the soft tissue envelope of the face and mouth (muscles of mastication, muscles of expression, glands, and skin). External carotid to the facial complex consists three branches: maxillary, lingual, and superficial temporal.

During development, the first and second pharyngeal arches merge together as soon as PA2 is formed. PA3, PA4, and the puny PA5 remain distinct. During the merger process, the first and second aortic arch arteries that serve PA1 and PA2 disintegrate, leaving behind dorsal *remnant vessels* dangling from the dorsal aortae. The dorsal remnant of first aortic arch artery, the *mandibular artery*, eventually supplies the pituitary. The dorsal remnant of second aortic arch artery, *the* hyoid artery, gives off the all-important stapedial artery. With growth, the hyoid comes to lie just beneath the future tympanic cavity. It is the only extracranial branch of internal carotid. Hyoid persists as the carotid-tympanic artery.

Birth and Death of the Stapedial Artery System

Hyoid artery, being a second arch structure, is associated with cranial nerve VII. It sends a branch upward (in conjunction with CN VII) into the embryonic middle ear, which is eventually enclosed by tympanic cavity. This is **stapedial stem.** Within the tympanic cavity, stapedial divides. Both divisions of stapedial follow branches of the seventh nerve and exit the tympanic cavity.

Upper division stapedial follows greater petrosal all the way to trigeminal ganglion; it divides to follow V1 and V2. V1 stapedial supplied all dura, bone, and skin and vestibular lining, conjunctiva, and orbital structures innervated by V1. V2 stapedial supplies dura, lacrimal gland, and lateral orbit. Superior division does not have the opportunity to follow V3 because it already has exited the skull.

Lower division stapedial follows chords tympani (VII) to reach V3 — where it anastomoses with internal maxillary from ECA. This pathway is marked by the remnant anterior tympanic artery. From this anastomosis, it immediately sends out a ventral branch, inferior alveolar, following V3 to the mandible and a dorsal branch following V3 to the dura, middle meningeal. It then continues forward to with ECA until it reaches the sphenopalatine fossa where it provides all remaining branches following V2 into the zygomatico-maxillary-palatine complex.

The return of StV3 middle meningeal to the dura has drastic hemodynamic consequences for the previous two intracranial stapedial arteries. Middle menineal ascends and connects at trigeminal ganglion with the original superior division originating at tympanic cavity. Thus, bifurcation of StV1 and StV2, formerly dependent on long distance from a relatively small stapedial stem, is exposed to a high pressure system. Greater flow leads to an involution and disintegration of the proximal upper division associated with greater petrosal leading back to the tympanic cavity. So extracranial SstV3 finds itself in the cranial cavity where it will form the meningeal system and supply the orbit via StV1 branch to superior fissure and StV2 branch to the meningo-orbital foramen. Within the orbit, these two embryologically distinct arteries will unite to form the supraorbital stapedial. They plug into the ophthalmic to supply all not ocular tissue of the orbit.

Note that when StV1 joins primitive ophthalmic, its proximal stem back to the trigeminal ganglion involutes. Thus, middle meningeal does NOT supply StV1 directly. STV1 is fed by primitive ophthalmic from internal carotid. StV1 supplies dura innervated by V1, principally via its ethmoid branches. However, orbit *does* receive StV2 from the meningeal system. It comes into the lateral orbit via a foramen and helps supply the lacrimal gland. This is the axis of Tessier cleft zone 9. This anatomy is explained in greater detail in Chaps. 6 and 7.

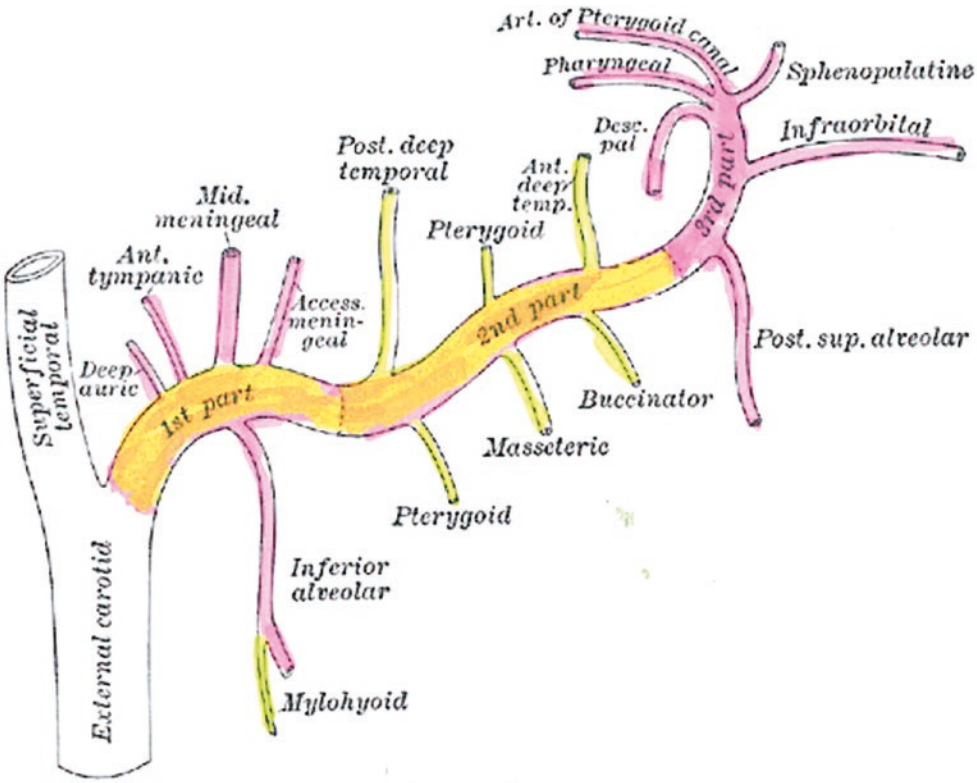

Fig. 2.41 Maxillo-mandibular artery
First part
Non-neural crest mesenchyme—ECA
- **Mastication**

Neural crest mesenchyme—stapedial—all V3
- **External ear**
- **Tympanic membrane**
- **Dura**
- **Mandible**

Second part
Nonneural crest mesenchyme—ECA
- **Mastication**

Third part
Neural crest mesenchyme—stapedial—all V2
- **Maxillary fields**

(Reprinted from Lewis, Warren H (ed). Gray's Anatomy of the Human Body, 20th American Edition. Philadelphia, PA: Lea & Febiger, 1918)

Internal Maxillo-Mandibular Arterial Axis Summarized

Facial circulation is the topic of Chap. 7. But, as our discussion of neuromeric derivatives is based on the blood supply, let's review the IMMA (Fig. 2.41).

ECA neuroangiosomes supply soft tissue fields.

Stapedial neuroangiosomes supply bone fields innervated by V2 and V3.

Segment 1 (Mandibular): Dorsal Branches

- *Deep auricular artery* represents one of two escape routes for the inferior division of stapedial as it exits tympanic cavity. It supplies r3 tympanic membrane and r3 temporomandibular joint.
- *Anterior tympanic* passes through pterotympanic fissure and represents a surviving remnant of stapedial.
- *Middle meningeal* proceeds epaxially with V3 middle meningeal nerve to supply the dura. Entry via foramen spinosum makes an anastomosis with StV2 of the superior division at the takeoff of StV2. The StV2 remnant becomes *anterior branch of middle meningeal* to supply alisphenoid and frontolateral dura. Alisphenoid is innervated by V2 and remains an r2 derivative. The StV3 segment becomes *posterior branch of middle meningeal* to supply the dura of the middle and posterior cranial fossae.
- *Accessory meningeal* goes through foramen ovale to trigeminal ganglion. Represents remnant of the primitive trigeminal artery. Remnant of dorsal aorta.

Segment 1 (Mandibular): Ventral Branches—Mixed

- Inferior alveolar artery: The principal artery to the lower jaw was not necessarily a stapedial derivative in the early gnathostomes Recall that in the primitive state lower jaw is initially supplied by ECA. It is possible that full expression of the maxillo-mandibular artery with stapedial reaching the maxillary stem does not occur until later in evolution. This is evidenced by the evolution of the meninges. Fishes have a single layer of meninx. Reptiles add a second layer, the pachymeninx (dura). Note: the three-layer model of meninges, with an arachnoid and subarachnoid space, is a mammalian invention.
- Mylohyoid artery derived directly from the original stem external carotid: supplies muscles of mastication.

Segment 2 (Infratemporal): Dorsal Branches

- Posterior deep temporal—squamous temporal/muscle
- Pterygoid—mastication
- Anterior deep temporal—squamous temporal/muscle anastomose with lacrimal

Segment 2 (Infratemporal): Ventral Branches

- Pterygoid (ECV3) supplies mandibular ramus
- Masseter (ECV3) supplies ramus
- Buccinator only muscle of second arch supplied by MMA

Segment 3 (Pterygopalatine)

- Zygomatic, temporal: zone 8
- Zygomatic, facial: zone 7
- Posterior superior alveolar: zone 6
- Infraorbital: zones 5 and 4
- Descending palatine zone 3
- Artery of the pterygoid canal: V3 part of auditory canal and tympanic cavity
- Pharyngeal branch: V2 part of auditory canal
- Nasopalatine branch lateral: zone 3—inferior turbinate and maxillary process
- Nasopalatine branch medial: zone 2/zone 1/premaxilla/vomer

Anatomy of Craniofacial Neural Crest

All students of the nervous system are familiar with neural crest cells. The importance of these cells for development is so great that they are often referred to as "the 4th germ layer." The biology of the neural crest is summarized in several authoritative reviews. In this section, we shall detail the neuromeric organization of the neural crest and the manner in which distinct anatomic zone of neural crest migrates in distinctive ways. We shall do so neuromere-by-neuromere. Because we must rely on nomenclature derived from neuroembryology, readers are advised to study because it shows the order in which the various neural crest populations migrate into their final position [54–56].

Building Blocks of the Face

The neural crest entering the face comes from three different sites with three different migration patterns (Fig. 2.42).

Forebrain: Prosencephalic Neural Crest (PNC) > Fronto-Orbito-Nasal Skin

The neural folds above the forebrain have two different zones, anterior and posterior. Tissues from these sites create the skin of the forehead, nose, and upper eyelid. Epidermis arises from *nonneural ectoderm* (NNE) of the anterior zone. Dermis arises from *neural crest* of the posterior zone (PNC). PNC migrates forward underneath NNE as a *single sheet* with distinct genetic zones. These correspond to Tessier cleft zones 10–13. FNO skin is unique; *frontonasal dysplasias* seen in the upper face are a consequence of its development.

Midbrain: Mesencephalic Neural Crest (MNC) > Upper Face

MNC develops from m1 to m2 from midbrain and r0 to r1 from isthmus. We'll refer to them as MNC or r1. These four

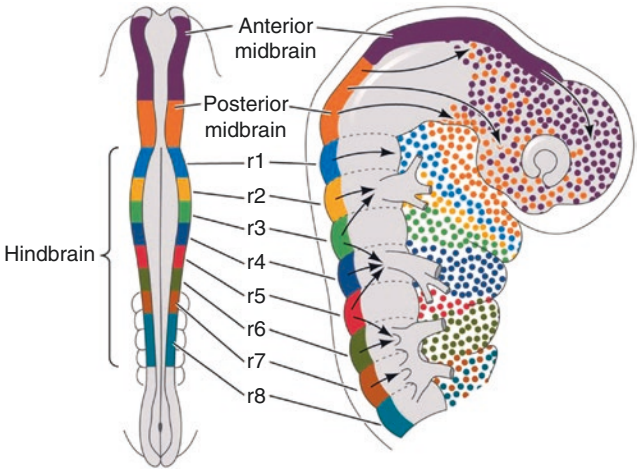

Fig. 2.42 Cranial neural crest map PNC vs. MNC vs. RNC. PNC (p1–p4) = frontonasal dermis (Stapedial V1). MNC (m1, r1) = dura, frontonasal and sphenethmoid mesenchyme (Stapedial V1). RNC (r2–r11) dura, maxilla-zygoma (stapedial V2), dura, mandible (stapedial V3), all remaining structures in first to fourth arches (external carotid system). Defects of midbrain neural crest: (1) Hypertelorism: failure of apoptosis. (2) Encephalocoele: field deficiency defects. (3) Holoprosencephaly: failure of MNC to separate the prechordal mesoderm. (Reprinted from Creuzet S, Couly G, Le Douarin NM. Patterning the neural crest derivatives during development of the vertebrate head: insights from avian studies. J Anat 2005; 207:447–459. With permission from John Wiley & Sons)

populations travel forward in *streams* over the lateral aspect of the forebrain to reach the midline. They produce the entire V1-innervated dura. MNC bone are: the sphenoid complex (except alisphenoid), the ethmoid complex, the lacrimal bone, the frontal bone, and the membranous bones of the orbital series. When the optic cup evaginates from diencephalon, it becomes coated with MNC. The fields of MNC are supplied by V1-induced branches of stapedial ophthalmic axis. These neuroangiosomes are referred to as StV1,

Hindbrain: Rhombencephalic Neural Crest (RNC) > Midface

RNC develops from r2 to r11 in the hindbrain and migrates into the five pharyngeal arches. Each arch is supplied by a pair of rhombomeres. Blood supply for all these derivatives is external carotid. In the first arch, a separate population of RNC from r2 and r3 is responsible for synthesizing the mandible, zygomaticomaxillary complex, and alisphenoid. These *non-pharyngeal arch jaw fields* are supplied by V2 and V3-induced branches of the stapedial maxillo-mandibular axis. These neuroangiosomes are referred to as StV2 and StV3.

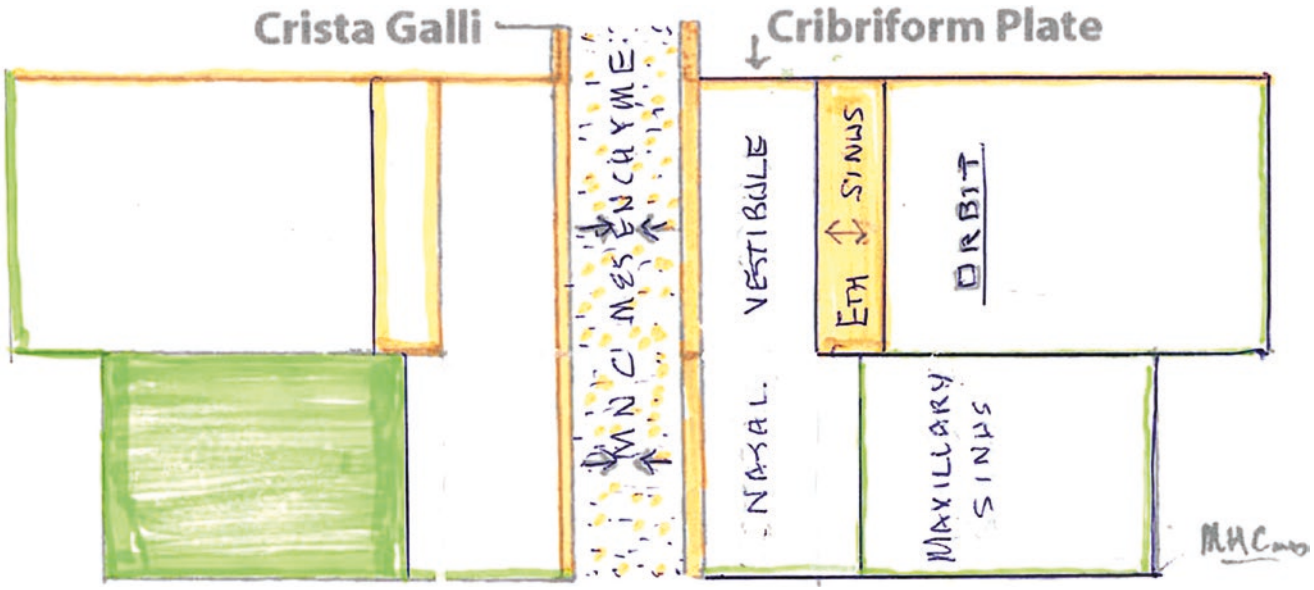

Fig. 2.43 Frontonaso-orbital and maxillary mesenchyme. MNC (orange) is also the source of anterior cranial base frontal bone, ethmoid, and sphenoid. Ethmoid sinuses are separation planes between MNC programmed by r1 sclera (overlying the p5 globe) and p6 vestibular epidermis with r1 submucosa. (Courtesy of Michael Carstens, MD)

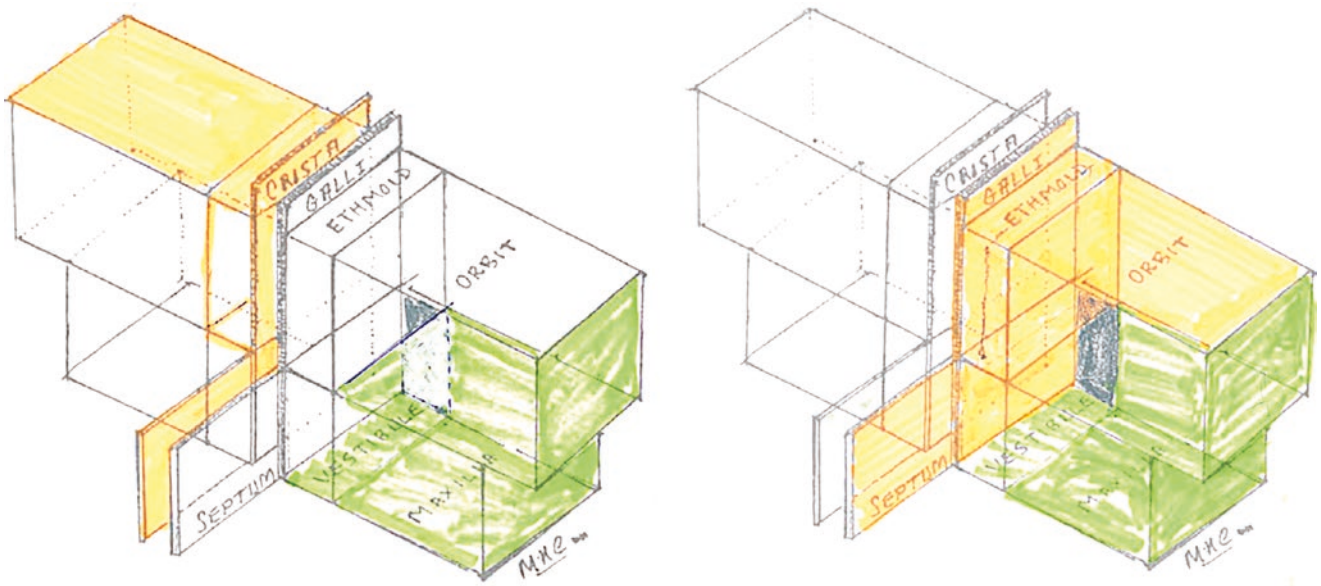

Fig. 2.44 Naso-orbital-maxillary complex: five-sided box. MNC (orange): ethmoid, sphenoid. RNC (green): maxilla, a five-sided box. (Courtesy of Michael Carstens, MD)

Developmental Fields Can Be Lumped into Three Groups: A + B + C

The face is constructed from three blocks of fields on either side of the midline. We can classify them by their blood supply and innervation. This in turn is based on the stapedial arterial system (Figs. 2.43 and 2.44).

A field neuroangiosomes consist of an *FNO skin coverage* and *bone fields of the anterior cranial fossa and medial-superior orbital walls*. The epidermis contains *nasal and optic placodes*, islands of specialized nonneural ectoderm that form the nasal cavity, and complete development of the globe. The MNC bone fields are: sphenoid (except alisphenoid), the ethmoid complex, the frontal bone, and the orbital series (lacrimal, prefrontal, and postfrontal). These are innervated by V1. The blood supply is V1-induced branches of the stapedial ophthalmic axis.

B field neuroangiosomes are ***non****-pharyngeal arch bone fields* of the jaws and supporting bones: mandible, vomer,

Table 2.3 Neuromeric organization of craniofacial neural crest

Field	NCrest	Neuromeres	Blood supply	Derivatives
A	PNC	p3–p1	StV1	Fronto-naso-orbital dermis
A	MNC	m1–m2, r0–r1	StV1	Fronto-naso-orbital bone fields
B	RNC	r2–r3	StV2/StV3	Jaws and supporting bones to skull
C	RNC	r2–r11	Ext carotid	All other arch structures

premaxilla, maxilla, palatine, zygoma, and alisphenoid. These are innervated by V2. The blood supply is V2-induced branches of the stapedial maxillo-mandibular axis. Mandible, supplied by StV3, is not included in our discussion.

C field neuroangiosomes: *pharyngeal arch tissues* (except the jaws). These are innervated by V2. The blood supply is from the branches of external carotid (Table 2.3).

In conclusion, the formation of facial fields occurs in this following sequence: (1) MNC and PNC complete the formation of the frontal fields. (2) $RNC_{ROSTRAL}$ (first and second arches) moves into position. (3) MNC forms the anterior cranial base and orbit. (4) RNC_{CAUDAL} completes formation of the pharynx. (5) PNC produces frontonasal dermis. Let's first take a look at each of these populations. Then we will consider a model of spatial assembly.

Migration Patterns of Neural Crest

Neural crest cells from the level of the r0 posteriorly are produced in a cranio-caudal order and from m1 forward in caudal-order. *Three groups of neural crest*, each defined by their level of origin from the embryonic brain, mature in a fixed temporal order, and migrate in unique patterns [57–63].

First to depart from the neural folds are those neural crest cells associated with the mesencephalon. These are, from the midbrain, **m1** and **m2**, and from anterior-most hindbrain, **r0** and **r1**. These MNC cells do not participate in pharyngeal arch formation. Instead, beginning at stage 9, they migrate forward in three distinct *streams* toward the orbit and interorbital midline. These pathways are lengthy; therefore, MNC fronto-nasal migration is not complete until **stage 14** (at the same time after pharyngeal arches are filled).

Next to mature are those cells from the *rostral* rhombencephalon **r2–r7**. These neural crest cells are assigned to pharyngeal arch formation. RNCr cells migrate in a strictly *segmental* fashion. Although these cells begin traveling in time immediately MNC, they have a shorter distance to travel and thus arrive at their destination by **stage 12.** However, these cells have to be positioned in space which takes them until stages 14–15. Cells from the *caudal* rhombencephalon **r8–r11** start later still. These cells also travel in *segmental* fashion over a relatively short distance within their respective segments. It is therefore logical that these RNCc cells arrive at their destination concomitantly with those from the mesencephalon, i.e. at **stage 14**.

Cells from the neural folds above the caudal prosencephalon (i.e. at neuromeric levels **p1**, **p2**, and **p3**) migrate forward as a large *sheet*. They begin their journey after the departure of the MNC. These PNC cells travel a great distance forward; their migration is not complete until **stage 16**. Recall that facial assembly begins at stage 17.

Prosencephalic Neural Crest: Anatomic Considerations

The New Prosomeric Model

The model used in this book represents an amalgamation of the neural crest fate mapping studies of Couly and LeDouarin and the neuromeric system of Puelles and Rubenstein. The neuromeric anatomy of the prosencephalon was initially described in 1993 and went through subsequent iterations [63–68]. So far, we have seen a relatively straight-forward relationship between the neuromeres of the hindbrain and midbrain and their derivative tissues. In order to map out structures that relate to the forebrain, here is a brief refresher on the prosomeric system.

First, the developing vertebrate brain is subdivided into transverse building blocks arranged longitudinally down the entire neural tube, much like the watertight compartments of a submarine. These are repetitive (metameric). Although the neuroanatomic content of individual neuromeres can vary, they all share a common dorsoventral organization (roof, alar plate, basal plate, and floor plate). The initial segmentation of the CNS occurs immediately after gastrulation based on *Otx-2* signals from down the anterior visceral endoderm, prechordal plate, and notochord. In the subsequent stage, gradients of Engrailed are laid down on either side of the r0 isthmus (Fig. 2.45).

The anatomic boundaries and neuroanatomy of each neuromere are determined by a unique combination of developmental (homeotic) genes that defines the position of the neuromere along the neuraxis and also what structures it contains. In the mammalian (mouse) model, the activity of homeotic genes within the neuromeres continues to be active into the perinatal period.

The concept of mapping the forebrain into genetically based developmental units, prosomeres, is anatomically sound, but has undergone a number of modifications, The original 1994 model divided the forebrain into six proso-

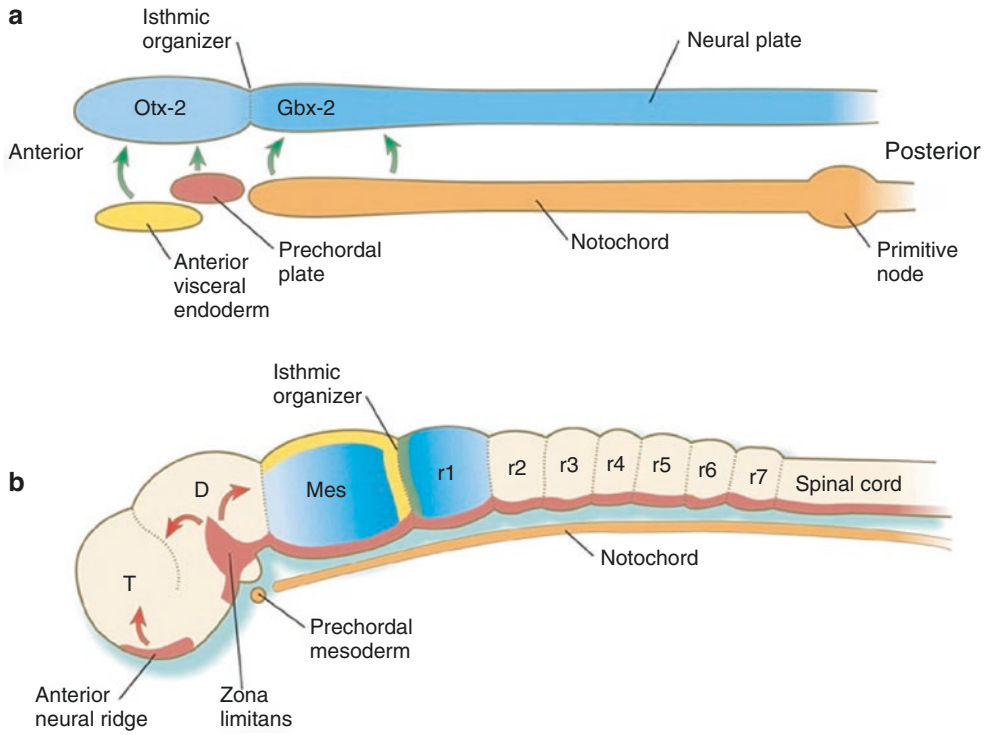

Fig. 2.45 Schematic representation of signaling centers acting on and within the early embryonic brain. (**a**) In response to signals (greens arrows) from the anterior visceral endoderm, the prechordal plate, and the notochord, the neural tube express Oyx-2 in the future forebrain/midbrain and Gbx-2 in the hindbrain/spinal cord. (**b**) Later in development, signals fFGF-8 (green) and Wnt-1 (yellow) from the isthmic organizer induce decreasing gradients of En-1 and En-2 (blue) on either side. Sonic hedgehog (red) is secreted from the other two organizers, the anterior neural ridge and the zona limitans, as well as the ventral part (floor plate) of the neural tube. *D* diencephalon, *Mes* mesencephalon, *r* rhombomere, *T* telencephalon. (Reprinted from Carlson BM. Human Embryology and Developmental Biology, 6th edition. St. Louis, MO: Elsevier; 2019. With permission from Elsevier)

meres, three for the telecephalon and three for the diencephalon. These six prosomeres were discrete developmental units, each with a unique genetic identity. The prosomeres were vertically oriented columns such that the neural folds above the alar zones would share a common homeotic coding with those of the basal zones. Thus, neural crest could be mapped out using the same markers as the base of the brain. This model contradicted well-established studies, done with traditional anatomic methods such as Nissel stains, carried out *without* the use of genetic markers, in which four identifiable units were described [69] (Fig. 2.46a).

Further work showed increasing complexity of the genetic subunits of the telencephalon. The floor plate and basal fields did not run directly upward to the roof, as was previously thought. Time honored dogmas such as the vertical "stacking" of epithalamus, thalamus, and hypothalamus were disproven. As genetic mapping work proceeded, the prosomeric model underwent successive iterations. The 2009 model clarified the anatomy of p1–p3, but made the boundaries of p4–p6 more complex [67]. In 2013, the existence of diencephalon with prosomeres p1–p3 was retained, but the concept of a telencephalon with p6–p4 prosomeres was dropped [68] (Fig. 2.46b).

In Chap. 5, prosomeric system will be discussed in detail but for purposes of this chapter it is important to understand its terminology because this will be used to map out neural crest arising over the prosencephalon.

How can we make use of this model? Caudal forebrain neural folds do *contain neural crest*, so they can be mapped from p1 to p3. This neural crest is the source for the dermis of all frontonasal skin innervated by V1. Rostral forebrain neural folds are utterly *devoid of neural crest* cells. Instead, the rostral folds will form the epidermis of frontonasal skin. They also contain specialized epithelial structures, from proximal to distal: the optic olfactory, and adenophypophyseal placodes. The derivatives of the rostal neural folds have been mapped out by LeDourain and we can extrapolate them to the model of Puelles model. Caudal secondary prosencephalon is zone p4 and contains the *calvarial ectoderm*, the "program" for the upper frontal bone. Rostral secondary prosencephalon has two zones. Zone p5 contains the optic placode, the eventual source of the lens. Zone p6 contains the nasal placode and the adenohypophyseal placode. Although the model proposed by this author is hypothetical, the neural fold fate map continues to be refined in the mouse and correlated with the human prosomeric system.

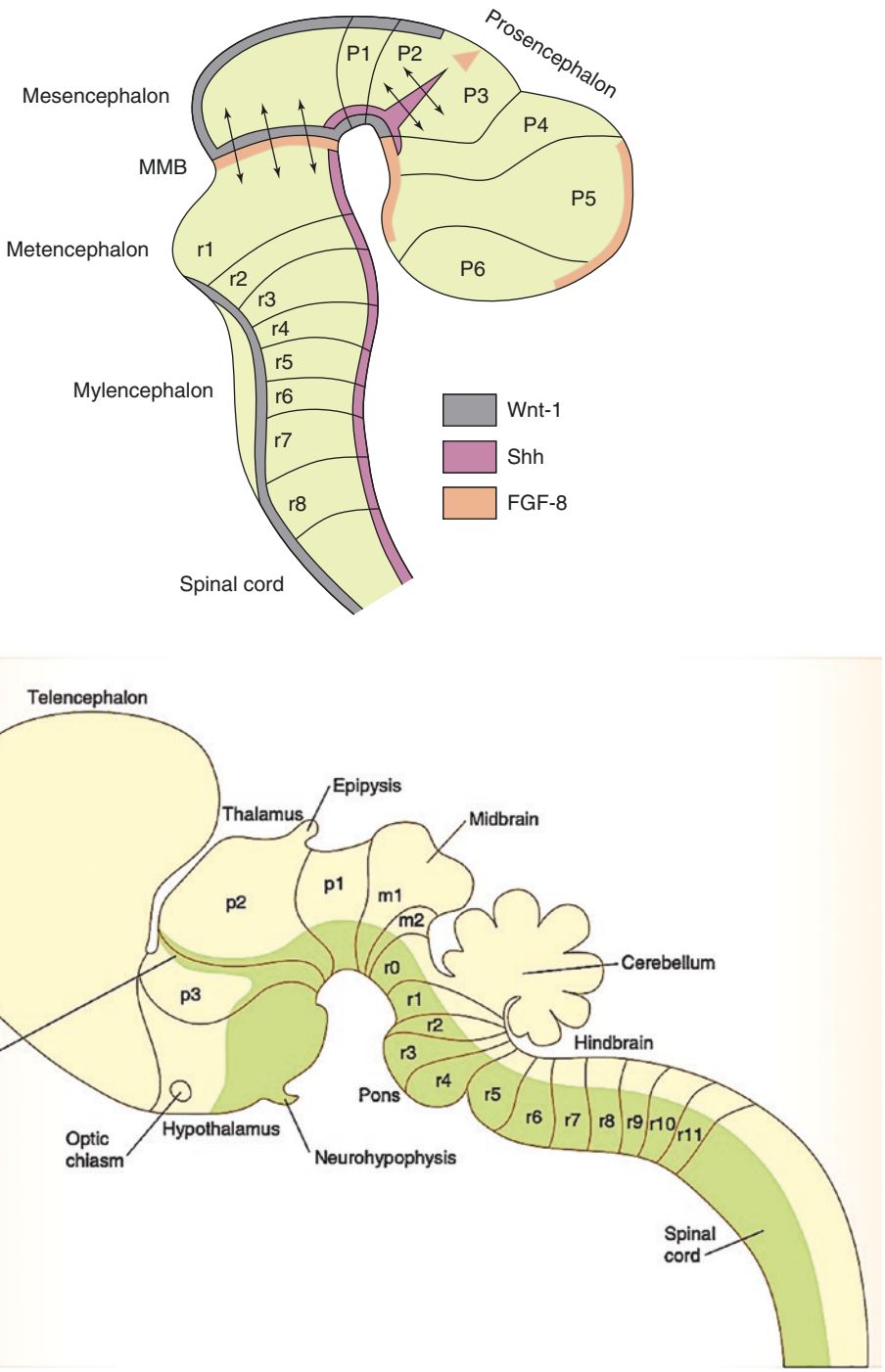

Fig. 2.46 Previous iterations of the prosomere model. Generalized vertebrate embryo showing neuromeres and distribution of major signaling molecules. Mindbrain/hindbrain signaling regions = arrows just rostral to first rhombomere. Arrows between second and third rhombomeres represent a hypothetical signaling region in the forebrain. Model subsequently revised by 2013 with defined prosomeres restricted to the diencephalon. Prosomeres p6, p5, and p4 are now not assigned to neural folds but map of neural fold derivatives remains valid. (Left: Reprinted from Carlson BM. Human Embryology and Developmental Biology, 6th edition. St. Louis, MO: Elsevier; 2019. With permission from Elsevier. Right: Reprinted from Puelles L, Harrison M, Paxinos G, Watson C. A developmental ontology for the mammalian brain based on the prosomeric model. Trends Neurosci 2013; 36(10):570–578. With permission from Elsevier)

For the purposes of mapping out facial structures, we shall adopt the following conventions:

- Rostral forebrain nonneural ectoderm (NNE) can be divided into zones corresponding to the placodes.
- Placodes are ectodermal structures that maintain a relationship to the CNS.
- Zones p5 and p6 are repositioned basal to the forebrain.
- Zones p4–p6 participate in the development of the face.
- V1 stapedial connects p4–p6 facial fields and the subjacent anterior cerebral artery.
- Field defects in the ACA fields relate to and may predict defect segments of the StV1 system that supply the p4–p6 facial fields.

Prosomeric Mesenchyme and Nonneural Epithelium: General Considerations

Why are these distinctions so important? Recall that frontonasal skin (FNO) is mapped out by the sensory distribution

of V1. How this skin develops is utterly unique. Recall that the gastrulation process that produces germ layers at stage 7 does not extend forward from level r0. Thus, *ectoderm and mesoderm are simply not available to make the skin of the eyes*, *nose*, *and forehead*. The embryo uses a different strategy using three different tissue sources to accomplish the same thing [68].

- Frontonasal epidermis develops from the neural folds overlying the rostral prosencephalon (telencephalon). This zone is devoid of neural crest and is termed the *nonneural ectoderm* (NNE). The contributions of NNE to craniofacial skin have been mapped by Couly et al. [70].
- Frontonasal dermis arises from the caudal prosencephalon (diencephalon); the folds that produce neural crest are in register with prosomeres p4–p1. We shall refer to the prosencephalic neural crest as PNC.
- Subcutaneous frontonasal tissues are derived from midbrain neural crest (MNC); it covers the entire forebrain and upper face.

Survival of the FNO epidermis requires the acquisition of an underlying support network in order to survive. PNC cells from caudal forebrain migrate forward to populate the subepithelial plane of p4–p5–p6 with neural crest-derived dermis. In this way, PNC ensures the viability of the nonneural epithelium.

Cellular movement of PNC into the forward position takes place more in the form of a sheet than as clearly identifiable streams. How do these populations migrate? The order in which the target zones of the rostral folds are populated is from back to front (caudal-to-rostral). This is supported by the known *sequence of placode development*, which is: otic, optic, and then olfactory. *Failure of neural crest to populate the sub-placodal zone leads to placodal dysfunction or outright absence*. We shall discuss the derivatives of placodes that result from these interactions in the next section [71–74].

Prosomeric Placodes

Development of the face is dominated by behavior of three important placodes: pituitary, nasal, and optic. Development of the ear is controlled by the optic placode of the hindbrain. A placodal region is one in which the *specialized zone of ectoderm is in direct contact with the CNS*. Cellular migration of three types takes place from all placodes. (1) Specialized sensory cells are represented by structures such as the otoliths of the labyrinth from the otic placodes of r4–r5 hindbrain and the vomeronasal organs flanking the septum from the medial nasal placodes. (2) Neuroblasts arising from the lateral olfactory placodes provide the apparatus of smell, whereas those from the medial olfactory placodes transmit chemoreceptive data to the brain. (3) Neural crest or PAM cells interact with invading placodal tissue to form into the cartilaginous capsules of the presphenoid, the nasal cavities, the orbits, and the temporal bone (Figs. 2.47, 2.48, 2.49, and 2.50).

The natural behavior of placodes is to penetrate (more accurately to become incorporated) into the embryonic CNS. As these placodes "sink beneath the waves," they interact with the brain to induce additional structures. These simple relationships are readily seen in the neural fold state prior

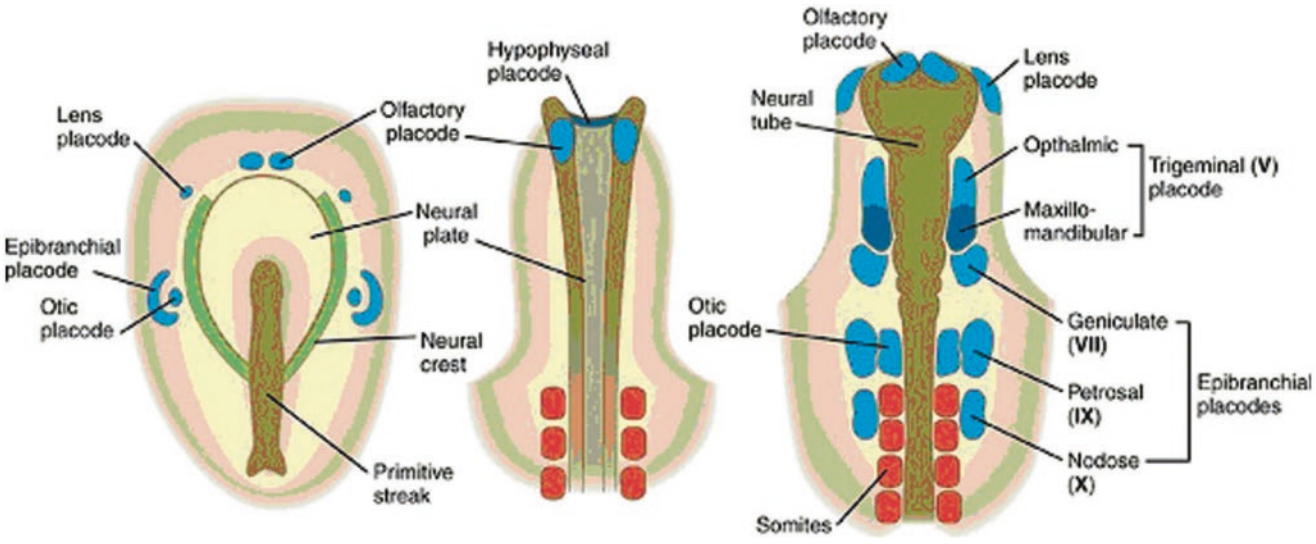

Fig. 2.47 Neural folds and placodes. Early stages in the formation of cranial ectodermal placodes (blue) in the chick embryo, as viewed from the dorsal aspect. These specialized zones of the neural folds interact with neural crest cells to produce the neurosensory-endocrine apparatus of the embryo (the pituitary, olfactory systems, lens, inner ear, and specialized ganglia). (Reprinted from Carlson BM. Human Embryology and Developmental Biology, 6th edition. St. Louis, MO: Elsevier; 2019. With permission from Elsevier)

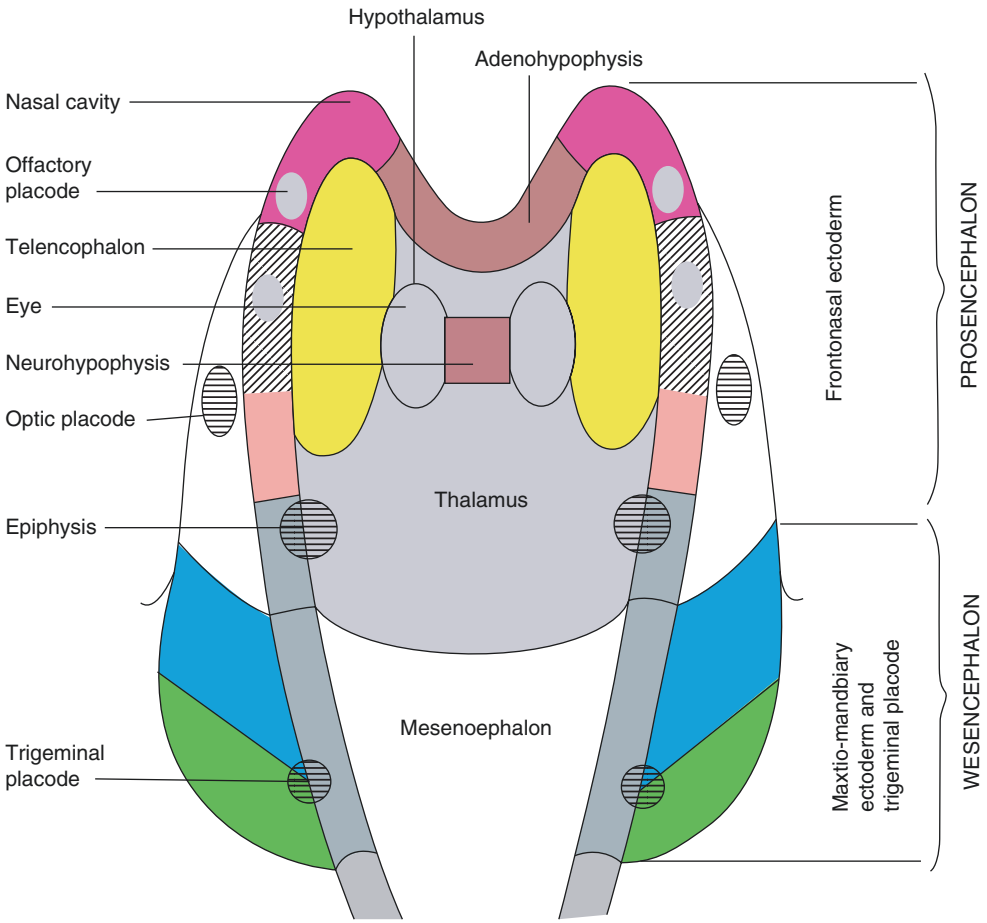

Fig. 2.48 Nonneural ectoderm of the anterior folds and epidermal derivatives. Adenohyophyseal placode/Rathke's pouch, p6 (brown), nasal epithelium, p6 (pink), upper beak/nose epidermis, p5 (green), calvarial epidermis, p4 (orange), eyelid epidermis/cornea epithelium, r1 (white), midface oral-maxilla-zygoma epidermis, premaxilla mucoperiosteum r2 (blue), lower face mandible epidermis, r3 (light blue). (Reprinted from Standring S (ed). Gray's Anatomy 40th ed. New York, NY: Churchill Livingstone; 2008. With permission from Elsevier)

to closure of the neuropore and head folding. Growth of the telencephalon at this point involves the formation of paired hemispheric vesicles that push laterally from the sidewalls of the neural tube. These cerebral vesicles push rostrally and caudally. They expand so greatly that they eventually envelop the entire neuraxis. Tucked within the hemispheres are the midbrain and hindbrain. The cerebellum sprouts forth from r0 and r1; it projects backward beneath the hemispheres. Neuromeric pathologies in r0–r1 can be seen as facial tissue defects and cerebellar hypoplasia or aplasia.

Adenohypophyseal Placode

The most rostral/cranial placodes in p6 neural folds are the adenohypophyseal placodes. These are repositioned by forebrain expansion and folding until they come to lie tucked below the brain into the future nasopharynx at Rathke's pounch. At this point, they fuse to form the epithelial component of the pituitary, the adenophypophysis. Rathke's pouch also marks the epithelial boundary zone between p6 nasal vestibular lining anteriorly and likely third arch endothelium posteriorly (Figs. 2.51 and 2.52) [75, 76].

The most distal zone of each p6 NNE to be populated by PNC is that of the *adenohypophysis (pituitary) placode* (AP). These are bilateral but, at the anterior extreme of the embryo, the p6 zones are continuous with each other, resembling a handlebar moustache. Textbooks describe the AP as if it were a single entity when, in point of fact, the placodes are *bilateral* and fuse. For this reason, in the presence of forebrain pathology, the ipsilateral adenohypophysis can be smaller. Tumors of a given cell type can also be unilateral.

With formation of the primary head fold, the most anterior nonneural ectoderm is tucked ventrally and caudally below the forebrain until it lies just beneath the presphenoid/basisphenoid junction. This can be visualized by imagining the fingernail of your right index finger as the placode and the metacarpo-phalangeal joint of the same finger as the PS/BS "joint." This is the topology of the neural plate. If you then make a fist with the hands supine, the tip of the index finger (containing the placode) will come to rest beneath your MP (PS/BS) joint.

At any rate, the relocation of the APs into the future nasopharynx beneath the PS/BS junction permits upward "penetration" by these placodes to take place. Once within the "potential space of the sphenoids," the adenohypophysis will ultimately be married up with the neurophypophysis from the caudal diencephalon. Neurohypophysis emerges from basal p1. It descends and is affixed to the posterior aspect of adenohypophysis. At this site, primitive tumors, such as *cra-*

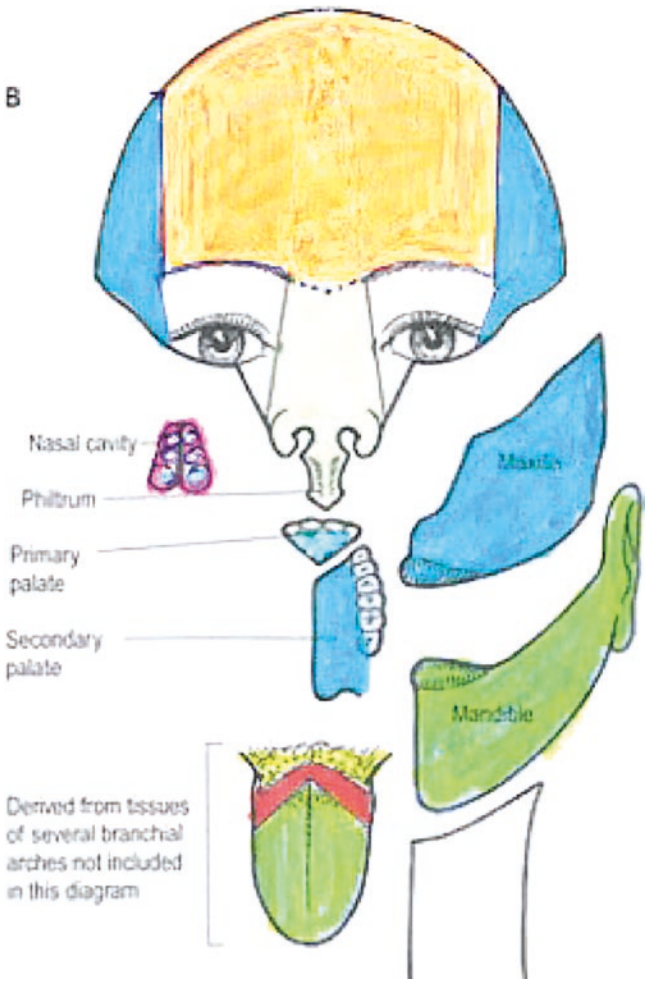

Fig. 2.49 Internal nose: lining (p6), superior and middle turbinates (r1), inferior turbinate (r2). Forehead (p4), external nose (p5). Medial and lateral nasal processes both p5 but induced by their respective half of the nasal placode. Upper eyelid and lacrimal skin (r1) with lower eyelid skin lateral to punctum (r2). Oral cavity floor: anterior 2/3 tongue from first arch (r3) abuts against posterior 1/3 from third arch (r7). Root of tongue fourth arch (r8) abuts against larynx r8–r9. Note: buccopharyngeal membrane separates first and third arches at tongue, anterior palatal pillars, and the proximal 1/3 of the soft palate. (B) Neuromeric derivations of craniofacial soft tissue structure (Reprinted from Standring S (ed). Gray's Anatomy. 40th ed. New York, NY: Churchill Livingstone; 2008. With permission from Elsevier)

Fig. 2.50 Rostral prosencephalic folds (zones p4–p6). The neural folds of the prosencephalon extend all the way forward from midbrain to neurohypophysis. Caudal folds over diencephalon have neural crest. Rostral folds over secondary prosencephalon have nonneural ectoderm bearing placodes but no neural crest cells. Most anterior folds can be mapped into p6 epithelium (red) surrounding the adenohypophyseal and nasal placodes, p5 epidermis (green) upper beak ectoderm, and p4 calvarial ectoderma (orange). Note the bulge of the optic vesicle just lateral to p5. Ectoderm from r1 is responsible for the epidermis of the upper eyelid and corneal epithelium. Neural crest from the caudal neural folds flows forward beneath the NNE in sheet-like fashion to create dermal substrate for frontonasal skin and the submucosa of the nasal vestibular lining. MNC flowing forward between brain and skin comes in contact with the nasal lining to form the sphenethmoid complex, nasal and lacrimal bones. (Courtesy of Prof. Kathleen K. Sulik, University of North Carolina)

niopharyngiomas, can bulge beneath the mucosa into the pharynx. At times, this can even disrupt palatal formation [77–80].

Nasal Placodes

Located more caudally along p6 neural folds, the nasal placodes contribute three separate sets of neurons that ultimately find their way to three different sites in the p6 telencephalon! Without this incorporation, areas of the basal forebrain (the rhinencephalon) are hypoplastic as in *Kallman syndrome* [81–83] (Fig. 2.53).

The anatomic fate of the nasal placode is determined by the furious proliferation of MNC around the placode which throws the surface ectoderm into relief. This produces as an elongation of the snout. It also results in an "invagination" of the nasal placode "backward" into the ethmoid mesenchyme, owing to its physical connection to the primitive basal forebrain, rhinencephalon. As the nasal placode is drawn inward, it pulls along with it the most distal zone of p5 nasal skin into the introitus of the nasal vestibule. In so doing, the p5 skin doubles back on itself. MNC associated with this skin is programmed by the *p5 intranasal dermis* to form the *lower lateral cartilage*. Further inward, MNC associated with *p6 vestibular lining* will form the upper lateral cartilage and septum. Note: Nasal bones should *not* be considered p5 derivatives. They are MNC derivatives programmed by p6 vestibular lining (Fig. 2.54).

Nasal placodes are essential to the formation of the nasal cavity. If a placode is aberrantly placed, *heminose* results with a tubular proboscis marking the ectopic placode. Complete absence of placodes causes arrhinia which can coexist with normal ocular development (Fig. 2.55) [84].

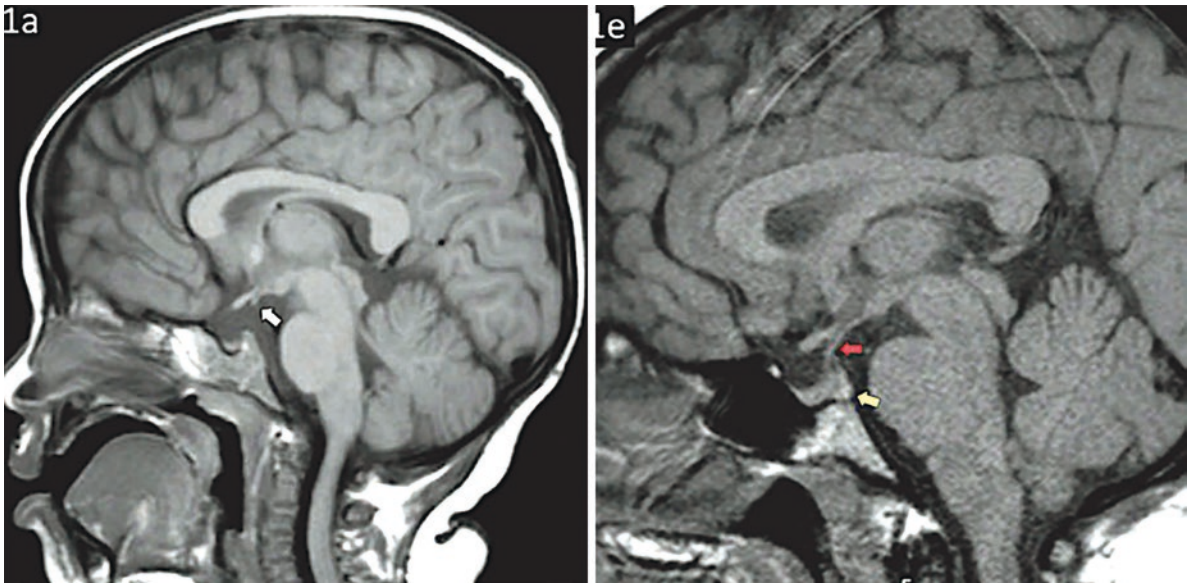

Fig. 2.51 Four-year-old male patient with congenital hypopituitarism presented as global developmental delay and growth retardation. Workup showed hormonal deficiencies and MRI abnormalities. (**a**) T1-weighted MRI shows partially empty sella turcica, pituitary stalk cannot be identified. Anterior pituitary tissue seen along the floor of the sella. The posterior pituitary is ectopic, seen as a 2 mm hyperintense nodule at the median eminence (white arrow). (**b**) T1-weighted MR shows normal 30-year-old patient are provided for comparison. Note the normal infundibulum extends from the hypothalamus to the pituitary gland (red arrow). Sella turcica is well-developed and contains both the anterior pituitary lobe and T1 hyperintense posterior pituitary lobe (yellow arrow). (Reprinted from Omer A, Haddad D, Pisinski L, Krauthammer AV. The Missing Link: A case of absent pituitary infundibulum and ectopic neurohypophysis in a Pediatric Patient with Heterotaxy Syndrome. J Radiology Case Reports 2017; 11(9): 28–38. DOI: https://doi.org/10.3941/jrcr.v11i9.3046. with permission from Journal of Radiology Reports)

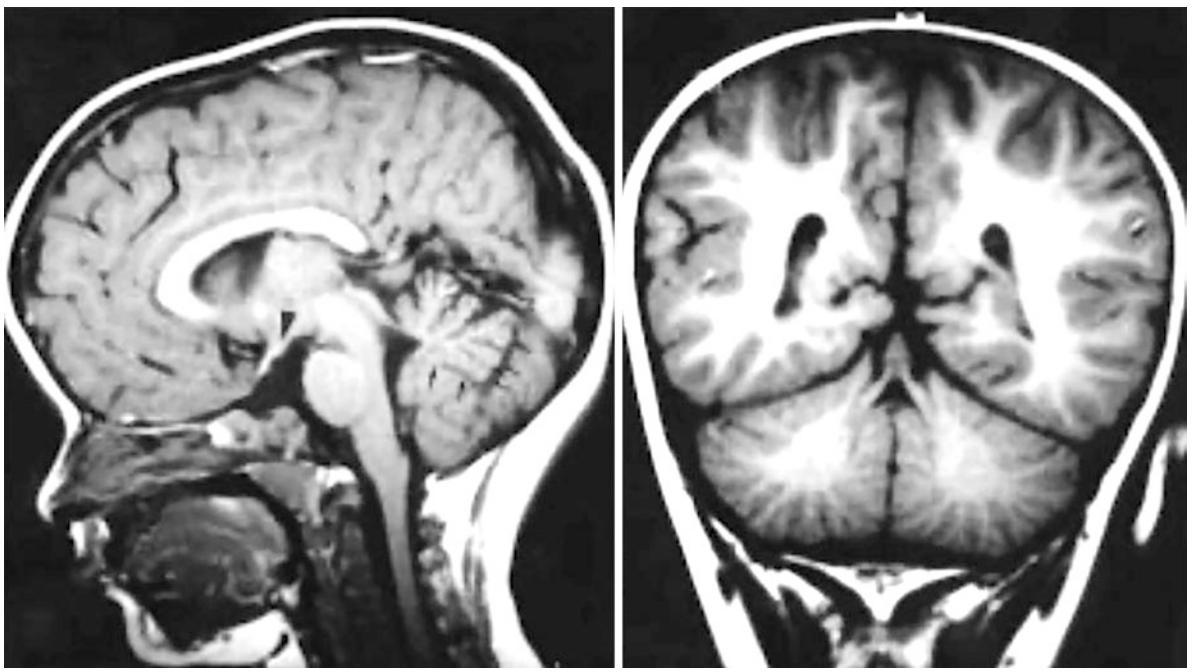

Fig. 2.52 Cerebellum arises from r0 to r1. Sella turcica arises from the same level. MR image shows cerebellar hemispheres are separated by a cleft because the posterior lobe of the vermis is absent. (Reprinted from L I Al-Gazali, L Sztriha, J Punnose, W Shather, M Nork. Absent pituitary gland and hypoplasia of the cerebellar vermis associated with partial ophthalmoplegia and postaxial polydactyly: a variant of orofaciodigital syndrome VI or a new syndrome? Journal of Medical Genetics 1999; 36(2):161–166. With permission from BMJ Publishing Group Ltd.)

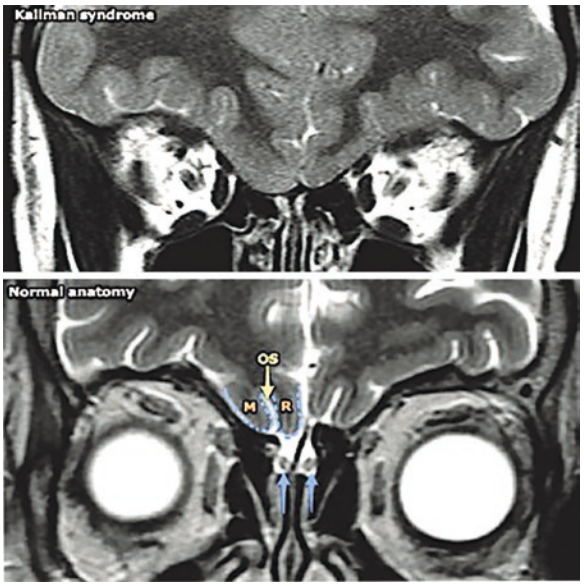

Fig. 2.53 **Kallmann syndrome** is a rare genetic disorder characterized by hypogonadotropic hypogonadism associated with anosmia or hyposmia. When anosmia is absent, a similar syndrome is referred to as normosmic idiopathic hypogonadotropic hypogonadism. MRI is the modality of choice in assessing for the absence of olfactory bulbs, and coro\nal T2 sequences are most effective. It is a rare disorder with an estimated prevalence of one in 10,000 males and one in 50,000 females. Although patients with Kallmann syndrome are anosmic from birth, this usually is not apparent to either the parents or the child. The diagnosis is only made when puberty does not occur. At that time gonadotropin levels (FSH and LH) and sex hormones (testosterone and estradiol) are low, whereas other pituitary hormones are normal. Associated findings include enlarged paranasal sinuses, small anterior pituitary, septo-optic dysplasia, CL/P, sensorineural deafness, and renal agenesis. The olfactory nerves, bulbs, and sulci are absent (arhinencephaly). Importantly the hypothalamus and pituitary are most often morphologically normal in appearance. However, the anterior pituitary can appear small. (Case courtesy of Assoc. Prof. Frank Gaillard, Radiopaedia.org, rID: 6083. https://radiopaedia.org/cases/6083/)

Optic Placodes

The placodes are located still more caudally along the prosencephalic neural folds, in zone p5. They are required for the proper formation of the eye, specifically the lens apparatus. In *aphakia*, absence of the placode, the globe has no lens. If the Pax-6 gene expressed by the placodes is more globally suppressed, the globe itself will be phthisic (shrunken), a condition known as microphthalmia or absent, resulting in anophthalmia (Fig. 2.56) [85].

Otic Placodes

The otic placodes develop from the neural folds of the hindbrain at neuromeres r4–r5. They share common characteristics with those of the forebrain and are therefore included here for the sake of completion. The otic placodes induce the cochlear and vestibular systems using mechanisms of mechanosensory hairs. Abnormalities of these structures are another form of neurocristopathy (Fig. 2.57) [86].

Blood Supply for Fronto-Orbital-Nasal Skin

Vascular development for FON skin takes place in two phases. Recall that, as a neuroepithelium, PNC has no intrinsic blood vessel-forming capacity. In the initial phase, invasive angioblasts create a primitive head plexus which surrounds the developing forebrain. The origin of these cells is unclear; they may come from the prechordal plate. In any case they provide the mesodermal substrate for the subdermal plexus. The subcutaneous plane is then populated by midbrain neural crest. This combination of mesodermal cells and neural crest cells forms a vascular head plexus. Neuroangiosomes from the StV1 system (lacrimal, supraorbital, and supratrochlear) connect with this plexus and provide stable support for the skin. Later on, as we shall see, the

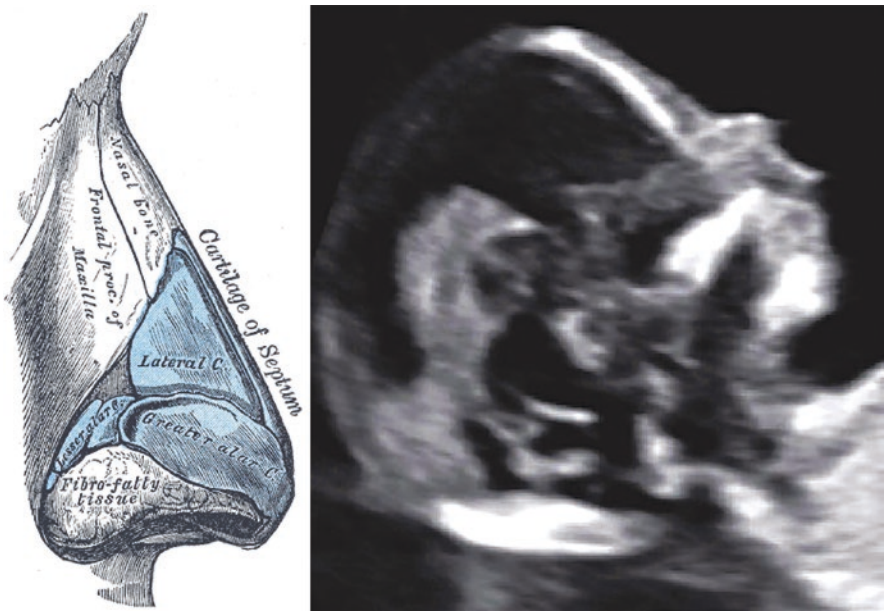

Fig. 2.54 Nasal bones and upper lateral cartilages are synthesized based on a program embedded in the underlying r1 vestibular lining. The lower lateral cartilages are programmed by the r2 skin. Hypoplastic nasal bones are seen in Down syndrome (43–62%). Absent nasal bones seen in trisomy 21 (60–73%), trisomy 18 (53–57%), trisomy 13 (32–45%), Turner's syndrome (9%). (Left: Reprinted from Lewis, Warren H (ed). Gray's Anatomy of the Human Body, 20th American Edition. Philadelphia, PA: Lea & Febiger, 1918, Gray fig. 582. Right: Case courtesy of Dr. Ayush Goel. Radiopaedia.org, rID: 54486. https://radiopaedia.org/articles/absent-nasal-bone)

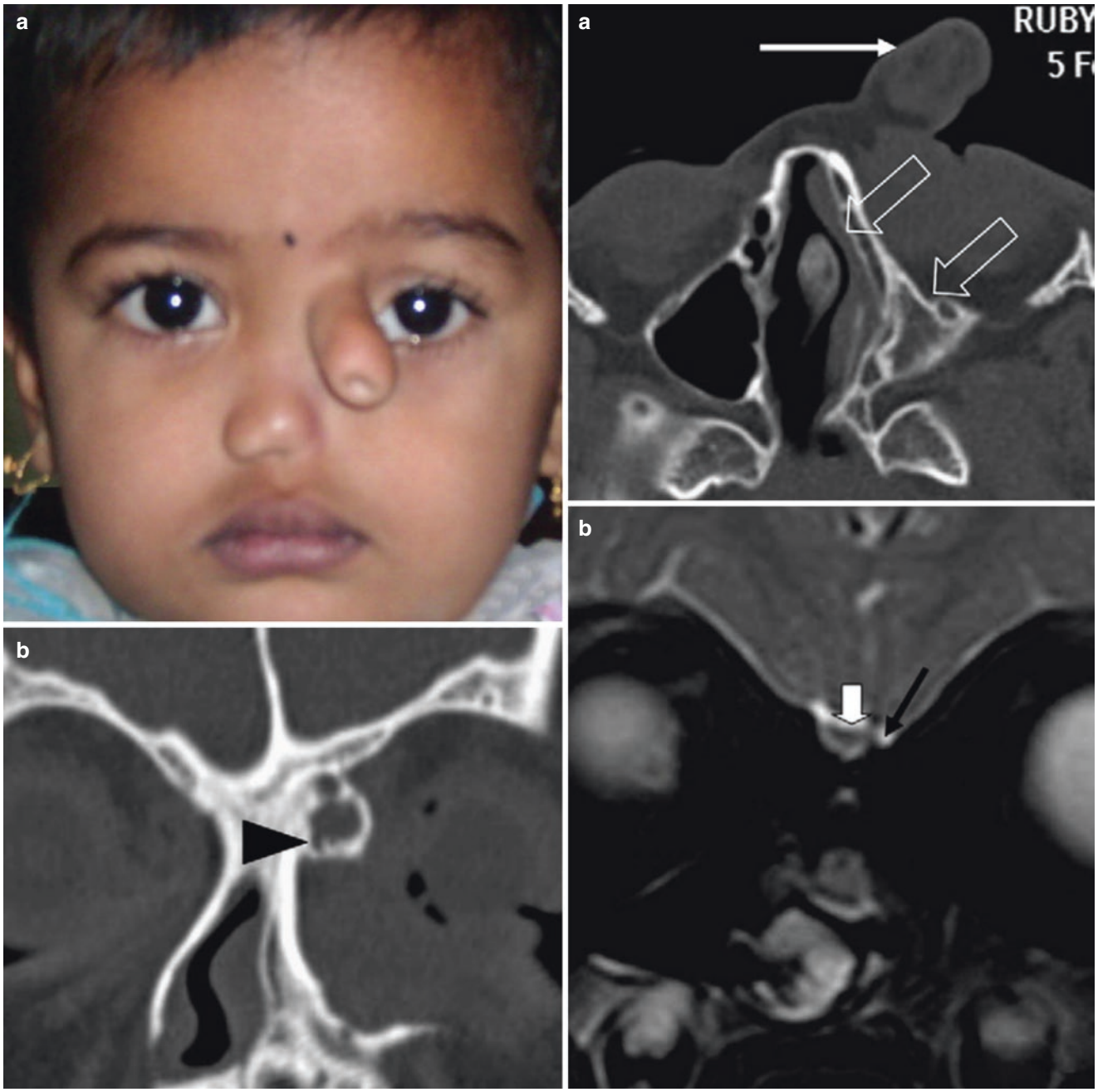

Fig. 2.55 Abortive development of left nasal placode proboscis lateralis in a 2-year-old girl with associated ipsilateral sinonasal aplasia, orbital cyst, absent olfactory bulb and olfactory tract. Ipsilateral olfactory pathway is missing. Upper left: Tubular trunk-like process arising from medial canthus of left orbit. Upper right: HRCT image (**a**) showing a tubular trunk-like process (white arrow) arising from superomedial aspect of the left orbit with aplasia of ipsilateral nasal cavity and maxillary/ethmoid sinuses (open arrows). Note septum pulled over to the left. Lower left: Coronal HRCT image (**b**) shows well-formed bony canal in superomedial compartment of the left orbit (black arrowhead). Lower right: normal right olfactory bulb and groove (white block arrow) and hypoplastic left olfactory groove with absent left olfactory bulb (black arrow). (Reprinted from Vaid S, Shah D, Rawat S, Shukla R. Proboscis lateralis with ipsilateral sinonasal and olfactory pathway aplasia. J Pediatric Surg 2010; 45: 453–456. With permission from Elsevier)

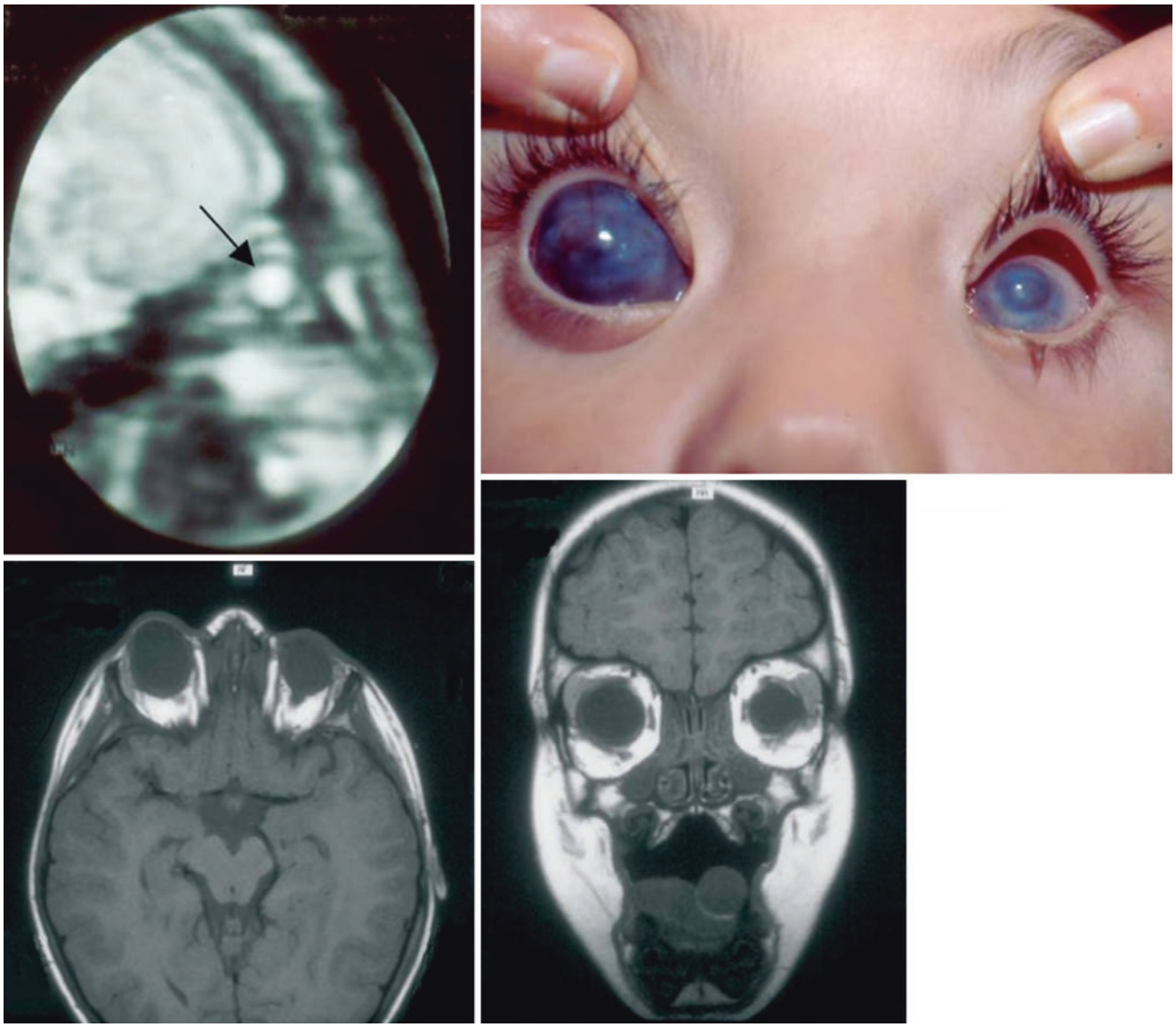

Fig. 2.56 Congenital primary aphakia (CPA) consists of absence of a lens, induction of which takes place in weeks 4–5, causing complete aplasia of the anterior segment (the diagnostic histologic finding in CPA). Primary (congenital) aphakia can occur in isolation or as part of a complex anterior segment abnormality, i.e., microphthalmia, absence of the iris, anterior segment aplasia, and/or sclerocornea. Absent placode at 4–5 weeks prevents the formation of any lens structure in the eye. This leads to complete aplasia of the anterior segment, Secondary aphakia is characterized by absorption of the lens after it is formed. The causation is unknown but may involve a mutation in the *FOXE3* gene. Upper left: MRI of 28.5 week fetus showing eyeball as white sphere without the lens, normally seen inside as a black sphere. Upper right: 1 month baby with left-sided microopthalmia and right-sided CPA. Lower left and right: axial and coronal MRI of 4-year old demonstrating bilateral microopathalmia and right-sided aphakia. The brain tissue is otherwise normal. (Reprinted from Valleix S, Niel F, Nedelec B, et al. Homozygous nonsense mutation inf the FOXE3 gene as a cause of congenital primary aphakia in humans. Am J Hum Genet 2006; 79(2): 358–364. With permission from Elsevier)

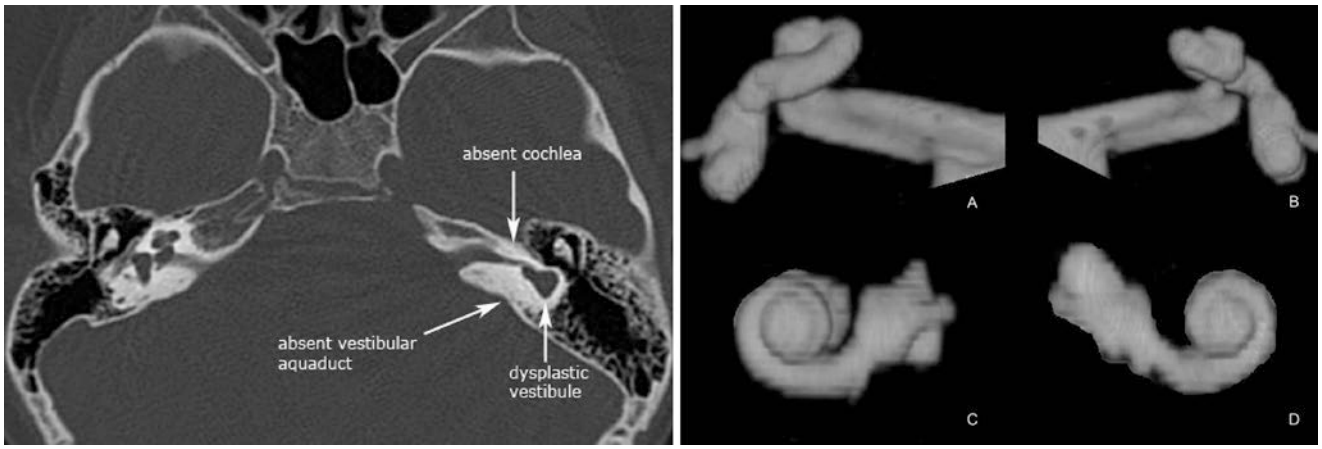

Fig. 2.57 Michel Syndrome. Absent/hypoplastic otic placode follows a sequence: 3–4 weeks: Michel (complete labyrinthine aplasia). 4–5 weeks: cochlea and vestibular system confluent. 5–6 weeks: cochlear aplastia/hypoplasia (vestibular system forms earlier and is spared). Left: Michel syndrome (oculopalatalskeltal). Right: unilateral SCC hypoplastic (left side with intact cochlea and hearing loss). (**a**) Superior left, (**b**) lateral left, (**c**) superior right, (**d**) lateral right. (Left: Reprinted from Wikimedia. Retrieved from: https://en.wikipedia.org/wiki/Michel_aplasia. With permission from Creative Commons License 1.0: https://creativecommons.org/publicdomain/zero/1.0/deed.en. Right: Reprinted from Breheret R, Brecheteau C, Tanguy J-Y, LacourreyeL. Bilateral semicircular canal hypoplasia European Annals of Otorhinoloaryngology, Head and Neck Diseases 2013; 130:225–228. With permission from Elsevier)

MNC plane is invaded by facial muscles from the second arch that are supplied by laterally based vessels of the facial artery system. This arrangement permits elevation of skin flaps from above the muscle plane based on their vascular pedicles.

MNC Schizophrenia

PNC does not have the capacity to form bone or cartilage. What the skin envelope does have is the "template" of information that instructs underlying substrate to produce bone. The mesenchymal "raw materials" necessary for the synthesis of all cartilage and bone structures of the nose, eyes, anterior cranial fossa, and sphenethmoid complex come from midbrain neural crest. But the instructions for bone formation reside within the epithelial structures of the brain and skin. MNC mesenchyme must obey orders from two different masters and therefore splits into two laminae.

- Epidermis/dermis induces outer ectomeninx to produce frontal bone.
- Brain tissue induces inner endomeninx to make dura.

Recall that membranous ossification requires a "*stimulating mesenchyme*" (neural crest dura or dermis) that contains a genetic program for the bone and a "*responding mesenchyme*" (neural crest or PAM) that forms the bone itself. Recall that neural crest, by virtue of being both epithelial and mesenchymal, can serve an epithelial function. In some parts of the skull, a responding mesenchyme may be sandwiched between two layers of stimulating ectoderm or endoderm. *Bilaminar* membranous bone formation occurs. In the calvarium, the interface between the laminae constitutes a potential space that is later manifested as a *diploic space* [87]. This model for bilaminar bone fields explains the anatomy of the *sinuses of the skull*. These occur at sites where mucosa from oropharyngeal cavity has anatomic access to that potential space. By exploiting field separation planes, the mucosa will expand into the frontal, ethmoid, sphenoid, and mastoid bones to create their respective sinuses, *but it will never transgress a neuromeric boundary*, i.e., a suture.

All calvarial bones formed by neural crest and PAM cranial to the first motion segment (r11–c1 junction the proatlas) are *segmental*, i.e., the bone boundaries correspond to neuromeres. At the craniocervical junction, vertebrae become, for the first time, *parasegmental*, i.e., each vertebral body results from contributions of the caudal somite above and the rostral somite at that level.

Forebrain Neural Crest Migration

The neural folds of the anterior secondary prosencephalon (zones p4–p6) contain nonneural ectoderm; they do not have neural crest. PNC develops from the neural folds of the posterior secondary prosencephalon (zones p1–p3). It then migrates forward into the FNO in caudal-to-rostral process. That is, it proceeds forward away from the midbrain. PNC cells come in, like guided missiles, seeking "target zones" of nonneural ectoderm: the calvarial epithelium, the optic placode, the upper beak epithelium, the nasal epithelium, the nasal placode, and the adenhypophyseal placode. In every case, the migration of PNC involves a succession of lateral-to-medial cell movements, each zone advancing further forward, building upon its predecessor. Thus, the flow of PNC through prosomeric zone p4 is forward and medial; each zone of p5 is "newer" than its predecessor. Neural crest entering the sixth prosomeric zone is the most recent of all.

Fig. 2.58 Multiple displaced nasal placodes. Right side with double nostril and left side interorbital position. Note left #10 zone cleft affecting upper eyelid and orbit with concomitant hairline abnormality. (Reprinted from NIH National Library of Medicine Images. Retrieved from: https://openi.nlm.nih.gov/imgs/512/315/3119293/PMC3119293_MEAJO-18-192-g001.png)

Pathologic correlations follow from this anatomy:

1. Placodes can be defective per se due to the dysgenesis of NNE itself.
   - Selective neuroepithelial defects in either the lateral or medial half of the nasal placode can lead either to *anosmia* or to *Kallman's* syndrome.
2. Placodes can also be dysfunctional due to failure to properly interact with PNC.
3. Placode pathology can be unilateral or bilateral.
4. Pathology in one placode may not necessarily affect other placodal zones.
   - Isolated failure of AP, with consequent pituitary insufficiency, can occur in the presence of a normal face.
   - Nasal placode defects resulting in *heminose* or *arhinia* can occur in the presence of a normal eye.
   - Defects in the activity of *Pax-6* may affect the ability of the optic placode to form a lens with the nose remaining normal.
5. Placodes also affect surrounding structures.
   - The nasal placode is required for creation of a nasal passage within the underlying MNC of the ethmoid complex.
6. Finally, multiple placode dysfunctions may occur in the presence of an underlying vascular sequence, such as in complex *craniofacial clefts* (Fig. 2.58).

Development of Frontonasal Bone and Skin: Prosomeric Zones p4 and p5

Development of the frontal bone will be discussed in detail in the osteology chapter. For now, suffice it to say that the frontal bone in an MNC derivative is defined by two distinct sets of fields. The upper (forehead) component is defined by zone p4 *calvarial epithelium*. MNC in this zone is programmed by forebrain dura and forehead skin. The lower (supraorbital) component is defined by zone p5 *perioptic epithelium* surrounding optic placode. MNC in this zone gets its program from the dura of the floor of the anterior cranial fossa, the sclera (an) extension of dura, and caudal forehead skin.

Frontal bone anatomy is thus complex. The upper zone (frontal bone proper) is bilaminar and occurs between two inductive substrates of dermis and rostral forebrain dura. The lower zone (fronto-orbital bone) is also bilaminar, but from different sources: it occurs between the inductive substrates of basal forebrain dura, the periocular extension of dura (i.e., sclera), and p5 skin. Sclera is an MNC tissue. These differences in induction are demonstrated in anencephaly, an r1 deficiency state that always deforms the sphenoid, but has a selective effect on the frontal bone, wiping out the upper zone while sparing the lower zone. The presence of normal orbital and nasal structures seen anencephaly bespeaks of the interactions and reflects of a second and independent source of programming for frontal bone.

Frontal bone development in zones p4 and p5 can be summarized as follows. This bone is a composite structure considered by many comparative anatomists to represent the amalgamation of previous distinct membranous bones in ancestral tetrapods. The first zone of formation of the prefrontal zones occurs from lateral-to-medial to producing *postfrontal bone* (PF) and *prefrontal bone* (PrF). The orbital rim zones may thus represent the previously separate medial and lateral prefrontal bones, separated by the supraorbital neurovascular of V1. Neural crest then stacks up beneath the calvarial epithelium. Ossification of the orbital rims takes place before that of the frontal tubers. This could likely result from two factors: (1) periorbital MNC migration is complete before that of the forehead, or (2) ascending pathway of the arterial axis provides blood supply to the orbit and then to the frontal zone.

MNC in zone p4 occupies a potential space between two osteoinductive substrates: the *r1 dura* over the frontal lobes and *p5 dermis*. Each of these layers will induce membranous osteogenesis to take place in the residual mesenchyme creating a bilaminar frontal bone with sinus cavities. This potential space communicates with the nasal cavity via the frontonasal duct. When the nasal epithelium invades and exploits that potential space, the *frontal zone of the frontal sinus* results.

MNC in zone 5 has a similar fate. It is programmed by r1 dura of the anterior cranial fossa and r1 sclera, so a potential

space exists for an orbital zone of the frontal sinus in communication with its predecessor. Let's examine how this process works.

PNC flows around the *optic placode* (OP) and causes it to become "activated." Interaction between the optic placode and the optic vesicle induces the latter to form the *optic cup* into which the placode is incorporated as the lens. At the same time, placodal neural crest mesenchyme flows inward to surround the globe. This neural crest is stimulated to form membranous bone by the dura of the basal forebrain laid down previously by r1 MNC. This can be called the *cranial lamina of the front-orbital bone*. At the same time, r0/r1 dura/sclera associated with the globe serves as an inducing agent causing placodal p5 neural crest to form a transient cartilaginous orbital capsule surrounding the globe. (In birds, this forms a ring of chondral bones arranged much like ball bearings around the orbital rim.) In mammals, the orbital capsule is converted into the *orbital lamina of the fronto-orbital bone*. Exploitation of the potential space between these two layers by nasal epithelium results in the *orbital zone of the frontal sinus*.

Note that dysgenesis/agenesis of the optic placode have manifestations in the development of the globe itself. These can be isolated and total such as *anophthalmia* or partial such as loss of the lens in *congenital aphakia*.

The neural crest making up the two laminae of the fronto-orbital bone is divided into two bone fields by the supraorbital neurovascular pedicle. The lateral *postfrontal bone* field (PF) is the site of the Tessier #10 cleft. Frontal sinus pneumatization usually does not extend into this zone, hence PF tends to be very thin. This may explain why clefts in this zone present as an *encephalocele* herniating through the orbital roof into the lateral orbit. PF of the lateral orbital rim is in continuity with postorbital bone of the lateral orbital rim; therefore, zone 10 clefts tend to affect the lateral eyebrow. Dermoid cysts are common here as well (Fig. 2.59) [88, 89].

The medial *pre-frontal* bone field (PrF) is the site of the Tessier #11 cleft. This zone is always pneumatized. Perhaps this is why encephaloceles are not as common here. PrF of the medial orbital rim is in continuity with the nasal process of frontal bone. Therefore, zone 11 clefts tend to affect the medial eyebrow. Orbital dermoid can occur here as well. Neural crest excess or tumors in either zone of the fronto-orbital rim can result in significant *orbital dystopia*.

The final r1 product within the orbit is the *lacrimal bone*. This bone sits anterior to orbital plate of ethmoid. A medial extension of r2 called the *frontal process of the maxilla* (MxF) forms the most medial aspect of the inferior orbital rim and approaches L, but must straddle around the lacrimal

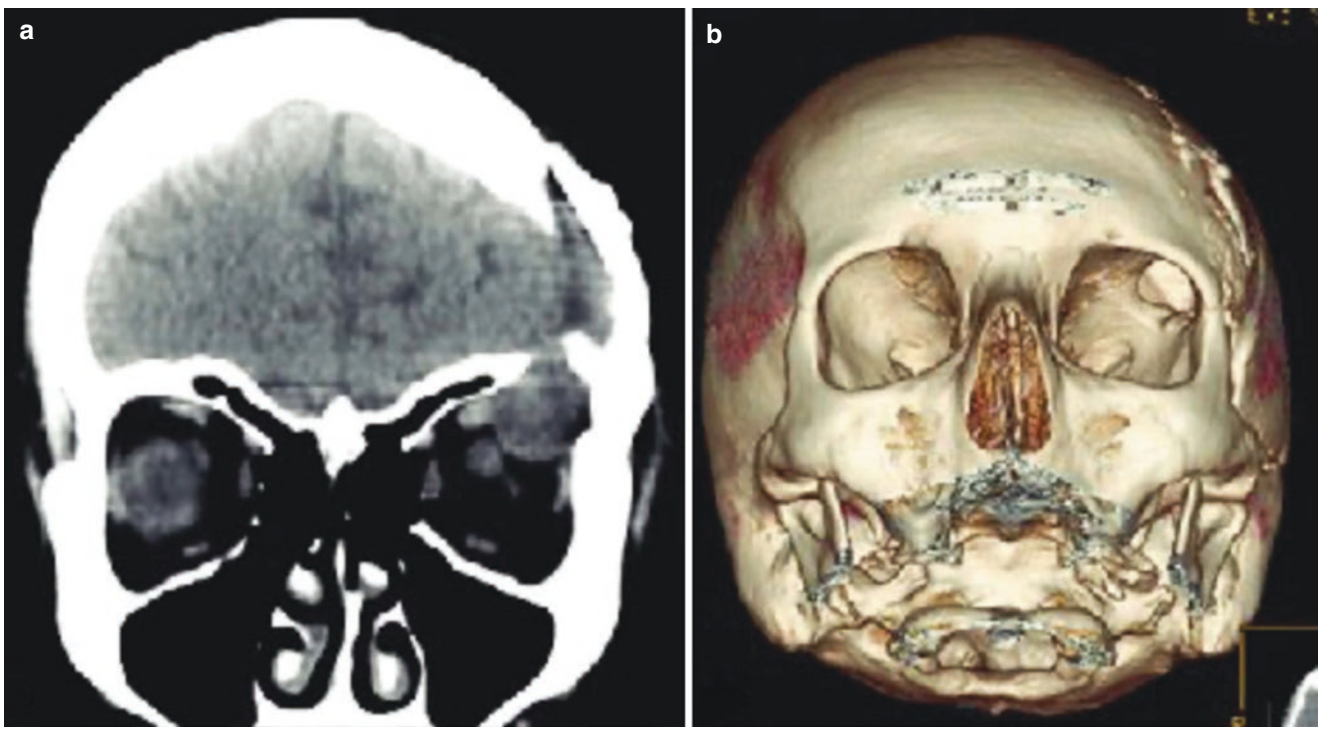

Fig. 2.59 Orbital roof encephalocoele. Lateral orbital roof (zone 10) corresponds to the lateral prefrontal bone field. Defects in this zone allow for the herniation of the brain into the orbital. (Reprinted from di Somma L, Iacoangeli M, Nasi D, Balercia P, Lupi E, Girotto R, Polonara G, Scerrati M. Combined supra-transorbital keyhole approach for treatment of delayed intraorbital encephalocele: A minimally invasive approach for an unusual complication of decompressive craniectomy. Surg Neurol Int Suppl 1, 2016;7(2): S12–S16. With permission from Surgical Neurology International)

sac to reach it. MxF accomplishes this goal by producing two tongues of mesenchyme, anterior and posterior. Where these contact the lacrimal bone, *the anterior and posterior lacrimal crests* are produced. The lacrimal bone extends caudally downward from the orbit as a lamina that terminates just lateral to the inferior turbinate. Lacrimal bone is bilaminar, being programmed externally by p5 and internally by p6 vestibular lining. *The space between these two laminae (r2 medial and r1 lateral) is exploited by mucosa to form the lacrimal sac and duct*. The proper formation of the lacrimal bone is dependent on the physical integrity of the r2 inferior turbinate. If no IT is present, the caudal portion of lacrimal will be deformed or absent. On the other hand, excessive neural crest in the lacrimal field or failure of this field to undergo appropriate apoptosis may result in *lacrimal duct stenosis* or frank *obliteration* of the lacrimal sac.

The skin covering the nasal dorsum and extending down to the columella and philtrum is constructed from p5 nonneural ectoderm populated by PNC and supported by MNC. In birds, this is known as the *upper beak epithelium* (UBE). In mammals, the external nasal skin is continuity with that of the internal nasal skin (nasal vestibular epithelium). Within each nostril, the boundary between p5 skin and p6 vestibular epithelium is readily visible; it lies at the caudal margin of the upper lateral cartilage.

Coda: Additional pathologies of frontal p5 would have to include states of developmental deficiency or excess. *Anencephaly* separates the p4 upper calvarial component of frontal bone from existence of independent p5 prefrontal and postfrontal bone fields of the orbital roof and rim. Clinically, it is manifested as gross absence of the frontal bone in concert with loss of forebrain dura; at the same time, the orbital rims and the remainder of the face are preserved [90–97] (Fig. 2.60). Mesenchymal excess is illustrated by *frontonasal dysplasia* [98–102] (Fig. 2.61). These conditions demonstrate the p5 fields to be shield-shaped with distinct manifestations in the skin. Bone abnormalities in this condition reflect MNC populations that are distinct for that of the sphenethmoid complex. On the other hand, failure of normal process of apoptosis of the entire MNC sphenethmoid complex creates a state of residual excess termed *hypertelorism* with stretched and distorted sphenethmoid fields accompanied by otherwise normal frontal bone fields and frontal lobes [103, 104]. Surgical correction of hypertelorism corrects a physical deformity that is superimposed on an otherwise normal CNS [105, 106] (Figs. 2.62 and 2.63).

- In sum: p4 and p5 nonneural ectoderm is supported by a glacier-like migration of PNC forward from the caudal secondary prosencephalon which reaches the facial midline via successive waves of lateral to medial migration, each more distal, anterior, and midline than its predecessor. The order of formation of p5 components is as follows: orbital rim (postfrontal, prefrontal, nasal process of frontal bone), a separate frontal bone, optic placode flanks by orbital rim of prefrontal and postfrontal bones, labyrinth, and nasal. These are Tessier clefts #10, #11, #12, and #13.

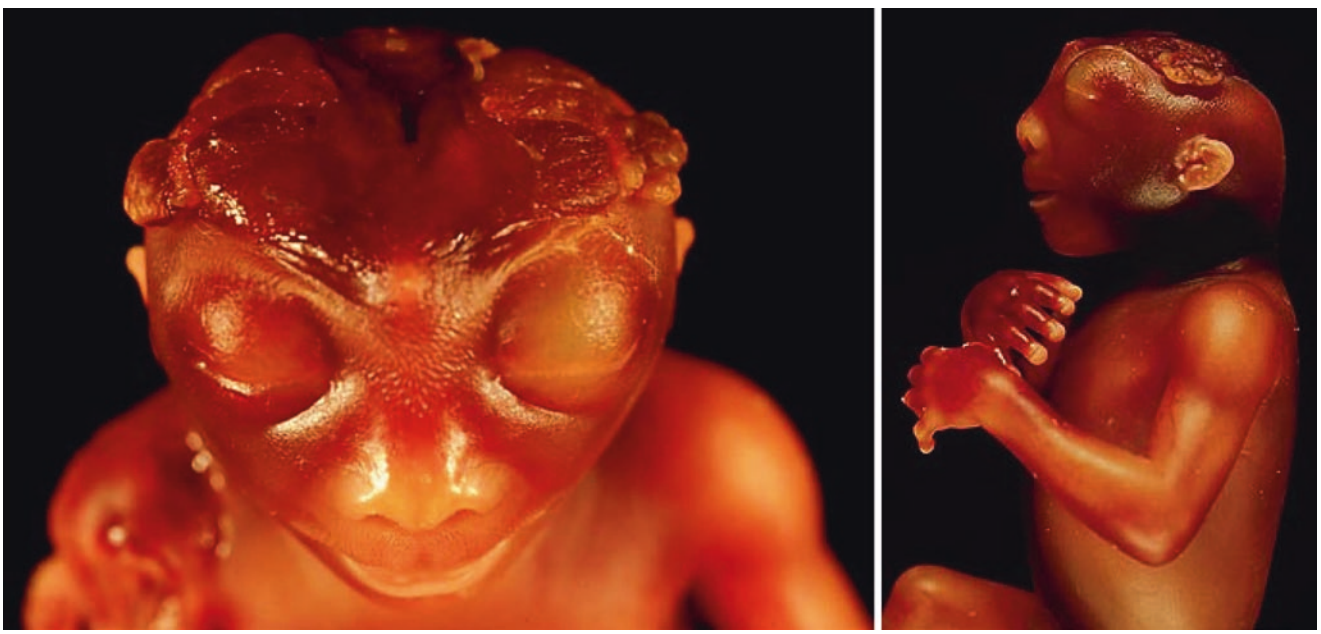

Fig. 2.60 Anencephaly. Note the recessed surface areas of zones 10 and 11. (Left: Reprinted from Wikimedia. Retrieved from: https://commons.wikimedia.org/wiki/File:Anencephaly_front.jpg. Right: Reprinted from Wikimedia. Retrieved from: https://commons.wikimedia.org/wiki/File:Anencephaly_side.jpg)

Fig. 2.61 Frontonasal dysplasia and hypertelorism. Hypertelorism reflects inadequate apoptosis of the central ethmoid fields. It is seful to examine the ethmoid sinuses to see if they are broadened. This condition involves r1 neural crest cranial bone and neural crest midline soft tissues over the nose. (Reprinted from Sin Young Song, Joon Woo Choi, Han Wook Lew, Kyung S Koh. Nasal reconstruction of a fronto-nasal dysplasia deformity using aesthetic rhinoplasty techniques. Arch Plast Surg 2015; 42(5): 637–639. With permission from Archives of Plastic Surgery)

Fig. 2.62 Severe hypertelorism and vertical deficit in zone 11 affecting lateral branch of external nasal field and causing retraction of the alae upward and the medial brow pulled downward. Note notches in the nasal alae. Columella is virtually absent. (Courtesy of Prof. Dr. S. M. Balaji, MDS)

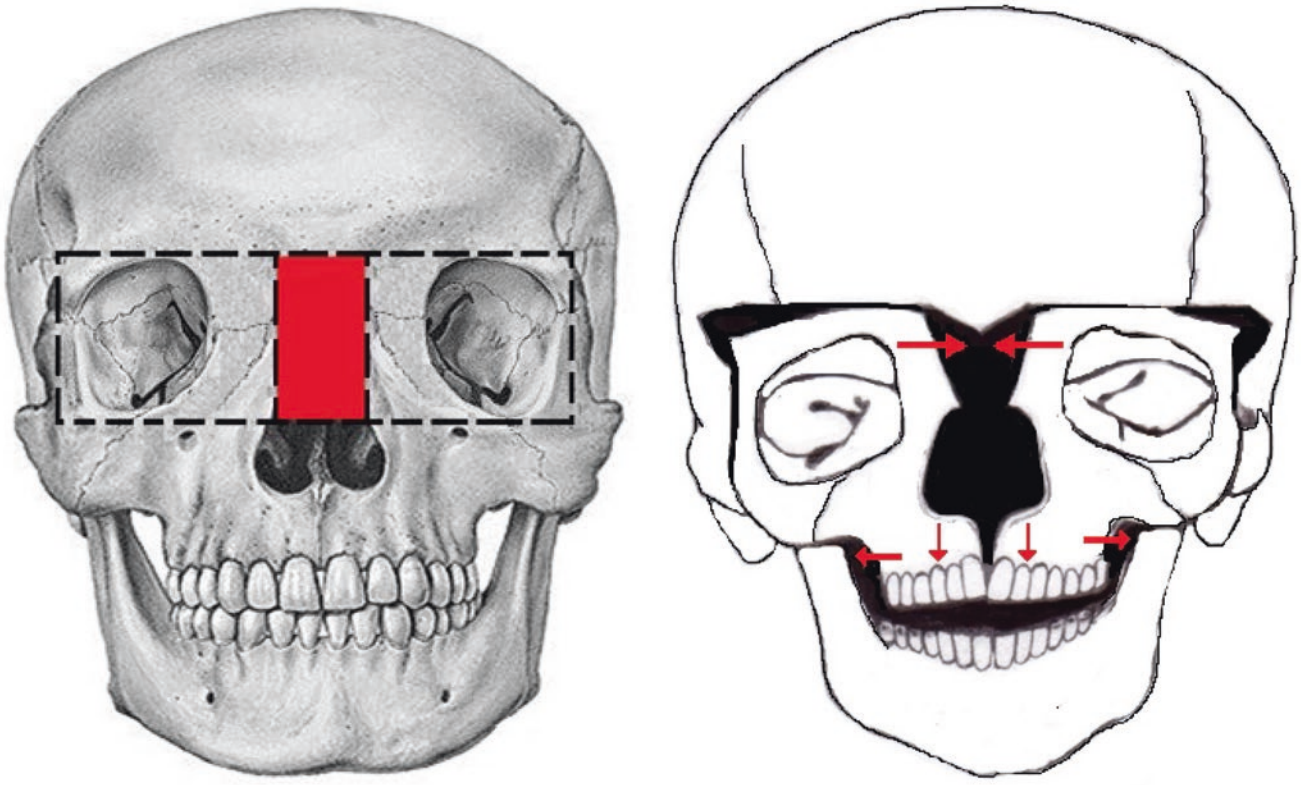

Fig. 2.63 Box osteotomies pioneered by French surgeon Paul Tessier resolved the issue of mesenchymal excess in zones 13 and 12. Hypertelorism affects ethmoid fields in two dimensions: transverse excess and possible vertical deficiency. Surgical correction of hypertelorism recognizes the excess mesenchyme in the ethmoid fields. Choice of procedure depends, in part, on the existence of vertical foreshortening affecting the palate. Left: "box" osteotomy. Right: facial bipartition. (Left: Reprinted from Wikimedia. Retrieved from: https://commons.wikimedia.org/wiki/File:Picture_box_osteotomy.jpg. With permission from Creative Commons License 3.0: https://creativecommons.org/licenses/by-sa/3.0/deed.en. Right: Reprinted from Wikimedia. Retrieved from: https://commons.wikimedia.org/wiki/File:Picture_median_fasciotomy.jpg. With permission from Creative Commons License 3.0: https://creativecommons.org/licenses/by-sa/3.0/deed.en)

Naso-Oral Lining, Nasal Bones, and Nasal Cartilages: Prosomeric Zones p6–p5

The nonneural ectoderm of the sixth prosomere has three subzones: the *adenohypophyseal placode* (AP), i.e., the pituitary, the *nasal epithelium* (NE), and the *nasal placode* (NP). We shall see how the nature of the placodes, coupled with the proliferation of surrounding MNC mesenchyme, leads to the formation of bilateral nasal chambers. The vestibular epithelium lining the nasal chambers all the way backward from the vibrissae located at the lower border of the upper lateral nasal cartilages is of p6 derivation, whereas the remaining external to the vibrissae is p5 skin.

We shall also see that two factors influence how both sides of the face approximate each other in the midline: (1) the pattern of closure of the rostral neuropore and (2) the natural apoptosis of MNC nasoethmoid mesenchyme. Defects in the former can produce encephalocoels, while defects in the latter cause hypertelorism [107, 108].

Along with proliferation of the brain, mesenchymal structures are also being positioned. The developing eye is tucked directly beneath somitomeres 1–3, providing easy access for the myoblasts of the extraocular muscles to reach their scleral targets. Recall that the eye projects initially 90° from the neuraxis. Hence, the most caudal aspect of the globe is the *lateral sclera*. This is spatially positioned close to the fifth somitomerewhich obligingly sends out lateral rectus. Meanwhile, the fourth somitomere is positioned just posterior to the AP, where it forms the basisphenoid.

At the same time, r1 neural crest invading anterior to AP forms the trabecular and nasal cartilages. Trabecular cartilage gives rise to presphenoid bone and subsequently the remainder of the sphenethmoid complex. The sphenoid sinus occupies the interface between PS and BS These mesenchymal tissues force the adenohypophyseal placode to assume new position facing ventrally within the future pharynx. Work by Kjaer demonstrates that basisphenoid (BS) always forms before presphenoid (PS). This is consistent with the idea that somitomeres are closely apposed to the neuraxis and develop earlier in time compared with neighboring neural crest populations.

A similar process explains how the p6 nasal epithelium gets drawn inside the nasal chamber. The traditional view holds that ingrowth of the nasal placodes, a "burrowing" into the underlying MNC ethmoid complex, is responsible for forming the inner nasal architecture. Persistent placodal neuroanatomic connection to the rhinencephalon of the p6 basal forebrain is the key element here. Explosive expansion of MNC beneath the nasal skin forces the nose to grow *outward* from the face. The adhesion of the p6 nasal placode to the brain is so strong that the nasal epithelium is drawn inwards. At the same time, placodal traction may be responsible neuroectodermal tissue being drawn out from the central nervous system as the olfactory bulbs. Alternatively, placodal structure may simply contain the cell adhesion molecules required for neuronal growth.

Formation of Nasal Cartilages: Prosomeric Zones p6–p5

Zone of p5 nonneural ectoderm is known as *upper beak ectoderm* and becomes the nasal skin. It surrounds nasal placode and proliferates, causing the nasal placode to become internalized. This draws epithelium inside the naris where it become *nasal vestibular epithelium* (NE). When MNC migrates into the nasal tissues, it follows the subcutaneous plane. Later, SMAS fascia lies superficial to it. Inside the naris MNC is contact with skin proximal to the external nasal valve and with vestibular lining distal to the valve.

Every rhinoplasty surgeon takes advantage of this embryology. The upper lateral cartilages are derived exclusively from MNC programmed by p6 vestibular lining. *The actual "program" that determines the size and geometry of the nasal cartilages resides in the p6 NE*. In a similar manner, the lower lateral cartilages are MNC structures programmed by the p5 epithelium. The nasal epithelium dictates to the neural crest exactly where to make the cartilages. For this reason, *variations in vestibular lining may explain differences in size or angulation of the nasal cartilages*. Deficiency states of the p6 nasal fields would explain the clinical picture of *short nasal bones* described by Sheen (Fig. 2.64) [109–111].

Note that septum is an MNC structure programmed by a sandwich between two walls p6 vestibular lining brought together by the programmed death of ethmoid tissue. The floor beneath the septum consists of fused vomerine bone fields of the medial nasopalatine neuroangiosome. The septum develops temporally after the perpendicular plates. In holoprosencephaly MNC, ethmoid tissue is affected: the perpendicular plate and the septum can be completely absent. This is accompanied by absence of the vomer/premaxilla resulting in wide bilateral "cleft." In less severe states, the septum and premaxilla may be attenuated. On the other hand, a widened *bifid septum* results if failure of normal midline apoptosis resulting in persistent MNC mesenchyme prevents approximation of the nasal and optic fields (Fig. 2.65) [112].

Prior to closure of the rostral neuropore (RNP), the two potential nasal cavities are widely separated. The remnant of the RNP is the *foramen cecum* (just above the nasal bones). Recall that closure of the neural folds concludes neurulation. This process is initiated at the fourth occipital somite, i.e., at the 11th rhomobomere. From that direction, closure pro-

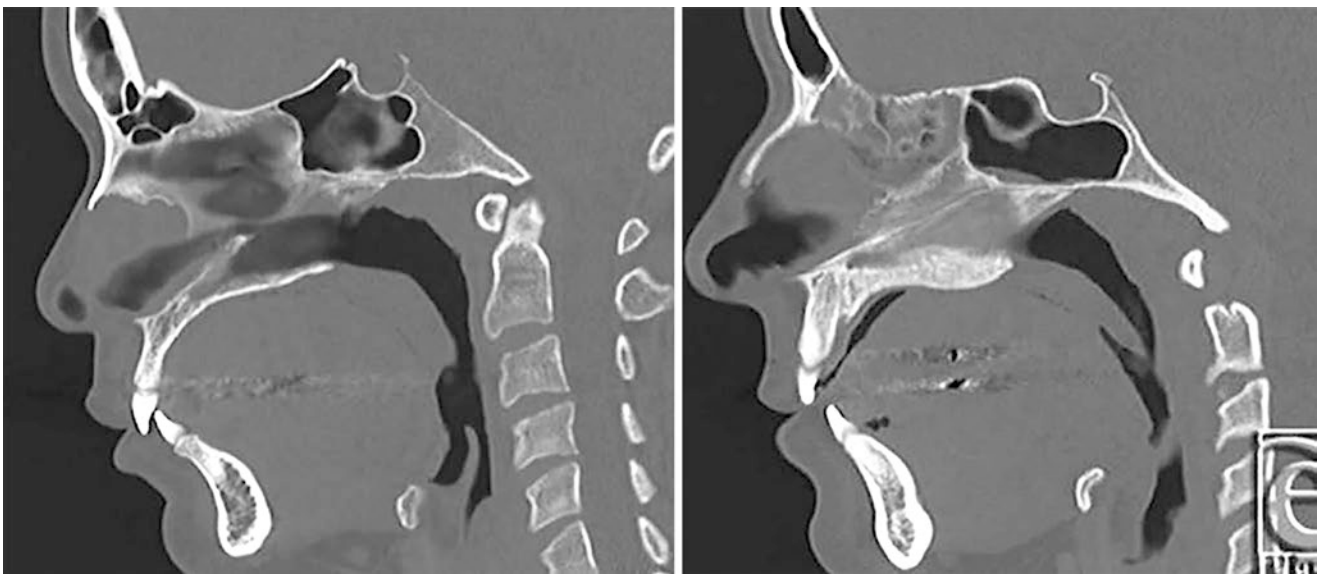

Fig. 2.64 Short nasal bones. (Reprinted from Mowlavi AS, Chamberlain TL, Melgar A, Talle A, Saadat S, Sharifi-Amina S, Willhelmi BJ. Upper Vault Septal Anatomy and Short Nasal Bone Syndrome: Implications for Rhinoplasty Eplasty 2018; 18: e29. With permission from ePlasty)

Fig. 2.65 Bifid nasal septum. (Reprinted from Karakor-Altuntas Z, et a. Isolated Congenital Nasal Bifid Septum Separated by a Wide Layer of Soft Tissue. Arch Plast Surg 2015; 42(5): 640–642 With permission from Archives of Plastic Surgery)

ceeds both rostrally and caudally. Closure of the rostral neuropore occurs *one stage before* that of the caudal neuropore. However, closure of the RNP is a *bidirectional* process. Starting from the adenohypophyseal placode, closure is directed *backward*. Rostral to the RNP, the pattern of closure is directed *forward*. These two "zippers" meet at nasofrontal foramen. Defects in this process may lead to a patent foramen cecum and the development of dermoid, encephalocoele or *glioma* (Fig. 2.66).

No nasal chamber can be constructed without a placode. Unilateral or bilateral absence of placodes is the developmental basis for hemi-nose or *arrhinia* [113–119]. The high position of the single nasal placode seen in *ethmocephaly or cyclopia* can be understood in terms of a gross deficiency of p5 mesenchyme [120–122]. In this contracted state, the nasal placode is drawn up to the position of the RNP and therefore appears above the common orbit (Fig. 2.67).

When PNC populates the *nasal placode* (NP), it initiates within the NP three neuronal populations. The lateral zone contains neurons of the olfactory system. These process odors. The medial zone contains neurons of the accessory olfactory system. These process chemicals such as pheromones. Also contained in the medial zone are neurons associated with release of gonadotropin releasing hormone (GnRH). Each set of neurons is relayed to separate areas of the frontal and temporal lobes. These pathologies are well-illustrated in Kallman syndrome [81].

Deep to the fifth and sixth prosomeric zones lies a vast deposit of midbrain neural crest that forms the sphenethmoid complex, nasal bones, nasal cartilages, and septum.

Mesencephalic Neural Crest Derivatives

Definition of MNC: Mesomeres m1–m2, Rhombomeres r0–r1

Midbrain neural crest has a rather loose definition because, from a functional standpoint, its sources include the most anterior zone of hindbrain. It develops from neuromeres m1, m2, r0, and r1. Midbrain proper has two mesomeres, m1 and m2, with the first mesomere being much larger in size than m2. Known contents of m1 are separate colliculi (hills) for vision and hearing, and two distinct nuclei for cranial nerve III. The *presisthmic tectum*, m2, develops as a subdivision of m1. Its anatomic contents are unclear.

The *isthmus* forms the junction between midbrain and hindbrain. Isthmus is coded r0 and is much smaller than first rhombomere r1, which contains the nucleus of IV. Isthmus is also in direct contact with the midline prechordal mesoderm. Isthmus develops as an anterior subdivision of r1. It contains the decussation of trochlear nerve IV.

For purposes of our discussion, the two populations of greatest interest are m1 and r1 (cf Fig. 2.46).

Although soft tissue and bone derivatives of MNC are known, *the specific contributions of its component neuromeres are not mapped out*. MNC dura covers the entire anterior cerebrum and cerebellum. MNC as broadly defined is responsible for producing the anterior cranial fossa, sphenoid, ethmoid complex, and the anterior cranial fossa, sclera, and orbital contents.

MNC migrates ventrally and anteriorly on its way to the orbit and face. It hugs the axis of the embryo. It moves

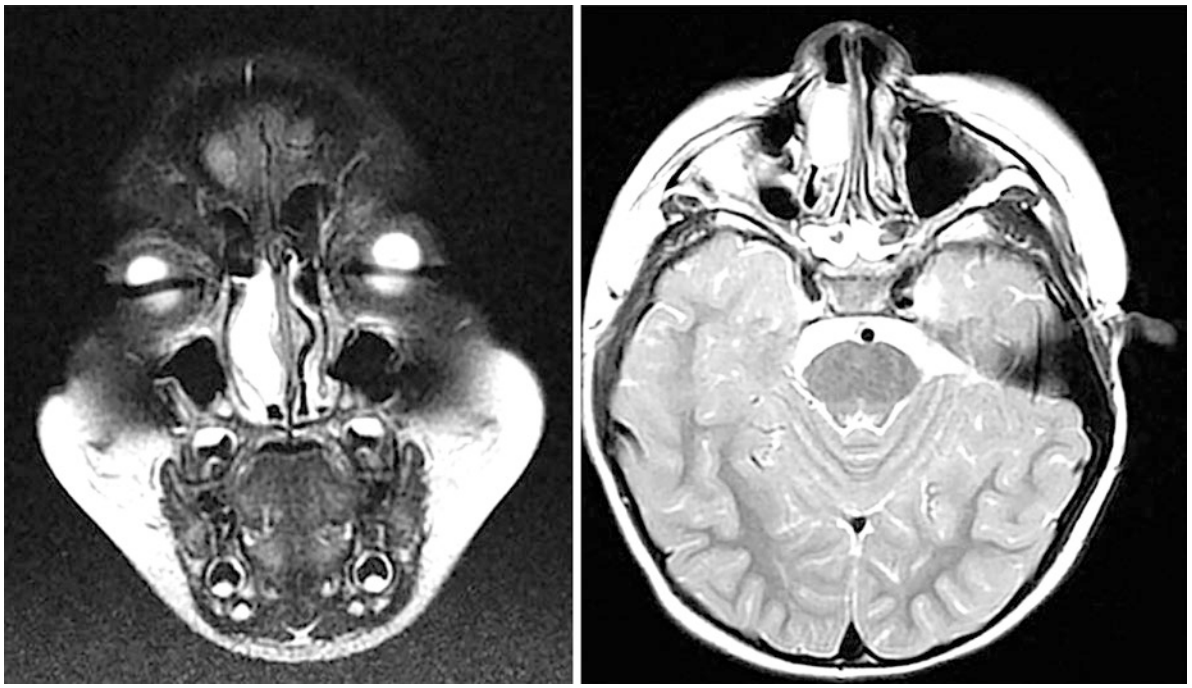

Fig. 2.66 Nasal glioma. Nasal gliomas are composed of dysplastic glial tissue and are congenital non-neoplastic lesions best categorized as heterotopia. They are rarely associated with other congenital malformations [2]. A nasal glioma may be connected to the brain by a stalk of tissue in up to 15% of cases, but the stalk does not contain a direct fluid-filled tract that communicates with the subarachnoid spaces; therefore, a nasal glioma is distinct from a nasal encephalocele. # Types extranasal (60%), intranasal (30%), and mixed (10%). Nasal gliomas occur near the root of the nose (where the cranial portion of the nose joins the forehead). Extra-nasal gliomas are usually seen in a paramedian location at the bridge of the nose external to the nasal passage, whereas intranasal lesions are usually located within the nasal passage medial to the middle turbinate bone. Ultrasound is useful for determining if the mass is cystic or solid. Doppler flow studies of nasal gliomas reveal a characteristic low arterial flow velocity during the end-diastolic phase Nasal gliomas are often isointense relative to the normal brain at MR imaging, which is the imaging modality of choice. High-resolution surface coil MR imaging is often useful in demonstrating the intracranial stalk. (Reprinted from Radiopaeida. Courtesy of Dr. Francis Deng)

directly in front of the notochord to interact with the prechordal mesoderm located between the rostral notochord and the buccopharyngeal membrane. MNC migration sequence is determined by the spatial order of CNS development. Hindbrain development is rostral-caudal. Thus, r0 migrates first, followed by r1. The two populations probably do not remain distinct. Midbrain development follows that of hindbrain and is caudal-rostral; thus, m2 is followed by m1. Given the small size of isthmus, we can also assume the two populations are combined.

The immediate task of MNC is to protect the brain by providing tissues that will complete the preexisting vascular plexus, lay down the meninges, and support the skin. Synthesis of the anterior cranial base and orbit follows. As the optic primordium emerges from p5 basal diencephalon, it pushes its way through this MNC like a fist through a sock. The future globe thus acquires a coating of neural crest that will provide the future sclera. The globe is genetically divided into two developmental sectors: ventro-nasal and dorso-temporal. Neural crest of the sclera will form binding sites for the extraocular muscles according to this system.

Directly lateral to caudal forebrain are positioned the first three somitomeres Sm1–Sm3. These contain all extraocular muscles except lateral rectus. Sm4 lies directly opposite the tip of the notochord. This mesoderm is sessile and forms the basisphenoid. Sm5 sits just behind it and contains the remaining extraocular muscle, LR. Since m1 and m2 contain the nuclei of III, it makes sense to assign them both to the sclera, although, given the small size of m2, this may not be functionally significant.

In thinking about MNC, keep in mind that it is not that MNC from r1 or m1 carries a particular "message" that will produce a derivative, rather it is the *interaction* of MNC with the local environment it populates that will determine the outcome.

The embryonic axis defined above has many implications for the future developmental sequence of the eye. The initial blood supply for the eye is from primitive maxillary artery. This vessel is ultimately reassigned to supply the hypothalamus. It is replaced first by primitive dorsal ophthalmic and later by primitive ventral ophthalmic. These arteries are held together to form the definitive ophthalmic artery (prior to arrival of stapedial). Via prDOA and prVOA (primitive dor-

Fig. 2.67 Holoprosencephaly with hypotelorism sequence. Upper left: bilateral cleft lip and palate with hypoplastic premaxilla (loss of lateral incisor subfields) and vomer; Upper right: cleft lip and palate with absent premaxilla and/or vomer; Lower left: cebocephaly (single chamber proboscis in correct position); Lower center: ethmocephaly (proboscis in the ethmoid field, bilateral orbits); Lower right: cyclopia (proboscis above the plane of single orbit). (Reprinted from Bianchi D. Fetology: Diagnosis and Management of the Fetal Patient, 2nd ed. McGraw Hill; 2010. With permission from McGraw-Hill Education)

sal ophthalmic and primitive ventral ophthalmic arteries, respectively), neural crest cells arrive at the iris to form the intrinsic striated muscles of the eye.

Given the above, can we deduce which population of MNC supplies what sector of the globe? The temporal-dorsal sector of the optic vesicle (supplied by prDOA) is biologically "older" than the nasal-ventral sector [123–127].

The insertion sequence of the extraocular muscles is as follows: LR[13] (Sm5) > SO[14] (Sm3) > SR[14] (Sm2) > MR[16] (Sm1) > IO[16] (Sm2) > IR[17] (Sm1) > LPS[19–21] (Sm2).

Dura innervated by V1 is continuous with the sclera of that side of the globe as well. For this reason, sensory nerves to the eyes are exclusively V1. Myoblasts from Sm1 to Sm3 and Sm5 migrate into the orbit where they are ensheathed by MNC fascia. This means that the cell source for the muscular arteries will be V1 stapedial.

MNC Bone Fields

Mesencephalic bone fields can be abbreviated as: presphenoid (PS), orbitosphenoid (OS), lateral pterygoid plate (MPt), ethmoid lamina (EL), ethmoid perpendicular plate (PP), and septum (S).

Bone fields of the anterior cranial fossa and orbit develop from neural crest via two mechanisms: (1) by the formation of an intermediate cartilage that becomes a membranous bone; or (2) via direct osteogenesis in membrane. Of particular value is the construction of the sphenoid complex. The principle cartilages are demonstrated in Figs. 2.68 and 2.69. Development follows a pattern ventral to dorsal, caudal to rostral, and medial to lateral. Bone fields build quickly, one upon another to produce the sphenoid complex (Figs. 2.70 and 2.71).

We arrive therefore at three extremely important generalizations.

- At a given neuromeric level, *bone derived from somitomeric PAM will be laid down* ***prior*** *to that derived from neural crest*. Basisphenoid precedes presphenoid. Temporal bone precedes squamous occipital bone.
- PAM bones are not found in the viscerocranium (pharyngeal arches).
- PAM bones of the skull are chondral, the sole exception being the parietal bone in which r2–3 neural crest is admixed with Sm4 PAM.

Rhombencephalic Neural Crest Derivatives: r2–r7

The relationships between the homeobox genetic code in the hindbrain, neural crest migration, and the pharyngeal arches were worked out in the late 1980s with contributions by

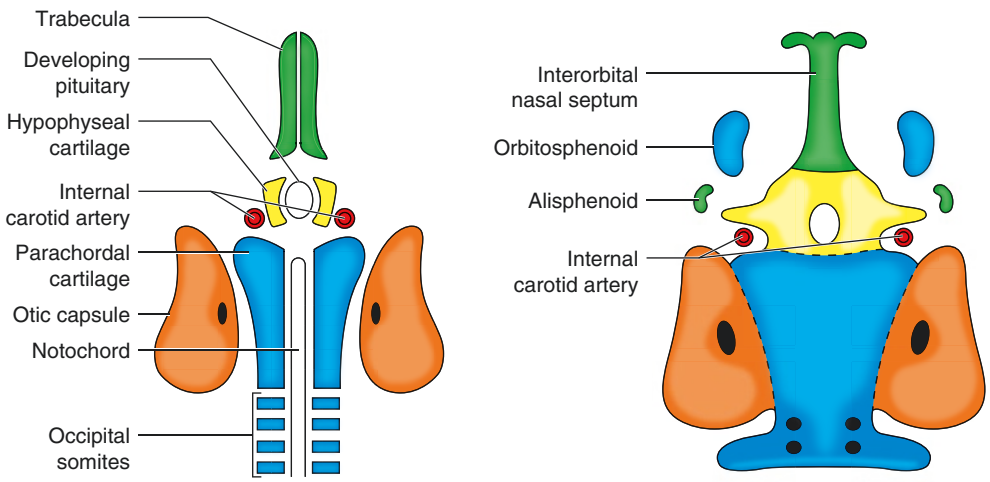

Fig. 2.68 Chondrocranium 1. Occipital somites [4] consolidate to form the basioccipital bone

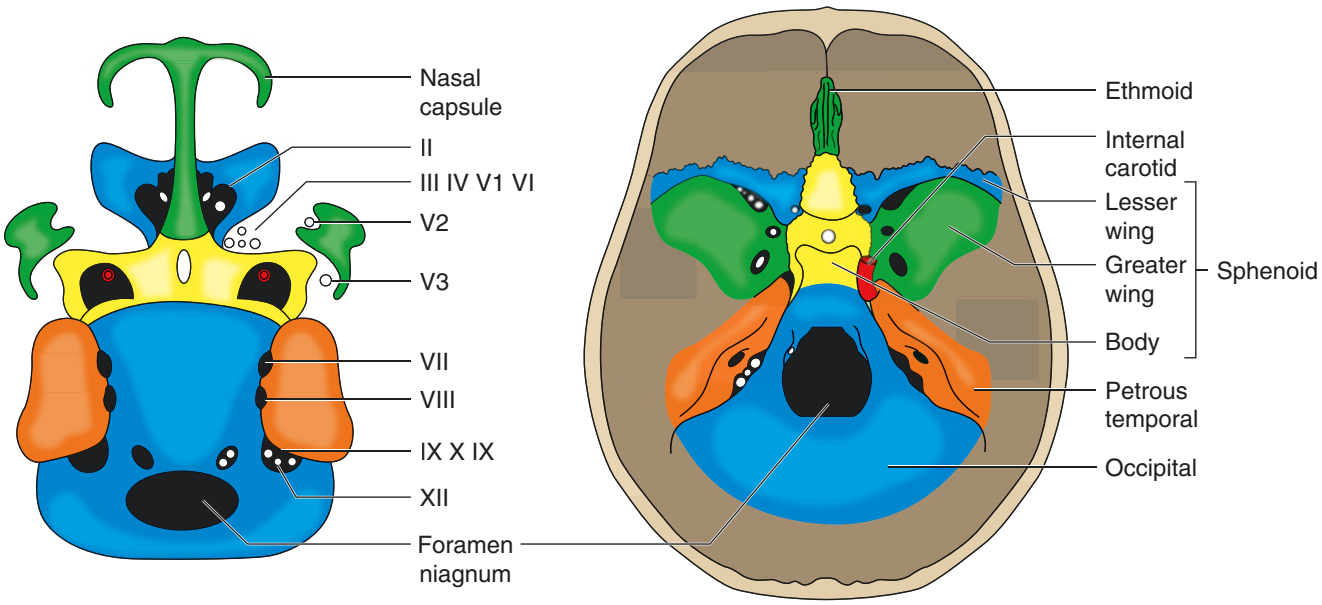

Fig. 2.69 Chondrocranium 3. Note sphenoid mesenchyme condensing around the nerves

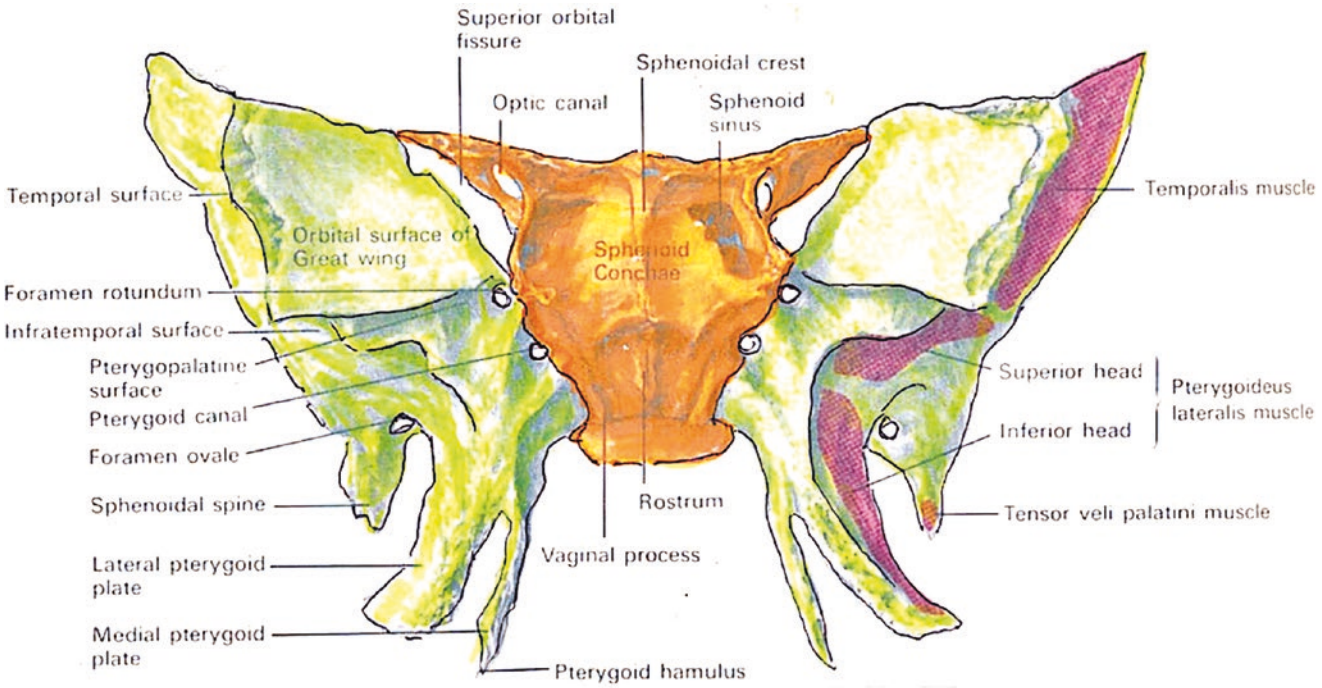

Fig. 2.70 Sphenoid, anterior. (Reprinted from Lewis, Warren H (ed). Gray's Anatomy of the Human Body, 20th American Edition. Philadelphia, PA: Lea & Febiger, 1918)

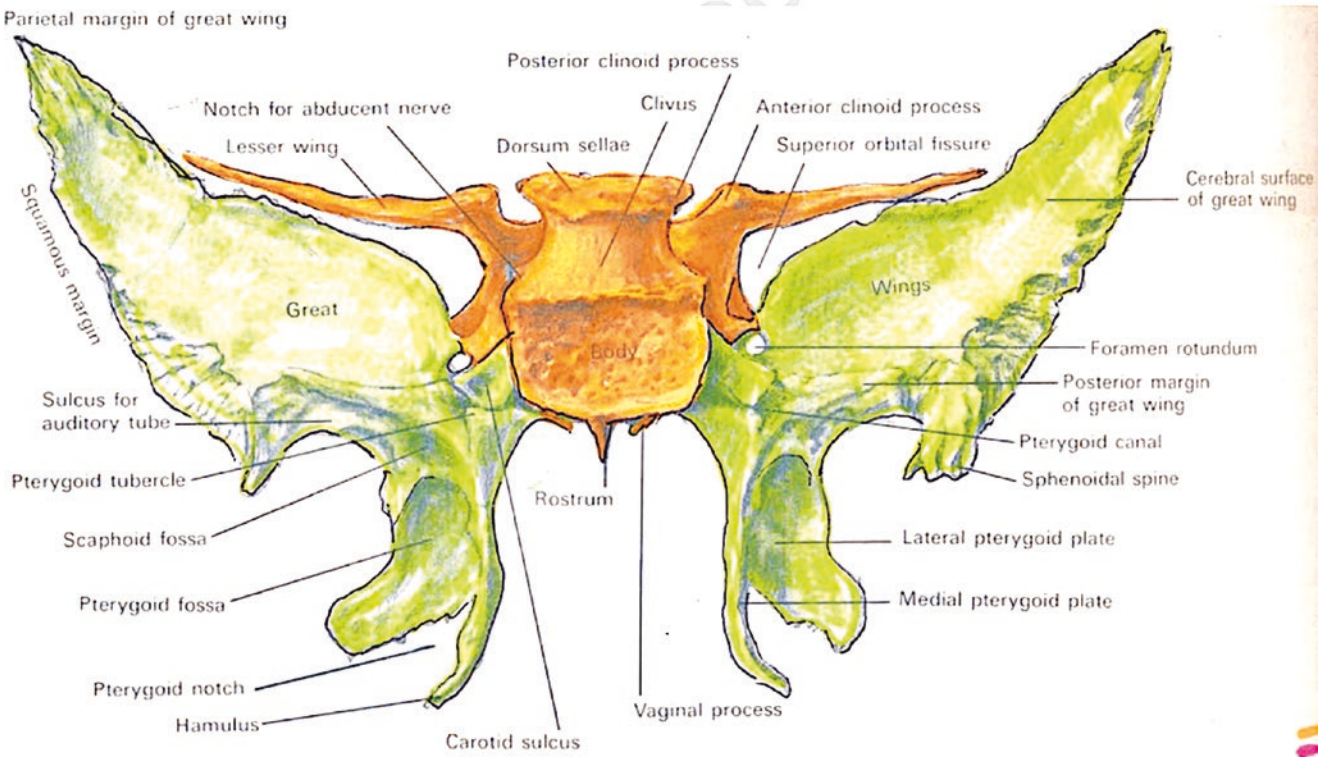

Fig. 2.71 Sphenoid, posterior. (Reprinted from Lewis, Warren H (ed). Gray's Anatomy of the Human Body, 20th American Edition. Philadelphia, PA: Lea & Febiger, 1918)

Lumsden and from Krumlauf [32, 33, 128–130]. Herein we will concern ourselves with the patterning of the first three pharyngeal arches.

The earliest neural crest migrations to be completed are those originating from the rostral rhombencephalon, i.e., from rhombomeres r2 to r7. This type of neural crest (RNCr) is intimately involved with the formation of the first three pharyngeal arches. RNCr pathways are *segmentally restricted* between rhombomeres; RNC cannot participate in craniofacial development independent of the pharyngeal arch to which it is assigned. Subsequently, RNC is physically transported to the face (frontonasal mesenchyme) by the processes of pharyngeal arch translocation and embryonic folding. The very first fold in the neuraxis, called the *mesencephalic flexure*, is hinged at the midbrain. It results in the CNS being tucked back on itself almost 150°. The most rostral zones of the prosencephalon (p6 and p5) are brought ventrally until they are in almost direct contact with the rapidly growing first and second pharyngeal arch amalgam. Epithelial contact between the frontonasal and lateral masses results in fusion. Neural crest and PAM mesenchymal derivatives then move into their appropriate locations.

This type of RNCr migration is very different from that observed in neural crest of prosencephalic or mesencephalic origin. The biologic behavior of PNC and MNC is not constrained by a secondary reorganization into a pharyngeal arch. These neural crest cells move directly under the epithelium to their destinations, set up shop, and go to work.

Timing is everything, especially in craniofacial development. We know that RNCr migration into the first three arches is complete by the 11-somite stage. On the other hand, the mesenchyme to which the RNCr will directly attach to form the facial skeleton comes from MNC. However, MNC migration is not complete until the 14-somite stage. What happens during the intervening time? *CNS folding occurs in this interval*. At this point in time, the first and second pharyngeal arch "sandwich" has swung into position. All potential RNCr fields are now ready to make contact with their MNC counterparts. Note further that, although MNC interacts with PNC via the r1 perpendicular ethmoid plates, *no direct anatomic contact exists from RNCr and those from PNC*.

When the pharyngeal arches arrive on the scene, they are composite entities. Recall that the five arches are not completely separate. The external surface of the arches shows deep grooves in the epithelium. These grooves are not of full thickness; it would be theoretically possible for neural crest and PAM from one arch to meld into its neighbor. For this reason, the first and second pharyngeal arches, once formed, promptly meld into each other to create a "sandwich." In this case, neural crest cells from r2 interact with those of r4, whereas those from r3 interact and meld with those of r5. For this reason, myoblasts from r4 populate the maxillary fields and those from r5 populate the mandibular fields.

Let's turn our attention to the osseous derivatives of the first and second pharyngeal arches. By the time the PA1/PA2 sandwich arrives on the scene, it has two visible components. An upper maxillary mass contains derivatives of r2 and r4. It comes into direct contact with the frontonasal "process" (sic), i.e., the orbito-spheno-ethmoid complex. A lower mandibular mass contains derivatives of r3 and r5. Unlike the maxillary mass, the mandibular mass bears no physical relationship to the orbito-sphenoid complex. It is suspended from the cranial base r6 petrous temporal bone at the temporomandibular joint.

First Pharyngeal Arch: Rhombomere 2

Migration Pathways

The anatomic pathways taken by the r2 neural crest are dictated by the neuroanatomy of V2 and by preexisting MNC fields of the orbit and nose, the presence of which force it to follow along their boundaries or to make detours around them. Perigrinations require a pathway for the pilgrim to follow. *The mechanism of r2 RNC migration is to take advantage of previously established MNC structures*. Just as in gastrulation mesoderm has a "leading edge," the pioneering cells of which leave a trail for later mesoderm to follow, so do the initial cells of a neural crest pathway leave signals behind for their successors. Succeeding waves of angiosomes will follow each other *based upon their ordinal anatomic site of origin* along the vascular axis.

RNC from r2 follows two principal pathways forward. An *intracranial pathway* pursues the course of the meningeal branch of V2 which is given off before foramen rotundum. It proceeds to the backwall of the future orbit where it deadends as alisphenoid. The *extracranial pathway* courses through foramen rotundum as described below.

Playing "follow the leader" means respecting obstacles. The r1 MNC blastema responsible for synthesis of the *lesser sphenoid wing of the sphenoid* and the lateral pterygoid plate "pushes" RNC laterally. It therefore completes the back wall of the orbit by producing greater wing of sphenoid. Once the blastema of *alisphenoid* mesenchyme is already in place, additional r2 RNC pathway is forced to pass beneath the greater wing. By this "underhanded move," it gains entrance to the pterygopalatine fossa. There it breaks up into individual pathways dictated by the branches of V2 that fan out from the fossa to the oro-nasal cavity, maxillary complex, and the zygomatico-orbital complex.

The Premaxillary-Vomerine Complex

We shall follow the pathway of the terminal branch of StV2, the nasopalatine axis (NP), as it turns medially from the pterygopalatine fossa and heads toward the midline. In so doing, it encounters a physical obstacle, the upwardly growing *palatine bone*. NP inserts itself between palatine bone and the

cranial base. The palatine bone is derived from STV2 descending palatine, the stem of which is given off prior to that of NP. The palatine bone consists of a *horizontal plate* that forms the posterior hard palate and a *perpendicular plate* projecting up into the orbit from the superior border of which are projected upward a posteriorly directed *sphenoidal process* and an anteriorly directed *orbital process*. These are two separate processes because of the presence of the nasopalatine axis, which they must straddle. Thus, the presence of the sphenopalatine notch represents a "footprint" of the migratory pathway used by NPA on its way to the midline. *All notches and foramina of the skull are tacit recognitions for the prior existence of neurovascular structures*.

After passing over the palatine, NPA bifurcates. A lateral branch (NPm) is dedicated to the nasal wall of the maxillary complex and the medial branch (NPm) is directed toward the nasal midline. Here it encounters the previously synthesized perpendicular plate (PPE) of ethmoid. As it grows forward, the neurovascular axis of NPm is forced to follow its inferior border of perpendicular plate.

We have said before that the derivatives of NPm are the premaxilla and the vomer and that these are *bilateral* field complexes. Beneath the presphenoid is a midline axial structure (probably bilateral in origin), the *sphenoidal rostrum*. Inserted on either side of the rostrum are two flanking lamine from the posterior margins of the vomerine bones. These are known as the *vaginal processes*. As the vomers extend anteriorly from the vaginal processes, they descend beneath the perpendicular plates of the ethmoid (PPE). The ability of NPm to follow along the fused midline laminae of r1 (i.e., the perpendicular ethmoid plates), determines whether or not one or both premaxillary bones will be produced. The r1 PPE is a bilateral structure.

Holoprosencephaly (HPE) involves neurovascular territories of the ventral and anterior forebrain and the r1 spheneth-moid complex upon which the brain rests [131–135]. Because r1 neural crest is involved in the synthesis of the branches of anterior cerebral circulation, an r1 deficiency state may be a possible cause of HPE. HPE can exist in a unilateral form that includes ipsilateral attenuation or absence of the perpendicular plate. In these cases, hypoplasia or frank absence of the ipsilateral premaxilla can be present. If the palatal shelves must fuse to vomer in order to achieve union at the midline, then unilateral HPE, by destroying the pathway for medial nasopalatine migration, will create an ipsilateral palatal cleft.

The lamination sequence of NPm is completely different from that of r0 and r1. Building upon the PAM derivative basisphenoid, r1 neural crest spreads to form the central anterior cranial fossa. One does not see absence or deformation of the sphenoid in the presence of a normal ethmoid. The ethmoid capsule forms a lattice for r2 migration. Earliest in time to migrate is the premaxillary neural crest. At about the time PMx neural crest arrives at the anterior base of the presphenoid, the r1 perpendicular plates of the ethmoid are forming. These make up the "perpendicular plate pathway" by which PMx passes along the future roof of the mouth and arrives at its final position in the facial midline. As PMx migrates, it leaves behind it a molecular "slime trail" for vomerine neural crest to follow [136].

Once in the midline, PMx forms a common alveolar process that subsequently splits into two independent zones. Neural crest "flow" into zone PMxA creates the central incisor and alveolus. This field is a pie-shaped wedge with the apex pointing toward the incisive foramen. A "split-second" later, a second neural crest population containing the future lateral incisor and ascending process of the premaxilla arrives on the scene. It too has the form of a pie-shaped wedge with its apex at the incisive foramen. Thus, zone 2 does not "spill over" from zone 1, but arises just posterolateral to it. Zones 1 and 2 are in continuity, just as are zones 3, 4, and 5.

From its most distal aspect, PMx produces a cellular outgrowth of vital importance to plastic surgeons. This *frontal process* of the premaxilla (PMxF) is responsible for the internal piriform rim. *Deficiency states in PMxF are the cause of the isolated cleft lip nasal deformity* (vide infra) [137–139].

The vomerine neural crest migrates into position later in time than that of PMx. The premigratory position of V field cells is thus *caudal to PMx along the neural fold*. Isolated deficiency states of the V population can exist. It is therefore possible to have hypoplastic vomer in the presence of a perfectly normal lip and an intact premaxilla. This can lead to a spectrum of problems. Thus, even though primary contact between the premaxilla maxilla has resulted in fusion of the alveolar arch, small vomer bone may be physically unavailable for fusion with the ipsilateral r2 palatal shelf, leading to secondary contact failure and a midline cleft palate.

PMx and V are supplied from a common neurovascular axis with which they can have two different types of relationship. In the first scenario, they follow each other "*Indian file*" down a common pathway. PMx neural crest is "pathfinder" for subsequent vomerine development. In other words, PMx is required but not sufficient for vomer. An absent premaxilla will always be accompanied by an absent vomer. On the other hand, an intact premaxilla could be accompanied by hypoplasia of vomer. A second scenario is on which each field represents an independent stem from the main axis. This model would permit a situation where vomer could be fully developed in the presence of an abnormal premaxilla. Clinical experience supports the first model. A third (unrelated) scenario occurs if there is developmental failure of the ethmoid fields, as in holoprosencephaly. Failure of the r1 "perpendicular plate pathway" makes migration of the medial nasopalatine axis impossible and leads to outright absence both vomer and premaxilla.

Organization of r2 RNC

Some superomedial r2 and r3 neural crest remains sessile alongside the developing brains. In conjunction with r1 neural crest, these populations produce the dura covering the prosencephalon. The neuromeric territories are defined by the sensory distributions of trigeminal to the dura.

The neural crest responsible for synthesizing the maxilla and lateral orbit can be organized into *three distinct osteogenic populations*. The segments arrive at the scene via spatially distinct migratory pathways. These pathways do not conflict with each other. The first population is the *orbital complex*. It follows intracranial V2 and is directed toward the orbit where it produces lateral pterygoid and greater wing of sphenoid. Neural crest cells within each segment produce bone derivatives in a strict time sequence. The second population contains the various components of the *maxillary complex*. The overall shape of these fields is that of a five-sided box, the medial wall of which is partially open into the nose. The third segment contains the two fields of the *zygomatic complex*, which forms secondarily over the malar eminence of the maxilla and the posterolateral orbit. We shall now describe the order in which these fields make their appearance.

Retro-Orbital Complex: Alisphenoid (AS) and Lateral Pterygoid (LPt)

Alisphenoid (AS) and *lateral pterygoid lamina* (LPt) are membranous bone with different blood supplies. These two fields are confluent with each other at the pterygopalatine fossa. From their juncture, each field is joined to the presphenoid bone by an osseous process. Where these processes straddle, the preexisting sensory nerve V2, the *foramen rotundum*, is created. They thus predate the remaining r2 neural crest populations as they pass through the foramen. Within the orbit, isolated deficiencies of the alisphenoid have been described that communicate with the external postorbital region. Alisphenoid develops from StV2 intracranial as the meningo-orbital artery. These may range from the reduced volume of the lateral orbit seen in trigonocephaly due to lacrimal defects to outright loss of the alisphenoid posterior wall.

The alisphenoid would appear to be an extension of the cranial base. It represents, however, an attachment of PA2 to the skull. This is a very ancient arrangement. The primitive palatoquadrate cartilage (from which the maxilla is derived) had three components, *autopalatine*, *metapterygoid*, and quadrate. The most anterior is the precursor of the maxilla and palate, the middle one forms the *alisphenoid*, and the latter forms the incus.

Lateral pterygoid lamina is the remnant of the ancient ectopterygoid bone of the palate series. It provides the primary insertion for lateral pterygoid muscle which spans to r3 mandible. Its arterial supply comes from the artery of the same name that is programmed by the second zone of IMMA and from StV2 lesser palatine artery.

Clefts occurring below the axis of the orbit are classified by Tessier as #3–7. All involve neural crest bones originating from the second rhombomere. The best way to understand the anatomic distribution of these clefts is to consider the neurovascular supply of the maxillary dentition. The anterior superior alveolar artery (ASAA), also known as infraorbital artery, produces medial and lateral branches to distinct groups of dental units. The posterior superior alveolar artery (PSAA) arises in the pterygopalatine fossa from the third part of the internal maxillary artery, proximal to the infraorbital artery. Thus, a developmental relationship exists between the developmental fields of the ASAA and the PSAA.

Maxillary Complex: Dental Zones (Mx1, Mx2, Mx3), Inferior Turbinate (It), and Palatine (Pl)

The Maxilla Is a Five-Sided Box

The maxilla is a five-sided box, the medial wall of which opens into the nose, permitting the development of a large maxillary sinus. Two additional bones, inferior turbinate and palatine, "patch up" the medial wall defect. The major supply for maxilla is the superior alveolar neuroangiosome. It trifurcates into three dental zones with each branch running through the membranous bony wall to reach the teeth creating within the anterior wall of the maxilla three developmental field zones.

The ASAN departs from the infraorbital nerve midway along its course through the canal. It traverses the *canalis sinosus* in the anterior wall of the maxillary sinus. The canalis sinosus swerves laterally away from the infraorbital canal and then hooks downward and medially to pass beneath the infraorbital foramen. It then runs downward to the canine and the incisors. The presence of the canalis is a tacit recognition of the prior existence of the anterior superior neurovascular bundle supplying those structures. The anterior superior alveolar artery arises from the infraorbital artery just prior to its exit from the infraorbital foramen. Just like its companion nerve, its course defines the canalis sinosus. Tessier clefts #3 and #4 occur here.

Mx1 is defined by *medial branch of anterior superior alveolar nerve* (MSA) and comprises those structures located medial to a vertical line dropped from the inferior orbital foramen. Mx1 is composed of: (1) the *mesial alveolus containing the lateral incisor and canine* and (2) the *anterior maxillary wall medial to the infraobital foramen*. The orbital rim and floor medial to the infraorbital fissure are formed by Mx1. This pedicle bifurcates into a medial branch that supplies the lateral incisor and a lateral branch supplying the canine. The dental units develop in a mesio-distal sequence, except that in most the lateral incisor from maxilla fails to develop, being supplanted by the lateral incisor unit from

premaxilla. Note that it is *normal* for both premaxilla and maxilla to produce an incisor tooth in the "lateral" position. Note that it is biologically normal to produce a second lateral incisor. That is why ectopic incisors are so common. In addition, in cases of complete cleft lip, where the premaxilla does not produce a lateral incisor, the presence of this tooth in the maxillary segment can be explained by this duality. It bifurcates as well to supply the medial and lateral premolars. Defects in MSA are the source of Tessier #4 cleft zone, while those of LSA are the basis for the Tessier #5 cleft zone.

From the medial edge and from the superomedial edge of Mx1 arise two extremely important structures for plastic surgeons; these are crucial for understanding Tessier clefts #3 and #4. These structures are the *inferior turbinate bone* (IT) and the *frontal process of the maxilla* (MxF). This thin lamina extends upward from the canine region, past the lateral margin of the nasal bone, and terminates by abutting with the prefrontal bone (PrF), i.e., the medial orbital rim. It receives a separate vessel from MSA. Defects of IT cause the #3 cleft, while defects of MxF cause the #4 cleft. More about inferior turbinate below.

Mx2 is defined by the *lateral branch of anterior superior alveolar nerve* (LSA). This arises from the inferior alveolar nerve in its course along the infraorbital groove. The nerve then tracks laterally and forward in the lateral maxillary wall. It bifurcates to supply the premolar teeth. These develop in a mesio-distal sequence. Defects of LSA produce the Tessier #5 cleft.

Mx2 is the field set for LSA (middle superior alveolar nerve) and is composed of the alveolar housing for the premolar teeth (supplied by the middle superior alveolar nerve and artery) and the maxillary wall lateral to the infraorbital foramen. The orbital rim lateral to the intraorbital foramen and the orbital floor lateral to the infraorbital fissure are formed by Mx2. It is thus in contact with the greater wing of the sphenoid. In zoologic term, this is called the alisphenoid (AS). As we shall see, neural crest forming AS arrives after Mx2 and thus potentially must be constructed upon it. An isolated defect of Mx2 causes a *Tessier #5 cleft*. When the alisphenoid is also affected, one sees (rarely) a *Tessier #5, #9 cleft.*

Mx3 is defined by the *posterior superior alveolar nerve* (PSA). The pedicle trifircates to supply the molar in mesial-distal fashion. The PSAN departs from V2 in the pterygopalatine fossa. It pierces the maxilla just along its infratemporal surface and descends beneath the sinus mucosa to supply the molars. This will be the site of Tessier cleft #6.

Mx3 is the field set for posterior superior alveolar nerve and consists of the alveolar housing for the molars and the maxillary wall projecting upward and lateral, the *zygomatic process of the maxilla* (buttress). The *Tessier #6 cleft* is associated with hypoplastic states in this zone. The postorbital field (PO) of the zygoma sits directly above Mx3 buttress. The *Tessier #8 cleft* localizes to PO. Dual affectation leads to the *Tessier #6, #8 cleft*.

The Sixth Side of the Box: Inferior Turbinate

This is a discrete bone forming 1/3 of the lower half of the lateral nasal wall. This structure is of critical importance in explaining the pathologic anatomy of the Tessier clefts #2, #3, and #4. To understand the clinical presentations of these clefts, we must dig into the role that IT plays in the separation of the nasal cavity from the maxillary sinus. Anterior to IT lies the ascending process of the premaxilla. Posterior to IT is the vertical plate of the palatine bone (Pl). As IT projects into the nasal cavity, it forms a caudally directed scroll. Beneath this scroll one encounters the terminus of the lacrimal duct. Thus, lower half of the lateral nasal wall is formed by three r2 neural crest derivatives (in antero-posterior order): MxF, IT, and Pl.

The upper half of the lateral nasal wall can likewise be divided into three discrete zones. The *posterior zone* is made from the vertical plate of the r2 palatine bone. The central zone contains the middle turbinate. This bone represents the caudal border of the r1 ethmoid complex. MT sits above IT and has the form of a Roman arch. An aperture between MT and IT results. This is hidden behind a scimitar-like projection of MT into the nasal cavity, the infundibulum. It is via this field boundary that the maxillary sinus drains. The anterior zone of the lateral nasal wall is made from the ascending process of the maxilla. The cranial margin of MxF abuts against the r1 bones: nasal bone medially, nasal process of the frontal bone posteriorly, and the r1 lacrimal bone laterally. Thus, the maxillary sinus is a five-sided box, five sides of which are exclusively of r2 derivation. The sixth side, the medial wall (the lateral nasal wall), is the combination of an upper tier of r1 fields with a lower tier of exclusively r2 fields.

As a mucous-producing structure, the maxillary sinus must have an obligatory escape route for its secretions. Fortunately, our six-sided box is not watertight. The field boundary between the anterior and posterior zones of the p6 lower ethmoid provides just the exit point for the maxillary sinus. It thus drains into the inferior aspect of the infundibulum, dripping out from beneath the middle turbinate. This messy situation neatly reinforces our previously described model of sinus development. ***All sinuses result from the expansion of oral mucosa into a potential space between fields***. Thus, the mucosa seizes the opportunity to insert itself into the opening between the anterior and posterior ethmoid zones and insert itself into the potential cavity between p6 and r2.

The structural integrity of the inferior turbinate is the prerequisite for the proper formation of two other structures that appear later in time. First, the r2′ frontal process of the premaxilla (PMxF) is constructed upon the scaffolding of IT. Second, p5 neural crest cells descend along the lateral

surface of IT to create the lacrimal bone. Because the inferior turbinate is such a crucial component of the lateral nasal wall, IT deficiency states will create a severe cleft condition that begins at the lateral piriform margin, eliminates the medial wall of the maxillary sinus, and ascends into the lacrimal system. This is the pathology of the *Tessier #3 cleft*.

The Sixth Side of the Box: Frontal Process of Maxilla

The second important element to be produced from Mx1 is the frontal process of the maxilla. As stated before, MxF in all but humans and higher primates is physically distinct from PMxF. Although MxF originates in the MSA zone of maxilla, it also depends on IT for its construction. The physical presence or absence of PMxF is *not* required for MxF synthesis. When MxF is deficient, additional forms of clefting can occur. Recall that the inner aspect of the piriform margin is composed of two laminae; a small upper one coming down from p5 and the lower one ascending from r2′. The superior lamina, the *descending nasal process of the frontal bone* (Fn), buttresses the undersurface of the nasal bones. The inferior lamina, the *frontal process of the premaxilla* (PMxF), arises from the distal (versus mesial) margin of the premaxilla just above region of the lateral incisor region.

The lateral piriform margin and the medial piriform margin are initially separated by the *nasolacrimal groove*. This closes over during fetal development, causing the lateral piriform rims to approach the midline from either side. They eventually overlap the medial piriform margins. *Due to this overlap, no suture is observed in the term fetus*. In the past, this led physical anthropologist Sir Ashley Montague to question the existence of the premaxilla in humans [140]. Definitive proof regarding the premaxilla has been provided by Barteczko and Trevizian [141, 142]. In the *Tessier #4 cleft*, the persistence of this groove spares the medial piriform margin. All the incisors ipsilateral to the cleft are intact. Tessier #4 and #5 clefts occur as gradations of severity within the Mx1 field. Therefore, the #5 is simply a more severe form extending all the way to the infraorbital foramen. Loss of dental units within Mx1 can also occur.

The developmental significance of the bilaminar piriform margin is that deficits of the r2′ PMxF will allow the r2 MxF to sit more laterally and the *vertical height of the lateral piriform margin will be lower*. This describes the pathologic osseous anatomy of the isolated cleft lip nose. In those r2′ deficiency states in which the PMxF is hypoplastic or missing, the piriform margin is unilaminar and extremely thin. This means that the actions of the nasalis and paranasalis muscle complexes acting over time will exert a more pronounced distracting force to displace the piriform margin out laterally.

Mammalian evolution demonstrates the development of a medial projection from Mx1 to Mx3, the hard palate. The palatal shelves extend from each of these fields. Palatal shelves have a bilaminar vascular supply. The nasal side is supported by lateral nasopalatine artery, while the oral size is supplied by greater palatine artery. For this reason, the hard palate is potentially bilaminar and can, on occasion, contain a sinus.

Just above the palatal shelves is located the medial maxillary wall. This is made up of three coplanar structures all lined up in a row. The fused frontal processes (PMxF and MxF) form the anterior third of the wall. The *inferior turbinate* (IT) bone forms the middle third of the wall. It is a derivative of Mx1m. The "sprouting" of IT from Mx1 occurs *prior to* that of MxF. The lateral ascending process is constructed upon an intact inferior turbinate. Thus, *a cleft in zone #3 will always destroy zone #4 but not vice versa*. An isolated defect of MxF causes a *Tessier #4 cleft*.

The Sixth Side of the Box: Palatine Bone

Immediately behind Mx3 lies the palatine bone (P). This structure ossifies after the maxilla. Descending palatine artery supplies the perpendicular plate; its lesser palatine branch is assigned to the horizontal plate.

Laterofacial clefts occur at the interface between the maxillary and mandibular regions of the first arch. They can penetrate deeply, affecting multiple fields, including the palatine bone. Deficiency states have been described with severe hypoplasia or absence of this structure. In such cases, the soft palate musculature will have nothing to insert upon. These muscles will remain as unfulfilled mesenchymal blobs over their sites of origin, i.e., the Eustachian tube (tensor veli palatini) and petrous apex (levator veli palatini). In the literature, this condition is described as an *ipsilateral absence of the soft palate*. This has also been reported in the context of severe Goldenhar's syndrome.

The Zygomatic Complex: Jugal (J) and Postorbital (PO)

This segment of r2 neural crest belongs to the zygoma and is ossified in cartilage after the maxilla is formed. Its arterial axis is the StV2 *zygomatic artery*. The zone is the composite of two previous bones seen in lower vertebrates. The *jugal bone* forms the temporal process of the zygoma and the inferior half of the malar eminence. It is the most distal and is synthesized first. It begins along the axis of the zygomaticofacial neurovascular bundle and spreads downward to contact the Mx buttress. It also spreads forward to contact the Mx2 lateral orbital rim. The *postorbital bone* forms the frontal process of the zygoma and the superior half of the malar eminence. It also begins at ZF axis and spreads upward to contact the p5 zygomatic process of the frontal bone. It also spreads backward to contact the r3 zygomatic process of the squamous temporal bone. The anatomic split between PO and J is indicated by the zygomatico-facial neurovascular axis. *Tessier clefts #8 and 7* correspond to these two fields,

respectively. These are commonly affected in Treacher-Collins syndrome, where the zygomatic arch is absent and the malar eminence is reduced or absent.

First Pharyngeal Arch: Rhombomere 3

The original lower jaw of tetrapods consisted of nine membranous bones organized around Meckel's cartilage. Over time, some of these fields disappeared (or were amalgamated). The most proximal bone fields became incorporated as components of the ear. Only the dentary bone remains to form the mammalian mandible. The mandible can be divided into four developmental fields. Three of these belong to the tooth-bearing alveolar bone. The ramus field contains also the coronoid process and the condyle. It develops after the alveolus. For this reason, in cases of craniofacial microsomia or Treacher-Collins, partial or total absence of the ramus can occur with preservation of the dental mandible.

Details of the formation of these fields are well-described by Kjaer. No clearer account of mandibular development can be found in the literature. Our purpose here is simply to identify the individual r3 fields and discuss their temporal order of formation. These concepts serve to rationalize the Kjaer's observations and permit additional clinical correlations (such as the anatomic rationale of the muscles of mastication).

Some superomedial r3 neural crest remains sessile alongside the developing brain. It helps form the dura covering the prosencephalon. This r3 zone is defined by the sensory distribution of V3 to the dura. Remaining r3 neural crest produces the bones of the second arch.

First r3 Segment: Mn1, Mn2, and Mn3

The alveolar zones of the mandible are similar to those of the maxilla. Three distinct sensory nerves supply the dental units of each zone. Mn1 contains both the incisors *and* the canine. Mn2 contains the premolars. Mn3 contains the molars. Each zone is supplied by a distinct sensory nerve. Early in development, each nerve has its own separate canal. These canals are organized in a strict time sequence. Derivatives in zone Mn1 represent the "oldest" mesenchyme; the incisors are the first teeth to erupt. Accordingly, the nerve to Mn1 occupies the most caudal canal. Just cranial to it lies the canal lies for nerve Mn2. Mn3 follows the same pattern. The three canals eventually become *roofed over* by the medial lamina of the mandible growing upward from its lower border. Thus, the inferior alveolar nerve is "three nerves in one!"

Individual variations in the number of dental units (both absence and excess) have been well-studied. These will affect the overall size and shape of the mandible from within their defined zone. Assuming that the number of teeth is constant, the AP length of the mandible is determined by the postdental segment. Under the same conditions, the vertical dimensions of the chin are determined by the fact that it represents a separate bone field from that of the dentary. *The majority of dentofacial skeletal deformities of the mandible result from deficiencies or excesses of mesenchyme in these two zones*.

Second r3 Segment: Ramus, Condyle, and Coronoid

The ramus forms via membranous ossification later in time than the alveolar bone. A portion of this periosteum converts to a cartilage cap that eventually forms the condyle. Pathologies affecting this zone may result in hypoplasia or absence but tend to spare neighboring fields. For example, craniofacial microsomia tends not to affect the tooth-bearing region of the alveolus. The coronoid forms at about the same time as the condyle. The cartilage goes on to form chondral bone. From this same PAM, the temporalis muscle is formed. For this reason, in Treacher Collins syndrome, absence of the coronoid is associated with an absent temporalis muscle.

Third r3 Segment: Derivatives "Assigned" to the Ear

The incorporation of the original angular bone becomes the tympanic bone. The reflected lamina of the angular held the original tympanic membrane; this is incorporated into the modern tympanic bone. The prearticular forms the anterior process of the malleus, the articular forms the malleus proper, and the quadrate forms the incus. In nonmammalian vertebrates, the jaw joint is represented by the quadrate and articular bones.

Second Pharyngeal Arch: Rhombomeres 4–5

The homeotic code defining rhombomere 4 is distinct from that defining rhombomere 5. As these populations sweep into the second arch, they do so at slightly different times. It is likely that they remain spatially distinct. We can hypothesize that r4 occupies the anterior (rostral) half of the arch and that r5 is distributed to the posterior (caudal) half of the arch. Motor branch of VII has upper and lower divisions, distributed to the anterior and posterior zones of the arch. The spatial arrangement of the branches of external carotid follows the geometry of the second arch once it has become repositioned.

Neural crest from r4 may represent the ancient hyoid suspension of the mandible. It likely forms the *styloid process* of the temporal bone. Fascia: all Sm6 muscles innervated by upper division of facial nerve are enveloped by r4 neural crest fascia. Neural crest from r5 forms the stylohyoid ligament and upper half of the hyoid bone. Sm6 muscles innervated by lower division of facial nerve are suspended in r5 neural crest fascia. Stapes is likely an r5 derivative.

The Extensive Distribution of Second Arch Mesenchyme

Second arch produces two layers of fascia which enclose functionally distinct muscles. Muscles of mastication work in concert with those of the first arch are located in the deep

plane of the face and are suspended in deep investing fascia (DIF). Thus, rostrally located buccinator has r4 fascia and caudally located posterior belly of digastric has r5 fascia. Muscles of facial animation are located in a superficial plane and are suspended in superficial investing fascia (SIF), otherwise known by surgeons as the superficial musculoaponeurotic system or SMAS. The SMAS is continuous with the epicranius layer of the head and therefore second arch facial muscles are distributed over the entire cranium and anterior neck down to the clavicles. This is because there is an uninterrupted subcutaneous plane which second arch can exploit and therefore distribute the facial muscles over a large surface area. The expansion respects the superficial cervical fascia and stays within the confines of the skull.

Third Pharyngeal Arch: Rhombomeres 6–7

This arch is often given short shrift in the literature with only a single muscle, stylopharyngeus, attributed to glossopharyngeal nerve. In reality, it plays a significant role in the construction of the upper pharynx and contains within its fascia multiple muscles the muscles of the palate and superior constrictor. The sensory distribution of third arch is exceptionally broad, from the skull base to the larynx and forward to the posterior third of the tongue. The muscles of the third arch all take origin in somitomere 7, which also provides mesenchyme for the mastoid component of the petromastoid complex. third arch is in register with r6–r7 and receives neural crest from these levels. Its motor innervation resides in the lateral motor column of medulla, specifically in cranial third of nucleus ambiguus. As we shall see in greater detail later, nucleus ambiguus contains neurons for glossopharyngeal in r6–r7, for vagus to larynx in r8–r9 (superior and inferior laryngeal nerves), for vagus to pharyngeal plexus in r8–r11, and for accessory nerve r8–r11. Additional fibers of vagus to the pharyngeal plexus are also found in r7 admixed with those for cranial nerve IX.

Gray's anatomy considers innervation of all the constrictors to come from accessory, in that XI is branchiomotor and takes over for IX. This is simply a question of neuromeric supply within nucleus ambiguus. In this model, soft palate and superior constrictor have motor nuclei in r6–7, middle constrictor is supplied from r8 to r9, and inferior constrictor is innervated from r10 to r11.

Third arch can be said to enclose the terminus of the nasopharynx with the hypopharynx being the province of the fourth and fifth arches. All palate muscles (with exception of tensor veli palatini) and superior constrictor are supplied by r6–r7, but fibers can arrive either via IX per se or via vagus nerve to pharyngeal plexus. This vagal contribution continues to cause confusion because fourth and fifth arches are associated with vagus and third arch is not. Soft palate is definitely not considered a fourth arch structure—in fact, its definition in most texts is rather vague. In sum, palate and constrictor are third arch structures—it does not matter what nerve conveys motor fibers to these muscles—the important neuroanatomic fact is that they are supplied from r6 and r7.

Localization of derivatives and fascia within third arch has not been well mapped-out, but we can use some commonsense neuromeric concepts to deduce its boundaries. Because second arch mucosa is eliminated within the oropharynx, third arch abuts with first arch along a line extending from pterygoid Hamulus to pterygomandibular raphe. It extends all the way back to pharyngeal tubercle of the occipital bone mylohyoid line and the posterior 2/3 of the tongue. Soft palate is halfway between the base of the tongue and the posterior pharynx. Laterally, it interfaces with first arch along Waldeyer's ring and the site of the ancient buccopharyngeal membrane. If there is indeed zonation, the r6 zone should be anterior and that of the palate and posterior to the cranial base should represent r7. The inferior boundary of superior constrictor contains stylopharyngeus muscle and cranial nerve IX, so it obviously borders with fourth arch. Motor innervation for the soft palate has not been mapped out, but is likely a mix between r6–r7. In terms of bone derivatives, r7 neural crest (possibly in combination with lateral plate mesoderm) forms the caudal half of the hyoid bone, the greater cornu, and the mastoid temporal bone.

Fourth Pharyngeal Arch: Rhombomeres 8–9

Fourth arch marks the transition from a nasopharynx to the hypopharynx. Its external boundaries are defined by middle constrictor enclosing an endodermal outgrowth for the respiratory apparatus. Fourth arch is in register with rhombomeres r8–r9, each of which contains a motor nucleus supplying the larynx via vagus nerves. Superior laryngeal nerve to cricothyroid originates from r8, while inferior laryngeal nerve to the remaining laryngeal muscles originates from r9. The laryngeal muscles are likely to arise and migrate from somitomeres 8 and 9 prior to their transformation into occipital somites 1–2. For that reason, they are not routinely listed as somite derivatives. Recall that the principle products of occipital somite myotomes S1–S4 are sternocleidomastoid and trapezius.

Middle constrictor is larger and thicker than its superior counterpart. It extends backward from second and third arch components, lesser and greater cornu. It is shaped like a fan with a broad posterior extension from the lower border of superior constrictor down to the lower pharynx. The lower border of middle constrictor with inferior constrictor admits internal laryngeal nerve and superior thyroid artery, laryngeal branch. For these reasons, it is likely that middle constrictor (like its laryngeal counterparts) arises from *both* Sm8 and Sm9. Motor supply originates from r8 to r9 of nucleus ambiguus via the vagus to the pharyngeal plexus (or accessory). Thyroid cartilage is a fourth arch derivative.

Derivatives of the Fifth Pharyngeal Arch: Rhombomeres 10–11

Fifth arch remains poorly defined. Some consider it nonexistent. But since rhombomeres r10 and r11 remain intact and produce neural crest, since somitomeres Sm10 and Sm11 are present, and since blood supply is available from superior thyroid with collaterals from inferior thyroid, it seems reasonable to assign the final derivatives of the pharynx to this arch. Fifth arch is the putative source of cricoid cartilage. This is an obvious boundary. Below it, trachea forms from cervical lateral plate mesoderm, as does the esophagus, both in register with neuromere c1 and below.

Inferior constrictor is the largest of the three constrictor and overlaps its middle counterpart. It has two parts, *thryopharyngeus* and *cricopharyngeus.* Since the latter abuts with esophagus, it must arise from Sm11; the former arises from Sm10 or perhaps Sm9–Sm10. Passing under the lower border of inferior constrictor, one finds the recurrent laryngeal nerve and the laryngeal branch of inferior thyroid artery. Innervation of thryopharyngeus is from nucleus ambiguus r10–r11, while that of cricopharyngeus may also be recurrent laryngeal nerve.

Formation of the Larynx and Trachea

The exact contributions of neural crest and lateral plate mesoderm to the laryngeal, arytenoid, and cricoid cartilages are unclear, but these structures arise from levels r8–r11. The multiple nuclei of the vagus nerves supplying these structures are distributed along the length of this segment of medulla. The tracheal cartilages display a unique structure that is anticipated by the cricoid. These cartilage units are U-shaped, being incomplete posteriorly. Because endoderm provides the pattern for so many other cartilages in the oropharynx, it is tempting to think that lateral plate mesoderm responds in the same way. The endodermal bud grows downward into an unorganized central mass of LPM and forces it to form rings of cartilage. But what might explain the periodicity of the trachea? Let's speculate a bit.

The origins of LPM in the neck that could contribute to the trachea are the very same as that of the cervical esophagus. The cervical esophagus displays a curious vascular pattern of axial segmental vessels, 4–5 in number (one per neuromeric level). At the level of the thorax, the esophageal vasculature comes from the celiac axis. In mammals, this situation suggests that four neuromeric units are involved in producing the esophagus, i.e., from c5 to c8. At the same time, the musculature of the cervical esophagus gradually changes from striated to smooth, the transition being complete at the thoracic inlet.

It would appear that there is something segmental about the cervical esophagus. The reason for this might be that LPMs and LPMv are unsplit in the neck. Readers will recall that the formation of the bony body wall requires that these two layers separate with LPMv forming the internal mesoderm of the body cavity, while LPMs encircles the visceral organs. Indeed, the anatomy of ribs is nothing more than segmental extensions of PAM from each vertebra that bud outward into the mass of LPMs. We know that somatic LPM follows the same *hox* code as the vertebrae. Thus, within the neck, lateral plate mesoderm maintains an occult segmental pattern. Although cervical LPM is an unsplit fusion of visceral and somatic laminae, it is the somatic component that imposes a segmental order to the esophagus and trachea. *As soon as LPMs and LPMv part company (at the thoracic inlet), all segmentation of visceral structures disappears*.

We therefore arrive at the following hypothetical mechanism for tracheal development. The endoderm confers cartilage-forming signals on the unsplit LPM from neuromeric levels c1 to t1–2. The spaces between the tracheal rings are occult manifestations of individual neuromeric units of LPM. As soon as LPM splits apart at the inlet, gene expression within LPMv responds by formation a carina and the appearance of lung buds. The lungs are appropriately enclosed within the ensheathing visceral pleura. Sensory innervation of the visceral pleura is non-segmental. It is organized around the neuromeric units of the sympathetic autonomic nervous system (SANS). The parietal pleura, on the other hand, is formed from LPMs, innervated segmentally and thus is capable of exquisite, localizing pain.

Spatial Relationships of Pharyngeal Arches

Mammalian facial muscle anatomy represents a significant departure from the initial arrangement of pharyngeal arch muscles in other tetrapods. These muscles were designed to be co-planar. Deep layer muscles fulfill a sphincteric function, while superficial muscles act as dilators. The original branchial arch gill structure had anterior (pre-trematic) and posterior (post-trematic) elements. We advance the hypothesis that the neuromeric arrangement of the pharyngeal arches is a holdover of this anatomic plan. Every arch is in register with two rhombomeres. The cranial neuromere produces anterior structures, while the caudal neuromere produces posterior structures. With embryonic folding, these become to rotate 90°. Hence, the r2 maxillary complex is cranial to r3 mandible.

Only a few second arch muscles remain co-planar with those of the first arch. Most second arch mesenchyme is positioned superficial to envelop the first arch with the facial muscles positioned superficially with an entirely separate fascia, the SMAS. The third arch (r6–r7) remains co-planar with the first two, however. It abuts up against the r8/first occipital somite muscle, the sternocleidomastoid. One could

surmise that the amalgamation of PA2 with PA1 occurs concomitant with or shortly after the formation of PA3. The fourth and fifth arches are formed in continuity with the caudal aspect of PA3 and thus are "tucked in" deep to the plane of the first three arches. Thus, at the level of PA3, the pharynx becomes a *tube within a tube*.

Formation of the Cranial Base

Posterior Cranial Base

Analysis of the order of ossification of the facial skeleton from a neuromeric perspective reveals several important observations. The development of the neurocranium is in direct proportion to the need for brain coverage. Bone made from somitomeric PAM will at all times form before that formed by neural crest. The chondral neurocranium preceeds the membranous neurocranium. For example, basipostsphenoid (PAM from the first somitomere) forms before the presphenoid (r1 neural crest). Why might this be so?

We can envision a spatial relation between the neuraxis and the somitomeres versus the eventual position of the pharyngeal arches. Although the somitomere may not possess a sclerotome per se, the physical position of the PAM next to the neural tube makes it likely to be converted into paraxial bone. Just like company of firefighters provides the "first response" to an emergency in their neighborhood, so does PAM represent the mesodermal "first response" to brain formation and the need for structural support.

The timing of neural crest migration occurs well after somite formation. Neural crest thus represents a "second response" to brain formation. Just as in the formation of a house, the foundation of the cranial base is first laid down by PAM, because this mesenchyme is physically situated at the ground floor. Subsequently neural crest takes over, making the ensheathing bones of the calvarial roof. This happens as the sidewalls of the neural tube grow upward and approximate. Neural crest from the neural folds follows this process right along. It is thus no accident that the ossification sequence of the frontal and parietal bones is ventral to dorsal.

The layout of the chondrocranium demonstrates these concepts. Somitomeres Sm1–Sm3 lie just lateral to forebrain. They do not contribute bone. Sm4 makes basisphenoid. From the sphenooccipital synchondrosis backwards, basioccipital is laid down by parachordal cartilages from Sm5 to Sm7. Sm6–Sm7 contribute laterally to the otic capsule. Sm8–Sm11 become occipital somites S1–S4. Because the somitomeres are sessile and located immediately next to the notochord, they can be rapidly converted to cartilage. From basisphenoid forward, all derivatives are mesencephalic neural crest from r0/r1. These include the trabecular and ethmoid cartilages that fuse to make presphenoid and ethmoid. Lateral to these cartilages are the nasal and optic capsules. Refer again to Figs. 2.68 and 2.69.

Cranial base anatomy displays both segmentation and parasegmentation. PAM forming the basisphenoid is strictly an r1 derivative. So too, the temporal bone comes from Sm6–7 plus corresponding r6–r7 neural crest. *Parasegmentation begins at the spheno-occipital suture*. Each of the four occipital somites contribute to the basioccipital, exoccipital, and supraoccipital bones in a laminar manner. If the sclerotomes of these somites produced vertebrae, it would be as if the four bodies were fused in succession like Russian dolls forming BO. The lateral elements around the foramina would likewise be laminated, with r8 on the outside and r11 closest to the ring. These laminae would produce the exoccipital bone. Finally, fusion of the neural arches would yield the supraoccipital bone (Figs. 2.72, 2.73, 2.74, and 2.75).

Experimental work provides solid evidence that this is so. The avian model described by Huang has five occipital somites [22, 23]. Using tracing maker methodology, the contributions of each somite to the skull base are depicted in color. O'Rahilly demonstrated the mammalian model to have only four somites [24]. The pattern of these is similar to that of birds, so it is reasonable to suppose that the same topology of assembly holds true as well.

Anterior Cranial Base

We have completed our survey of the mesenchymal derivatives involved in head and neck. We are now in a position to understand facial bone formation in terms of neuromeric derivatives. This is a visual exercise involving migratory pathways by which neural crest and PAM arrive at their final destinations in the face and skull. A description of this entire process is beyond the scope of this paper. Nonetheless, we can use a model of the *fronto-orbito-sphenoid complex* as a convenient model to study how these migrations can be understood on a neuromere-by-neuromere basis. (Assembly of the facial midline will be covered in greater detail in Chap. 3).

This science has direct relevance for the surgical correction of congenital based on the painstaking clinical observations of Paul Tessier regarding the various forms of craniofacial clefting [1–3]. Tessier documented that these anomalies seemed to follow certain occult anatomic patterns that he classified numerically. The Tessier system, derived purely on an empiric basis, has a remarkable fit with neuromeric fields. By understanding the face as an assembly of fields with a neuromeric basis, clefting takes on an entirely new relevance for neuroscientists and surgeons alike.

Analysis of craniofacial clefts provides the means by which we may understand the developmental anatomy of the

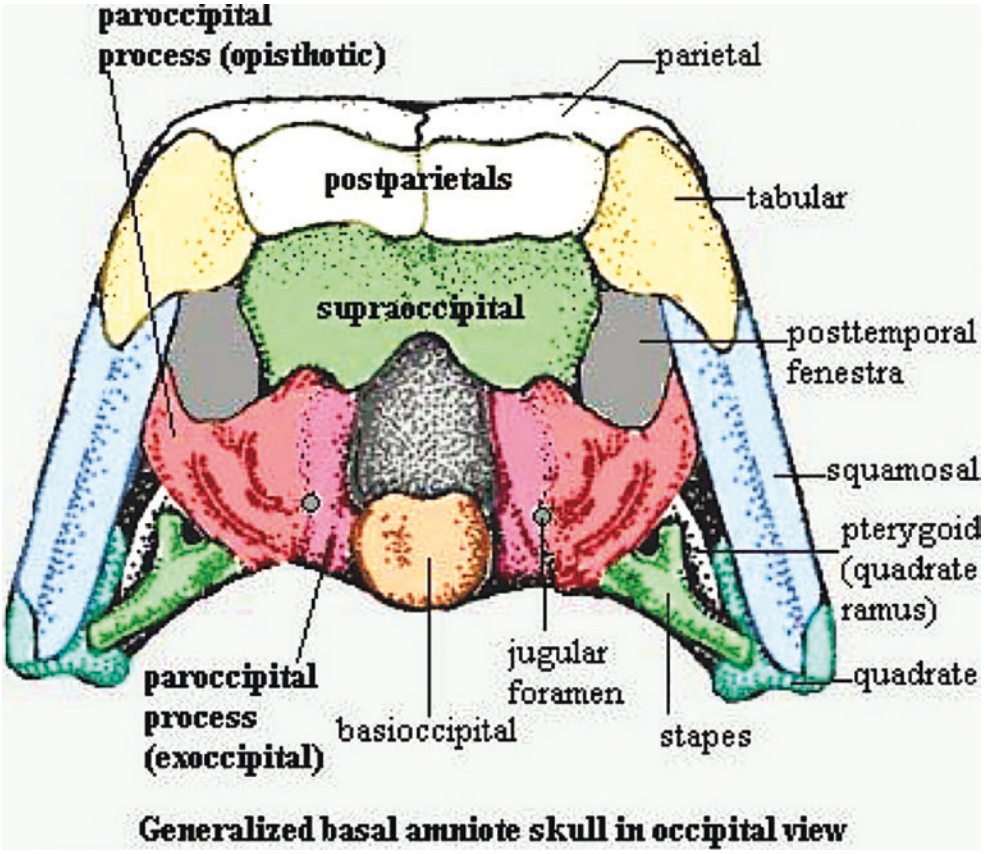

Fig. 2.72 Occipital bone complex of basal amniote. (Courtesy of Augustus T. White, Palaeos.com. http://palaeos.com/vertebrates/bones/braincase/images/Opisthotic2.jpg)

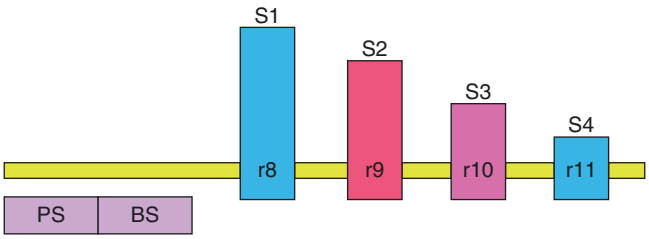

Fig. 2.73 Posterior cranial fossa development 1. Embryogenesis of the posterior cranial base involves amalgamation of the first four occipital somites. These can be considered as primitive vertebrae. The ventral hemal arches combine to make the basioccipital bone(s), the lateral pedicles produce the exoccipital bones, and the neural arches form the supraoccipital bone(s). Purple = r1 presphenoid and basisphenoid. Turquoise = r8 first occipital somite. Red = r9 second occipital somite. Pink = r10 third occipital somite. Blue-green = r11 fourth occipital somite. (Courtesy of Michael Carstens, MD)

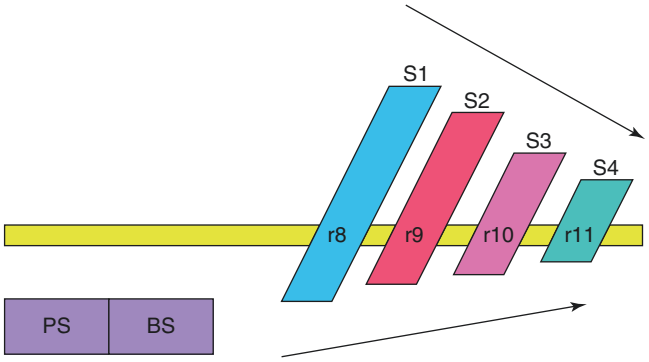

Fig. 2.74 Posterior cranial fossa development 2. Although somites 1–4 initially appear as somite-like masses, they undergo a topologic transformation in which they become inclined and stack up sequentially inside each other like Russian dolls. Under the influence of occipital lobe, development of the fused neural arches undergoes expansion posteriorly and superiorly. Each of the occipital somite myotomes contributes myoblasts to the tongue. The low hairline and large tongue seen in Down's syndrome reflect misallocation of paraxial mesoderm away from the occipital braincase and toward the tongue muscles. (Courtesy of Michael Carstens, MD)

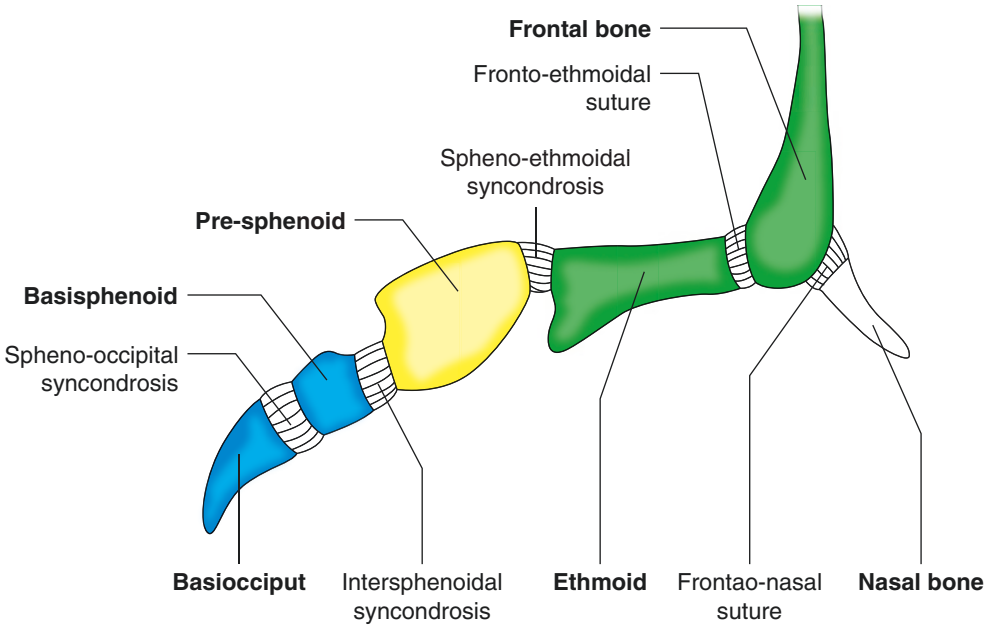

Fig. 2.75 Cranial base sutures

fields themselves. It is a secret window into the spatiotemporal order of neural crest migration. Let us examine a theoretical diagram of the anterior cranial base in which each field is color-coded to match its neuromeric level of origin. The pathways by which neural crest cells arrive at the orbit and the structures created by each neural crest are indicated by color-code arrows. The physical location of all neural crest cells is understood to be from sites above and behind the orbitosphenoid complex. Derivatives listed most distally along each pathway migrate earlier and develop earlier.

The discerning reader will note that most neural crest bones of the face form via membranous ossification. However, when neural crest cells are grown in isolation in vitro, they form cartilage. Craniofacial neural crest, in order to form a membranous bone, requires signaling from epithelium. In the absence of such interaction, cartilage will form. But this does not determine that the cartilage will automatically become chondral bone. Subsequent signals can convert a neural crest cartilage to a membranous bone. Another example of this process is the zygoma, attached first to the maxilla as a neural crest cartilage derivative and subsequently converted into membranous bone.

Orbitosphenoid Derivatives Neural Crest

These bones originate from MNC and are programmed by dura and sclera.

The anterior surface of the neural crest presphenoid (PS) is facing us. Hidden behind it is the basisphenoid (BS) produced from paraxial mesoderm of somitomere 4. Although these two bones have differing mesenchymal sources, both PS and BS belong to the axial cranial base. Both are formed by chondral ossification. *All components of the cranial base, be they from paraxial mesoderm or from neural crest, develop as* cartilage. Recall that pituitary represents the dividing line for the anterior cranial base. All bone fields anterior to it are neural crest; all those posterior to it are PAM (Fig. 2.75).

Arriving later in time, two neural crest *orbital cartilages* flank the presphenoid. These ossify to make the orbitosphenoid (OS), better known as the lesser wing. OS is joined to PS via two bony pedicles. These form an arch around the preexistent optic nerve, the optic foramen. Projecting like a beak from the anterior-inferior (rostral-ventral) surface of presphenoid is the *pharyngeal tubercle*. Hanging down caudally from the underbelly of PS are two neural crest laminae, the medial pterygoid plates (MPt). These are remnants of ancient pterygoid. A secondary chondral extension later develops: the pterygoid hamulus, around which the sling of tensor veli palatini will be draped.

Fronto-Orbital Derivatives

These bones originate from MNC programmed by p5 dermis and r1 dura (light blue). MNC sweeps into position over the frontal lobes and below FNO skin producing dura and subcutaneous tissue. The programming for frontal bone relates to frontal lobe developmental fields. The ossification center for each frontal bone is centered between two branches of V1 stapedial: frontal artery via supratrochlear supplies Tessier cleft zones 13 and 12, while supraorbital supplies zones 11 and 10.

Below the horizontal axis of the artery, the orbital rim has two fields that appear to be in continuity with frontal but are biologically distinct. Medial is *prefrontal* bone (PrF) and lateral is *postfrontal* bone (PF): they belong to zones 11 and 10, respectively. These bones form by a wave of ossification which starts inside the orbital roof, moves outward and ascends from the orbital rim. Recall that MNC makes the

dura of the anterior cranial base and that sclera is an extension of dura as well. Thus, the orbital roof component of these two fields is potentially bilaminar and can make a sinus.

These upper frontal fields are exquisitely sensitive to perturbations in the underlying r1 zone, whereas PrF and PF are resistant. Thus, in *anencephaly*, the orbital rims remain intact. The mediolateral axis of the frontal fields displays a clear-cut time line. The more medial fields form last. Thus, global deficiency states first manifest themselves medially and, with greater severity, progress laterally. Trigonocephaly, frequently accompanied by frontal lobe deficits,

Palatine Derivatives

Attached only the ventrolateral aspect of the presphenoid is the alisphenoid bone (AS), forming the greater wing of the sphenoid. AS is the remnant of ancient epipterygoid. Its axis is meningo-orbital artery which is sole anterior branch from StV2 intracranial to the orbit. Ossification of AS occurs in two ways. The lateral margin of the superior orbital fissure forms in cartilage. The remainder of the AS is a membranous bone. Hugging the external face of the r1 MPt is a second laminar bone; the lateral pterygoid plate (LPt) is the remnant of ectopterygoid and is r2 RNC. Just like MPt, LPt is formed in membrane.

Sitting directly in front of the medial pterygoid plates just like two bookends are the r2 palatine bones. They develop from the descending palatine neuroangiosome. These strictly membranous bones have perpendicular and horizontal laminae joined at a 90° angle. At the anterior and superior corner of the perpendicular lamina, each palatine bone projects a quadrangular, superiorly directed *orbital process*. These orbital processes are not obvious within the eye socket. (Designed by nature expressly for purposes of the plastic surgery oral board examination.) Just posterior to the orbital processes, smaller prominences project upward to make contact with the anterolateral corners of the presphenoid. Between these anterior orbital processes and the posterior sphenoid processes lies the sphenopalatine foramen. *This is an absolutely critical anatomic landmark with enormous significance for the formation of cleft lip and palate*.

Nasopalatine Derivatives

Through the sphenopalatine foramen passes the most medial branch of the StV2, the axis of medial nasopalatine artery (NPm). Neurovascular pedicles are like paleontologic footprints; they serve as evidence of the earliest cellular migrations in the embryo. In this case, the sphenopalatine axis shows us the pathway by which neural crest passes forward toward the orbit, is forced by *preexistent r1 mesenchyme* to take a posterior and inferior route, and gains access to the midline of the future nasal cavity. The nasopalatine field contains within it two neural crest osteosynthetic "packets." The most anterior is that of the premaxilla; this is followed up by the vomer. The presence of r1 neural crest in the roof of the nasal midline guides NPm into the midline of the future face. Without this r1 "superhighway," vomer and premaxilla will be unable to arrive at their destination in zones 1 and 2. Pathologies that affect the ethmoid complex, such as holoprosencephaly, can create varying degrees of deficiency or outright absence of the vomer/premaxilla complex.

Assembly of the Face

Herein we present a preview of a topic which is the subject of Chap. 4. What we have accomplished in this chapter is to catalog one-by-one the mesenchymal components that are used to construct the face based upon their neuromeric level of origin. So far, our discussion has been static. We will now illustrate the dynamics of this assembly process. This topic is so important that it merits in-detail treatment in Chap. 4. Our purpose in this section is to integrate what we have covered so far and show the basics of how this process works.

Facial construction occurs in three related steps: (1) The frontonasal skin envelope is created by epidermis from rostral forebrain nonneural ectoderm and dermis from caudal forebrain neural crest. (2) A massive migration of midbrain neural crest creates paired fronto-naso-orbital units that (with apotosis and the approximation of the nasal placodes) fit together like the letter "T." (3) Rostral hindbrain neural crest + PAM from somitomeres 4 and 6 creates the non-jaw components of first and second arches. The two arches are amalgamated masses of soft tissue. They move medially under the wings of the "T" to fill out the facial midline. The timeline for this process is very tight and precise.

Like an origami puzzle, the face "comes together" when two lateral components (the pharyngeal arch complexes on either side) sprout out from the rhombencephalic zone of the embryo, extend towards each other in the midline like pincers, and make contact with a central pair of units organized around the forebrain. This process is driven by apoptosis of nasoethmoid MNC discussed in greater detail in Chap. 4.

An apology straightaway to the reader is due here. Although experimental work has defined the end point of neural crest migration, the start point on a zone-by-zone basis is less clear. ***Here are our working hypotheses***.

1. Neural crest populations *migrate in a strict time sequence*.
2. A developmental zone contains *several populations*, each producing a specific anatomic structure or field.
3. Fields develop according to their vascularization.
4. Adjoining developmental fields are interdependent. Substances produced in one field may affect the function of another.
5. Developmental zones are autonomous; if a neural crest field N in zone X is deficient, it will not affect the ability of fields to develop appropriate cell mass in adjacent zone Y.

6. The presence of a deficiency in zone X can affect the physical shape of fields in adjacent zone Y. These other normal fields will have normal volume and surface area, but, with growth, they can undergo *secondary deformation* as they collapse into the deficiency site. This is known as *deficiency-induced field mismatch*.

Neuromeric Production of Soft Tissues

In subsequent sections, we shall be discussing the mechanisms by which a spectrum of clefts is produced using a neuromeric field model in which deficits in specific fields lead to specific types of clefts. To do so, we shall need to expand our vocabulary one step further. Neuromeric concepts must be applied to soft tissue structures as well.

To this point, the anatomy of facial fields has been presented in terms of the mesenchymal components that make them up, emphasizing neural crest and paraxial mesoderm. Our discussion of neural crest has focused on: (1) *where* the neural crest components arise in the embryo prior to their migration, (2) the *sequence* in which these neural crest fields migrate to the face, (3) the *pathways* they use to get there, (4) the *spatial arrangement* of the fields once in final position, and (5) the *developmental relationships* that exist among fields that enable them, like Lego® pieces, to fit together in a precise time sequence to build the face.

Our discussion of mesoderm has focused on: (1) distinguishing its various *anatomic types* (paraxial PAM, lateral plate LPM), (2) its *mechanism of formation* during gastrulation, (3) the *neuromeric basis of segmentation* as it applies to the gastrulation process, (4) *somitomeres and somites* as segmental units, (5) *neural crest contributions* with these mesodermal structures, (6) the *reorganization* of facial mesenchyme into head mesoderm, pharyngeal arches, and occipital somites, and (7) the *spatial origami of head folding* by which these units are positioned for final integration into the face.

Because the facial bones are so readily distinguished and because they form in such a strict time sequence, much of our discussion of developmental fields has to date centered on these bony building blocks. But we must now change our emphasis completely to that of the soft tissues. ***The bones of the craniofacial skeleton, like all bones in the body, are merely the products of soft tissue developmental fields*** (functional matrices, if you will). Any defect in a bony is merely the manifestation of a problem in the functional matrix that produced it. A field/functional matrix disturbance can therefore manifest itself in bone, in soft tissue structures, or in both.

Skin

Cutaneous coverage of the head and neck has its own separate chapter. For our purposes, consider the following. The *skin of the forehead, nose, and philtrum* is composed of p5 nonneural ectoderm epidermis and p5 neural crest dermis. The *upper eyelid* epidermis comes from p5 NNE and the dermis is made from r1 MNC. The epidermis of the *lower eyelid* is made of r2 ectoderm, while the dermis is produced by r2 neural crest. For this reason, the sensory supply to the upper lid *and the entire conjunctiva* is from V1, while that of the lower lid is from V2. The remainder of the facial skin is produced in accordance with its innervation patterns. Ectoderm corresponding to r2–r11 is initially present in the five pharyngeal arches, but as these fold up upon one another, r6–r11 ectoderm disappears. The remaining facial skin is produced from r2 and r3 (with a small representation of second arch r4–r5 skin over the external auricle).

The dermatomes of the occiput come from cervical neuromeres c2–4. Neural crest likely produces the *hair of the face and scalp* from r1 to r3 and from c2 to c4. It is intriguing that the hair pattern corresponds to the dermis innervated by the dorsal (epaxial) branches of C2–4, while the dermis supplied by ventral (hypaxial) branches of C2–4 is hairless. In the same manner, a dorsal/ventral pattern might be seen in V2 and V3-derived dermis. The epaxial dermis would produce hair, while the hypaxial dermis would produce beard. Most patterns of human hair formation fit this model. Eyebrows, for example, would occur at the interface between r1 RNC dermis and p5 PNC dermis. They also correspond to the surface anatomy of orbital bone fields: prefrontal and postfrontal.

Mucosa

Nasal vestibular lining develops from the nonneural ectoderm of the nasal placode. *Oral mucosa* develops from ectoderm of pharyngeal arches 1–2. Representation from the second arch is quickly crowded out and disappears due to expansion of the first and third arches. The oropharynx posterior to Waldeyer's ring is produced from endoderm of pharyngeal arches 3 and 4, like a series of Michelin tires stacked one aside the other.

Facial Muscles, Fascia, Fat

Muscles of mastication originate from somitomere 4 (first arch) and somitomere 6 (second arch). They are covered by neural crest deep investing fascia from r2 to r3 and r4 to r5, respectively.

Facial muscles develop from somitomere 6. Those supplied by the upper division of the facial nerve are covered in neural crest fascia likely to originate from the proximal second arch (i.e., from r4), while the fascia corresponding the muscles supplied by the lower division of the facial nerve would originate from the distal second arch (i.e., from r5). *Salivary gland* formation would result from neural crest mesenchyme from r4 to r5 invaded by oral epithelium. The connective tissue within the salivary glands is r3 oral epithe-

lium. This has implications for understanding the derivation of the parotid gland. Because this structure is penetrated by the facial nerve, it may be reasonable to assign it to r4 and r5 (being distributed along the upper and lower divisions, respectively). Facial *fat* is a neural crest derivative.

Biologic Basis for Developmental Fields

At this juncture, the discerning reader must be queried by nettlesome questions such as: Does the functional matrix concept have any provable experimental basis? Why should I bother learning this stuff? The best answers to the first question reside in a plethora of papers stemming from the quail-chick chimera system popularized in developmental biology literature by Couly and LeDourain. These investigators showed that visible differences in neural crest cells existed in quail and chick embryos such that microsurgical extirpation experiments could be carried out. When NC cells from one type of embryo are transplanted into the other, their derivatives can be distinguished under the light microscope. Using the neuromeric map, these authors were able to demonstrate what derivatives came from what levels. For example, the mandible, malleus, and incus are all neural crest products from level r3.

The Couly-LeDourain model also allowed for assessment of programming function. How does r2 neural crest "know" to make zygoma or r5 neural crest to make hyoid bone? The answer is not surprising. Mesenchyme responds to an occult *program in the surrounding epithelium* [143–147]. Ectodermal zone patterns influence the development of dermal bones. More recently, foregut endoderm (FE) has been shown to instruct neural crest what to do. By taking out a certain zone of FE, specific parts of the hyoid bone fail to appear. The spatial layout of the hyoid fields is faithfully reflected in the organization of the FE. Finally, if a given zone of FE is reversed 180°, then the corresponding part of the hyoid bone is reversed as well.

Thus, all neural crest bone and cartilage derivatives associated with the foregut arise as the result of programming embedded in the endoderm. Because the endoderm in each region arose from a spatially dedicated zone of epiblast cells, it can truly be said that the overall organizational plan of the organism is set up prior to gastrulation.

Future research will undoubtedly result in the understanding of the fate of foregut endoderm. Specific zones will correspond to specific structures. Each zone will ultimately be categorized by a unique pattern of gene expression, alterations of which will lead to predictable abnormalities in the neural crest products associated with that zone.

Developmental fields do not occur in isolation. Interaction with other fields is often required. This is particularly well demonstrated in the formation of facial bones. Many of these structures result when specific populations of neural crest migrate from their nascent position in the neural fold to distant locations. Here they interact with local epithelial cells (ectoderm or endoderm) from which they receive signals that determine cellular mitotic rate (volume) and the physical confines in which such population expansion may take place (shape). Moreover, the presence of one field may be required in order for another field to correctly develop. The footplate of the lacrimal bone is positioned just lateral to the inferior turbinate (IT). *The formation of the inferior turbinate occurs earlier in time than does that of the lacrimal bone*. A disturbance in the formation of IT may lead to defective or absent lacrimal system. By the same token, problems within the lacrimal system (stenosis of the duct) can occur without affecting the inferior turbinate.

It should be thus apparent that developmental fields are the results of tightly regulated sequence of field creation, field positioning, and field assembly. Process such as flexion of the embryonic neuraxis, spatial repositioning of pharyngeal arches, and programmed cell death (apoptosis) are required in order for field assembly to take place correctly. All students of the nervous system will recognize that brain growth is critical to the development of the face. It should be understood, up front, that the migration of neural crest cells refers to a point in time before embryonic folding takes place. All the populations have arrived and are positioned with respect to epithelial developmental zones and pharyngeal arches.

Recall that positional genes, such as the *DLX* system, map out the arches into spatial regions, each with its own developmental fate. ***Thus, the spatial position of a neural crest population on the neural fold or in the pharyngeal arch does not confer specificity. Once the cells arrive at their destination, they are "instructed" as to their final anatomic form***. Thus, r1 neural crest does not "know" to become the sphenethmoid complex. Those cells that become physically positioned in front of the notochord will be instructed by it to form the trabecular cartilages from which develop first the presephenoid and later the ethmoid.

Toward a Neuromeric Theory of Facial Cleft Formation

The purpose of this chapter has been to demonstrate how neuromeric concepts can be used to understand facial development. From this, an integrative theory of cleft formation will be presented. We shall begin with facial bones and then proceed to soft tissue structures. This distinction is completely artificial! Recall that facial bones are mesenchymal responses to an epithelial (soft tissue) environment. *Bone does not "grow itself": it is the product of a developmental field*. Each developmental field is neuromeric in nature and includes ***all soft tissues associated with a given bone***.

Muscle insertion into its "target" bone is a good example. Muscles take their origin from a specific somitomere, somite, or group of somites. This origin corresponds to the neuromeric level of its motor nerve. The muscle then makes a primary insertion into a bone developing from the *same* neuromeric level. Supraspinatus is innervated by C5 and therefore originates from somite S9. The supraspinous fossa of scapula arises from neuromeric level c5 as well; therefore, it receives the primary insertion of the muscle. The secondary insertion of a muscle is into the nearest available binding site, preferably one arising from the same neuromeric level. Hence, supraspinatus seeks out the c5 developmental zone of humerus. Infraspinatus is larger. It is innervated by both C5 and C6 and therefore takes origin (distal to infraspinatus) from S9 and S10. Its primary insertion into infraspinous fossa occurs because this zone of scapula arises from both levels c5 and c6—and therefore has a larger surface area. It then seeks a secondary insertion more distal on the humerus (Fig. 2.76).

Understanding the pathways by which neural crest cells migrate into position is a crucial first step in our discussion. Facial bone synthesis occurs in a rigid spatiotemporal order There are three general populations of neural crest involved in constructing the face; the behavior of each depends on its anatomic zone of origin.

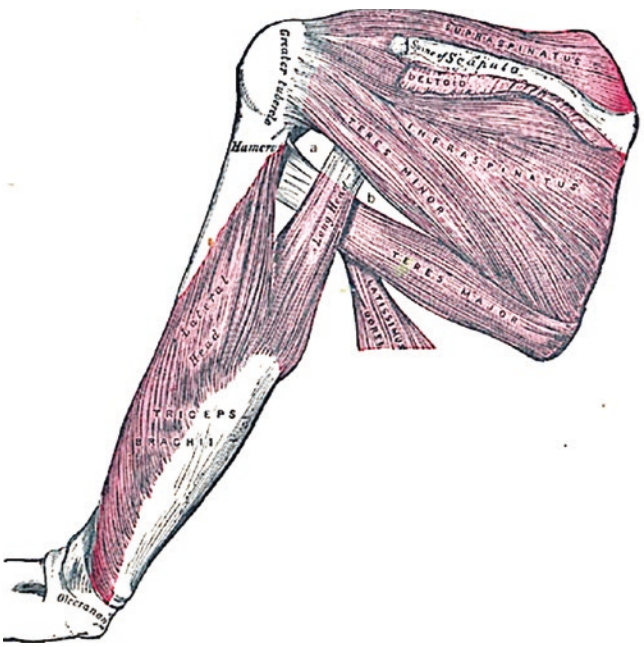

Fig. 2.76 Muscle origin/primary insertion/secondary insertion: the scapula model. Suprapinatus C5 suprascapular nerve, infrasinatus C5–C6 and teres minor C5–C6 axillary nerve—c5 zone of humerus. Teres major C5–C6 lower subscapular nerve—more distal has c6 zone. Note triceps is c6–c7 zone on the humerus. (Courtesy of Michael Carstens, MD)

- Prosencephalic neural crest (PNC) arises from the neural folds above the caudal forebrain. PNC migrates forward like a *glacier-like sheet* to populate the neural folds of the rostral forebrain (which are lacking in neural crest). PNC has a limited but important role. It produces fronto-naso-orbital skin.
- Mesencephalic neural crest (MNC) arises from the neural folds above the midbrain proper (an enormous structure in the embryo) and from rhombomeres r0 and r1. MNC departs and the midbrain develops—in caudal-cranial order—as *individual streams* and migrates forward beneath the nonneural ectoderm outside the brain where it is responsible for the synthesis of forebrain dura, anterior cranial fossa, the sphenethmoid complex, the primary nasal cavity, and the superomedial orbit.
- Rhombencephalic neural crest (RNC) arises from the neural folds above the hindbrain. RNC migrates in strictly defined *segment*s into the pharyngeal arches. It produces the remainder of the inferolateral orbit, supporting bones, fascia, the caudal components of the nasal chamber, (e.g., vomer, premaxilla, inferior turbinate, and hard palate), the oropharynx, and larynx.

A detailed description regarding the anatomy of these populations, how they relate to the neuromeric system, and how isolated defects in a component population lead to a craniofacial cleft is the subject of this chapter. Our model will focus on the fronto-naso-orbito-maxillary complex—as this is where facial clefts occur. We shall examine first how the bone fields form and then turn our attention to the soft tissue anatomy of the nose and mouth. The interactions between underlying bone fields and soft tissue fields that characterize the common labiomaxillary cleft will be detailed as these provide a common biologic model for craniofacial cleft formation in general.

Zygomatico-Maxillary Complex

The ZMC consists of the upper jaw and the r2 bones that constitute its medial wall (palatine, inferior turbinate) and connect it with the face.

Melding of individual fields to form the face is *not* a slow process. Although the four types of neural crest that migrate into the head and neck (RNCc, MNC, and RNCc, PNC) complete their migrations at different times of embryonic development, all neural crest are in place within a matter of 15 h or so. These components of the future face are initially located in parts of the embryo that are widely separated. The PNC and MNC are positioned together initially around the brain, while the rostral RNC is found in the pharyngeal arches. Furthermore, by the time PNC has populated the future frontonasal zone of the embryo (Carnegie stage 10), reorganization of the first 11 somitomeres into pharyngeal arches and occipital somites is complete. These quite dispa-

rate components must be physically approximated in order for facial assembly to occur. Cephalic folding accomplishes this goal in less than 24 h.

Human embryos at day 22 have cephalic neural folds that are broad and thick. These stick up in the air like the fins of some ancient Cadillac limousine. The reason for this neural fold projection is the tremendous proliferation of head mesenchyme lying just beneath them. This mesenchyme is, of course, a product of the explosive growth of MNC. Somitomeres lie astride the future cranial base like saddlebags. Their individual contributions have been described.

The rapidly growing embryo lies atop a yolk sac that is not growing much at all. As the cephalic part of the embryonic axis expands, its yolk sac "tether" forces the neural plate to bend at specific sites. The first of these flexures occurs at the site of the future mesencephalon. At day 22, the *cranial* (*mesencephalic*) *flexure* bends the prosencephalon ventrally toward the pharyngeal arches. In less than 24 h, the angle between the forebrain and the rest of the neuraxis decreases from >150° to <100°. Voila! The first and second pharyngeal arches now have ready access to the frontonasal mesenchyme. Although these mesenchymal masses are covered with epithelium, when contact is made between the frontonasal and lateral masses, epithelial fusion quickly ensues. The underlying mesenchymal fields can now interact.

What does the field geography look like at the time of arrival of the pharyngeal arches? Let's pretend we are standing in front of the embryo, directly opposite the future embryonic mouth. In front of us on either side we see the combined first and second arch complexes containing all the future bone and muscle fields of PA1 and PA2. The mesenchyme of these arches has had ample time to fuse, thus forming the first-second arch "sandwich." The upper (maxillary) half of our sandwich contains all the bone fields produced by r2 and r4 RNC. Although the maxillary mesenchymal mass seems just a shapeless blob, in reality these fields are all lined up in precise spatial order, ready to develop into specific bone and soft tissue structures. Superficial to these bone fields lie the blastema of the future facial muscles produced by Sm5 PAM with the fascia provided by r5 RNC. Laid out in exactly the same manner is the lower (mandibular) half of our sandwich, the bones and muscles of which are made from the same precursors. A hidden "fault line" exists in the pharyngeal arch separating the soft tissue mesenchyme of the maxilla and the mandible. In the Tessier #7 cleft (lateral orofacial cleft), the soft tissues are divided by a fissure extending from the oral commissure back to the ear.

In the neuromeric model, the development of each pharyngeal arch follows certain hypothetical rules. We shall discuss them and see how they are applied to the formation of the face. (1) Tetrapods possess five pharyngeal arches. The fate of the original sixth and seventh arches in tetrapods is to become transformed into the upper neck (c1–c4). (2) Aortic arch arteries are formed by the fusion of a bud from the dorsal aortae and a bud from the ventral aortic outflow tract. (3) In each arch, blood supply becomes preferentially available to the caudal mesenchyme such that the distal end of each pharyngeal arch is first to develop. (4) In each arch, the bone derivatives of the caudal and distal sectors will form earlier in time than those of the cranial and proximal sectors.

Initially, the pharyngeal arches project outward from the embryo like sidearms. Explosive growth of the PA1/PA2 arch complex takes place at the very same time as the embryo undergoes head flexion. This differential growth causes the sidearms to physically become repositioned toward the ventral midline of the embryo. This takes place concomitant with massive apoptosis of the MNC nasoethmoid complex. In so doing, they come into a "docking position" below the frontonasal mesenchymal mass. The PA1/PA2 field complex locks on to, and then interacts with the previously constructed fronto-naso-orbital mass. Thus, preexisting pathology of FNO fields can impact upon the development of the RNC fields.

The concept that a given field is the prerequisite for proper development of subsequent fields has a sound experimental basis. Neural crest cells respond differently according to their epithelial environment. In the presence of pharyngeal endoderm, NC will form cartilage, whereas, when in contact with ectoderm, NC forms membranous bone. Furthermore, neural crest-derived cartilages can serve as precursors of membranous bone. When strips of foregut endoderm were removed in chick embryos, specific cartilaginous bones failed to develop. Adjacent neural crest membranous bones normally destined to ossify later on from PNC or PA1 also failed to develop. Absence of Meckel's cartilage (subsequently the quadrate and articular bones) led to developmental failure of the pterygoid, quadratojugal, angular, supra-angular, opercular, and dentary bones.

We shall now describe how MNC and RNC become physically positioned. The facial midline consists of three complexes of fields.

- A fields: MNC fronto-naso-orbital skin and bone fields are supplied by V1 stapedial branches of ophthalmic artery.
- B fields: $RNC_{ROSTRAL}$ mesenchyme forms the jaws and supporting bone fields; it is supplied by V2 and V3 stapedial branches of internal maxilla-mandibular artery.
- C fields: $RNC_{ROSTRAL}$ mesenchyme forms all remaining structures of the first and second arch complex (except the jaws) and is supplied by branches of external carotid artery.

The maxillary fields are assembled from seven populations (fields) of r2 neural crest, all of which sweep forward

toward the developing face in a strict spatiotemporal order according to their site of origin on the neural fold. Their target, the r0/r1 primordium of the sphenethmoid and orbit, is already in place. The blood supply to each field comes from the stapedial V2 branches of internal maxillary. *The physical anatomy of these arteries, the order in which they form the internal maxillary axis, replicates the spatiotemporal order of the fields they serve*. First to arrive is the r2′ premaxillary and vomerine MNC supplied by the terminal branch of the IMA, the *medial sphenopalatine artery*. (All subsequent fields come from r2 proper.) Next on the scene is the r2 inferior turbinate field supplied by the *lateral sphenopalatine artery*. Behind IT comes the palatine bone supplied by the *greater palatine artery*. Note the horizontal plate of palatine bone and the anterior palatine aponeurosis are supplied by *lesser palatine artery*. Mx1, Mx2, and Mx3 follow in succession, each supplied by their respective superior alveolar branches off the *infraorbital artery*. *Zygomatic artery* arises from infraorbital and supplies the latera wall of the orbit.

Construction of the malar fields occurs around the axis of the zygomatic nerve. In zoologic terms, the zygoma has a cranial field, the *postorbital bone*, and a caudal field, the *jugal bone*. Persistence of this transverse separation is occasionally seen as the *os japonicum* [142]. The post-orbital bone articulates with the zygomatic process of the frontal bone to form the lateral orbital rim. Isolated failure of the field is the Tessier #8 cleft. It also articulates with the posterior maxillary wall Mx3. Hence, the association between the Tessier #6 cleft with the #8 cleft. The more caudal field, the jugal bone, bridges between r3 zygomatic process of the squamous temporal bone and the maxillary buttress above the first molar. The zygoma is an example of a neural crest derivative that begins as a cartilage and then is converted into membranous bone. The ossification process is exactly analogous to that of the coronoid process of the mandible.

Connecting the ZMC with the Cranium

Previously, we have seen how brain growth forces the embryo to flex. This brings the cranial base of the anterior fossa into contact with pharyngeal arch mesenchyme to assemble the face. Interaction between A and B fields at critical contact points results in horizontal (lateral to medial) and vertical (cranial to caudal) approximation. The tissues for the letter "T." These processes are well depicted in the SEM work by Hinrichsen and schematically illustrated by this author in a previous communication [143].

The first relevant A-B contact is between the r1 sphenethmoid mesenchyme and the r2 premaxillary mesenchyme. As the future PMx/V fields travel toward the face, they encounter a physical obstacle, the previously synthesized r1 back wall of the orbit. Unable to advance further, they are forced ventrally. They duck beneath the orbit, seeking the midline. PMx and V pile up beneath the presphenoid. They then "see" their respective ethmoid lamina and beneath which they "hitch a ride" to their final destination. Apoptosis of the MNC ethmoid mesenchym in the center of the face causes the nasoethmoid-premaxillary-vomerine masses to approximate each other. They eventually fuse, uniting the facial midline. Failure of this to take place is the basis of hypertelorism.

The external appearance of the early embryonic face is dominated by huge disc-like nasal placodes made from p6 epithelium. Placodal adherence to the brain is the key to understanding the formation of nasal cavities. Rapid proliferation of MNC mesenchyme surrounding the p6 placodes forces the surrounding skin to be pushed forward creating a "hemi-nose." The topology of this process can be envisioned by a humble analogy. The tip of an elastic structure shaped like a condom is glued to a flat surface. The peripheral rim is likewise glued. A needle is then placed and the structure is insufflated. The central disc represents the placode, while the periphery is the facial skin. A donut-like chamber results.

In the hemi-nose, the internal skin is p6 while the surrounding outer skin is p5. The heminasal chambers approximate in the midline and fuse. Into the common p6 medial wall mesenchyme of the future nose, the r1 perpendicular ethmoid plate and septum develop. The process of nasal fusion takes place from inside-out/back-to-front. Thus, the vomerine bones approximate from the sphenoid forward. The two premaxillae follow suit. The presence of bifid frenulum and a wide diastema between the central incisors are forem fruste signs of inadequate premaxillary approximation (the Tessier #0 cleft). The process of palatal development is vividly depicted by Kaufman [91].

Various nasal anomalies can occur from defective embryogenesis. Absence of a nasal placode will lead to hemi-nose. Very rarely, complete nasal duplication is seen. This is likely due to additional nasal placode on either side of the midline. A notch in the nasal rim (sometimes with defect between the central and lateral incisors) is the Tessier #1 cleft. This represents a "fault line" in the soft tissues of the nasal roof between the medial nasal process and the lateral nasal process.

(A + B) + C contact between the maxilla and orbit follows a similar closure pattern. At the postero-lateral corner of the nasal cavity, ascending processes of the r2 palatine bone make contact with the p5 orbit and the r1 sphenoid. This represents a "hinge" for what will be a lateral to medial rotation. When this is complete, closure of the palate can take place. This requires two contact points. Proliferation of premaxilla and Mx1 provides the *first contact point* between the maxilla and the midline. The frontal processes of these two fields (PMxF and MxF) ascend to make contact with the r1 nasal and lacrimal bones. Lamination between frontal process of maxilla and the lacrimal provides a potential space by which the lacrimal duct gains access to the nose. Successful contact

between PMxF and MxF positions the internal aspect of the respective alveolar processes in space such that fusion of the primary palate can occur. This is initiated just in anterior to the nasaopalatine nerve and takes place *posterior to anterior*.

The second contact point is between the more proximal fields of both ethmoid complex and r2. Just behind the premaxillae, the vomerine bones represent neural crest mesenchyme that migrated a bit later than premaxilla. It is thus biologically "younger," and will ossify later than that of the premaxilla. The palatal shelf develops from Mx1 later in time than either the frontal process or the inferior turbinate. Palatal shelf projection and elevation take place in an anteroposterior sequence. Mx1 is developmentally "older" than Mx2 and Mx3; hence, it produces the shelf first. Successful contact between the vomer and palatal process of the maxilla takes place just posterior to the nasopalatine nerve. The fusion pattern is *anterior to posterior*.

Assembly of the Oronasal Soft Tissues

Time and again, we have emphasized that craniofacial osseous structures are mere by-products of soft tissue function matrices, i.e., of developmental fields that were preexistent in the embryo, are correctly positioned by folding, and interact in a tightly controlled time sequence to produce the recognizable anatomic features of the fetus. Why so much obsession with bones? What about the soft tissues?

The answer to the first question stems (in large part) from a plethora of experimental data pertaining to ossification patterns. Radiologic studies by Kjaer of these patterns constitute a treasure trove of incalculable worth for all those interested in craniofacial development. Most all the bones in question are neural crest derivatives. When the ossification sequence is combined with neuromeric compartments, a neural crest "map" of the embryo can be constructed. Such a map displays all bone fields organized along the neural folds into their respective neuromeric zones. Within each zone, the relative position of each bone field to its confreres is reconstructed.

Bone fields have readily defined sutures and ossification centers. Sutures represent truly separate compartments; neural crest cells have been demonstrated diving into every one. Bone fields allow us to think neuromerically about the overlying soft tissue. For example, we can position the lateral border of the p5 nasal skin envelope precisely over the interface between r2 frontal process of maxilla and the r1 nasal bone. The medial border of the cheek sandwich with r2 dermis lies directly over r2 MxF. In the palate, the tensor veli palatini originates from somitomere 4 and spans from the r3 lateral Eustachian tube to the r2 palatine horizontal lamina. The levator veli palatini originates from Sm6 and the Sm6 petrous apex. Levator forms later in time than tensor. TVP inserts into the lateral margin of the anterior palatine aponeurosis, an r2 derivative supplied by lesser palatine artery. LVP inserts the middle 1/3 of palatine aponeurosis, a derivative of r5–r6 neural crest supplied by ascending palatine branch of facial to the muscle and ascending pharyngeal to the fascia.

Muscle origins and insertions, from a neuromeric perspective, develop mathematically. The *origin* of a muscle corresponds to its somitomere or somite(s). After migration, the myoblasts, "packaged" by fascia, will seek out the nearest site of exposed collagen II. The *primary insertion* is to a bone that develops in the neuromeric zone as its motor nerve. The *secondary insertion* will occur at the first available bone in the surrounding environment displaying an ossification center.

Formation of the Normal Lip and Prolabium

As the nasal chambers move toward midline fusion, the r2 premaxilla is covered over by a layer of p5 skin and MNC mesenchyme. This becomes the columella and philtrum as follows [148]. Note the importance of BMP4 in midline fusion [149] (Fig. 2.77).

Recall that dorsal nasal skin has p5 dermis and MNC subcutaneous tissue. With r1 septal growth, the nasal tip rises and projects. This stretches the skin anterior to the septum to form the columella. The skin remaining atop the premaxilla, the prolabium is completely devoid of muscle. When the prolabium unites with the lateral lip elements, it encounters biplanar orbicularis. Superficial orbicularis will bind to the mesenchyme of prolabium, but cannot penetrate it. It stays bunched up on the sides to create the *philtral columns* of *Cupid's bow*. Deep orbicularis penetrates below the plane of prolabium and above the bone to unite with itself across the midline. How does this take place? How do the outlying maxillary fields gain access to the midline? What causes epithelial breakdown such that these skin-covered fields can fuse with each other?

At Carnegie stage 13, no true mouth-nose distinction can be made. Breakdown of the floor of the primitive nasal cavities occurs at stage 14, thus creating the primary choane. During this stage, the maxillary process fills out the lateral nasal process with r2 mesenchyme, while the medial nasal process is filled by MNC mesenchyme. Beneath these soft tissue structures lies bony support: That of the lateral nasal process is Mx1 (Tessier zone 4), while the support for medial nasal process is premaxilla. Between stages 15 and 16, an epithelial edge emanates from the LNP termed "Simonart's band" and attaches to the MNP. Multiple studies confirm that this process involves a burst of oxygen consumption and RNA synthesis at the alar base. In mice, fusion of lateral to medial nasal process takes just 4 h. Oxygen deprivation or environmental exposure, such as carbon monoxide, can interfere with this critical event [150].

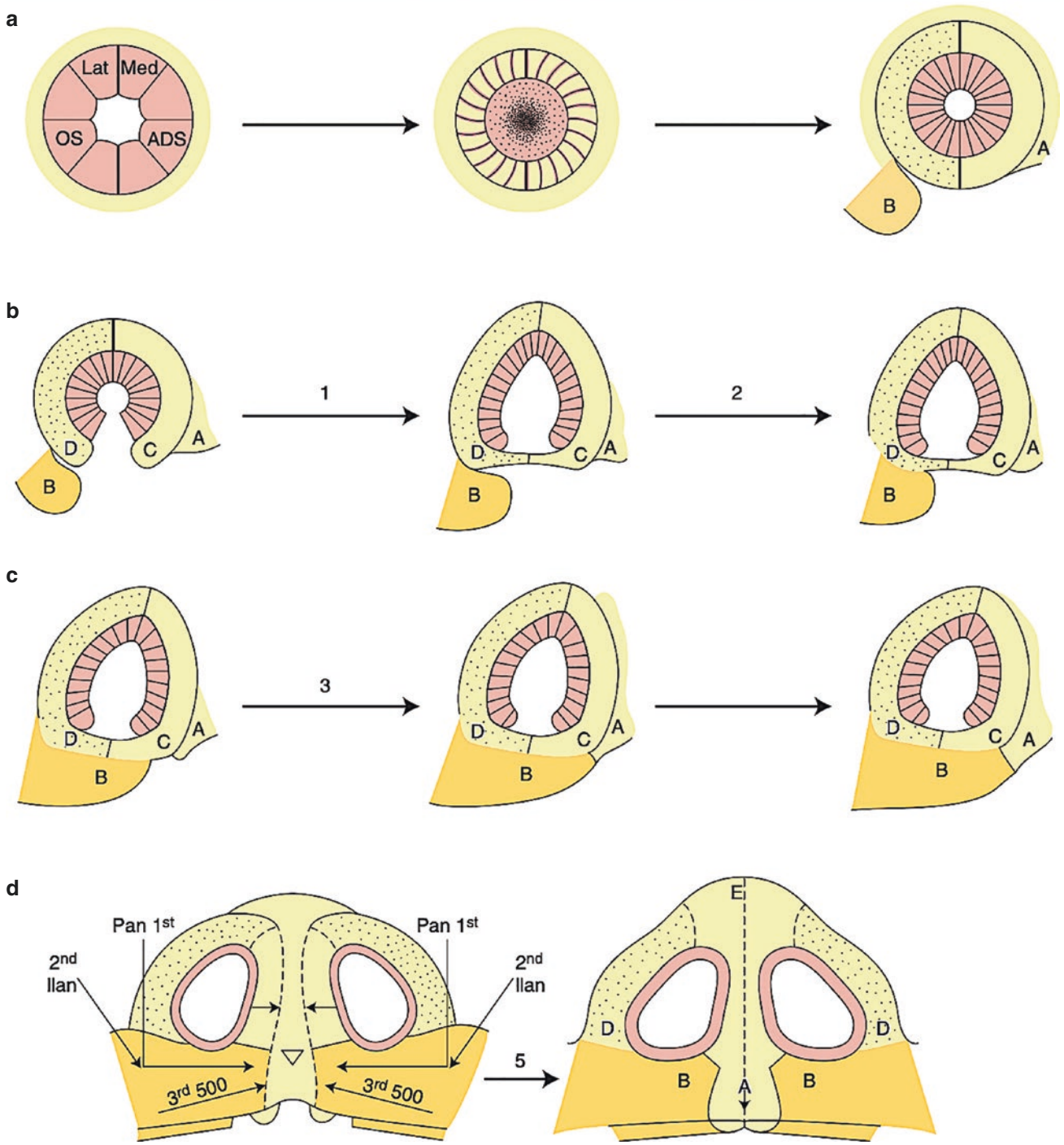

Fig. 2.77 Lip closure sequence. (Courtesy of Michael Carstens, MD)

persistence of epithelium, and failure of mesenchymal fusion. Since the signal emanates from the PMx, it diffuses down from the piriform fossa to the lip. Therefore, as the BMP-4 signal is progressively weaker, lip cleft severity worsens: i.e., from a vermilion notch, to an incomplete form involving half of the lip, and finally to a complete cleft lip. Variations of this mechanism are the likely basis for the final pathologies seen in the entire spectrum of Tessier clefts [151, 152] (Figs. 2.81 and 2.82).

In summation, *the volume of the premaxilla determines whether or not lip closure can occur*. First, small premaxillae make small amounts of BMP-4. The amount of BMP-4 produced is critical to produce the epithelial breakdown necessary to permit mesenchymal merger. Second, when the premaxilla is too small, the physical distance between it and maxilla will exceed a critical dimension. Epithelial bridge formation between the alar base and the prolabium cannot occur. Third, if this critical distance exists at the

Concomitant with the biochemical activity of the LNP, the underlying maxillary bone fields are developing as well. The zone #3 inferior turbinate develops immediately behind zone #4 Mx1. Building on the scaffolding of IT, the maxillary frontal process is synthesized. Construction of neural crest bone can be monitored by BMP-4. The cellular mass of Mx1 and PMx determines the transverse distance between LNP and MNP. Work by Johnston in cleft-forming rodents demonstrated a consistently *abnormal angle* between MNP and LNP. When a critical transverse distance between these fields exists, bridge formation will fail and a soft tissue cleft results. Reduction in physical size of the premaxilla can also cause the *critical contact distance* to be exceeded.

Prolabium is constructed from p5 skin and MNC mesenchyme; it has a vermillion consisting of r2 mucosa covering the premaxilla. The mucosa has an odd "flaky" appearance for the lack of underlying muscle. Epithelial breakdown allows maxillary myoblasts to gain access to the prolabium. In accordance with other pharyngeal arch derivatives, first arch muscle maturation follows a strict sequence: deep-to-superficial, caudal-to-cranial, and lateral-to-medial. The orbicularis muscles, being very medial, are late-forming (compared to platysma). The deep (sphincter) layer of orbicularis (DOO) forms well before the superficial (dilator) layer. DOO shows common characteristics with the buccinator. Both belong to the deep plane and develop in contact with the oral mucosa. They are innervated by VII from above. Because DOO is programmed by the mucosa, it curls around the lip but terminates at the white roll. SOO forms later in time. It makes physical contact with the p5 prolabial mesenchyme with which it fuses. For this reason, when one pares the edge of a unilateral cleft prolabium only a single muscle layer is observed: DOO from the opposite, non-cleft side.

The Pathologic Anatomy of Cleft Formation

The pathologic anatomy of unilateral and bilateral labiomaxillary clefts stems from a tissue deficiency state localized to the lower lateral piriform fossa. The developmental field at fault is the premaxilla. Such clefts always have an osseous component consisting of a scooped-out nasal floor. The extent of bone involvement is variable, up to and including a complete cleft of the primary palate. Soft tissue involvement occurs likewise as a spectrum (Figs. 2.78, 2.79, 2.80, 2.81, 2.82, and 2.83).

Formation of the premaxilla results from interactions between these tissues. The premaxilla has several anatomic subcomponents; these are assembled in a strict sequence. The medial incisor field (PMxA) forms first, followed by the lateral incisor field (PMxB). This can be understood as the "flow" of neural crest mesenchyme forward from the ipsilateral vomer. The time sequence of dental eruption (central incisor A > lateral incisor B) is a manifestation of the relative biologic "maturity" of the mesenchymal field within which each tooth develops. The frontal process field (PMxF) is a vertical offshoot of PMxB; this subfield is the biologically "newest" tissue. These zones of premaxilla correspond to the vascular axis of medial nasopalatine artery.

Pathology affecting the premaxilla occurs as a spectrum based on this original developmental pattern. Deficits in the neuroangiosome leading to a deficiency state of the premaxilla first occur in the most distal aspect of the frontal process (i.e., at its most cranial extent). As the mesenchymal deficit worsens, frontal process will be reduced in a cranial-caudal gradient. "Scooping out" of the piriform rim results; the nasal lining is pulled down as well. This causes depression of the alar base and a downward-lateral displacement of the lateral crus. Biologic signals from PMxF do not affect lip formation. Therefore, the *forme fruste* manifestation of premaxillary deficiency is a cleft lip nose with a perfectly normal lip.

Once the frontal process is eliminated, the deficiency state shows up in the lateral incisor field. Progressive degrees of premaxillary deficiency in the lateral incisor field cause progressive loss of alveolar bone substance. Alveolar bone development follows a gradient from the incisive foramen forward. Mild deficiency causes notching on the labial surface. As the deficiency worsens, the notch deepens *backward* toward the incisive foramen. A critical lack of alveolar bone mass results in outright failure of lateral incisor development.

The reader should now be quite comfortable with the mechanisms by which bone is affected in a cleft. But a little more detail is required to spell out how a deep osseous field can affect the overlying soft tissue. Tessier's series includes colobomas, eyebrow absence, as well as skin deficits. It is herein proposed that the soft tissue deficits seen in craniofacial clefts represent either failures of fusion or failures of formation. The notch in the alar rim is a boundary zone fusion failure, whereas the absence of eyelashes on the lateral lower eyelid represents the failure of that field to produce a product. Neural crest mesenchymal cells that participated in lash formation in an adjacent field fail to behave correctly in the target field. Failure of formation is a more difficult topic to discuss (and out of our scope here), but the mechanism of fusion may well be universal throughout the head and neck.

Let's take the role of the LNP-MNP nasal bridge as a case in point. Migration of myoblasts containing mesenchyme along the Simonart's band cannot occur without a generalized breakdown of the epithelium covering the lateral lip element, the skin bridge, and the p5 prolabial skin. Stability of the epithelia in facial processes is maintained by repression activity of *Sonic Hedgehog* (*SHH*) within the skin. BMP-4 causes derepression of *SHH*; epithelial breakdown results. Thus, absence or deficiency of an appropriate BMP-4 signal will lead to restricted expression of SHH, abnormal

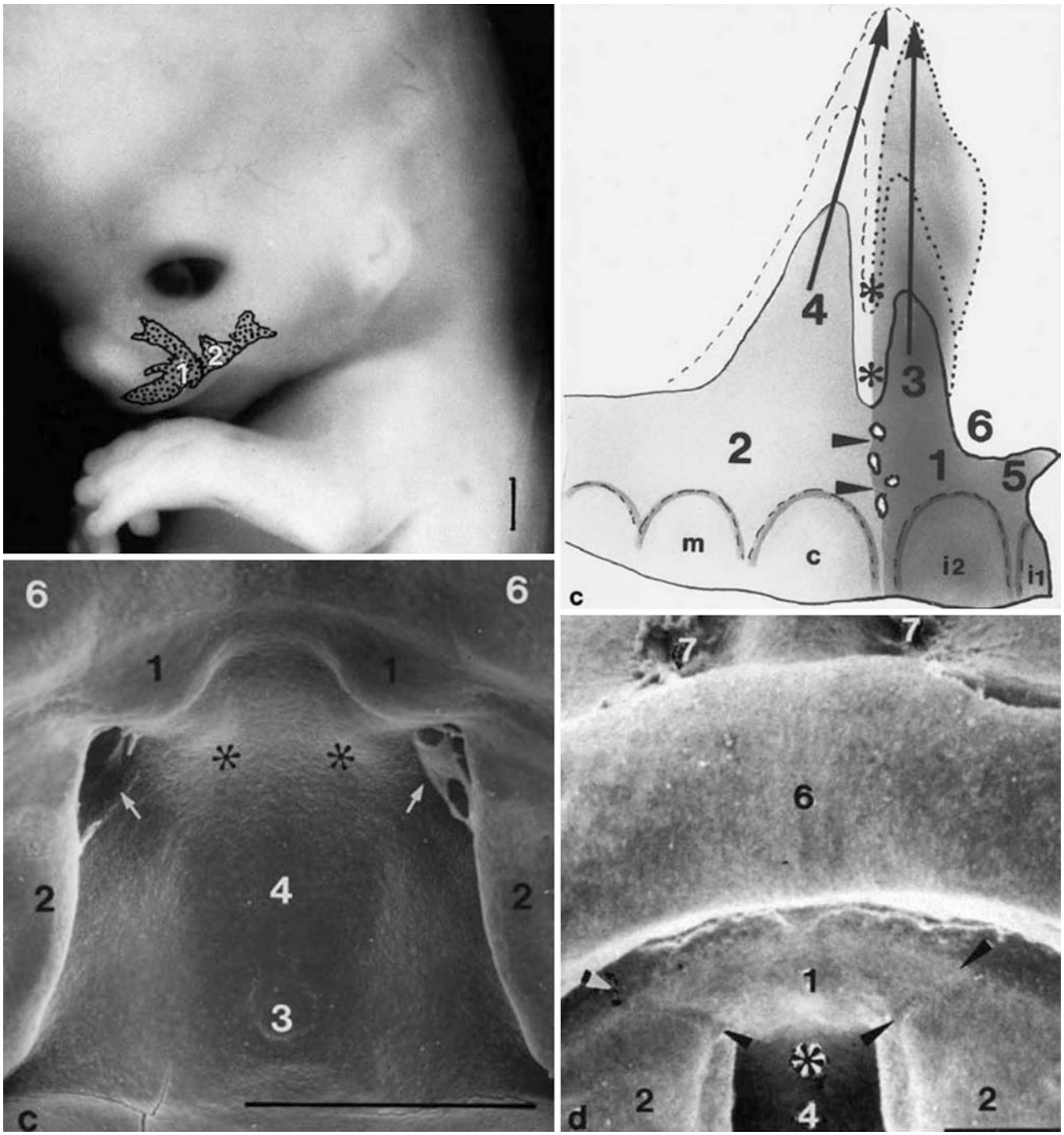

Fig. 2.78 Premaxillary frontal process seen before it becomes overlapped by the frontal process of the maxilla. Upper left: embryo stage 23. Upper right: Reconstruction upper jaw in a human fetus in the fifth month. Schematic drawing to demonstrate the progressive growth of the facial processes from maxilla as well as premaxilla including the fusion line. 1. Premaxilla, 2. maxilla, 3. processus frontalis premaxillaris, 4. processus frontalis maxillaris, 5. processus stenonianus/spina nasalis, 6. apertura piriformisremaxilla, i1 medial incisor, i2 lateral incisor, c canine, m molar, arrowheads former sutura incisiva, *sutura incisiva, long arrow direction of growth towards the os frontale. Lower left: Embryo stage 19. 1. Premaxillary anlage/primary palate, 2. secondary palate, 3. adenohypophysis/remnant of Rathke's pouch, 4. roof of the oral cavity, 5. mandibular arch and floor of the oral cavity removed, 6. upper lip anlage, 7. nasal plug, *intermaxillary bulge at the ventral roof of oral cavity, short arrows choanae, arrowheads sutura incisiva between primary and secondary palate. Lower right: Embryo stage 23. (Reprinted from Bartezco K, Jacob M. A re-evaluation of the premaxillary bone in humans. Anat Embryol (Berl) 2004 Mar;207(6):417–37. With permission from Springer Nature)

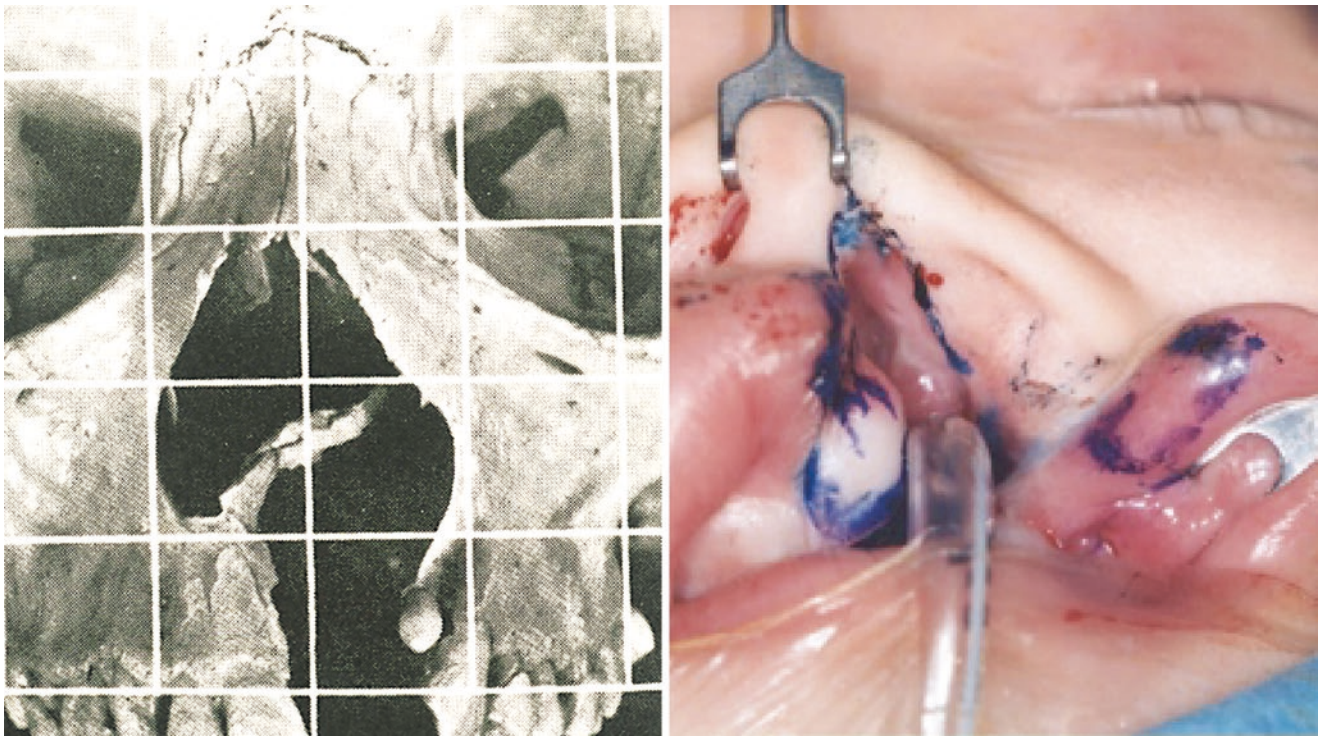

Fig. 2.79 UCL soft tissue and bone defects. Note the scooping out of the piriform fossa on the side of the cleft. Note as well that the maxilla is capable of producing an incisor which is not really "ectopic," but rather constitutes part of three dental units supplied by the medial branch of anterior superior alveolar neuroangiosome. Soft tissues are displaced downward and laterally to fit into the piriform fossa. (Courtesy of Michael Carstens, MD)

Fig. 2.80 Bilateral cleft lip showing the prolabium to consist of four neurovascular fields. Philtral prolabium (PP): V1 anterior ethmoid: these two fields are the width of the columella. Non-philtral prolabium (NPP): V2 medial sphenopalatine: these fields flank the PP. (Courtesy of Michael Carstens, MD)

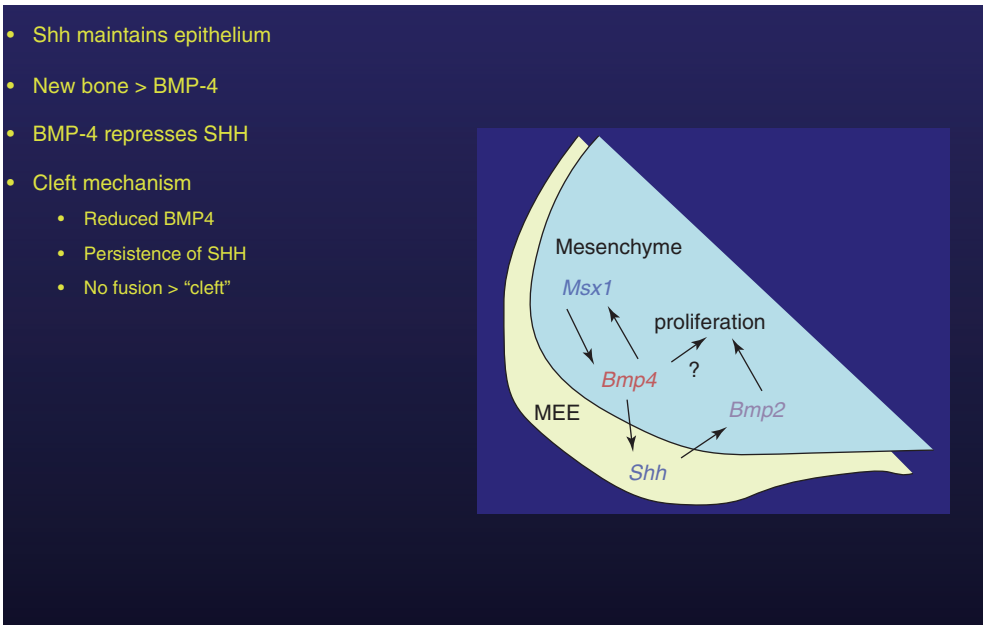

Fig. 2.81 BMP4/SHH interaction controls lip fusion. Epithelial integrity/cohesion is regulated by signals from the underlying mesenchyme. Epithelial cohesion depends on local expression of Sonic Hedgehog (Shh). Osteogenesis of membranous bone underlying the epithelium involves expression of BMP-4; the protein diffuses outward from the piriform fossa into the soft tissues and thence downward into the lip. The most distal target of BMP-4 in upper lip is the vermillion border. BMP-4 represses expression of Shh and permits epithelial disintegration. Mechanism of cleft lip: (1) Fusion of the lateral lip element to the prolabium involves breakdown of epithelium which requires presence of adequate BMP-4. (2) Reduced volume of underlying membranous bone > reduced (BMP-4). (3) This permits the persistent expression of Shh in epithelium of the lateral lip element and/or prolabium. (4) Intact epithelium resists fusion processes—creating a "cleft" which proceeds from caudal to cranial and deep to superficial. (Reprinted from Zhang Z, Song Y, Zhao X, et al. Rescue of cleft palate in Msx-1 deficient mice by transgenic Bmp4 reveals a network of BMP4 and Shh signaling in the regulation of mammalian palatogenesis. Development 2002; 129:4135–4146. With permission from the Company of Biologists)

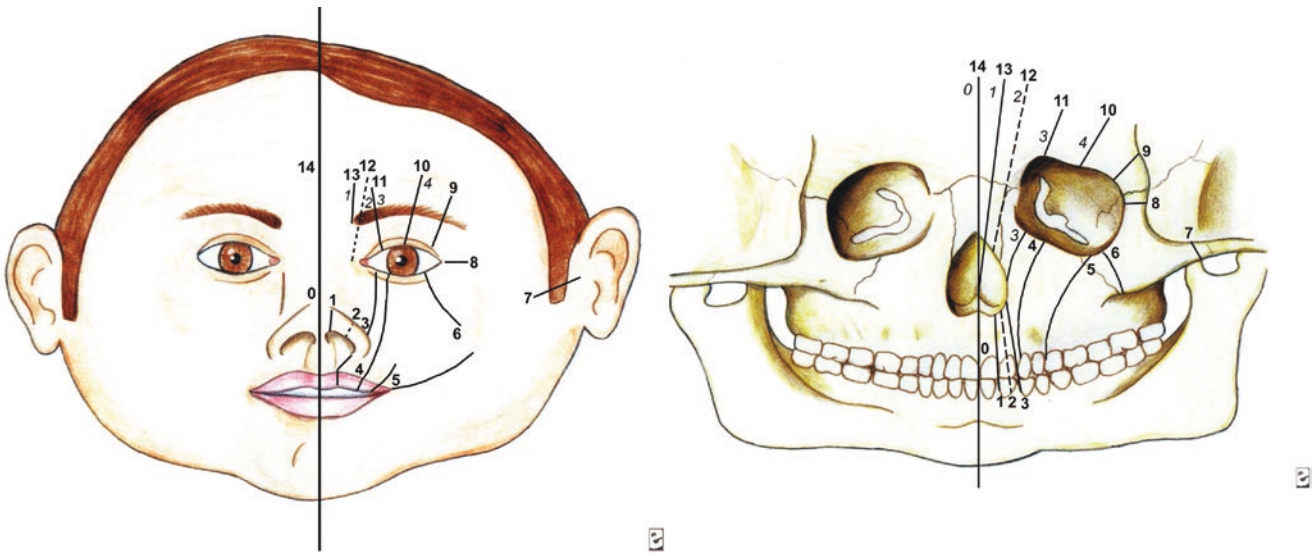

Fig. 2.82 Paul Tessier's numeric classification of craniofacial clefts. This model recognized two tiers, above and below the orbit. Maxillary clefts are numbered 0–7, while orbitofrontal clefts are numbered 8–14. Empirically, the two zones display pairing in which the sum of the lower and upper clefts is 14, the system has several minor flaws. It does not distinguish between states of field deficiency and field excess. Lumping together of developmental fields occurs thus, the common cleft involving PMx belongs to zone #2 rather than the inferior turbinate zone #3. Clefts in zone #3 are much more devastating because they involve an entirely different mechanism. (Reprinted from Sari E. Tessier Number 30 Facial Cleft: A rare maxillofacial anomaly. Turkish J Plast Surg 2018; 26: 12–19. With permission from Turkish Journal of Plastic Surgery)

Fig. 2.83 Developmental field reassignment. Repositioning fields into their embryonic relationships facilitate formal symmetrical facial growth over time. Upper left and right: secondary repair. Lower left and right primary repair. (Courtesy of Michael Carstens, MD)

level of the incisive foramen, a cleft of the secondary palate will form. This is because the horizontal repositioning of the palatal shelf from the maxilla must make contact with the vomer just posterior to the incisive foramen. The process is just like a zipper. If initial contact is not made, fusion of the palatal shelf to the vomer cannot take place. Even if initial contact is made, a secondary palatal cleft can still result due to displacement of the vomer away from the midline. The vomer can become warped by the inequality of growth forces on either side of the cleft. Thus, the zipper may get started anteriorly, but as it proceeds posteriorly, when it encounters the deviated vomer, a palatal cleft will ensue.

Clinical Consequences of the Developmental Field Model Applied to Facial Clefts

- The repair of facial clefts involves the identification and repositioning of misplaced fields.
- Fields should be dissected to conserve the entire neuroangiosome basis—virtually no tissue should be discarded.
- Such fields should, when replaced into their proper anatomic relationships, grow symmetrically making use of the entire mesenchymal substrate.
- Reconstructive procedures based on embryologic principles offer the best chance to maintain near-normal growth and preserve their esthetic relationships.

How to Understand the Assembly of the Face: A Method of Study

Understanding of how component fields of paraxial mesoderm and neural are assembled together to form the face and skull is not easy task. It involves visualizing structure arising from one anatomic site and then moving into new positions via migration or folding. This is a ***four-dimensional process***. The physical development of certain fields may be dependent upon the correct development of precursor fields. Errors in this developmental sequence lead to varying forms of craniofacial clefts.

Craniofacial development is thus like a complex play in several acts. The challenge for both author and reader alike is to set the stage wherein all the actors are properly introduced; their respective roles and relationships with one another are clearly presented. Then and only then can the action begin and the plot unfold. Shakespeare understood this well. His plays commonly begin with a *dramatis personae*. After the characters are introduced, the temporal logic of the acts must be presented. When and where does each act take place? Now the reader is ready to follow the dramatic action.

Step 1: Summary of Ideas

Major ideas introduced by previous papers in this series include: (1) the segmental organization of the early embryo based upon the neuromeric system, (2) the mechanism by which gastrulation forms a trilaminar embryo, (3) the anatomy of the resulting germ layers, including the neural crest, (4) the segmental reorganization of mesenchyme into somitomeres and somites, (5) formation of pharyngeal arches and neural crest migration patterns, and (6) derivative analysis of final anatomic structures.

Step 2: Key Definitions and Point of Clarification

Craniofacial development is an interdisciplinary study. Interested readers may find themselves entering an uncharted territory between the basic science laboratory and the operating room. Several contemporary texts are worth consulting. The reader should review the definitions and anatomic abbreviations presented at the beginning of part 1.

Step 3: Staging of Embryos (General Principles)

Embryology is the analysis of relationships between order and form. The timing with which anatomic structures make their appearance is all-important to understand the overall process. Several parameters traditionally used to describe development in the first 8 weeks of life make the literature confusing. These parameters are: (1) time/age, (2) crown-rump length, (3) the observable number of somite pairs, and (4) Carnegie stage. Each system has its own degree of (im) precision and overlap.

Lumping the events of embryogenesis into weeks is quite imprecise. Critical events may take place within the space of a single day. Fusion between the lateral nasal prominence and the medial nasal prominence may occur in as little as 6 h. Embryo size (measured as C-R length in millimeters) is a more accurate measurement of maturation. The Carnegie staging system, originally described by Streeter and refined by O'Rahilly, categorizes development into a series of stages defined by the formation and maturation of key structures. The system derives its name from the leadership role played by the Carnegie Institution as a sponsor of embryological research in the early twentieth century. Each stage is tightly linked to C-R length, intervals of which are as small as 2 mm through stage 15 (3–36 days).

Morphologic studies correlating developmental stage with the number of observable somites are useful but are limited to a certain window of embryogenesis. Carnegie stage 9 (days 20–21) is defined by the appearance of the first 1–3 somite pairs. The first occipital somite, previously described by von Baer and others and confirmed by Huang, may indeed be present at Carnegie stage 8. Why the confusion? It turns out that the first occipital somite is incompletely segmented at its rostral end (i.e., from Sm7), but fully epithelialized at its caudal end. Thus, the boundary between somitomeres 7 and somite 1 is indistinct but that between somite 1 and somite 2 is complete. In this scenario, Carnegie stage 9 would include up to four somite pairs. Using this numbering system, formation of the 31st pair (observed between days 29 and 31) would define Carnegie stage 13. The bottom line is the human embryo.

Although the number of somite pairs ceases to be of importance in defining subsequent embryonic stages, these entities play a vital role in the segmentation of the spine and the organization of the trunk. In addition to four occipital somites, human spines are constructed of 8 cervical, 12 thoracic, 5 lumbar, and 5 sacral somites. Fusion of these latter to form the sacrum is evidenced by the presence of four individual foramina. The coccyx is constructed with an additional 2–5 somites bringing the total count in humans to approximately 37–40 pairs. The final somite bearing a myotome is the first coccygeal; therefore the total number of spinal nerves sums to 31 pairs. The time required for somitogenesis is 10 days.

Step 4: Carnegie Staging System: With Special Reference to the Head and Neck

The best way to follow the events of craniofacial formation is by Carnegie stage. Key aspects of this system are summarized below as they apply to specific anatomic sites (e.g., cranial base synthesis, the formation of the nose). Carnegie staging will be discussed and illustrated in depth in Chap. 3. Our purpose here is paint an overview of the developmental

timeline so that the reader may refer to in through the course of the test. Measurements of crown-rump length are in millimeters. The beautiful SEM studies of embryos, both human and murine, constitute an excellent way to visualize these processes; the reader is encouraged to obtain a copy of this invaluable works and study them with care [153–156].

Major Themes of Craniofacial Development

First: The formation of mesenchyme is a more primordial event than the development of the brain. Gastrulation sets up the trilaminar embryo in 48 h during stage 7. Neural plate and folds appear in stage 8. From a teleological standpoint, proper protection of the nervous system must be ensured. Brain development must take place in the presence of a preexistent mesenchyme into which it can expand. The covering layers outside the CNS come from either neural crest NC or paraxial mesoderm PAM.

Second: Formation of mesoderm via gastrulation is a craniocaudal process beginning at the level of the tip of the notochord. The anterior extent of the notochord lies at the junction of the presphenoid and basisphenoid bones. This corresponds to neuromeric level r0. Mesodermal segmentation results as a response to gene signals emanating from different levels of the notochord. No definitive endoderm and intraembryonic mesoderm can be produced anterior to r0. All mesodermal and endodermal tissues anterior to the notochord represent forward migrations of tissues produced by gastrulation.

Third: The forebrain sitting in front of the notochord is an evolutionary "after-thought." It arises from induction signals from the tip of the notochord, the anterior visceral endoderm (just in front of the notochord), and from a zone of ectoderm located at the extreme anterior aspect of the trilaminar embryo. No mesoderm is associated with forebrain development. All mesenchyme associated with forebrain coverage comes via two mechanisms: (a) migration of neural crest from the caudal prosencephalic neural folds and (b) migration of midbrain neural crest from m1 to m2, and r0 to r1.

Fourth: The forebrain arises as a vesicular structure that, under normal conditions, becomes divided into two hemispheres. Only the forebrain and r0/r1 cerebellum have dura and it is derived exclusively from neural crest. There is no dura around the hindbrain. Dura coverage of the spinal cord begins at foramen magnum and is exclusively of paraxial mesoderm. Growth of the forebrain occurs in all directions such that the two hemispheres eventually surround the midbrain and hindbrain. *Intracranial dural anatomy can be mapped on the basis of sensory supply to neural crest from rhombomeres 1, 2, and 3*.

Fifth: Epithelium surrounding the brain is not stable without a supporting layer of mesenchyme. Neural crest from diencephalon creates the *dermis* underlying ectoderm above the skull (the future skin of the upper face and scalp). Neural crest creates the *submucosa* underlying the ectoderm of the oropharynx beneath the skull base.

Sixth: The brain case (neurocranium) has two primary units. The *membranous neurocranium* consists of dermal bones formed by signals (and some PAM), differentiates due to signals from the dermis above and meninges below to an intermediate layer of mesenchyme. *The chondral neurocranium* forward from the sella turcia is of neural crest origin. Backward from the sella turcica it all comes from PAM.

Seventh: By Carnegie stage 10 all sources of PAM for the growing brain have been synthesized. Eleven somitomeres have formed. The dorsal aortae and primitive hindbrain channels that constitute circulation of the embryo are derived somitomeres. Transformation of the last four (Sm8–Sm11) creates the occipital somites.

Eighth: By Carnegie stage 11, the physical provision of mesenchyme to the brain and face is complete. This requires four elements: (a) neural crest, (b) paraxial mesoderm for striated muscles, (c) pharyngeal arches; and (d) folding. Organization of paraxial mesoderm into somitomeres begins with notochord development in stage 8. In stage 9, all somitomeres contributing to the head are present. This includes the transformation of somitomeres 8–11 into the four occipital somites. All neural crest migration to the head (begun at stage 9 in mammals) is complete by stage 11. Pharyngeal arches first appear as when populated by neural crest from rostral hindbrain. Embryonic flexion brings all these mesenchymal sources into contact with the forebrain.

Summary

The idea of common neuromeric definition provides us with a new understanding of the anatomic rationale behind the bones, muscles, and fascia of the craniofacial skeleton. These structures, be they derived from neural crest, PAM or both, can be traced back to the level of the embryo from which its cells originated. The neuromeric system offers a unique perspective on craniofacial deformities. Pathologic states involving a particular neuromeric level can affect one or all of its derivatives. Deformities involving seemingly unrelated bones or muscles can be understood in terms of common neuromeric levels of origin. Genes found at multiple levels of the embryo may be mis-expressed within a single neuromeric level or on only one side of the body.

The purpose of this communication was to outline the principles of the neuromeric system and to describe the manner in which the craniofacial skeleton originates. Each bone was assigned to a neuromere(s) of origin using a color code. The time course of assembly of the craniofacial bones was discussed. In subsequent chapters, this information will be related to the clinical patterns of the common craniofacial conditions. The application of these principles to the rare craniofacial clefts described by Tessier enables us to understand that these pathologies are variations in the craniofacial field system.

References

1. Tessier P. Fentes orbito-faciales verticales et obliques (colobomas) completes et frustes. Ann Chir Plast. 1969;19:301–11.
2. Tessier P. Anatomical classifications of facial, craniofacial, and laterofacial clefts. J Maxillofac Surg. 1976;4:69–92.
3. Tessier P. Plastic surgery of the orbit and eyelids (trans: SA Wolfe). Philadelphia: Mosby Inc. (Masson); 1981.
4. Carlson BR. Human embryology and developmental biology. 6th ed. St. Louis: Mosby/Elsevier; 2020.
5. O'Rahilly R, Muller F. Human embryology and teratology. 3rd ed. New York: Wiley-Liss; 2001.
6. Gilbert SF, Barressi MJF. Developmental biology. 12th ed. New York: Sinauer/Churchill Livingstone; 2020.
7. Liem K, Bemis WE, Walker WF, Grande L. Functional anatomy of the vertebrates: an evolutionary perspective. 3rd ed. Belmont, CA: Thompson; 2001.
8. Kjaer I, Fischer-Hansen B. The prenatal human cranium. Copenhagen: Munsksgaard; 1999.
9. Tan PPL, Beddington RSP. The formation of mesodermal tissues in the mouse embryo during gastrulation and early organogenesis. Development. 1987;99:109–26.
10. Tan PPL, Trainor PA. Specification and segmentation of the paraxial mesoderm. Anat Embryol. 1994;189:379–90.
11. Tan PPL, Ziou SX. The allocation of epiblast cells to ectodermal and germ-line lineage is influenced by the position of the cells in the gastrulating mouse embryo. Dev Biol. 1996;1778: 124–32.
12. Tan PPL, Behringer RR. Mouse gastrulation: the formation of a mammalian body plan. Mech Dev. 1997;68:3–25.
13. Tan PPL, Parameswaran M, Kinder SJ, Weinberger RP. The allocation of epiblast cells to the embryonic heart and other mesodermal lineages: the role of ingression and tissue movement during gastrulation. Development. 1997;124:1631–42.
14. Tan PPL, Goldman D, Camus A, Schoenwolf GC. Early events of somitogenesis in higher vertebrates: allocation of precursor cells during gastrulation and the organization of a meristic pattern in the paraxial mesoderm. In: Ordahl CP, editor. Somitogenesis, part I. San Diego: Academic Press; 2000. p. 1–32.
15. Meier SP. Development of the chick mesoblast: morphogenesis of the prechordal plate and cranial segments. Dev Biol. 1981;83:4.
16. Jacobson AG. Somitomeres: the primordial body segments. In: Bellairs R, Ede DA, Lash JW, editors. Somites in developing embryos. New York: Plenum; 1986.
17. Jacobson AG. Somitomeres: mesodermal segments of the head and neck. In: Hanken J, Bk H, editors. The skull, Development, vol. II. Chicago: University of Chicago Press; 1993.
18. Meier SP, Tam PPL. Metameric pattern in the embryonic axes of the mouse. I. Differentiation of the cranial region. Differentiation. 1982;21:95–108.
19. Pourquie O. Segmentation of the paraxial mesoderm and vertebrate somitogenesis. In: Ordhal CP, editor. Somitogenesis, part I. San Diego: Academic Press; 2000. p. 165–70.
20. Bronner Fraser M. Rostrocaudal differences within the somites confer segmental pattern to trunk neural crest migration. In: Ordahl CP, editor. Somitogenesis, part I. San Diego: Academic Press; 2000. p. 279–96.
21. Meier SP. Development of the chick mesoblast: pronephros, lateral plate and early vasculature. Dev Biol. 1980;55:299–306.
22. Huang R, Zhi Q, Ordahl CO, Christ B. The fate of the first avian somite. Anat Embryol. 1997;195:435–49.
23. Huang R, Zhi Q, Patel K, Wilting J, Christ B. Contribution of single somites to the skeleton and muscles of the occipital and cervical regions in avian embryos. Anat Embryol. 2000;202:375–v383.
24. Müller F, O'Rahilly R. Segmentation in staged human embryos: the occipitocervical region revisited. J Anat. 2003;203:297–315.
25. Noden DW. Origins and patterning of craniofacial mesenchymal tissues. J Craniofac Genet Dev Biol Suppl. 1985;2:15–31.
26. Noden DW. Cell movements and control of patterned tissue assembly during craniofacial development. J Craniofac Genet Dev Biol. 1991;11:191–213.
27. Noden DM, Trainor PA. Relations and interactions between cranial mesoderm and neural crest populations. J Anat. 2005;207:575–601.
28. Jiang X, Iseki S, Maxxon RE, et al. Tissue origins and interactions in the mammalian skull vault. Dev Biol. 2002;241:106–16.
29. Kuratani S, Matsuo I, Aizawa S. Developmental patterning and evolution of the mammalian viscerocranium: genetic insights into comparative morphology. Dev Dyn. 1997;209:139–55.
30. Kuratani S. Craniofacial development and the evolution of the vertebrates: the old problems on a new background. Zool Sci. 2003;22:1–19.
31. Lumsden A, Keynes R. Segmental patterns of neuronal development in the chick hindbrain. Nature. 1981;337:424–8.
32. Lumsden A, Sprawson N, Graham A. Segmental origin and migration of neural crest cells in the hindbrain region of the chick embryo. Development. 1991;113:1281–91.
33. Krumlauf R. Hox genes and pattern formation in the branchial region of the vertebrate head. Trends Genet. 1993;9:106–12.
34. Lumsden A, Krumlauf R. Patterning the vertebrate neuraxis. Science. 1996;1996(274):1109–15.
35. Carstens MH, Chin M, Ng T, Tom WK. Reconstruction of #7 facial cleft with distraction assisted in situ osteogenesis (DISO): role of recombinant human bone morphogenetic protein-2 with Helistat activated collagen sponge. J Craniofac Surg. 2005;16: 1023–32.
36. Depew M, Lufkin T, Rubenstein JLR. The specification of jaw subdivisions by *DLX* genes. Science. 2002;298(5592):381–4.
37. Depew MJ, Simpson CA. 21st Century neontology and the comparative development of the vertebrate skull. Dev Dyn. 2005;235:1256–91.
38. Brand-Saberi B, Whiting J, Ebesperger C, Christ B. The formation of somite compartments in the avian embryo. Int J Dev Biol. 1995;40:411–20.
39. Christ B, Schmidt C, Huang R, et al. Segmentation of the vertebrate body. Anat Embryol. 1998;197:1–8.
40. Burke AC. Hox genes and the global patterning of somatic mesoderm. In: Ordahl CP, editor. Somitogenesis part 1. San Diego: Academic Press; 2000. p. 155–81.
41. Kemp TS. The atlas-axis complex of the mammal-like reptiles. J Zool (Lond). 1969;159:223–48.
42. Schoenwolf G. Cell movements in the epiblast during gastrulation and neurulation in chick embryos. In: Kellar R, Clark Jr WH, Griffin F, editors. Gastrulation: movements, patterns, and molecules. New York: Plenum; 1991. p. 1–28.
43. Lemire L, Kessel M. Gastrulation and homeobox genes in chick embryos. Mech Dev. 1997;67:3–16.

44. Graham A, Smith A. Patterning of the pharyngeal arches. BioEssays. 2001;23:54–61.
45. Evans DH, Piermarini PM, Choe KP. The multifunctional fish gill: dominant site of gas exchange, osmoregulation, acid-base regulation, and excretion of nitrogenous waste. Physiol Rev. 2005;85(1):97–177.
46. Gasser RF. Development of the facial muscles in man. Am J Anat. 1966;120:357–75.
47. Padget DH. The development of the cranial arteries in the human embryo. Contrib Embryol. 1938;32:205–61.
48. Noden DM. Development of craniofacial blood vessels. In: Feinberg RN, Silver GK, Auerbach R, editors. The development of the vascular system. Basel: S Karger; 1991. p. 1–24.
49. Ruberte J, Carretero A, Marcucio R, Noden DM. Morphogenesis of blood vessels in the head muscles of the avian embryo. Spatial, temporal and VEGF expression analyses. Dev Dyn. 2000;27:470–83.
50. Hiruma T, Nakajima Y, Nakamura H. Development of pharyngeal arch arteries in the early mouse embryo. J Anat. 2002;201(15):29.
51. Etchevers HC, Couly G, Le Douarin NM. Morphogenesis of the branchial vascular sector. Trends Cardiovasc Med. 2002;12:299–304.
52. Mukouyama Y-S, Shi D, Britsch S, et al. Sensory nerves determine the pattern of arterial differentiation and blood vessel branching in the skin. Cell. 2002;109:693–705.
53. Morris-Kay GM. Derivation of the mammalian skull vault. J Anat. 2001;199:143–51.
54. LeDouarin NM, Kalcheim C. The neural crest. 2nd ed. Cambridge: Cambridge University Press; 2001.
55. Hall BK. The neural crest and neural crest cells in development and evolution. 2nd ed. New York: Springer-Verlag; 2009.
56. Trainor P. Neural crest cells: evoution, development, and disease. San Diego: Academic Press; 2013.
57. Serbedzija GN, Fraser SE, Bronner-Fraser M. Pathways of neural crest migration in the mouse embryo as revealed by vital dye labeling. Development. 1990;108:605–12.
58. Serbedzija GN, Bonner-Fraser M, Fraser SE. Vital dye analysis of cranial neural crest migration in the mouse embryo. Development. 1992;116:297–307.
59. Osumi-Yamashita N, Ninomiya Y, Doi H, Eto K. The contribution of both forebrain and midbrain crest cells to the mesenchyme in the frontonasal mass of mouse embryos. Dev Biol. 1994;164:409–19.
60. Osumi-Yamashita N, Ninomiya Y, Eto K. Mammalian craniofacial embryology in vitro. Int J Dev Biol. 1997;41:187–94.
61. Couly GF, Le Douarin NM. Mapping of the early neural primordium in quail-chick chimeras I. Developmental relationships between placodes, facial ectoderm, and prosencephalon. Dev Biol. 1985;110:422–39.
62. Couly GF, Le Douarin NM. Mapping of the early neurala primordium in quail-chick chimeras II. The prosencephalic neural plate and neural folds: implications for the genesis of cephalic human congenital abnormalities. Dev Biol. 1987;120:198–214.
63. Creuzet S, Couly G, Le Douarin NM. Patterning the neural crest derivatives during development of the vertebrate head: insights from avian studies. J Anat. 2005;207:447–59.
64. Puelles L, Rubenstein JLR. Expression patterns of homeobox and other putative regulatory genes suggest a neuromeric organization. Trends Neurosci. 1993;16(11):472–9.
65. Rubenstein JLR, Shimamura K, Martinez S, Puelles L. Regionalization of the prosencephalic neural plate. Annu Rev Neurosci. 1998;21:445–77.
66. Puelles L, Rubenstein JLR. Forebrain gene expression domains and the evolving prosomeric model. Trends Neurosci. 2003;26:469–76.
67. Puelles L. Forebrain development: prosomere model. In: Squire LR, editor. Encyclopedia of neuroscience, vol. 4. Oxford: Academic Press; 2009. p. 315–9.
68. Puelles L, Harrison M, Paxinos G. A developmental ontology for the mammalian brain based on the prosomeric model. Trends Neurosci. 2013;36(10):570–8.
69. O'Rahilly R, Muller F. The embryonic human brain: an atlas of developmental stages. 3rd ed. New York: Wiley-Liss; 2004.
70. Couly GF, Le Douarin NM. Head morphogenesis in avian chimeras: evidence for a segmental pattern in the ectoderm corresponding to the neuromeres. Development. 1990;108:543–58.
71. Webb JF, Noden DM. Ectodermal placodes: contributions to the development of the vertebrate head. Am Zool. 1993;33:434–47.
72. Streit A, Streit A. Early development of the cranial sensory nervous system: from a common field to individual placodes. Dev Biol. 2004;276:1–15.
73. Singh S, Graves AK. Molecular basis of craniofacial placode development. Wiley Interdiscp Rev Dev Biol. 2016;5(3):363–76.
74. Pathey C, Schlosser G, Schimeld SM. Evolutionary history of vertebrate cranial placodes. Dev Biol. 2014;389(1):82–97.
75. Omer A, Haddad D, Pisinski L, Krauthammer AV. The missing link: a case of absent pituitary infundibulum and ectopic neurohypophysis in a pediatric patient with heterotaxy syndrome. J Radiol Case Rep. 2017;11(9):28–38. https://doi.org/10.3941/jrcr.v11i9.3046.
76. Al-Gazali LI, Sztriha L, Punnose J, Shather W, Nork M. Absent pituitary gland and hypoplasia of the cerebellar vermis associated with partial ophthalmoplegia and postaxial polydactyly: a variant orofaciodigital syndrome VI or a new syndrome? J Med Genet. 1999;36:161–6.
77. May JA, Krieger MD, Bowen I, Geffner ME. Craniopharyngioma in childhood. Adv Pediatr Infect Dis. 2006;53:183–209.
78. Garrè ML, Cama A. Craniopharyngioma: modern concepts in pathogenesis and treatment. Curr Opin Pediatr. 2007;19(4):471–9. https://doi.org/10.1097/MOP.0b013e3282495a22.
79. DiRocco C, Caldarelli M, Tamburrini G, Massimi L. Surgical management of craniopharyngiomas—experience with a pediatric series. J Pediatr Endocrinol Metab. 2006;19:355–66.
80. Koral K, Weprin B. Sphenoid sinus craniopharyngioma simulating mucocele. Acta Radiol. 2006;47:494–6.
81. Dodé C, Hardelin J-P. Kallman syndrome. J Hum Genet. 2008;17:139–46.
82. Junklass J. Atypical presentation of a patient with both Kallman's syndrome and craniopharyngioma: case report and literature review. Case Rep. 2005;11(1):30–6.
83. Boehm U, Bouloux PM, Dattani MT, et al. Expert consensus document: European Consensus Statement on congenital hypogonadotropic hypogonadism—pathogenesis, diagnosis and treatment. Nat Rev Endocrinol. 2015;11(9):547–64. https://doi.org/10.1038/nrendo.2015.112.
84. Vaid S, Shah D, Rawat S, Shukla R. Proboscis lateralis with ipsilateral sinonasal and olfactory pathway aplasia. J Pediatr Surg. 2010;45:453–6.
85. Vulleix S, Niel F, Nedelec B, et al. Homozygous nonsense mutation of the FOXE3 gene as a cause of congenital primary aphakia in humans. Am J Hum Genet. 2006;79:358–64.
86. Breheret R, Brecheteau C, Tanguy J-Y, Lacourreye L. Bilateral semicircular canal hypoplasia. Eur Ann Otorhinoloaryngol Head Neck Dis. 2013;130:225–8. https://doi.org/10.1016/j.anorl.2012.10.005.
87. Hu D, Marcucio RS, Helms JA. A zone of frontonasal ectoderm regulates patterning and growth in the face. Development. 2003;130:1749–58.
88. Tirumandas M, Sharma A, Gbenimacho I, Shoha MM, Tubbs RS, Oakes WJ, Loukas M. Nasal encephalocoeles: a review of the etiology, pathophysiology, clinical presentations, diagnosis, treatment, and complications. Childs Nerv Syst. 2013;29(5):739–44. https://doi.org/10.1007/s00381-012-1998-z.
89. Di Somma L, Iacoangeli M, Nasi D, Balercia P, Lupi E, Girotto R, Polonara G, Scerrati M. Combined supra-transorbital key-

hole approach for treatment of delayed intraorbital encephalocele: a minimally invasive approach for an unusual complication of decompressive craniectomy. Surg Neurol Int. 2016;7(Suppl 1):S12–6.
90. Siebert JR, Kokich VG, Warkany J, Lemire RJ. Atelencephalic microcephaly: craniofacial anatomy and morphologic comparisons with holosprosencephaly and anencephaly. Teratology. 1987;36:279–85.
91. Marin-Padilla M. Study of the sphenoid bone in human craniooschisis and craniorachischisis. Virchows Arch A Pathol Anat Histopathol. 1965;339:245–53.
92. Kjaer I, Keeling JW, Graem N. Midline maxillofacial skeleton in human anencephalic fetuses. Cleft Palate Craniofac J. 1994;31(4):250–6.
93. Medical Taskforce on Anencephaly. The infant with anencephaly. N Engl J Med. 1990;322:699–74. https://doi.org/10.1056/NEJM199003083221006.
94. Dambska M, Schmidt-Sidor B, Maslinska D, et al. Anomalies of cerebral structures in acranial neonates. Clin Neuropathol. 2003;22:291–5.
95. Dias MS, Partington M. Embryology of myelomeningocele and anencephaly. Neurosurg Focus. 2004;16:E1.
96. Lemire RJ, Cohen MM Jr, Beckwith JB, Kokich VG, Siebert JR. The facial features of holoprosencephaly in anencephalic human specimens I. Historical review and associated malformations. Teratology. 1981;23:297–303.
97. Siebert JR, Cohen MM Jr, Sulik KK, Shaw C-E, Lemire RJ. The facial features of holoprosencephaly in anencephalic human specimens II. Craniofac Anat Teratol. 1981;23:305–15.
98. Guion-Almeida ML, Richeiri CA. Fronto-nasal dysplasia, macroblepharon, eyelid colobomas, ear anomalies, macrostomia, mental retardation and CNS structural abnormalities defining the phenotype. Clin Dysmorphol. 2001;10:191–202.
99. Richieri Costa A, Guion-Almeida ML. The syndrome of frontal-nasal dysplasia, callosal agenesis, basal encephalocele, and eye anomalies: phenotypical and etiological considerations. Int J Med Sci. 2004;1:34–42.
100. Kawamoto HK, Keller JB, Mell MW. Craniofacial-nasal dysplasia: Surgical treatment algorithm. Plast Reconstr Surg. 2007;120(7):1943–56.
101. Balci S, Mavili ME, Son YE, et al. A female patient with frontonasal dysplasia sequence and frontonasal encephalocele. Ann Plast Surg. 1999;43:457–9.
102. Song SY, Cho JW, Lew HW, Koh KS. Nasal reconstruction of a frontonasal dysplasia deformity using aesthetic rhinoplasty techniques. Arch Plast Surg. 2015;42(5):637–9. https://doi.org/10.5999/aps.2015.42.5.637.
103. Sharma R. Hypertelorism. Indian J Plast Surg. 2014;47(3):284–92.
104. Lightwood RC, Sheldon WPH. Hypertelorism: a unilateral case. Arch Dis Child. 1928;3(15):168–72. https://doi.org/10.1136/adc.3.15.168.
105. Tessier P, Guiot G, Derome P. Orbital hypertelorism: II. Definite treatment of hypertelorism (OR.H.) by craniofacial or by extracranial osteotomies. Scand J Plast Reconstr Surg. 1973;7:39–58.
106. Balaji SM, Modified facial bipartition. Ann Maxillofac Surg. 2012;2(20):170–3.
107. Smith JL, Schoenwolf GC. Neurulation: coming to closure. Trends Neurosci. 1997;20(11):510–7. https://doi.org/10.1016/s0166-2236(97)01121-1.
108. Copp AJ. Neurulation in the cranial region: normal and abnormal. J Anat. 2005;207:623–5.
109. Sheen J, Sheen AP. Aesthetic rhinoplasty. 2nd ed. St. Louis: Quality Medical Publishers; 1998.
110. Gruber RP, Tabbal GN, Sheen J, Toriumi D. Treatment of complex nasal deformities. Aesthet Surg J. 1999;19(6):475–82.
111. Mowlavi AS, Chabelian TL, Melgar A, et al. Upper septal vault and short nasal bone syndrome: implications for rhinoplasty. Eplasty. 2018;18:e29.
112. Karakor-Altuntas Z, et al. Isolated congenital nasal bifid septum separated by a wide layer of soft tissue. Arch Plast Surg (Korean Society of Aesthetic Plastic Surgery). 2015;42(5):640–2.
113. Shino M, Chikamatsu K, Yasuoka Y, et al. Congenital arhinia: a case report and functional evaluation. Laryngoscope. 2005;115:1118–23.
114. Zhang M-M, Hu Y-H, He W, Hu K-K. Congenital arrhinia: a rare case. Am J Case Rep. 2014;15:115–8.
115. Newman MH, Burdi AB. Congenital alar field defects: clinical and embryologic considerations. Cleft Palate J. 1989;19(6):475–82.
116. Abulezzi T. Case of heminasal aplasia: clinical picture, radiologic findings, and follow-up after early surgical treatment. J Craniofac Surg. 2019;30(3):e199–202.
117. Meyer R. Total external and internal reconstruction in arhinia. Plast Reconstr Surg. 1997;99:534–42.
118. Gong A. Proboscis lateralis type IV: a report from the Indian subcontinent. Acta Chir Plast. 1991;33:34–9.
119. Olsen OE, Gjelland K, Reigstad H, Rosendahl K. Congenital absence of the nose: a case report and literature review. Pediatr Radiol. 2001;31:225–32.
120. Toraynski E, Jacobiec FA. Cyclopia and synophthalmia: a model of embryologic interactions. In: Jacobiec FA, Duane TD, Jaeger EA, editors. Ocular anatomy, embryology, and teratology, Biomedical foundations of ophthalmology, vol. I. Philadelphia: JB Lippincott; 1982.
121. England SJ, Blanchard GB, Mehadevan L, Adams RJ. A dynamic fate map of the forebrain shows how vertebrate eyes form and explains two causes of cyclopia. Development. 2006;133:4613–7.
122. Bianchi D. Fetology: diagnosis and management of the fetal patient. 2nd ed. New York: McGraw-Hill; 2010.
123. Suzukui DG, Fukumoto Y, Yoshimura M, Yamazaki Y, Kosaka J, Kuratani S, Wada H. Comparative morphology and development of extraocular muscles in the lamprey and gnathostomes reveal the ancestral state and developmental patterns of the vertebrate head. Zool Lett (Zoological Society of Japan). 2016;2:10.
124. Plock J, Contaldo C, Von Ludinghausen M. Extraocular muscles in human fetuses with craniofacial malformations: anatomical findings and clinical relevance. Clin Anat. 2007;23(3):239–45.
125. Noden DM. Patterning of avian craniofacial muscles. Dev Biol. 1986;116:347–56.
126. Noden DM, Francis-West P. Differentiation and morphogenesis of craniofacial muscles. Dev Dyn. 2006;235:1194–2018.
127. Ziermann JM, Diogo R, Noden DM. Neural crest and the patterning of vertebrate craniofacial muscles. Wiley Genesis. 2018;56(6–7):e23097. https://doi.org/10.1002/dvg.23097.
128. Lumsden A, Keynes R. Segmental patterns of neuronal development in the chick hindbrain. Nature. 1989;337:424–8.
129. Lumsden A, Krumlauf R. Patterning the vertebrate neuraxis. Science. 1996;274:1109–15.
130. Hunt P, Krumlauf R. Hox codes and positional specification in vertebrate embryonic axes. Annu Rev Cell Biol. 1992;8:227–56.
131. Cohen MM, Sulik KK. Perspectives on holoprosencephaly: part I. Epidemiology, genetics and syndromology. Teratology. 1989;40(3):211–35.
132. Cohen MM, Sulik KK. Perspectives on holoprosencephaly: part II. Central nervous system, craniofacial anatomy, syndrome commentary, diagnostic approach, and experimental studies. J Craniofac Genet Dev Biol. 1992;12(4):196–244.
133. Cohen MM, Sulik KK. Perspectives on holoprosencephaly: part III. Spectra, distinctions, continuities and discontinuities. Am J Med Genet. 1989;34(2):271–88.

134. Hendry JM, Nemerofsky R, Stolman C, Granick MS. Plastic surgery considerations for holoprosencephaly patients. J Craniofac Surg. 2004;15:675–7.
135. Nagase T, Nagase M, Osumi N. Craniofacial anomalies of the cultured mouse embryo induced by inhibition of sonic hedgehog signaling: an animal model of holoprosencephaly. J Craniofac Surg. 2005;16:80–8.
136. Gui T, Osama-Yamashita N, Eto K. Proliferation of nasal epithelia and mesenchymal cells during primary palate formation. J Craniofac Genet Dev Biol. 1993;13:250–8.
137. Carstens MH. The spectrum of minimal clefting: process-oriented cleft management in the presence of an intact alveolus. J Craniofac Surg. 2000;11(3):270–94.
138. Carstens MH. Functional matrix cleft repair: principles and techniques. Clin Plast Surg. 2004;31:159–89.
139. Carstens MH. Developmental field reassignment in unilateral cleft lip: reconstruction of the premaxilla. In: Losee J, Kirschner R, editors. Comprehensive cleft care. Boca Raton, FL: CRC Press/Taylor & Francis; 2007.
140. Montague A. The premaxilla in primates. Q Rev Biol. 1935;10(1):32–59.
141. Barteczko Barteczko K, Jacob M. A re-evaluation of the premaxillary bone in humans. Anat Embryol (Berl). 2004;207:417–37.
142. Trevizan M, Consolaro A. Premaxilla: an independent bone that can base therapeutics for middle third growth. Dental Press J Orthod. 2017;22(2):21–6. https://doi.org/10.1590/2177-6709.22.2.021-026.oin.
143. Burdi AR, Lawton TJ, Grosslight J. Prenatal pattern emergence in early human facial development. Cleft Palate Craniofac J. 1988;25:8–15.
144. Graham A, Smith A. Patterning the pharyngeal arches. BioEssays. 2001;23:54–61.
145. Couly G, Cruezet S, Bennaceur S, et al. Interactions between Hox-negative cephalic neural crest cells and the foregut endoderm in patterning the facial skeleton in the vertebrate head. Development. 2002;129:1061–73.
146. Ruthin B, Creuzet S, Vincent C, et al. Patterning of the hyoid cartilage depends upon signals arising from the ventral foregut endoderm. Dev Dyn. 2003;228:239–46.
147. Tapadia MD, Cordero D, Helms JÁ. It's all in your head: new insights into craniofacial morphogenesis. Development. 2005;132:851–61.
148. Johnston MC, Millicovsky G. Normal and abnormal development of the lip and palate. Clin Plast Surg. 1985;2:521.
149. Gong S-G, Guo C. Bmp4 gene is expressed at the putative site of fusion in the midfacial region. Differentiation. 2003;71:228–36.
150. Carstens M. Development of the facial midline. J Craniofac Surg. 2002;13:129–87.
151. Ashique AM, Fu K, Richman JM. Endogenous bone morphogenetic proteins regulate outgrowth and epithelial survival during avian lip fusion. Development. 2002;129:4647–60.
152. Zhang Z, Song Y, Zhao X, et al. Rescue of cleft palate in Msx-1 deficient mice by transgenic *bmp4* reveals a network of BMP and Shh signaling in the regulation of mammalian palatogenesis. Development. 2002;129:4135–40.
153. Jirasek JE. Atlas of human prenatal morphogenesis. Amsterdam: Martinus Nijhof; 1983.
154. Jirasek JE. An atlas of the human embryo and fetus. CRC Press; 2000.
155. Hinrichsen K. The early development of morphology and patterns of the face in the human embryo. In: Advances in anatomy, embryology, and cell biology, vol. 98. New York: Springer; 1985. p. 1–72.
156. Kaufman MH. The atlas of mouse development. San Diego: Academic Press; 1992. p. 429.